Nuclear Structure Calculations using many-body perturbation theory with a separable interaction

Paul Stevenson

Balliol College

A thesis submitted in partial fulfillment of the requirements for the degree of Doctor of Philosophy in the University of Oxford

Trinity Term 1999

Nuclear Structure Calculations using many-body perturbation theory with a separable interaction

Paul Stevenson

Balliol College

Abstract

A new form of the effective nuclear interaction is presented which is density-dependent and separable in coordinate space. Calculations are made of the properties of the even-even closed-shell nuclei ^{16}O, ^{34}Si, ^{40}Ca, ^{48}Ca, ^{48}Ni, ^{56}Ni, ^{68}Ni, ^{78}Ni, ^{80}Zr, ^{90}Zr, ^{100}Sn, ^{114}Sn, ^{132}Sn, ^{146}Gd and ^{208}Pb as well as infinite symmetric and asymmetric nuclear matter and neutron stars. Ground state observables are calculated in the Hartree-Fock approximation. Corrections are calculated for binding energies by summation of the perturbation series up to third order. The correction terms in the series are found to be small and convergent, giving confidence that the method is applicable to the interaction presented.

Acknowledgements

Any errata to this Thesis will be available on the World Wide Web at:

`http://csep2.phy.ornl.gov/theory_group/people/spaul/thesis-errata.html`

Contents

Chapter 1

Introduction

1.1   Nuclear Structure Theory

The science of nuclear structure attempts to explain the phenomena arising in the atomic nucleus in terms of the protons and neutrons which constitute it and the forces under which they interact. The type of phenomena which are seen include the nuclear mass, its size and shape, and the rich spectra of excited states, each with certain good quantum numbers and excitation energies which may be well-defined or broad resonances, and may be identifiable as single-particle or collective behaviour. In weakly bound nuclei near the neutron drip line such exotica as neutron skins and halos are in evidence. At the other extreme, near the proton drip-line, proton radioactivity is observed. As well as these observables in the time-independent problem, one observes phenomena in nuclear reactions which a theory of nuclear structure needs to address such as the reaction cross sections, fission barriers and lifetimes. The number of particles of a self-bound nuclear system ranges from two nucleons in the deuteron to nearly three hundred in the super-heavy nuclei currently being studied[1, 2, 3]. Furthermore neutron stars are thought to be made of nuclear matter, bound due to gravitational forces, and under more extreme physical conditions than "ordinary" nuclear matter, but presumably subject to the same interactions.

The ability to explain all these phenomena is complicated by two things. The more fundamental of these is the fact that the nuclear interaction is not fully understood, despite a considerable amount of effort spend in studying it. In fact, Hans Bethe once suggested that more endeavour had been spent in studying the nuclear force problem than any other problem in the history of science, and this was in 1956[4]. The force between two nucleons must be ultimately described by the combined effect of the forces between their quark and gluon constituents or even from more fundamental constituents, should such things exist. Work exists which describes the forces between observed particles as derived from the underlying quark-quark interactions[5] but, as yet, no full nucleon-nucleon interaction derived just from more fundamental microscopic considerations is available. All

interactions used in calculations of nuclei contain, at least in part, phenomenol-ogy. That nucleons are made of more fundamental constituents is not to say that one should be solving the many-body Schrödinger equation for a system of $3A$ (or more) quarks. Since nucleons are the only particles actually observed in nuclei, it is certainly to be expected that an expression for the interaction binding the nu-cleons together can be written in terms of the nucleon coordinates and quantum numbers without necessary recourse to the presumed substructure. This argument is analogous to the fact that one describes atoms and molecules in terms of the electron coordinates and degrees of freedom even though such systems manifestly contain protons and neutrons.

The second difficulty in producing results in the field of nuclear structure is the calculational complexity involved in solving the microscopic equations of many-body quantum mechanics, especially given the rather complicated nuclear inter-actions posited. At the present, and for the foreseeable future, approximations need to be made to perform calculations of the majority of nuclei. These approx-imations are often considerable.

1.2   Nuclear forces and the many-body problem

1.2.1   Realistic Interactions

The most fundamental nucleon-nucleon interactions currently used in nuclear structure calculations are the so-called "realistic" potentials. These are based around the assumption that the force between two nucleons is dominated by me-son exchange. This approach agrees with the quark model at large separations when the finite meson size and underlying quark structure are not relevant. The short and intermediate range parts are phenomenologically parameterized to fit nucleon-nucleon scattering data and the binding energy of the deuteron. Mod-ern versions of these potentials, such as the Argonne $v18$ potential[6] are usually used in conjunction with three-nucleon potentials[7, 8, 9] since three-nucleon effects seem to be important in nuclei, as evinced by so-called Borromean nu-clei, which are bound and consist of a core and two loosely bound particles, but which would not be bound if one of these particles were absent. The necessity of three-body interaction is also seen in the way the two-body interactions fitted to two-body data alone fails to fit the binding energy of the triton and heavier nuclei. The great drawback with using a "realistic" potential is that they are functionally rather complicated, consisting of many terms, each dependent upon the states of the particles, and they have a hard-core, which is to say that the potential be-comes very strongly repulsive at small separation, so that "obvious" techniques of many-body quantum mechanics such as perturbation theory, or the standard Hartree-Fock approximation may not be used and rather more complicated tech-niques need to be implemented. In addition, these forces are fitted to free nucleon
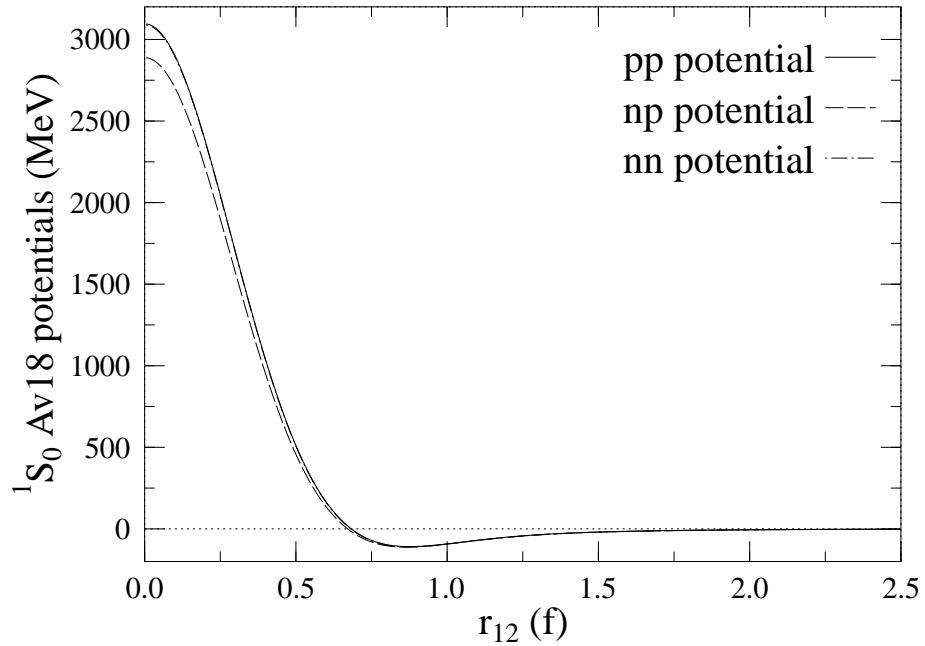
Figure 1.1: *The $^1S_0$ part of the Argonne v18 potential. The pp and nn potentials are identical and the pn potential is slightly different from both. The curve shows the strong repulsion common to most realistic interactions.*

data, so any effects which arise only when many nucleons are present are not accounted for, except by the addition of many-body forces. Currently, no attempt seems to be made to go beyond three-body interactions. Figure (1.1) shows the dominant part of the Argonne v18 potential. Note that the strength of the term for zero separation is ~ 3 GeV whereas the attractive mid-range part which is responsible for the binding is only about ~ 100 MeV. In the energy scale of nuclear physics, a GeV is a very large energy – it is roughly the rest mass of a nucleon.

There are a vast number of methods which have been used to solve the many-body Schrödinger equation with realistic interactions. The most venerable is the Bruekner Theory[10], also known as the independent pair approximation which takes the short range correlations into account by summing the ladder series of diagrams. Other successful techniques have been in the form of Fadeev [11], Variational Monte-Carlo[12], Green's Function Monte-Carlo[13], Correlated basis function [14] and coupled-cluster[15, 16] calculations. These have allowed for the study of a number of light nuclei up to $A \approx 7$, as well as the spherically symmetric ^{16}O and ^{40}Ca. As computational techniques and computer power advance, one would expect to calculate heavier and heavier nuclei with these methods; however, since the complexity of a full many-body problem increases combinatorially as a function of the number of particles, it is not expected that one would be able to calculate all, or even the majority of, known nuclei in this way in the immediate future.

1.2.2   Effective interactions

In using an effective interaction one is attempting to construct a form of the nuclear force which is typically simpler in form than the realistic interactions and is easier to use within calculational frameworks amenable to the calculation of medium and heavy nuclei. For instance an effective interaction may be parameterized in such a way as to avoid having a hard core. This is not as unreasonable as it might sound; if the force is intended for use in the calculation of finite nuclear properties rather than, say, scattering data, the Pauli exclusion principle keeps the nucleons sufficiently far apart that they very rarely feel this hard core repulsion. It is characteristic of effective interactions that they are suited for specific systems and calculational techniques. They are widely used in single-particle models, which dominate the microscopic calculations of medium and heavy nuclei.

The G-matrix expansion[17] provides a link between the realistic and effective interactions since it derives a "renormalized potential" from a realistic interaction which may be used for calculation in the same kind of situations as purely phenomenological effective interactions.

In single particle models it is assumed that each nucleon moves in an average field due to the action of the other nucleons. By this assumption one transforms the N-body problem into N one-body problems, which are much easier to solve. Single particle models are often used as the starting point for more sophisticated calculations. The archetype of this paradigm is the shell-model[32], which assumes a given static one-body potential which creates a spectrum of single-particle states, occupied by the nucleons. The nucleons in these states then interact with each other via effective interactions which are either phenomenological or microscopically derived from a realistic interaction to take into account the Hilbert space assumed in the single particle model[33]. Although this is a computationally easier process than the above methods with a full realistic interaction, one must be near a closed shell in heavy nuclei for a shell-model calculation to be feasible. Again, as techniques and computing advance, the boundaries of the nuclear chart of areas closed to the shell model will recede, but they will not be eliminated completely for some time. Furthermore, the theoretical basis of the shell model rests on a number of assumptions and approximations which are not always well justified[18], although this is true of the use of effective interactions in general. Furthermore, in the shell-model, there is typically no link between the interaction which produces the mean field, the single particle states and all the ground state properties, and the interaction which acts between the valence nucleons giving rise to the excited states.

1.2.3   Hartree-Fock calculations

The only fully microscopic models which are, at present, used to calculate the entire range of nuclei are the Hartree-Fock(HF) mean field method and its rel-

ativistic counterpart, the Relativistic Mean-Field(RMF) method. They provides the bulk properties of the ground state and single particle spectrum, which can then be used as a starting point for shell-model calculations, but from a nuclear effective interaction rather than an assumption. First introduced in atomic physics[19], the HF method was used to calculate nuclear properties with a wide range of interactions (see e.g. the exhaustive summary of Svenne[20]), but it was not until density-dependent interactions, such as Skyrme's interaction, used by Vautherin and Brink[21], and the surface delta interaction[44], were used that a Hartree-Fock calculation produced results which fitted both ground-state radii and binding energies at the same time. The key to this was the interactions' density-dependence, giving rise to an extra potential in the mean-field – the so-called "rearrangement potential". Since then, many parameterizations of the Skyrme interaction have been made, as well as some modification of its functional form. It has been applied to nuclei across the periodic table as well as to neutron stars[22]. A link between the density-dependent effective interactions like that of Skyrme and the realistic interactions was provided by Negele[23]. Extended versions of Skyrme's interaction have even been used in shell-model calculations to both generate the single particle basis and then, unaltered, as a residual interaction[24, 25]. By doing a shell model calculation, however, one again limits the range of nuclei that the technique may be applied to.

Despite the great achievements of the modern effective interactions used in mean-field calculations, they all have the characteristic of being short-, or zero-range, which makes them unsuitable for use in perturbation theory calculations, since the matrix elements involved are too large (the perturbation is not weak enough).

This means that one of the simplest and most elegant techniques for accounting for both single-particle and collective behaviour, and for both ground and excited state properties within one framework, with the same interaction, is not available for use with the forces so far mentioned. The great utility of the perturbation theory is that it is computationally feasible to calculate the lowest order diagrams for any nucleus, and so one could calculate a much better approximation to the exact wavefunction than in a mean-field alone without needing to stay close to the closed shells. As mentioned above, effective interactions may differ in form quite considerably from realistic interactions so that one need not have a short range repulsion. So too, then, one can attempt to parameterize the effective interaction in such a way that it is not of a very short range to use it in normal perturbation theory.

Motivated by the ideas presented above, this thesis supposes that there exists an effective nuclear interaction with which the techniques of standard many-body perturbation theory may be used to calculate observables, and that this interaction is of comparable quality to contemporary effective interactions. The focus is solely on the ground states of spherical closed-shell nuclei and nuclear matter since these are the simplest systems to calculate and therefore present the most convenient

systems for creating a new effective interaction. The thesis is organised as follows:

Chapter 2 discusses the methods used to solve the many–body Schrödinger equation for the interaction being used, which itself is the subject of chapter 3, in which its form and character are expounded. Chapter 4 deals with some of the computational details and approximations which affect the calculation. Chapter 5 discusses the numerical character of the force and explores how the different parts of the force affect observables. The following two chapters give the physical results; Chapter 6 contains details of the nuclear matter and neutron star calculations and Chapter 7 presents the results of calculation with finite nuclei. Chapter 8 summarises the work.

Chapter 2

Many-Body Perturbation Theory

2.1 Single-particle theories

An oft-used technique in quantum mechanics is to separate the Hamiltonian of an insoluble problem into two parts, one of which is solvable and the other not. The technique relies on the ability to choose the separation such that the solvable part gives the dominant effect and the remaining part is small and may be treated as a perturbation.

A useful way to perform this separation, in the case of a many-body system subject to two- (or more) body interactions, is to add and subtract a single particle potential, $U(r)$, term to the Hamiltonian to give

$$H = T(r) + V_1(r) + V(r_1, r_2) = \underbrace{[T(r) + V_1(r) + U(r)]}_{H_0} + \underbrace{V(r_1, r_2) - U(r)}_{H_1}. \tag{2.1}$$

The utility of this Ansatz is that the zeroth order problem of solving the many-body Schrödinger equation with H_0 as the Hamiltonian may be a good approximation to the true solution and will, for a sensible choice of $U(r)$ be much easier to obtain. In general, models which use this separation are termed singe-particle or independent-particle models. Since the independent particles are fermions, whether actual nucleons or quasi-particles, the ground state many-body wavefunction is a Slater determinant of single particle states, $\varphi_i(r_i)$,

$$\Phi(r_1, r_2, \ldots, r_N) = \mathcal{A} \prod_i \varphi_i(r_i). \tag{2.2}$$

Correlations are then defined as the corrections which need to be added to the independent particle model to arrive at the true solution. Since the results of the independent particle model depend upon the chosen potential, $U(r)$, in Equation (2.1) so, too, do the correlations. When one talks about single particle calculations already containing correlations, as is often the case with density-dependent HF calculations[97], it is usually meant that one considers an effective interaction to

be, in principle, a renormalized realistic interaction. The solution of the effective interaction in a single-particle model is then taken to include both single-particle and correlation effects of the realistic interaction. Of course, a purely single-particle model can never show certain correlation effects, such as the non-zero occupation probability of states above the Fermi level[26], unless one introduces quasi-particles.

There are many ways to calculate these correlations. The textbooks of Ring and Schuck[28], deShalit and Feshbach[27] and Eisenberg and Greiner[39] describe many of the methods used at the time of their publications (up to 1980). Some other methods were mentioned in the previous chapter. Presented here is the technique used in this Thesis, along with some mention of the relation to other methods.

2.1.1 One-body potential

The prescription for generating the one-body part, $U(r)$, facilitating the separation of the Hamiltonian varies between approaches. One approach is to make the one-body part essentially trivial by choosing a well-know single-particle potential to augment the kinetic energy term, such as a harmonic oscillator potential. This is the approach usually taken by the shell model. In its simplest form the shell model contains only this spherical single particle potential with a spin-orbit interaction [29] or for deformed nuclei, the extension to a deformed oscillator basis was provided by Nilsson[30]. More recently the residual interaction has been treated in which the calculational effort is spent in trying to solve the Schrödinger equation exactly by diagonalizing the full Hamiltonian in the basis given by the single particle potential. Typically this is a large problem which necessitates a truncation in configuration space, although "no-core" calculations have recently been performed for the lightest nuclei[31]. The large calculations are possible since the Hamiltonian matrices are typically sparse in this representation so can be diagonalized by the Lanczos method. These techniques are reviewed in [32]. By choosing the single particle potential in this way, one separates the potential which generates the single particle states from the interaction, which gives the spectroscopy.

Another choice of single particle potential is to pick the "best" potential. In this context, *best* means the potential which results in the Slater determinant solution which minimizes the expectation value of the full Hamiltonian, $H = H_0 + H_1$. The minimization procedure uses a variational principle which has, as the variational parameters, the single particle wavefunctions in the Slater determinant. Such a method for choosing the potential U is called the Hartree-Fock method and is described in Appendix A; it is the technique used in this work to obtain the single particle states which define the many-body ground state. Being a variational technique, only the lowest energy state is given as its solution, although one can extend the technique to excited states by including Lagrange multipliers

and performing so-called constrained Hartree-Fock calculations[28]. One major advantage with using the HF basis for perturbation calculations is that the Slater determinant of the single particle states has the property that matrix elements of the Hamiltonian between the ground state and any one-particle one-hole excitation vanish identically. This property is known as *Brillouin's Theorem*[35] and greatly simplifies the perturbation calculations if the HF Hamiltonian defines the unperturbed problem. In particular it means that the lowest non-zero term in the perturbation theory is the second order term. It should be pointed out that most HF calculations in nuclei are carried out without the intent of "going further"; i.e. it is possible to get a rather good description of nuclear ground states from the mean-field alone. This fact is one of the premises of the present study – that most of the ground-state properties arise from the mean–field. It is the additional contention that by a judicious choice of interaction one can calculate higher orders of perturbation theory and thereby describe effects beyond the mean field, which can not be accounted for by a single particle model alone.

2.2 Many-Body Perturbation Theory

The techniques of Many-Body perturbation theory provide a useful language for discussion of the methods of calculating correlations, as well as giving an intuitive graphical representation. Appendix B gives a derivation of the Rayleigh-Schrödinger perturbation theory and its application to a Hamiltonian with two-body interaction, using the Hartree-Fock states as the reference state. Alternative derivations are widely available in the literature[34, 35, 36, 37, 38, 39]. The graphical technique is discussed in Appendix C for Hugenholz diagrams. The alternative formulation in terms of Goldstone diagrams are discussed in the literature (see e.g. [40]).

The method used in this thesis is to evaluate diagrams directly for the vacuum amplitude diagram-by-diagram in a straightforward manner. This allows one to write down the total energy of the system in a series

$$E = E_{HF} + E_2 + E_3 + \cdots \tag{2.3}$$

and to evaluate each term one by one and examine the convergence properties. The contributions to the energy, E, to third order are given by

$$E_{HF} = \sum_{a<\epsilon_F} \langle a|T + V_1|a\rangle + \frac{1}{2} \sum_{ab<\epsilon_F} \langle ab|\tilde{V}|ab\rangle \tag{2.4}$$

$$E^{(2)} = \frac{1}{4} \sum_{a\neq b<\epsilon_F} \sum_{r\neq s>\epsilon_F} \frac{\langle ab|\tilde{V}|rs\rangle\langle rs|\tilde{V}|ab\rangle}{\epsilon_a + \epsilon_b - \epsilon_r - \epsilon_s}. \tag{2.5}$$

$$
\begin{aligned}
E^{(3)} &= \frac{1}{8} \sum_{a \neq b < \epsilon_F} \sum_{c \neq d \leq \epsilon_F} \sum_{r \neq s > \epsilon_F} \frac{\langle ab|\tilde{V}|rs\rangle\langle cd|\tilde{V}|ab\rangle\langle rs|\tilde{V}|cd\rangle}{(\epsilon_a + \epsilon_b - \epsilon_r - \epsilon_s)(\epsilon_c + \epsilon_d - \epsilon_r - \epsilon_s)} \\
&+ \frac{1}{8} \sum_{a \neq b < \epsilon_F} \sum_{r \neq s > \epsilon_F} \sum_{t \neq u > \epsilon_F} \frac{\langle ab|\tilde{V}|rs\rangle\langle rs|\tilde{V}|tu\rangle\langle tu|\tilde{V}|ab\rangle}{(\epsilon_a + \epsilon_b - \epsilon_r - \epsilon_s)(\epsilon_a + \epsilon_b - \epsilon_t - \epsilon_u)} \\
&+ \sum_{a \neq b \neq c < \epsilon_F} \sum_{r \neq s \neq t > \epsilon_F} \frac{\langle ab|\tilde{V}|rs\rangle\langle cr|\tilde{V}|at\rangle\langle st|\tilde{V}|cb\rangle}{(\epsilon_a + \epsilon_b - \epsilon_r - \epsilon_s)(\epsilon_b + \epsilon_c - \epsilon_s - \epsilon_t)}.
\end{aligned}
\tag{2.6}
$$

It is to this order that the diagrams are calculated in this Thesis. The explicit diagrammatic representation of these terms is given in Appendix C.

As a measure of the strength of the perturbative interaction, H_1, the dimensionless parameter κ is defined as

$$
\kappa = \frac{1}{4} \sum_{ab \leq \epsilon_F} \sum_{rs > \epsilon_F} \frac{\left|\langle ab|\tilde{V}|rs\rangle\right|^2}{|\epsilon_a + \epsilon_b - \epsilon_r - \epsilon_s|^2}
\tag{2.7}
$$

which is identified as the average number of particles the second order correlation excites from the Hartree-Fock ground state.

The perturbation theory gives a series for any observable, not just the energy since it produces a series for the exact wavefunction, $|\Psi\rangle$, which is of the form

$$
|\Psi\rangle = |\Phi_{HF}\rangle + \sum_{ab < \epsilon_F} \sum_{rs > \epsilon_F} C_{ab}^{rs}|\Phi_{rs}^{ab}\rangle + \cdots
\tag{2.8}
$$

where Φ_{HF} is the Hartree-Fock ground state Slater determinant, and Φ_{ab}^{rs} is a Slater determinant with two particles excited from the HF ground state into higher HF orbitals. The ellipsis indicates that higher order corrections exists which involve exciting more particles from the HF ground state into higher states. The wavefunction is then expressed as a sum of Slater determinants. The perturbation theory provides the coefficients, C_{ab}^{rs} etc., in terms of the interaction potential H_1. This Thesis, however, does not address corrections to any observables but the energy since the perturbation series for two-body observables such as the energy is thought to be much larger than for one-body observables such as the density if one uses the HF basis for perturbation theory. The purpose of this Thesis is to explore the possibility of finding a potential for which the perturbation theory converges and provides a reasonable fit in HF order for the ground state of spherical nuclei, rather than to calculate the large range of observables for all nuclei, which remains for future work.

2.2.1 Density-Dependent Interaction

In Appendix B it is seen that the separation of the Hamiltonian into the unperturbed (H_0) and perturbation (H_1) parts takes place in such a way that H_1 is just

the two-body interaction and H_0 is the solution of the normal Hartree-Fock equation. The omission of the density-dependence in this HF equation means that the methods used in this Thesis implicitly involve the assumption that, at the level of the perturbation theory, the densities are simple fixed functions which are not related to the creation and annihilation operators and do not directly result from many-body forces. If one did not make this assumption, the method would become too complicated. One would certainly be restricted to integral powers of the α and β parameters and even then, the appearance of a density in the denominator of a function would require special consideration.

2.3 Other Methods

While the method in this Thesis involves summing, in principle, all diagrams in the perturbation expansion, in practice, only a few are included since the series converges quite quickly. Other techniques used for nuclear structure calculations involve summing infinite series of diagrams. The Random-Phase-approximation[42] (RPA) method may be derived from the time-dependent Hartree-Fock equations[41], or by linearizing the equations of motion[39]. This is equivalent to summing the subclass of diagrams which include only the insertions given in Figure 2.1[37].

In Brueckner Theory[38] the ground state of a nucleus is calculated using a renormalized potential (the G-matrix) which includes the ladder diagrams, which is the series of diagrams featuring the insertion in Figure 2.2.

The second order diagram (Appendix C, Figure C.4) features in both these series. In the third order the particle-particle diagram of Figure C.5 contributes to the Brueckner theory calculation and the particle-hole diagram to the RPA.
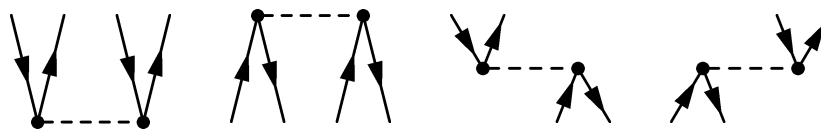
Figure 2.1: *Insertions included in the RPA calculation*
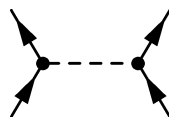
Figure 2.2: *Insertion in the series calculated by Brueckner theory*

Chapter 3

Nuclear Force: Theory

Having discussed some aspects of nuclear structure theory, ways in which it is usually approached, and discussed the methods used in the present work to attack the problem, it is clear that a new interaction needs to be used. The criterion which it must satisfy are that is must fit single particle properties well in the Hartree-Fock approximation and be weak enough to produce small and converging corrections in perturbation theory for many-body observables, particularly the binding energy.

3.1 Nuclear Interaction

The two-body force used in this work consists of a sum of terms each of which is separable in coordinate space. Each term consists of products of one body operators of definite angular momentum, and the terms are classified according to this value as monopole, dipole and quadrupole terms for angular momenta $l = 0$, $l = 1$ and $l = 2$ respectively.

3.1.1 Monopole Interaction

The monopole interaction is in the form of a separable function, each part of which is a scalar. In coordinate space it is written

$$
\begin{aligned}
V(r_1, r_2) \ = \ & W_a f_{\alpha_a} \rho^{\beta_a}(r_1) \rho^{\beta_a}(r_2) (1 + a_a(\tau_1^+ \tau_2^- + \tau_1^- \tau_2^+) + b_a \tau_{1z} \tau_{2z}) \\
+ \ & W_r f_{\alpha_r} \rho^{\beta_r}(r_1) \rho^{\beta_r}(r_2) (1 + a_r(\tau_1^+ \tau_2^- + \tau_1^- \tau_2^+) + b_r \tau_{1z} \tau_{2z}) \\
+ \ & k \nabla_1^2 \rho(r_1) \nabla_2^2 \rho(r_2),
\end{aligned} \tag{3.1}
$$

where the function f_ξ is defined as

$$
f_\xi = \left[\int_{\text{all space}} \rho^{\alpha_\xi}(r) d^3 r \right]^{-1}, \tag{3.2}
$$

and W_a, α_a, β_a, a_a, b_a, W_r, α_r, β_r, a_r, b_r, and k are parameters to be fitted to experimental data. The first two terms in Equation (3.1) are functionally identical in form, but have their own set of parameters. The subscript a denotes the attractive term, so the strength W_a is taken to be negative. The subscript r denotes the repulsive term, and W_r is always taken to be positive.

In addition to this two-body interaction there is a spin-orbit force which we postulate as a one-body field of the Blin-Stoyle form[43]. Its form is

$$V_{s.o}(r) = c\frac{1}{r}\frac{\partial \rho(r)}{\partial r}\mathbf{l} \cdot \mathbf{s}, \tag{3.3}$$

where $\mathbf{l}$ is the orbital angular momentum operator for the particle and $\mathbf{s}$ is the spin angular momentum operator. Note that this same *Ansatz* for the spin-orbit interaction has been used previously in HF calculations with effective interactions by Ehlers and Moszkowski[44] and Vautherin and Veneroni[45]. It has a single parameter c which is fitted to the spin-orbit splitting of nuclei.

3.1.2 Higher Multipole Interactions

The multipole interactions are written

$$V_D(r_1, r_2) = W_{D,q_1,q_2}f_D \sum_{M=-1}^{1} (-1)^M r_1\rho(r_1)Y_{1M}(\hat{r}_1)r_2\rho(r_2)Y_{1-M}(\hat{r}_2) \tag{3.4}$$

$$V_Q(r_1, r_2) = W_{Q,q_1,q_2}f_Q \sum_{M=-2}^{2} (-1)^M r_1^2\rho(r_1)Y_{2M}(\hat{r}_1)r_2^2\rho(r_2)Y_{2-M}(\hat{r}_2). \tag{3.5}$$

Here, W_{D,q_1,q_2} are constant strength parameters for the dipole force, with $q_1 = q_2 = p$ giving the strength for the proton-proton interaction and $q_1 = q_2 = n$ for the neutron-neutron interaction. Similarly constants W_{Q,q_1,q_2} and for $q_1 = q_2$ give the pp and nn quadrupole force strengths. In addition a term acting between proton and neutron states in the quadrupole force is considered with a strength $W_{Q,p,n}$. The functions f_D and f_Q are introduced to control the A-dependence of the force. In principle they may be of a similar form to the f of the monopole force since the integral of the density over all space gives just the particle number A. In the current work these functions are taken to be A^γ, since these terms in the force are not included in the mean-field and so no functional variation is performed where the results would depend on whether the force was written as density-dependent or not.

In addition the Coulomb interaction is included. The direct part is implemented exactly and the exchange term is treated in the Slater approximation[46].

3.2 Philosophy

Having stated the form of the force, some explanation is in order to describe why it is in the form it is. The following characteristics summarize the nature of the interaction, the rationale of which shall be discussed here. The force is separable. This term is used here rather loosely - in fact it is the sum of separable terms, but this usage seems common enough in the literature to be used in the present case, as well. By separable, it is meant that the terms in the force are written as the product of a function of the (space, spin and isospin) coordinates of particle one multiplied by a function of the coordinates of particle two. Since it cannot matter which particle is labelled "one" and which one is labelled "two", the two functions are always the same in each term. Furthermore, the terms are separated according to the multipolarity of the one-body functions which make them up. Each term in the monopole interaction consists of a product of two $l = 0$ functions. In the dipole term the functions are $l = 1$ and in the quadrupole term they are $l = 2$. Another important aspect of the force is that it is density-dependent. The motivation for writing the force in this way is discussed in the sections below.

3.2.1 Separability and Multipolarity

The separability of the force was chosen for two reasons. The first one is somewhat historical, and is also a reason behind the splitting up of the force into multipoles, and is based on the fact that a simple model of a separable force was used as a residual interaction called the pairing plus quadrupole (PPQ) model[47, 48, 49, 50]. In this older work, the interaction is not density dependent and is used in a truncated space of an harmonic oscillator potential. Their reasons for considering such a separable interaction were that it would make the calculations much easier so that the model would be applicable, with 1960s computer technology, to the calculation of a wide range of nuclei. This is not really an issue today, but the success of the model showed that a separable interaction was a viable way of parameterizing the effective nuclear interaction and despite its simplicity (or, perhaps, because of it), it is still used in shell-model calculations[51]. The PPQ Hamiltonian lacks a monopole interaction which is necessary to give the bulk properties of the nucleus like the binding energy and single particle energies and to provide a mechanism for saturation. If, then, one could produce a monopole interaction to complement the higher multipole forces, one would obtain a full interaction which could be used for a microscopic description of nuclei which would both generate the one-body field *and* be used as the residual interaction. A similar approach has been considered recently in the context of the shell model[52]. This gives some rationale behind why the force is split up into multipoles and why the dipole and quadrupole terms are separable. The separability of the higher multipoles is not really a sufficient reason for making the monopole force separable. In fact the main reason for doing so is so that the force

will be weak enough to perform perturbation theory. Standard effective interactions, such as the zero-range Skyrme interaction are too strong for this. In the paper which first used the Skyrme interaction in the HF approximation[21] the authors acknowledge *"a perturbation calculation would actually diverge because of the zero range"*. It is known that separable interactions, several of which are described in a review by Kerman[53], are weak enough for perturbation theory to be performed[54] so extending the separable multipole philosophy of the PPQ model to include the monopole interaction seems like a likely path to success. On the other hand, the quality of the results from earlier separable interactions has been rather poor by today's standards. The force of Bressel et al.[55] was too strong for normal perturbation theory to converge and the set of partially separable potentials of Rouben, Riihimäki and Zipse[56, 57, 58] have far too high binding energies in nuclear matter. The most successful separable potential has probably been that of Tabakin[59] which has been used in HF plus perturbation calculations similar to the present work[60, 54] but the finite nuclear properties of this force are not of the same quality as modern effective interactions.

3.2.2 Density-dependence

Neither the PPQ interaction as previously conceived nor separable interactions of monopole form have been density-dependent. In the case of the residual interactions, which is to say interactions between nucleons which determines the spectroscopy after the ground state is calculated or assumed, this has led to them to be considered in a restricted space. To do otherwise would be problematic since they have an infinite range. By including a density-dependence the range can be limited in the force itself and no truncations need to be made in the calculation to avoid such physical problems as an infinite potential. In the case of the monopole interaction, used to generate the bulk properties of the nucleus, it was found that without the density dependence and the extra "rearrangement" contribution to the binding energy which comes from it in the Hartree-Fock approximation, it was not possible to simultaneously fit nuclear radii and binding energies, for attempts to do so with density-independent separable interactions, see Kerman's review[53]. The introduction of density-dependence with the Skyrme interaction[21] and the finite-range Gogny interaction[62] changed this feature of HF calculations and shifted the focus of effective nuclear interactions to the class of density-dependent interactions.

3.2.3 Range

As well as being density-dependent, other successful phenomenological effective interactions are all characterised by a short range. In the case of Skyrme's interaction the range is zero. In the Gogny interaction parts of the Skyrme force were replaced by a finite range Gaussian which resulted in a force which drops

off quickly as the nucleons move apart. The separable density-dependent force stands in contrast to these in that the force is felt at long distance as well as short. From the terms of the form

$$V(r_1, r_2) \sim \rho(r_1)\rho(r_2) \tag{3.6}$$

it is seen that the only requirement for the force to be felt between two nucleons is that both the nucleons are situated inside the nucleus in a region where the density is non-zero.

3.3 Term by term rationale

3.3.1 HF Mean field

The Hartree–Fock energy, E_{HF}, and mean field are derived in Appendix E and the results are show here for discussion. The energy is

$$
\begin{aligned}
E_{HF} &= T + E_{coul} + \sum_{\xi=a,r} \left\{ \frac{1}{2} W_\xi f_{\alpha_\xi} N_{\beta_\xi}^2 - \frac{1}{2} W_\xi f_{\alpha_\xi} M_{\beta_\xi} \right. \\
&+ \frac{1}{2} W_\xi b_\xi f_{\alpha_\xi} (\Delta N_{\beta_\xi})^2 - \frac{1}{2} W_\xi f_{\alpha_\xi} \left[b_\xi M_{\beta_\xi}^{(\tau\tau)} + a_\xi M_{\beta_\xi}^{(\tau\bar{\tau})} \right] \left. \right\} \\
&+ \frac{1}{2} k N_d^2 - \frac{1}{2} k M_d + c N_w \\
&- \frac{1}{2} f_\Lambda \chi_{\Lambda, q_1, q_2} \sum_{i,j<\epsilon_F} \sum_{M=-\Lambda,\Lambda} (-1)^M \langle ij | [r_1^\Lambda(r_1)\rho(r_1) Y_{\Lambda M}(\hat{r}_1)] [r_2^\Lambda \rho(r_2) Y_{\Lambda-M}(\hat{r}_2)] | ji \rangle,
\end{aligned}
\tag{3.7}
$$

where T is the kinetic energy and E_{coul} is the Coulomb energy,

$$
E_{coul} = \frac{1}{2} e^2 \int \int d^3 r_1 \, d^3 r_2 \frac{\rho_p(r_1)\rho_p(r_2)}{|r_1 - r_2|} - \frac{3}{4} e^2 \left(\frac{3}{\pi} \right)^{1/3} \int d^3 r \, [\rho_p(r)]^{4/3}. \tag{3.8}
$$

The various quantities N and M with subscripts are integrals involving the one-body densities (in the case of the N functions) or the nonlocal densities (the M functions). They are all fully defined in the Appendix E.

The local Hartree–Fock potential is

$$
\begin{aligned}
U_\tau(x) &= \sum_{\xi=a,r} \left\{ W_\xi f_{\alpha_\xi} \left[N_{\beta_\xi}(\beta_\xi + 1) + b_\xi \Delta_\tau N_{\beta_\xi} \right] \rho^{\beta_\xi}(x) \right. \\
&- W_\xi(\alpha_\xi/2) \left[f_{\alpha_\xi} \right]^2 \left[N_{\beta_\xi}^2 + b_\xi(\Delta N_{\beta_\xi})^2 \right] \rho^{\alpha_\xi - 1}(x) \\
&- W_\xi f_{\alpha_\xi} \beta_\xi \left[G_{\beta_\xi}(x) + b_\xi G_{\beta_\xi}^{pp}(x) + b_\xi G_{\beta_\xi}^{nn}(x) \right] \rho^{\beta_\xi - 1}(x) \\
&+ W_a(\alpha_\xi/2)[f_{\alpha_\xi}]^2 M_{\beta_\xi} \rho^{\alpha_\xi - 1}(x)
\end{aligned}
$$

$$
\begin{aligned}
&+ \; W_\xi b_\xi \beta_\xi f_{\alpha_\xi} \left[\Delta N_{\beta_\xi} \right] \rho^{\beta_\xi - 1}(x) \delta\rho(x) \\
&+ \; W_\xi (\alpha_\xi/2) \left[f_{\alpha_\xi} \right]^2 \left(b_\xi \left[M^{pp}_{\beta_\xi} + M^{nn}_{\beta_\xi} \right] + a_\xi \left[M^{pn}_{\beta_\xi} + M^{np}_{\beta_\xi} \right] \right) \rho^{\alpha_\xi - 1}(x) \\
&- \; W_\xi a_\xi f_{\alpha_\xi} \beta_\xi \left[G^{pn}_{\beta_\xi}(x) + G^{np}_{\beta_\xi}(x) \right] \rho^{\beta_\xi - 1}(x) \Big\} \\
&+ \; 2 k N_d \nabla^2 \rho(x) - \frac{3}{2} (\nabla^2 \rho(x))^2,
\end{aligned}
\tag{3.9}
$$

where the functions $G(x)$ are defined in the Appendix E. The nonlocal Hartree–Fock potential is

$$
\begin{aligned}
\mathcal{U}_\tau(x, x') \phi_b(x) \;=\; & -\sum_{\xi=a,r} \Big\{ W_\xi f_{\alpha_\xi} \rho(x, x') \rho^{\beta_a}(x) \rho^{\beta_a}(x') \\
& + \; W_\xi b_\xi f_{\alpha_\xi} \rho_\tau(x, x') \rho^{\beta_\xi}(x) \rho^{\beta_\xi}(x') \\
& + \; W_\xi a_\xi f_{\alpha_\xi} \rho_{\bar{\tau}}(x, x') \rho^{\beta_\xi}(x) \rho^{\beta_\xi}(x') \Big\} \phi_b(x'),
\end{aligned}
\tag{3.10}
$$

and the state-dependent spin-orbit term is

$$
U_{so}(x) \phi_b(x) = c \left(\frac{1}{x} w_b \frac{\partial \rho(x)}{\partial x} - \frac{1}{x} \frac{\partial \rho_w(x)}{\partial x} - \frac{1}{x^2} \rho_w(x) \right) \phi_b(x).
\tag{3.11}
$$

The number w_b is a weight factor and the density $\rho_w(x)$ is the spin-orbit weighted density as defined in Appendix E.

This is just the potential which arises from the monopole force. As shown in Appendix A, the Hartree term due to the multipole forces is zero for closed-shell nuclei and the exchange term is assumed to be negligible for the purposes of calculating the mean-field. In addition, the Coulomb potential is

$$
U_{coul}(r) = e^2 \int d^3 r' \frac{\rho_p(r')}{|r - r'|} - e^2 \left(\frac{3}{\pi} \right)^{1/3} \rho_p^{1/3}(r).
\tag{3.12}
$$

3.3.2 Density dependence

Having decided to try to find a force which was *separable* and *density-dependent*, the most obvious choice seemed to be a term of the form $\sim \rho^\beta(r_1)\rho^\beta(r_2)$. Perhaps a form like this with $\beta = 1$ would be the most obvious choice, but parameters need to be included to give one the degrees of freedom necessary to fit nuclei. A term like this, with just a constant strength, has the problem that its contribution to the total energy goes roughly as A^2 not A, so it does not provide saturation of the energy. Furthermore, the direct term it gives in the HF potential has a coefficient which varies wildly across the nuclear chart, whereas it is known that the nuclear density and the depth of the single-particle potential is quite independent of A, so density-dependent HF potential should have largely A-independent coefficients,

as one finds with the successful Skyrme potential[21]. The reason for this too-strong dependence is that the direct energy of a separable force is always going to have the *square* of an integral of some function of the density, which in the present case is roughly proportional to A, when it would be preferable to have just one such function. The remedy is to include in the coefficient to the term a function which looks like one of these integrals and has a parameter which can be made, more-or-less, to cancel it out. Whence the f parameter,

$$f \sim \frac{1}{\int \rho^{\alpha}(x) d^3 x},$$ (3.13)

which cancels one of the two factors of the N integral in the energy

$$N \sim \int \rho^{1+\beta}(x) d^3 x.$$ (3.14)

In the direct HF potential, there is one factor of f and one of N so setting $1 + \beta = \alpha$ gives an A-independent coefficient to the density function in the mean-field which enables one to fit the whole range of nuclei with similar depths of the mean-field potential and similar central densities. The possibility exists to vary the condition $\alpha = \beta + 1$ to change the fit, but only small variations away from this turn out to produce anything sensible.

Some considerable effort was taken to try to fit a one-termed force of this form to a wide range of nuclei. By one-termed it is meant that the force consisted only of the kinetic, and Coulomb terms plus a one-termed potential of the form of the first line in Equation (3.1) without the second line. Although it was possible to fit the properties of a single nucleus this way, no overall parameterization presented itself, so a modification of the force was necessary. So far there is a term with a negative strength which, in the mean field, goes as $U(x) \sim \rho(x)$. A hint was taken from the Skyrme-like forces, which, as well as the leading term (proportional to t_0 – see [21]) have a extra term with an overall positive (i.e. repulsive) strength and a higher power of the density (the term proportional to t_3. Therefore, an extra term in the separable potential, like the first, but with its own set of α, β and strength (W) parameters is added. This is second line of Equation(3.1).

3.3.3   Isospin-dependence

Without this term there is nothing in the force which accounts for the different physics which arises in nuclei with extreme values of isospin. The necessity for such and effect has been known for a long time, which is reflected in the earliest semi-empirical mass formulæ[76] by the inclusion of the asymmetry term. The conventional choice for introducing isospin-dependence in a two-body interaction is to add a term with the operator $\tau_1 \cdot \tau_2$ or equivalently the isospin projection operator P^{τ}. In the present case there is a slightly generalized form of the operator $\tau_1 \cdot \tau_2$.

The isospin matrices are just the Pauli spin matrices

$$\tau_\xi = \begin{pmatrix} 0 & 1 \\ 1 & 0 \end{pmatrix} \qquad \tau_y = \begin{pmatrix} 0 & -i \\ i & 0 \end{pmatrix} \qquad \tau_z = \begin{pmatrix} 1 & 0 \\ 0 & -1 \end{pmatrix} \tag{3.15}$$

and the isospin operator is

$$\mathbf{t} = \frac{1}{2}\boldsymbol{\tau}$$

the action of which on proton and neutron states is

$$t_z|p\rangle = -|p\rangle, \qquad\qquad t_z|n\rangle = |n\rangle. \tag{3.16}$$

One can define raising and lowering operators which have the following properties:

$$t_+|p\rangle = |n\rangle, \qquad\qquad t_-|n\rangle = |p\rangle, \tag{3.17}$$

with other operations zero:

$$t_-|p\rangle = t_+|n\rangle = 0. \tag{3.18}$$

These operators can be expressed in terms of the operators t_ξ, t_y and t_z as

$$t_+ = t_\xi + it_y, \qquad\qquad t_- = t_\xi - it_y, \tag{3.19}$$

and the reverse relations are

$$t_\xi = \frac{1}{2}(t_+ + t_-), \qquad\qquad t_y = \frac{1}{2i}(t_+ - t_i). \tag{3.20}$$

Now rewrite the operator $\tau_1 \cdot \tau_2$

$$\begin{aligned}
\tau_1 \cdot \tau_2 &= 4t_1 \cdot t_2 \\
&= t_{1x}t_{2x} + t_{1y}t_{2y} + t_{1x}t_{2z} \\
&= (t_{1+} + t_{1-})(t_{2+} + t_{2-}) - (t_{1+} - t_{1-})(t_{2+} - t_{2-}) + 4t_{1z}t_{2z} \\
&= 2(t_{1+}t_{2-} + t_{1-}t_{2+}) + 4t_{1z}t_{2z} \\
&= 2(\tau_1^+\tau_2^- + \tau_1^-\tau_2^+) + \tau_{1z}\tau_{2z},
\end{aligned} \tag{3.21}$$

where the τ raising and lowering operators are the same as those for t (3.17) – i.e. they turn proton states in to neutron states and vice versa with no extra factor.

Generalizing this to allow different parameters for the first two terms and the last term allows one to have a force which breaks isospin symmetry, which is to say the p-p, n-n and n-p forces are not necessarily the same strength. The factor multiplying the density-dependent terms is then

$$(1 + a_\xi(\tau_1^+\tau_2^- + \tau_1^-\tau_2^+) + b_\xi\tau_{1z}\tau_{2z}), \tag{3.22}$$

with $\xi = a, r$ for the attractive and repulsive terms respectively.

Having this more general isospin operator gives one more degrees of freedom in fitting the force. Some modern realistic forces break isospin symmetry, such as the Argonne $v18$[6] potential and CD-Bonn[63], which they do because it fits the experimental data better[64]. In an effective interaction, then, one should not be afraid of doing so.

3.3.4   Surface Term

The force as constructed so far depends only on the magnitude of the density in the vicinity of the interacting nucleon. This means that the force is much weakened for nucleons at the surface, over the region where the density is dropping. The surface, however, ought to play an important part in the interaction since it is the weakly bound nucleons which must take part in most scattering events. The form of the surface term is chosen to be a derivative of the density since this will be peaked at the surface. The separable form was again chosen so that the perturbation theory matrix elements would be suitably small and the Laplacian operator was chosen so that each one-body function in the separable force would be a scalar.

3.3.5   Multipole terms

The reasons for including a multipole terms have been mentioned already. The particular form is that of the well-known separable multipole forces except that a density-dependence is added to allow the force to be used in an HF calculation in the full space.

3.4   Choosing parameters – Experimental observables

The parameterization of the force is chosen in a way that, it is hoped, may lend itself to the description of nuclear properties. The criterion, then, for choosing the parameters is to find the set which fits observable data the best. The function which describes the quality of the fit is the *Chi-squared* function which is defined as

$$\chi^2(C_1 \cdots C_N) = \sum_i^N \frac{(C_i - X_i)^2}{e_i^2}, \tag{3.23}$$

where i sums over all the observed quantities, C_i is the calculated values of the observable, X_i is the experimental value and e_i is the error in the experimental value, so that the better-known observables are given greatest weight.

3.4.1   Nuclei

To explore this separable interaction, a spherical HF code, which can be used with closed shell nuclei, has been written. In addition it provides a basis in which perturbation theory calculations may be performed. Only a few nuclei are truly spherical but it makes sense when developing a new interaction to begin with the computationally more simple cases and proceed to more difficult calculations only when one has shown the simple cases work. The nuclei taken in the fit in this work

nucleus	^{16}O	^{34}Si	^{40}Ca	^{48}Ca	^{48}Ni	^{56}Ni	^{68}Ni	^{78}Ni
Z	8	14	20	20	28	28	28	28
N	8	20	20	28	20	28	40	50

nucleus	^{80}Zr	^{90}Zr	^{100}Sn	^{114}Sn	^{132}Sn	^{146}Gd	^{208}Pb
Z	40	40	50	50	50	64	82
N	40	50	50	64	82	82	126

Table 3.1: *Nuclei included in fit*

are shown in table 3.4.1. Most of the numbers N and Z for the nuclei considered are generally considered to be magic. 40 is typically seen to be a shell closure (the fp shell) but the next state ($g_{9/2}$) lies very close above it; there is not a large shell gap. 14 is not usually considered to be a magic number, but the spin-orbit splitting between the first p-states in light nuclei is quite large so that it is a good closed sub-shell. The same is true of 64 as of 14 where the splitting between the d states provides a sub-shell closure and a moderate gap.

Data for these nuclei, as described in the next section are given in Chapter 7, in which the comparison of calculated and experimental properties is discussed.

3.4.2 Observables

The following observables are used in the fit:

- Ground state binding energy.

  The mass, M, of a nucleus is

  $$M(Z, N) = Zm_H + Nm_n - B(Z, N)/c^2. \tag{3.24}$$

  It is smaller than the mass of its isolated constituents, Z hydrogen atoms and N neutrons by an amount known as the binding energy. It is the energy of the interaction of the nucleons and is always positive for a bound nucleus. It is related to the *energy* E(Z, N) by the relation

  $$E(Z, N) = -B(Z, N). \tag{3.25}$$

  E is the quantity evaluated in quantum mechanics as the expectation value of the total Hamiltonian of the system of Z protons and N neutrons bound in the nucleus. It is the most reliable observable for ground state properties since it can measured quite easily and the observed quantity is directly comparable to the calculated expectation value.

- Single particle energies

The single particle energies are not observables as such in that there is no operator which acts on the many-body wavefunction to give as its expectation value a single particle energy. Koopmans' theorem [65, 35] for density-independent Hartree-Fock theory shows that the difference in energy between a nucleus $E(N, Z)$ and a nucleus $E(N, Z-1)$ or $E(N-1, Z)$ is equal to the single particle energy of the nucleus which was removed. With a density dependent potential it is no longer true; the removal of a nucleon alters the density making the force change. This means that the remaining nucleons "re-arrange" themselves to find the new lowest-energy configuration. In addition, as pointed out by Brueckner and Goldman[68], once a particle is removed, its set of quantum numbers becomes available as an intermediate state to the remaining nucleons for scattering events which will results in perturbative corrections. In the present density-dependent HF calculation, the effect of a change in the ground state density is already taken into account so that for the least bound state there is no correction but the removal of more deeply bound states may cause a substantial correction. No calculation along these lines is made in the present case. A similar calculation by Köhler[69] shows that the correction for the least bound states is small but the correction to deeply bound states may be as much as several MeV.

Despite these caveats, energies and quantum numbers can be assigned to resonances seen in scattering experiments and the results of nuclear stripping or pickup reactions which tally with the expected single particle states predicted by mean-field models. Although the absolute values of experimental single particle energies can not be compared with density-dependent HF values exactly, at least the relative orderings may be.

- Form factors

  The form factor of a given density distribution is its Fourier transform:

$$F(\mathbf{q}) = \int d^3r \, e^{i\mathbf{k}\cdot\mathbf{r}} \, \rho(\mathbf{r}). \tag{3.26}$$

For spherically-symmetric charge distributions the expression reduces to

$$F(k) = 4\pi \int_0^\infty dr \, r^2 \, j_o(kr)\rho(r), \tag{3.27}$$

where $j_0 = \sin(x)/x$ is the zeroth order spherical Bessel function. The charge form factor $F_C(k)$ is related to the experimental electron scattering cross-section[66]

$$\frac{d\sigma}{d\Omega}(k) \propto |F_C(k)|^2. \tag{3.28}$$

The charge density differs from the proton density in that it accounts for the finite proton size. The prescription for doing this in the present work is to

fold the intrinsic proton density with the nuclear proton density which is approximated by a Gaussian fitted to the proton size. This method is the same as that used by Negele[67] except that he also considers a centre–of–mass correction. In Fourier space, the correction becomes a simple product of form factors. Given the assumption of a Gaussian form for the single proton density, the Fourier transform is also a Gaussian and is, with a numerical fit to the proton size,

$$F_\pi(k) \propto e^{-\frac{(0.65k)^2}{4}}.\qquad (3.29)$$

The charge form factor is then

$$F_C(k) = NF_p(k)F_\pi(k),\qquad (3.30)$$

and is normalized so that $F(0) = 1$.

- Radii

  The mean square radius associated with a density distribution is defined, for a spherical distribution, as

  $$\langle r^2 \rangle_q \equiv \frac{\int dr\, r^4 \rho_q(r)}{\int dr\, r^2 \rho_q(r)}.\qquad (3.31)$$

  The subscript q labels the density and could be an isospin number to give the proton or neutron densities, or a label to indicate that it is the charge density, or the total particle density. The root mean square (rms) radius is then defined as

  $$r_{rms,q} \equiv \sqrt{\langle r^2 \rangle_q}.\qquad (3.32)$$

  The rms radius of the charge density calculated using the interaction may be compared with that of the charge density calculated as the Fourier transform of the electron scattering form factor.

Chapter 4

Computational Implementation

4.1   HF equations in a Basis

The Hartree-Fock equations involve a self-consistency problem in that the potential in the one-body Schrödinger equation depends on the wavefunctions which result as a solution of the equation. The usual method of solution of the HF equations is an iterative procedure shown schematically in figure 4.1.

| 1 | Make an initial guess of the single particle wavefunctions |

| 2 | Construct new potential from wavefunctions and solve HF equation |

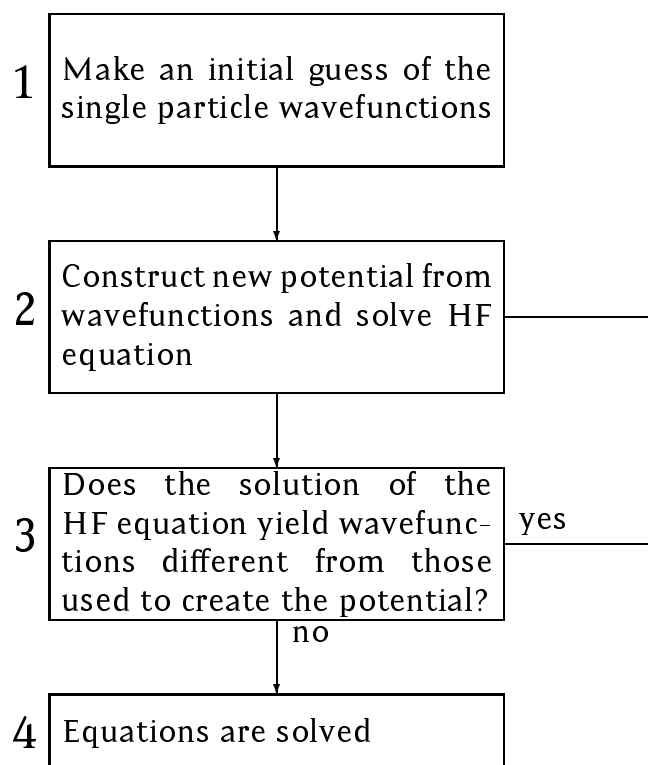| 3 | Does the solution of the HF equation yield wavefunctions different from those used to create the potential? | yes |

no

| 4 | Equations are solved |

Figure 4.1: *Schematic representation of the procedure for solving the HF equations*

Step 2 in Figure 4.1 is the one which can be difficult to accomplish. Constructing the potential from the wavefunctions can pose some difficulty since the potential includes the Fock (exchange) term which involves multidimensional integration for the functions denoted as M and G in the expression for the Hartree-Fock potential (E.91). In the case of spherical nuclei, the multidimensional integrals are never more than two-dimensional and are evaluated directly in coordinate space using the method of Gaussian quadrature[70].

The Hartree-Fock equations are integro-differential equations. The way they are usually solved it by either direct numerical solution on a grid, or expansion in a basis and the transformation to a matrix equation. In the present work it was found that the extremely non-local character of the potential, as well as the strong density-dependence, makes the first technique numerically unstable so the second method was used.

To solve the Hartree-Fock equations by basis expansion, a basis is chosen which is taken to be the simple harmonic oscillator. The choice of the oscillator is taken because the eigenstates are analytically calculable and matrix elements of simple functions (such as the kinetic energy) are already known. One proceeds by expanding a Hartree-Fock wavefunction, φ_a, in a truncated basis of harmonic oscillator wavefunctions, ϕ_β,

$$\varphi_a(x) = \sum_\beta C_{a\beta} \phi_\beta(x), \tag{4.1}$$

where a represents all the quantum numbers of the HF state and β represents all the quantum numbers of the harmonic oscillator state. x represents all relevant coordinates (including spin and isospin).

The symmetries of the problem are included in the basis wavefunctions. The spherically symmetric harmonic oscillator wavefunctions are used and the HF wavefunctions are assumed to have the same symmetries:

$$\begin{aligned}
\varphi_a(x) &= \mathcal{R}_{N_a j_a l_a}(x)\, \mathcal{Y}_{j_a l_a m_a}(\hat{x})\, \xi_{\tau_a} \\
&= \sum_{n_\alpha} C^{(lj\tau m)a}_{N_a n_\alpha} R_{n_\alpha l_\alpha}(x)\mathcal{Y}_{j_\alpha l_\alpha m_\alpha}(\hat{x})\xi_{\tau_\alpha}\delta_{l_a l_\alpha}\delta_{j_a j_\alpha}\delta_{m_a m_\alpha}\delta_{\tau_a \tau_\alpha},
\end{aligned} \tag{4.2}$$

where the relevant quantum numbers are written out in full. Here, the function $\mathcal{R}$ is the radial part of the HF wave function and the function R is the radial part of the oscillator wave function (see Appendix D). The rest of the wave function is kept the same in the two representation in Equation (4.2) so the HF wavefunctions are only, in fact, expanded in the principle quantum number. Rather then always make this explicit, the expansion coefficients may be more frequently written in the more compact form (4.1). The functions ξ are isospinors and $\mathcal{Y}$ are spinor-spherical harmonics, which are the tensor product of a spherical harmonic and a spinor:

$$\mathcal{Y}_{ljm_j} = \sum_{m_l m_s} \langle lm_l 1/2m_s | jm_j \rangle Y_{lm_l}\chi_{1/2m_s}. \tag{4.3}$$

Note that this basis expansion provides a convenient way to choose the initial wavefunctions in step 1 – they may be taken as the harmonic oscillator functions. Now consider the Hartree-Fock equation from appendix A (A.6)

$$\epsilon_i \varphi_i(x) = \left[-\frac{\hbar^2}{2m} \nabla^2 + u(x) + \int dy \rho(y) v(x,y) \right] \varphi_i(x) - \int dy \rho(x,y) v(x,y) \varphi_i(y). \quad (4.4)$$

This general HF equation does not explicitly include the rearrangement potential, since the form of the contribution of the rearrangement term to the HF local and non-local potentials depends on the exact form of the interaction. However, it is known from appendix E that the rearrangement potential for the interaction under study contributes local and non-local terms in just the form of the above equation with different integrands. Therefore the results that follow will hold true for a density-dependent interaction also, with suitable values of the local and nonlocal HF potentials.

One inserts the relation (4.1) into the above HF equation (4.4):

$$\epsilon_i \sum_\beta C_{\beta i} \phi_\beta(x) = \left[t(x) + u(x) + \int dy \rho(y) v(x,y) \right] \sum_\beta C_{\beta i} \phi_\beta(x)$$

$$- \int dy \rho(x,y) v(x,y) \sum_\beta C_{\beta i} \phi_\beta(y), \quad (4.5)$$

and acts at the left with $\int dx \phi_\alpha^*(x)$, to give

$$\epsilon_i \sum_\beta C_{\beta i} \int dx \phi_\alpha^*(x) \phi_\beta(x) = \int dx \phi_\alpha^*(x) \left[t(x) + u(x) + \int dy \rho(y) v(x,y) \right] \sum_\beta C_{\beta i} \phi_\beta(x)$$

$$- \int dx \phi_\alpha^*(x) \int dy \rho(x,y) v(x,y) \sum_\beta C_{\beta i} \phi_\beta(y)$$

$$\epsilon_i C_{\alpha i} = \sum_\beta h_{\alpha\beta} C_{\beta i}, \quad (4.6)$$

which is of the form of a matrix-eigenvalue equation

$$hC = \epsilon C, \quad (4.7)$$

in which **h** is the matrix whose elements are those of the HF Hamiltonian evaluated between the oscillator basis states and **C** is the matrix of expansion coefficients of the HF wavefunctions in terms of the harmonic oscillator wavefunctions. The Hartree-Fock equations written in this way are also called Roothan's equations[71]. The procedure described in Figure 4.1 is implemented then by making an initial guess for the matrix **C**. This then enables one to calculate the densities with which the matrix **h** is calculated. The matrix **h** is diagonalised to yield eigenvectors, **C**' and eigenvalues ϵ . If the new set of eigenvectors **C**' equal

the old set **C** then the problem is solved. In practice, the quantity which is checked for convergence is the Hartree-Fock energy.

Owing to the symmetries in (4.2), the Hamiltonian matrix **h** is in block-diagonal form with sub-matrices labelled according to the quantum numbers j, l, and τ. This is a great aid in calculation since it requires only the diagonalisation of small matrices.

4.1.1 Calculation of densities

To evaluate the HF field and energy, one must obtain the spatial density. Since this density depends upon the HF wavefunctions, it can be represented in terms of the harmonic oscillator wavefunctions:

$$
\begin{aligned}
\rho(x) &= \rho_p(x) + \rho_n(x), \\
\rho_{p,n}(x) &= \sum_{a<\epsilon_F \in p,n} \varphi_a^*(x)\varphi_a(x) \\
&= \sum_{a<\epsilon_F \in p,n} \sum_{\alpha\beta} C_{a\alpha}^* C_{a\beta} R_{n_\alpha l_\alpha}(x) R_{n_\beta l_\beta}(x) \mathcal{Y}_{l_\alpha j_\alpha m_\alpha}^*(\hat{x}) \mathcal{Y}_{l_\beta j_\beta m_\beta}(\hat{x}) \delta_{l_\alpha l_\beta} \delta_{j_\alpha j_\beta} \delta_{m_\alpha m_\beta} \\
&= \sum_{a<\epsilon_F \in p,n} \sum_{n_\alpha n_\beta} \sum_{ljm} C_{a\alpha}^* C_{a\beta} R_{n_\alpha l}(x) R_{n_\beta l}(x) \mathcal{Y}_{ljm}^*(\hat{x}) \mathcal{Y}_{ljm}(\hat{x}) \\
&= \sum_{a<\epsilon_F \in p,n} \sum_{n_\alpha n_\beta} \sum_{lj} C_{a\alpha}^* C_{a\beta} \frac{2j+1}{4\pi} R_{n_\alpha l}(x) R_{n_\beta l}(x), \quad\quad (4.8)
\end{aligned}
$$

assuming all the m-sub-states for each j-shell are filled. Note that each single-particle wavefunction exhibits a $(2j+1)$-fold degeneracy.

The fact that the density is represented in an analytic form is a great help when it comes to evaluating the derivative of the density since the derivative of the oscillator function is itself an analytic expression (See Appendix D).

4.2 Perturbation Corrections

The expressions for the perturbation corrections to the energy may also be simplified due to the assumption of spherical symmetry. This reduction is more involved than for the densities and is presented in Appendix F .It is the expressions derived in that Appendix which are directly computed and presented in Chapter 7.

4.3 Convergence in basis expansion

If the HF wavefunctions were expanded in an infinite basis then solving the matrix equation would be exactly equivalent to solving the Schrödinger equation. It is,

of course, impossible to solve an infinite-dimensional matrix eigenvalue problem so the basis must be truncated at some value of principal quantum number – the truncation in other quantum numbers is governed by the observed single-particle states. It is thus necessary to understand the effects of such a truncation on the physical results of the HF problem. Related to this is the fact that the oscillator basis expansion is characterized by a size parameter b (see Appendix D), or equivalently its energy quantum $\hbar\omega$. In a finite basis expansion the choice of b will affect the results since for one value of b the fraction of the HF wavefunctions which overlap with oscillator states outside the space will be different from that for another value of b. The prescription taken in this work is that since a variational principle is at play, the parameter b is treated as an extra variational parameter. For a given calculation, only a global b is chosen, whereas in some previous work each single particle state is given the oscillator parameter which produces the largest overlap with the actual wavefunction[67]. The justification for using a single parameter is that the convergence properties as a function of basis size seem to be good enough so introducing more b parameters would only result in a more complicated calculation.

Since it is desirable to apply this theory to all nuclei, including those which are weakly bound and have extended wavefunctions, and also since the perturbation theory calculation involves the use of excited and continuum wavefunctions, consideration must also be taken into account of the extent to which it is possible to represent the wavefunctions of unbound single particles, i.e. plane wave-like states, as an expansion in terms of eigenstates of an infinite potential, which produced only bound states.

4.3.1 Truncation effect in Hartree-Fock

Figures (4.2) and (4.3) show the Hartree-Fock energy for a sample parameterization of the force used to calculate the nucleus ^{40}Ca as a function of the oscillator size parameter, b, and the number of principle quantum numbers, N, in the expansion. The first plot shows that as one adds more states, the dependence on b becomes much flatter. This is to be expected since in the limit of an infinite expansion, the set of oscillator states forms a complete set no matter what the size parameter is. One also sees from Figs. (4.2) and (4.3) that the minimum occurs at different values of b as the size of the space is increased. The second figure shows more detail for the cases with larger N. In this plot one gets a view of the convergence of the HF energy with increasing space size and sees the rather complicated structure in the dependence of the energy on b. For the larger space sizes one observes secondary minima which, as one varies parameters, can take over as the true minimum.

The convergence of the Hartree-Fock energy as a function of space size is shown numerically in Table (4.1). The third column shows the pleasing result that as one adds more and more states in the basis expansion, the change in the HF results
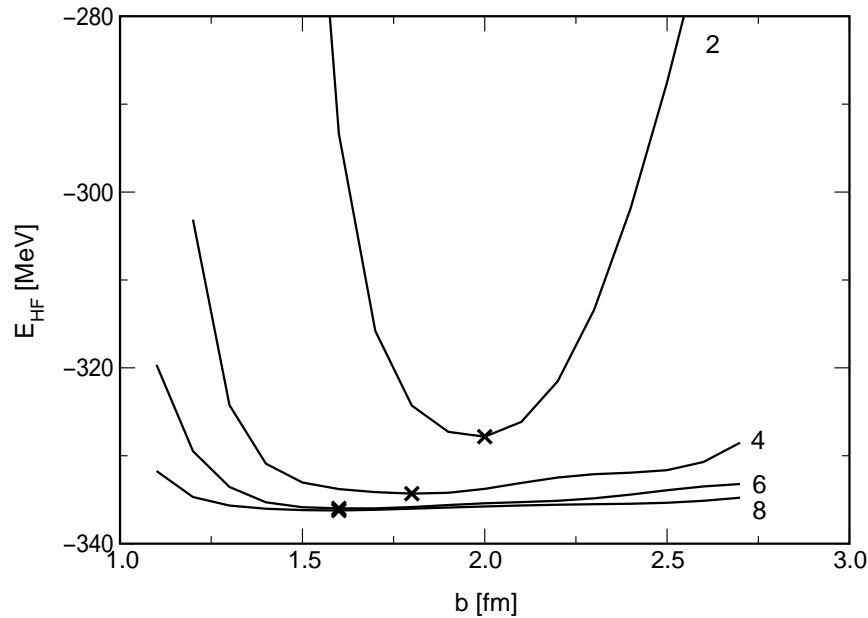
Figure 4.2: *Hartree-Fock energy, E_{HF}, as a function of oscillator parameter, b, for different Hilbert space sizes in ^{40}Ca. The crosses indicate the minima. The numbers on the plot show the size of the principal quantum number space.*

become less and less. Also shown is the convergence of the second order energy correction as a function of space size. This also converges to six significant figures by the time 20 states are reached, but as one sees from the last column, the convergence is somewhat slower than for the HF energy. This convergence is represented graphically in Figure 4.4.

4.3.2 Representation of continuum states

In HF calculations of nuclei around the valley of stability the continuum states play a rather small part. As one moves away from the valley of stability very weakly bound and extended states become occupied and need to be well represented numerically for a faithful calculation. When calculating correlations in perturbation theory one scatters particles into highly excited states of positive energy so the representation of these states is particularly important for perturbation calculations. These positive energy states are similar to plane waves and one would not naturally try and expand a plane wave in an oscillator basis were it not for the bound states being well represented in the expansion. It is only necessary for the wavefunctions to be well represented over the region of the nucleus since
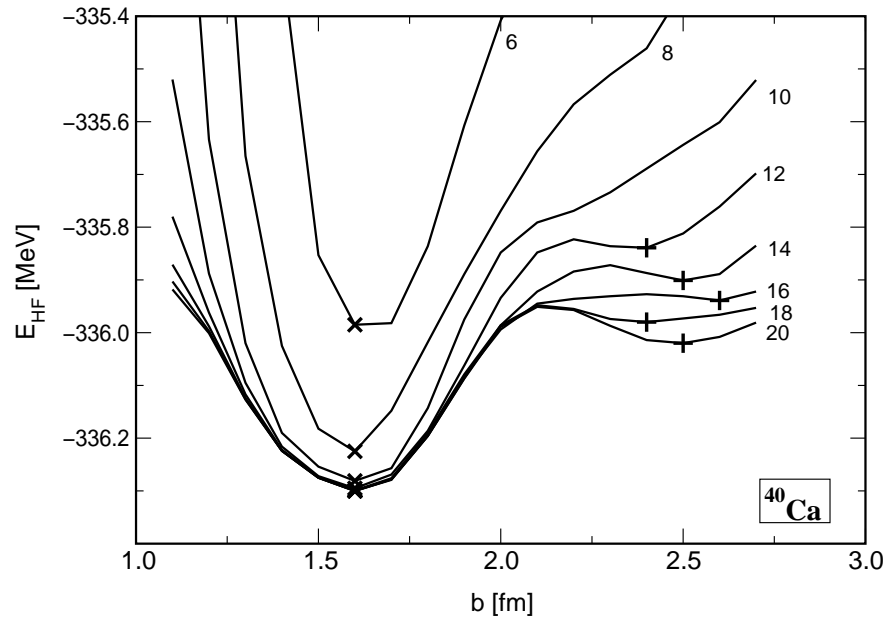
Figure 4.3: *Hartree-Fock energy as a function of oscillator parameter and size of Hilbert space for ^{40}Ca. The crosses indicate the global minima, while the pluses indicate local minima in the larger spaces, whose sizes are indicated by the numbers to the right of the lines.*

the matrix elements of the potential outside disappear very rapidly thanks to the density-dependence. In figure 4.5 some positive energy s-states are shown in the largest nucleus considered, ^{208}Pb, along with fitted plane wave states and the density profile on the same scale. As one can see all these states are well represented over the region of the nucleus.

4.4 Parameterization

As discussed in the previous chapter, the parameters are chosen to minimized a χ^2 function. This procedure was partially automated through the use of *MINUIT*[72], a minimization package which is part of the CERN libraries. The results obtained in this way were used as a guide to regions of parameter space where reasonable fits may be found, which are then obtained by hand.

Since it is assumed that the bulk of the binding energy comes from the HF mean field, and to ensure calculation in a reasonable time, the parameters are fitted first in the HF approximation. The calculation of the correlation effects then

Size of space, N	E^{HF} [MeV]	$|E_N^{HF} - E_{N-2}^{HF}|/E_N^{HF}$	$E^{(2)}$ [MeV]	$|E_N^{(2)} - E_{N-2}^{(2)}|/E_N^{(2)}$
2	-327.833	–	-0.80203	–
4	-334.318	0.019430	-0.98778	0.188047
6	-335.990	0.004976	-1.02875	0.039825
8	-336.230	0.000713	-1.03501	0.006917
10	-336.286	0.000166	-1.03683	0.001755
12	-336.300	0.000041	-1.03691	0.000077
14	-336.304	0.000011	-1.03704	0.000125
16	-336.305	0.000002	-1.03702	0.000019
18	-336.305	0.000000	-1.03701	0.000008
20	-336.305	0.000000	-1.03701	0.000000

Table 4.1: *Convergence of Hartree-Fock energy and second order energy correction as a function of size of basis expansion*

in principle would require the re-fitting of the force, but since the perturbation corrections to the energy are found to be smaller than deviations from experiment, re-fitting was not important.

Details of changes in observables as a function of the parameters are presented in the next chapter, which serves as a guide to fitting nuclear properties as well as being an exposition of the character of the force.

4.5 Centre-Of-Mass Correction

The nucleus in a Hartree-Fock calculation is centred on the mean-field. In reality, the nucleus is not localised and this anomaly in the HF calculation can lead to a significant error, especially in light nuclei. Several different techniques are used in the literature to compensate for this error(see Appendix E of Ref. [73]). In this work no such correction is undertaken since the philosophy of the present technique would suggest that this effect should be treated in the framework of perturbation theory. In this first calculation of the present interaction, only the straightforward evaluation of the lowest order vacuum amplitude diagrams is undertaken.
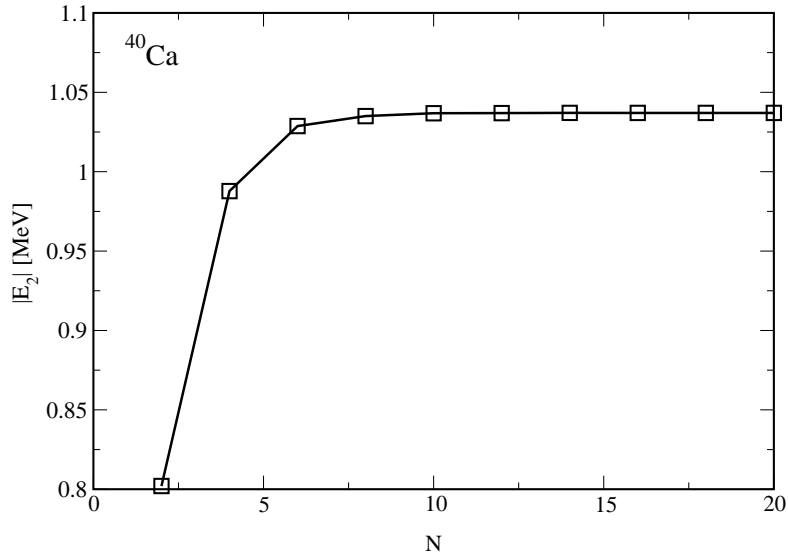
Figure 4.4: *Second order energy correction as a function of number of principal quantum numbers,* N, *in basis expansion, for* ^{40}Ca.
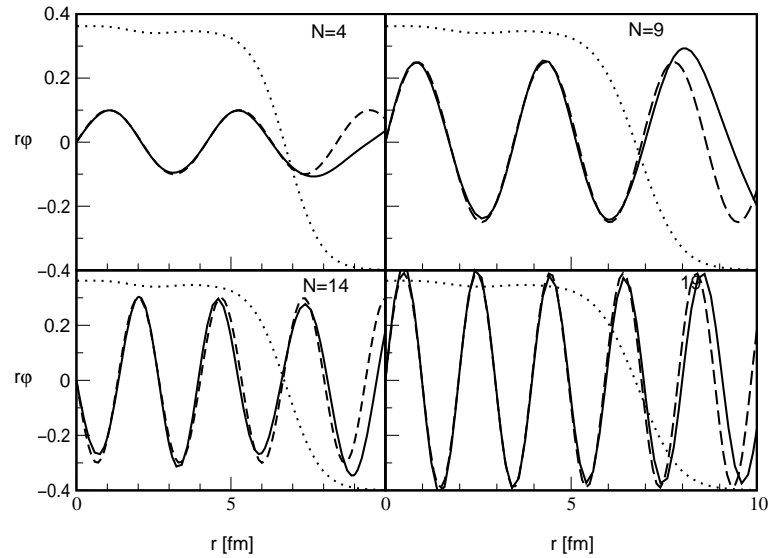

Figure 4.5: *Positive energy single particle* s-*states in* ^{208}Pb *up to the* 20th s-*state* $(N = 19)$ *for a calculation with 20 radial states per angular momentum state.*

Chapter 5

Nuclear Force: Results

This chapter shows results of HF and perturbation theory calculations for a typical set of parameters for some quantities of interest. Is does not show a comprehensive set of observables for all the nuclei under consideration with a comparison to data – that is the domain of chapter 7. Here the numerical properties of the force are examined in the region of parameter space, as explored during the process of fitting to finite nuclei, which produces a reasonable fit to give an overview of the character of the force in a quantitative way and as an aid to using the force and choosing and varying parameters.

5.1 Monopole Interaction

5.1.1 Contributions to the HF Energy

The Hartree–Fock Energy is (see Appendix E):

$$
\begin{aligned}
E_{HF} \;=\;\; & T + E_{coul} + \sum_{\xi=a,r} \left\{ \frac{1}{2} W_\xi f_{\alpha_\xi} N_{\beta_\xi}^2 - \frac{1}{2} W_\xi f_{\alpha_\xi} M_{\beta_\xi} \right. \\
& + \;\frac{1}{2} W_\xi b_\xi f_{\alpha_\xi} (\Delta N_{\beta_\xi})^2 - \frac{1}{2} W_\xi f_{\alpha_\xi} \left[b_\xi M_{\beta_\xi}^{(\tau\tau)} + a_\xi M_{\beta_\xi}^{(\tau\bar\tau)} \right] \left. \right\} \\
& + \;\frac{1}{2} k N_d^2 - \frac{1}{2} k M_d + c N_w .
\end{aligned}
\tag{5.1}
$$

The terms in (5.1) are labelled for discussion, term by term in the order of appearance, as the *kinetic energy*, *Coulomb* (which consists of a direct and exchange term), *direct* (attractive and repulsive), *exchange* (att. and rep.), *iso-direct* (att. and rep.), *iso-exchange* (which splits into *iso-exchange-a* and *iso-exchange-b*, both with attractive and repulsive parts), *derivative direct*, *derivative exchange* and *spin-orbit*.

Figure 5.1 shows the contribution to the Hartree-Fock energy per particle, η, from the various terms of the *attractive* monopole force and Figure 5.2 shows the
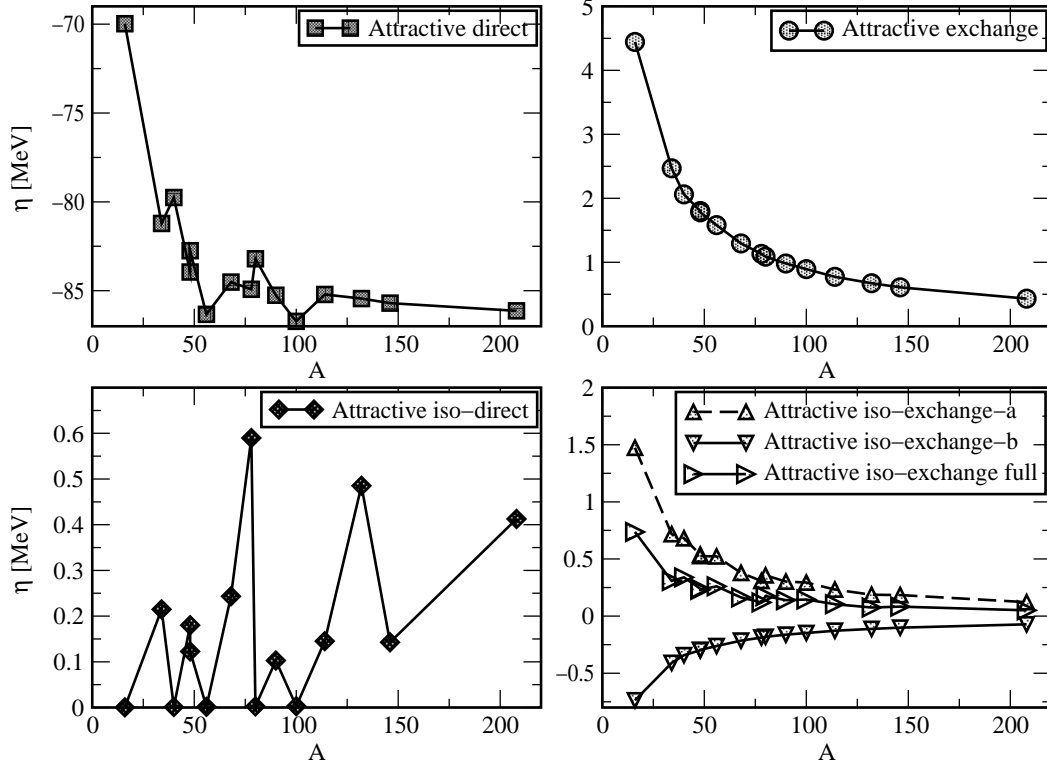
Figure 5.1: *Contributions to the HF energy, η, from the "attractive" parts of the monopole potential*

analogous contributions from the *repulsive* terms. Note the scales are such that the zero does not appear on every frame. The numbers for these two figures are combined in Figure 5.3 to show the total contribution, attractive plus repulsive, from the various components of the monopole force. In this, as in all figures which show a quantity as a function of A, the data points are for the nuclei mentioned in Chapter 3. In particular, there are two nuclei with $A = 48$ in each plot, so a sudden jump at $A = 48$, in those plots in which it occurs, is just a reflection of this.

There are several points to note. Firstly, the attractive parts of the force are always larger in magnitude than the repulsive parts, and follow the same A-dependence. The first part of this statement clearly must be true if the force is to be binding. The fact that the A-dependence is the same, i.e. the peaks and changes of direction appear in the curve in just the same places for both the attractive and repulsive terms, means that the sum of the two also has the same A-dependence.

The isospin-dependent direct interaction has a vanishing contribution to the $N = Z$ nuclei as it must since it depends on the isovector density $\delta\rho = \rho_p - \rho_n$. The
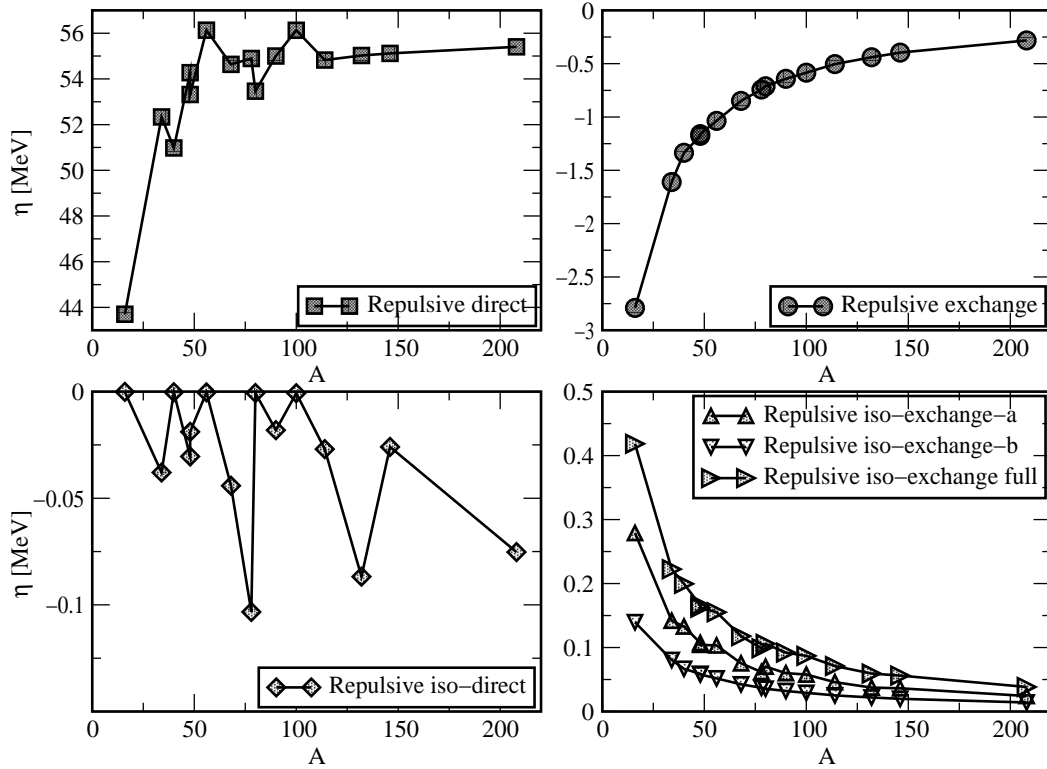
Figure 5.2: *Contributions to the HF energy, η, from the "repulsive" parts of the monopole potential*

contributions to the total energy from this term are much smaller than from the isospin-independent term partly due to the small isovector density, and also due to the fact the b parameters are usually fitted to be < 1. The exchange parts of the isospin-dependent force, on the other hand, *do* contribute to all nuclei and are on the same scale as the isospin-independent exchange since they depend on the same density matrices. The exchange terms are also notable for their smoothness – both the isospin -dependent and -independent terms have smooth A-dependence which approaches zero as A increases. In the next chapter it is shown that the exchange energy is zero in nuclear matter.

The contributions from the other terms in the potential are shown in Figure 5.4. The most significant contribution here is from the Coulomb term, about which there is little to say since it is a well known force with parameters not open for fitting. One can see the trend of increasing contribution to the energy per particle as A increases, with downward lines in the isotopic chains of calcium, nickel, zirconium and tin, as one would expect. In the exchange term one also sees the isotopic chains clearly forming straight lines. The derivative term has
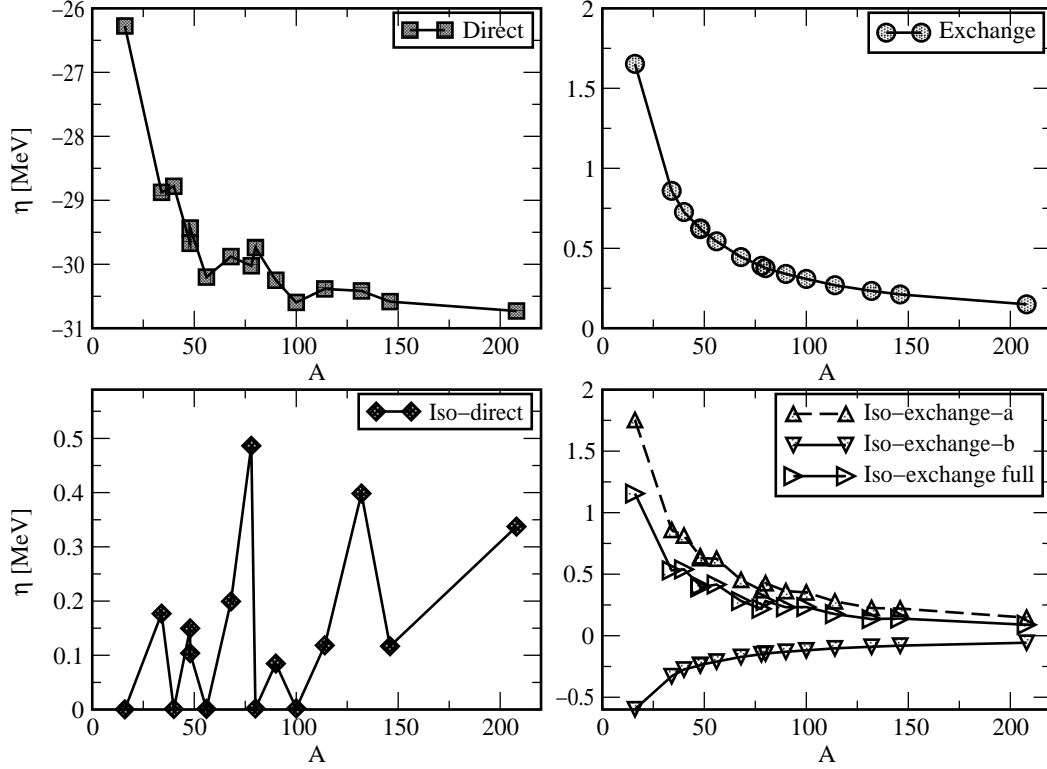
Figure 5.3: *Sum of contributions to the HF energy, η, from the attractive and repulsive parts of the monopole interaction.*

only the direct term calculated since the exchange term is rather too complicated. The sign of the parameter necessary to give correct single particle properties leads to a positive contribution to the Hartree-Fock energy, which is quite small, but not insignificant. The spin-orbit force is nearly zero for those nuclei in which the spin-orbit-split pairs are all fully occupied. The deviation from zero is due to the fact that the wavefunctions in the states of different j are not quite the same. For those nuclei which are not spin-orbit saturated there is a general trend of decreasing contribution with higher A, indicative of the fact that the force only contributes to the binding from a few states near the Fermi surface. The magnitude of the contribution is rather small and is fixed not by the binding energy, but to the spin-orbit splitting of the single particle energies.

5.1.2 Variation of monopole force parameters

Starting from a set of parameters used in the previous section, which is the result of a typical fit to the data, one may consider the act of singly varying any of the
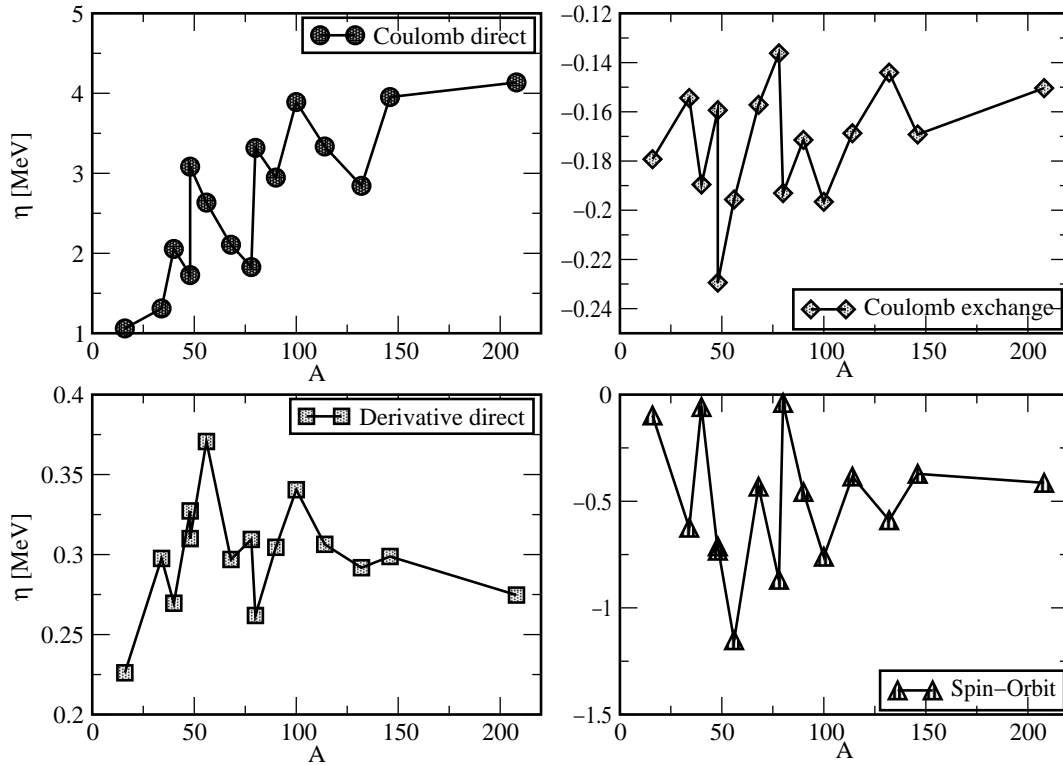
Figure 5.4: *Contributions to the HF energy, η, from the Coulomb, gradient and spin-orbit terms.*

parameters to examine the effect of each of them separately. Having observed that the attractive and repulsive forces give canceling contributions which have the same A-dependence, it suffices to look at varying the attractive parameters alone, since varying the repulsive parameters will just give the same results with opposite sign.

α_a **and** α_r

The α parameters enter the HF energy through the f functions (see Equation (3.2)) which appear in all the terms of the monopole force, except for the derivative term. In the HF potential, as well as through the f parameters, there are terms whose x-dependence is specifically α-dependent.

Taking a small increase in α_a, from 2.0 to 2.01 one sees a slight *increase* in the parameter f_{α_a} so from the action of this quantity alone one would expect an increase in the HF energy due to the strengthening of the attractive force and a deepening of the HF potential. On the other hand, the terms in the potential
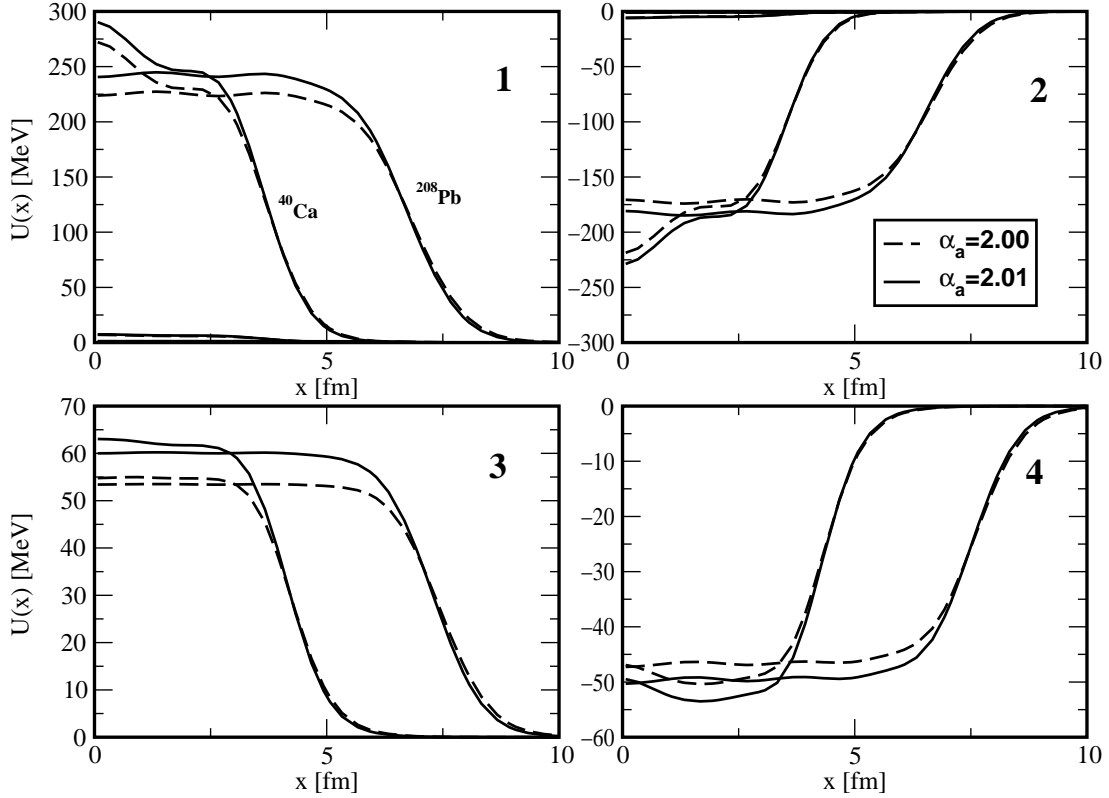
Figure 5.5: *Action of the variation of α_a upon various contributions to the HF potential, $U(x)$, in light and heavy nuclei (^{40}Ca and ^{208}Pb). The different contributions to the HF potential shown in the four frames are explained in the text.*

whose x–dependence depends on α_a has an extra factor of f_α and is repulsive so ought to counteract the effect of the general strengthening of the attractive term. The effect of varying α_a upon the explicitly α–dependent terns in the HF potential is shown in Figure 5.5. The first frame shows the terms in the isospin–independent part of the HF potential explicitly dependent on α_a for ^{40}Ca and ^{208}Pb. The large contribution is from the direct rearrangement term. The very small contribution near the x–axis is that from the exchange rearrangement term (that term which features the function $G(x)$ in Equation (3.9)). The second frame shows terms analogous to those in frame one, but for the repulsive force. Here one sees that a fairly significant change arises despite the lack of any dependence in α_a. The differences then must be due to the change in density which arises. The third frame shows the sum of the first two and the full HF potential (for neutrons) is shown in the final frame. Although the explicitly α–dependent terms show a reduction in binding, the overall change in the density and the effects of the change in the
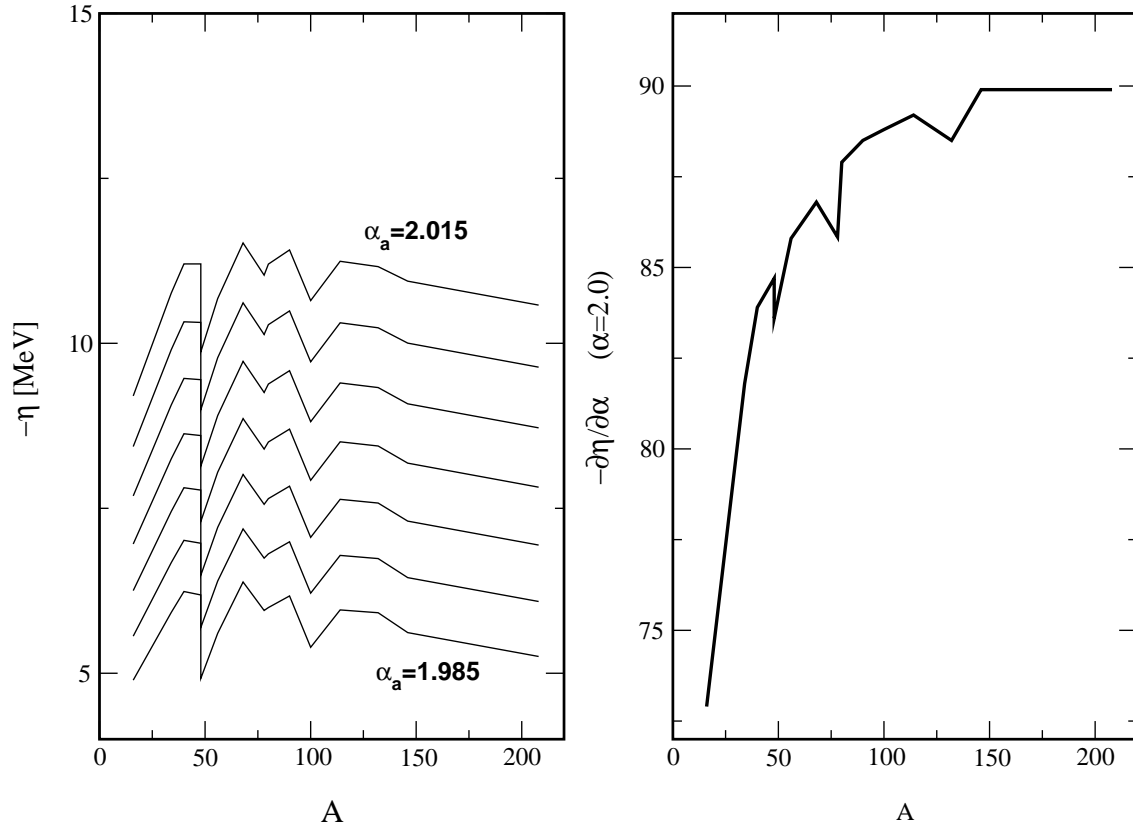
Figure 5.6: *A-dependence of the binding energy per nucleon,* $-\eta$, *for various values of* α_a, *and the change in* η *per unit change in* α_a *as a function of A.*

other parameters gives a net result of a deepened HF potential with a corresponding increase in binding energy and decrease in radius. The numerical changes are shown in Table 5.1 in which it is interesting to note that changing α_a changed f_{α_a} rather less than other of the parameters in the potential.

Figure 5.6 shows how the A-dependence of the binding energy per particle, η, changes as a result of varying α_a. As has been noted, an increase in α_a increases

Quantity	E_{HF} (MeV)	r_{ch}(fm)	f_{α_a}	N_{β_a}	f_{α_r}	N_{β_r}
Value$\|_{\alpha_a=2.00}$	-345.2	3.48	0.238	4.198	0.420	2.332
Value$\|_{\alpha_a=2.01}$	-413.1	3.43	0.233	4.385	0.398	2.465
Percentage change	19.7	1.4	2.1	4.5	5.2	5.7

Table 5.1: *Effect of a small change in* α_a *upon observables and parameters of the mean field for* ^{40}Ca.

the binding energy and this is seen, in the left frame, to occur across the whole range of nuclei. The right frame shows the change of binding energy per nucleon per unit change in α_a as a function of A. Here one notes that heavier nuclei are affected more strongly than light nuclei with about a 20% difference in strength. The dependence is quite smooth, with a small amount of shell structure in evidence. The scale of the y-axis shows that very large changes in the binding energy (and, in fact, in all other observables) result from small changes in α_a which is not surprising since α_a features as an exponent in the expression for the force (3.1).

β_a **and** β_r

Like the α parameters, the β parameters enter into each of the terms of the monopole force via their own functions, in this case the N functions (see Equation (3.9)). The form of these functions looks like a reciprocal of the f functions and one finds that an increase in a β results in a *decrease* in the corresponding N_β. The "leading" term of the HF potential, i.e. the Hartree term which is not part of the rearrangement potential has an x-dependence which is itself dependent on the β_a parameter. This term, for a small change in β_a is shown in the first frame of Figure 5.7, added to the functionally identical term from the rearrangement potential and the tiny part of the potential which arises from the exchange term but has the form of a local one-body potential (that part which features the function $G(x)$). The second frame again shows the corresponding action upon the same terms for the repulsive part of the force and the two parts are added together for frame 3. Frame 4 shows the effect of a small increase in β_a for the HF potential. As with the variation of α_a one concludes that the dominant effect of changing the parameter is not directly through the parts of the force which explicitly depend on it, but rather through the change in the density. Increasing β_a has the nett effect of decreasing the depth of the HF potential and increasing the rms radius of the density distribution.

The change in the A-dependence resulting from varying β_a is shown in Figure 5.8. The left frame gives a visual guide to the effect on the binding energy over the periodic table as β_a is varied. The obvious effect is seen to be a shifting of the energies *en masse*. The variation of this effect with A is shown in the second frame. The curve's shape resembles that of its analogue in the variation of α_a except for a change in sign. This suggests that the α and β parameters are not independent. In the next chapter the nuclear matter problem is studied in which it can be seen that in the limit of infinite nuclear matter the two parameters are indeed correlated.

Potential Strengths, W_a **and** W_r

The meaning of and the effect of changing the potential strengths are quite clear – they control the overall strength of the interaction and the extent to which they
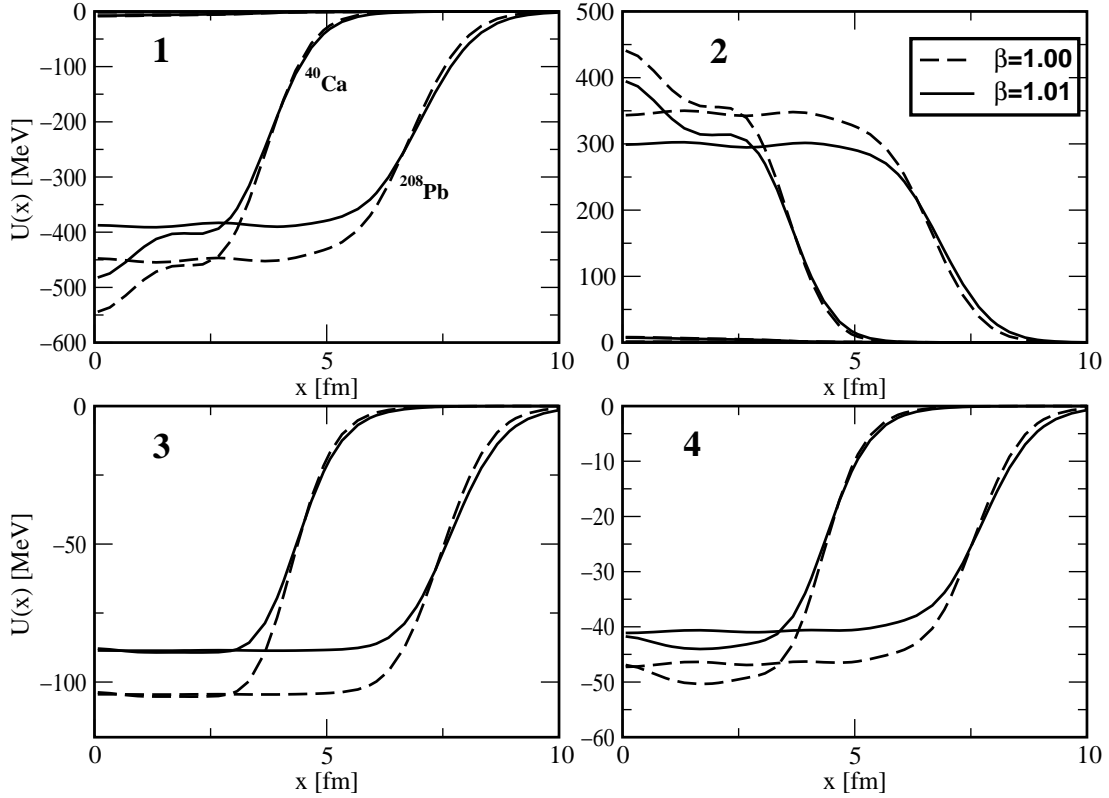
Figure 5.7: *Action of the variation of* β_a *upon the HF potential in light and heavy nuclei* (^{40}*Ca and* ^{208}*Pb). The different contributions to the HF potential shown in the four frames are explained in the text.*

cancel each other out.

Just varying W_a varies the depth of the potential and the HF energy in an obvious way. A more interesting way to examine the potential strengths is to vary them both while keeping an observable constant. Table 5.2 shows the effect

W_a	W_r	r_{ch} (fm)	$E^{(2)}$
-1320.0	1431.3	3.32	-1.19
-1420.0	1605.8	3.40	-1.09
-1520.0	1785.0	3.48	-1.01
-1620.0	1986.9	3.56	-0.95
-1720.0	2157.3	3.64	-0.90

Table 5.2: *Charge radius and second order energy correction in* ^{40}*Ca as attractive and repulsive potential strengths are varied at constant Hartree-Fock energy*
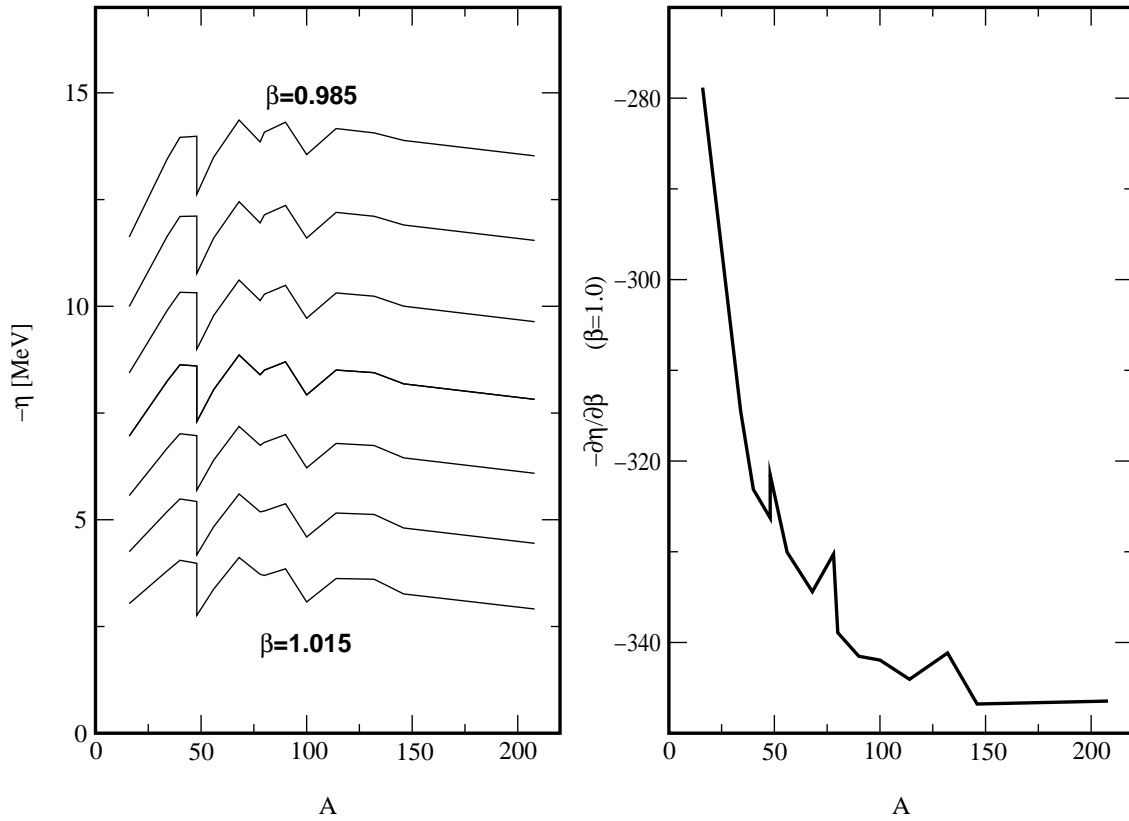
Figure 5.8: *A-dependence of the binding energy per nucleon, $-\eta$, for various values of β_a, and the change in η per unit change in β_a as a function of A.*

of varying W_a and W_r such that the binding energy of ^{40}Ca is kept fixed (at 345.2 MeV). One sees that there is a linear dependence upon the potential strengths of the charge radius so that one may fit both the energy and the charge radius simultaneously for at least one nucleus with fixed values of the exponents α and β.

The $\sim 30\%$ change in the second order energy correction shows that the amount of total energy which comes from the correlation depends on how one chooses the parameters. Clearly in this case one must choose the set of parameters which fits the charge radius, but the changes in the second order correction show that one may include as a fitting criterion the correlation energy.

Figure 5.9 shows how the binding energies of the other nuclei change between the most extreme values of the potential strengths in Table 5.2. The top two lines show the two curves of E/A as labelled by the left y-axis. Clearly there is only a slight difference between the two curves. The lower curve shows this difference and is labelled by the right y-axis. It can be seen that this curve of the differences
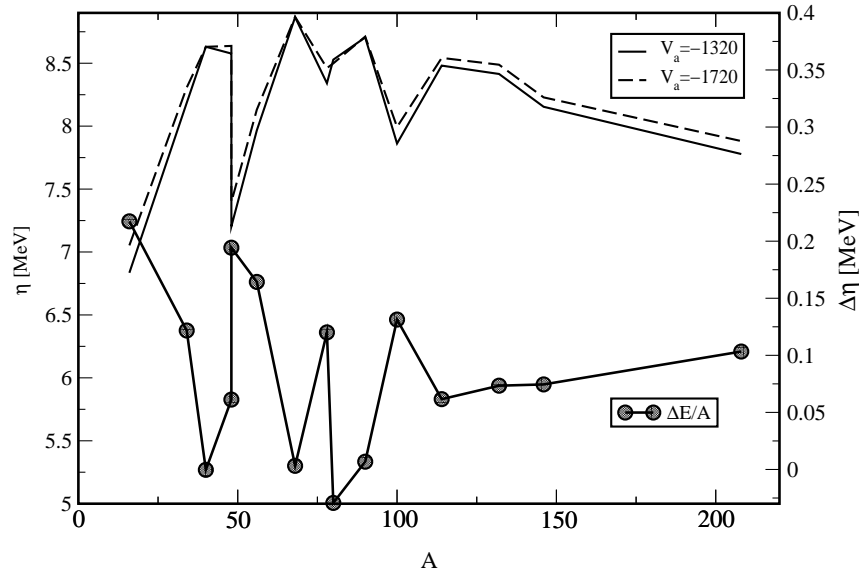
Figure 5.9: *Effect of varying W_a and W_r on the binding energy of a range of nuclei, keeping that of* ^{40}Ca *constant.*

mirrors the upper curves. This indicates that increasing the magnitudes of the potential strengths serves to flatten out the shell structure somewhat.

Isospin parameters, a_a, b_a, a_r, b_r

From Figures 5.1–5.3 the direct isospin-dependent energy is seen to depend strongly on the difference $N - Z$ with the largest contribution coming from the nuclei ^{78}Ni, ^{132}Sn and ^{208}Pb, those being the nuclei with the greatest neutron excesses. In Figure 5.10 one sees the result upon the total binding energy per nucleon of varying the b parameter for the attractive force. It is seen that there is a large variation the the contribution to the HF energy from the b-dependent terms. For a positive value of the b_a, that is to say an attractive force in the direct part, a large attractive contribution is seen for the nuclei mentioned above with large neutron excess. Also of note is the exchange contribution which acts with opposite sign to the direct term and results in reduced binding for the light $N = Z$ nuclei where its affect is strongest (see Figure 5.3).

As well as affecting the binding energy, the b parameters control the relative depths of the proton and neutron potentials and so also give one the freedom to fit the relative single particle energies of protons and neutrons. For the values of b_a used in Figure 5.10 and some values in between, the single particle energies
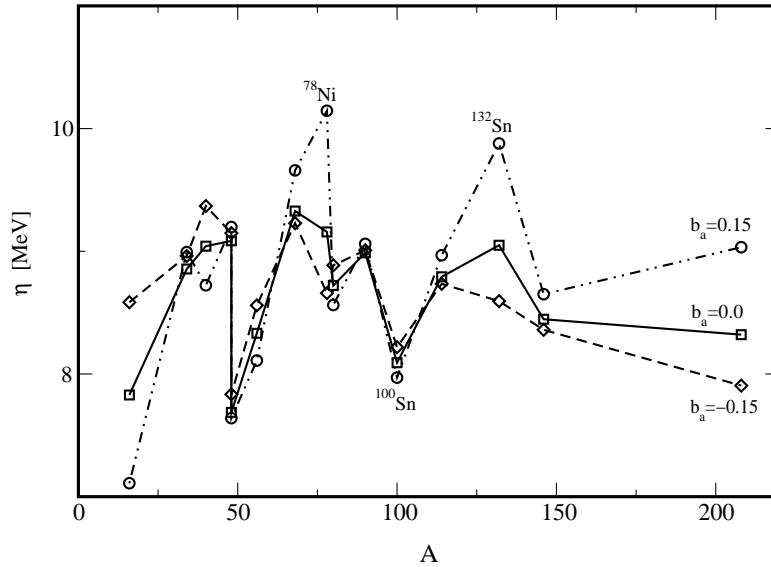
Figure 5.10: *Effect upon the binding energy per particle of the variation of the* b_a *isospin-dependent parameter*

of the few neutron and proton states either side of the Fermi level in ^{208}Pb are shown in Table 5.3. One sees making the parameter b_a more positive decreases the binding of the proton states and increases the binding of the neutron states. The action of b_r is reversed as shown in Figures 5.1 and 5.2.

The a parameters feature only in the exchange part of the energy and potential. Their effect then, as shown in Figures 5.1–5.3 is largest in light nuclei and smoothly varying. Varying a_a, as shown in Figure 5.11 reflects this behaviour and gives one the freedom to vary the A-dependence of the fit to the binding energy. An interesting effect of having a parameter which controls a part of the force which contributes quite weakly, only via exchange parts in the HF approximation, is that the contribution to the perturbation calculation to the energy may be large since there is no calculational distinction between direct and exchange forces at the level of perturbation theory. Figure 5.12 shows the size of the second-order energy correction as a function of a_a. The corrections are shown as contributions to the *binding energy*, so are positive since the second order correction is always binding. The quadratic behaviour of the energy with respect to a_a can be seen as contrasted to the more linear behaviour in the HF approximation. By increasing the magnitude of the a parameters one can then obtain large values of correlation energy for moderate changes in HF energy.

The figure also shows the difference in contributions to the N = Z and N $\neq$ Z

b_a	-0.15	-0.10	-0.05	0.00	0.05	0.10	0.15
$\pi 0h_{11/2}$	-11.9	-10.8	-9.5	-8.0	-6.2	-4.2	-1.4
$\pi 1d_{3/2}$	-10.7	-9.5	-8.1	-6.6	-4.8	-2.6	+0.2
$\pi 2s^*_{1/2}$	-10.1	-8.9	-7.6	-6.1	-4.3	-2.2	+0.6
$\pi 0h_{9/2}$	-6.7	-5.6	-4.2	-2.6	-0.7	+1.6	+4.2
$\pi 1f_{7/2}$	-5.7	-4.6	-3.4	-2.0	-0.4	+1.6	+4.5
$\pi 0i_{13/2}$	-5.0	-4.0	-2.9	-1.5	+0.0	+2.0	+4.6
$\nu 2p_{3/2}$	-9.7	-10.7	-11.8	-13.2	-14.8	-16.8	-19.3
$\nu 1f_{5/2}$	-9.6	-10.5	-11.6	-12.9	-14.4	-16.3	-18.8
$\nu 2p^*_{1/2}$	-8.9	-9.8	-10.9	-12.2	-13.8	-15.7	-18.2
$\nu 1g_{9/2}$	-5.5	-6.5	-7.6	-8.9	-10.4	-12.2	-14.6
$\nu 0i_{11/2}$	-3.9	-4.9	-6.1	-7.4	-8.9	-10.7	-12.9
$\nu 2d_{5/2}$	-3.1	-4.0	-5.1	-6.2	-7.8	-9.6	-11.9

Table 5.3: *Proton (π) and neutron (ν) single particle energies near the Fermi level in* ^{208}*Pb. The asterisks denote the highest occupied states.*

nuclei from the a-dependent terms. This is understandable in the following terms: An excitation arising from this term is non-zero if a single proton is excited to a
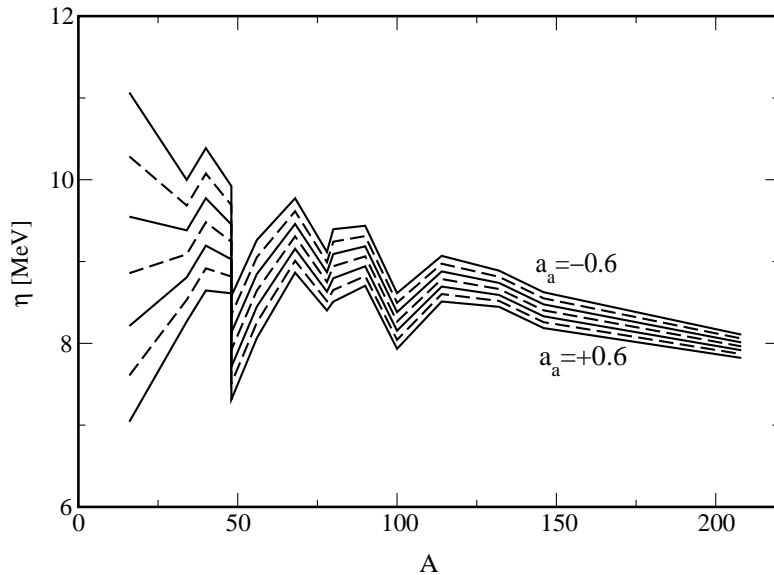

Figure 5.11: *Dependence of the binding energy per nucleon on the parameter* a_a. *Values of* a_a *range from* -0.6 *to* 0.6 *as labelled and increment in steps of* 0.2.
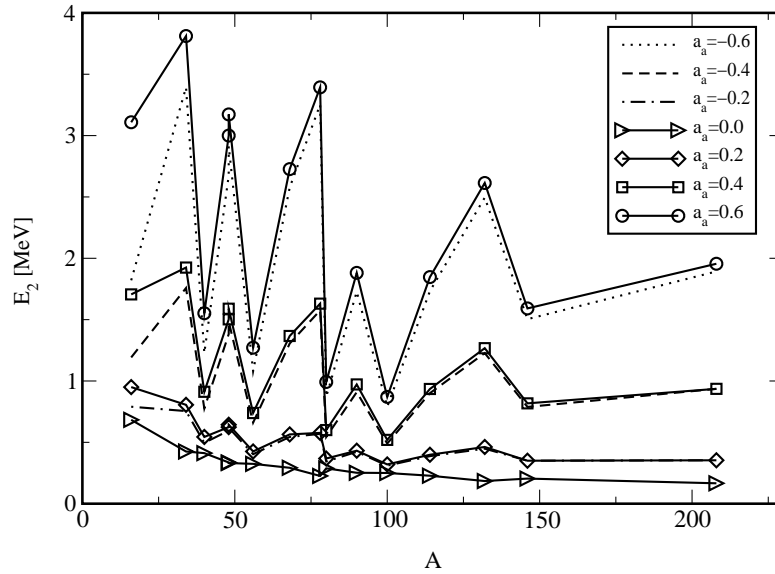
Figure 5.12: *Dependence of the total second order contribution to the binding energy on the parameter* a_a. *The parameter* a_r *is kept at zero.*

neutron orbital and a single neutron is excited to a proton orbital simultaneously. Since each excitation is an $l = 0$ excitation the lowest state a given proton can excite to is the lowest unoccupied neutron state of the same l and vice versa for a neutron exciting to a proton state. In an $N = Z$ nucleus the proton and neutron states are occupied to the same level so each excitation must involve a change in principal quantum number and thus incur quite a large energy denominator. In an $N \neq Z$ nucleus one can have the situation in which a neutron excites to a proton states in which all the (non-isospin) quantum numbers are exactly the same in which the matrix element is large and the energy denominator is small, giving rise to a large contribution.

Derivative force parameter, k

This part of the force controls rather strongly the density profile, particularly at the surface. Without it, there is always a large peak in the densities around the surface of the nucleus, which is particularly evident in heavy nuclei. Figure 5.13 shows the surface of the charge density in ^{208}Pb as the k parameter is varied. As one can see the peak is rather considerable if one omits this term ($k = 0.0$). In the figure, the parameter is increased in steps of 2.0 as indicated. At some value near 6.0 the charge density fits that of experiment quite well, and then becomes worse
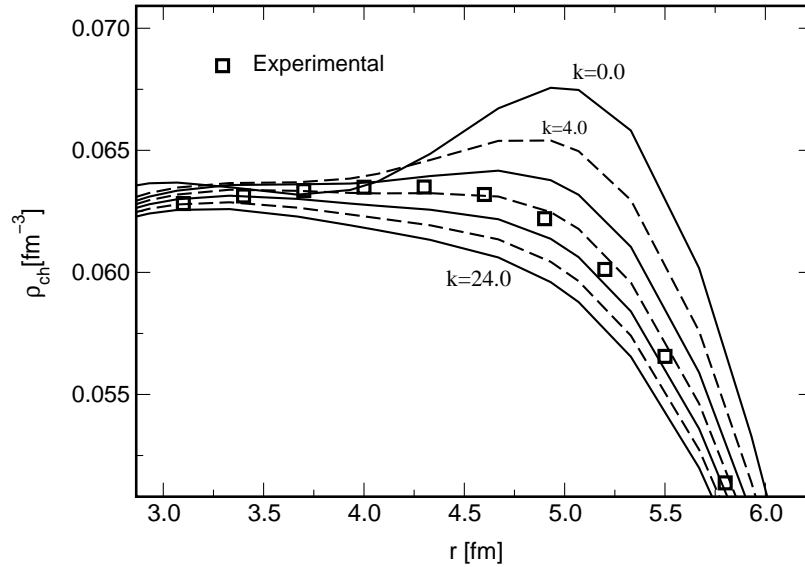
Figure 5.13: *Effect of varying* k *on the surface of the charge density*

as the parameter is increased. The experimental data are the Fourier transform of the charge scattering form factor[99].

k [Mev fm^{10}]	N$_d$	E$_{derv}$ [MeV]
0.0	–5.59	0.00
4.0	–4.72	44.63
8.0	–4.24	71.79
12.0	–3.90	91.36
16.0	–3.65	106.6
20.0	–3.45	119.2
24.0	–3.29	129.7

Table 5.4: *Hartree Energy contribution from derivative term as a function of term's strength in* ^{208}Pb

Table 5.4 shows how, as one increases the strength of the derivative term, the change in the density profile results in a decrease in the N$_d$ parameter, which is defined in expression (E.24) of Appendix E, so that, despite the term being proportional to the parameter k, the increase in energy is less than linear. The other significant effect of the derivative terms is related to change in the surface properties as shown in Figure 5.13. Since the shape of the HF potential is directly dependent upon the shape of the density, the rounding of the surface of the den-
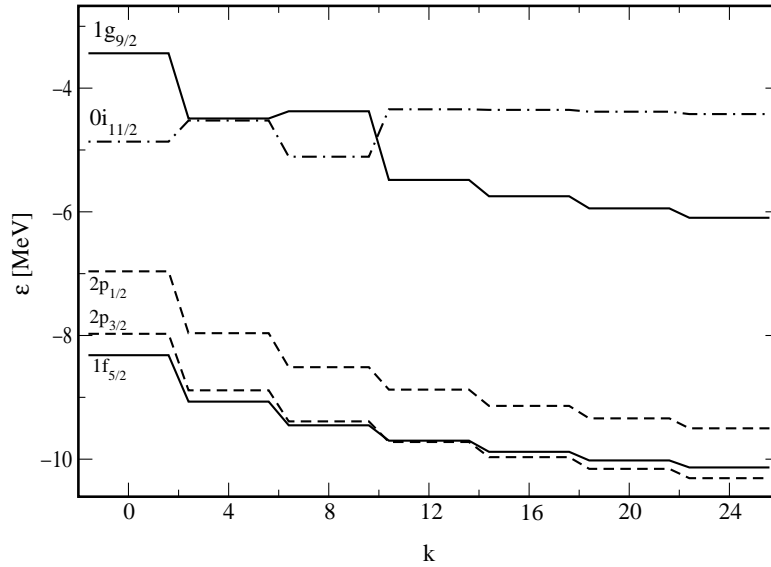
Figure 5.14: *Effect of varying* k *upon the neutron single particles energies near the fermi surface in lead.*

sity also smooths out the wall of the potential. The result of this is that those high angular momentum states which spend most of their time near this surface suffer a loss in binding. This is shown in Figure 5.14 for neutron states near the fermi surface in ^{208}Pb. When k = 0 the N = 126 shell gap is not pronounced, but as k increases the $i_{11/2}$ state moves up as the rest move down and the resulting shell gap is increased. Table 5.5 shows the numerical size of the gap between the highest occupied and lowest unoccupied neutron states in ^{208}Pb as shown in Figure 5.14.

k [Mev fm^{10}]	Gap [Mev]
0.0	2.10
4.0	3.44
8.0	3.43
12.0	3.39
16.0	3.39
20.0	3.40
24.0	3.49

Table 5.5: N = 126 *shell gap in* ^{208}*Pb as a function of* k. *Experimental value is 4.23 MeV[21]*
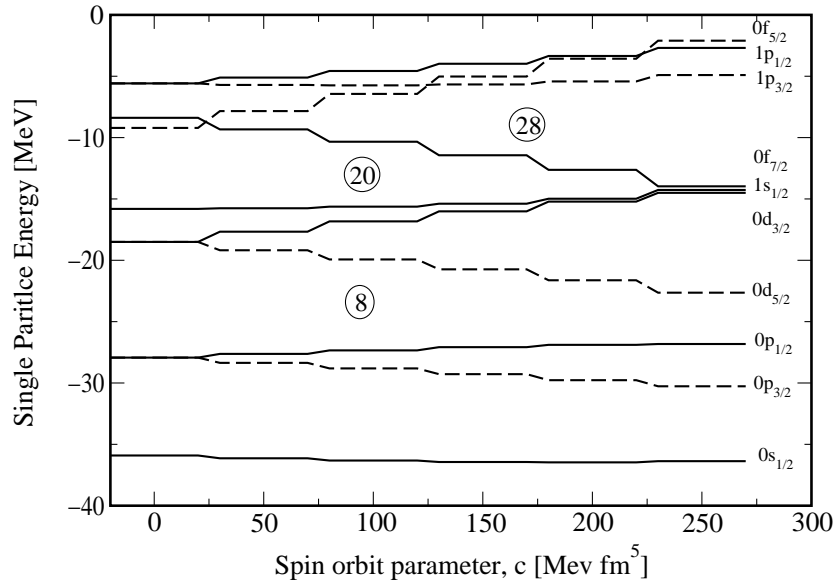
Figure 5.15: *Proton single-particle level spectrum of* ^{48}Ca *as spin-orbit paramter,* c *is varied.*

The reason that the single particle energies become more bound as k increases, even though the contribution to the Hartree-Fock energy of this term is positive is that the parameter N_d as shown in Table 5.4 is negative and appears with a single power in the mean-field, but squared in the HF energy.

Spin-orbit parameter, c

Figure 5.15 shows the variation of the proton single particle energies up to $Z = 40$ as a function of the spin-orbit strength, c. One sees that as the parameter is

c $\left[\text{Mev fm}^5\right]$	r_{ch} [fm]	E_{so}
0.0	3.50	0.00
50.0	3.49	-8.14
100.0	3.47	-17.34
150.0	3.44	-27.91
200.0	3.44	-40.43
250.0	3.43	-56.18

Table 5.6: *Charge radius and contribution to HF energy from spin-orbit force as* c *is varied in* ^{48}Ca.

increased the magic number 28 appears and upon further increasing the magic number 20 disappears. The correct value of the parameter is presumably around 150 Mev fm^5 where both magic numbers exist. The fact that the $0f_{5/2}$ and $0f_{7/2}$ states do not coincide in energy at $c = 0$ is due to the exchange part of the isospin-dependent force. The last term in the nonlocal HF potential (3.10) is, for protons

$$\mathcal{U}_p(x, x') \varphi_b(x) = -\sum_\xi W_\xi a_\xi f_{\alpha_\xi} \rho_n(x, x') \rho^{\beta_\xi}(x) \rho^{\beta_\xi}(x') \varphi_b(x') \tag{5.2}$$

which gives a different contribution according to whether the state which corresponds to the proton state φ_b is present in the neutron density $\rho_n(x, x')$ or not. Since the $0f_{7/2}$ neutron state is occupied but the $0f_{5/2}$ state is not, these two unoccupied proton states see a spin-orbit splitting even without the spin-orbit force.

5.2 Higher Multipole forces

The higher multipole forces do not contribute to the direct HF energy in spherical doubly-closed-shell nuclei (See Appendix E). There is an exchange contribution to the energy of the form:

$$E_{\Lambda,q_1,q_2} = -\frac{f_\Lambda}{2} W_{\Lambda,q_1,q_2} \sum_{i,j<\epsilon_F} \sum_{M=-\Lambda}^{\Lambda} (-1)^M \langle ij | (r_1^\Lambda(r_1) \rho(r_1) Y_{\Lambda M}(\hat{r}_1)) \, (r_2^\Lambda \rho(r_2) Y_{\Lambda-M}(\hat{r}_2)) | ji \rangle \tag{5.3}$$

Since the exchange part of the interaction is presumably small by analogy with the monopole field, its contribution to the HF field is neglected. The contribution to the HF energy *is* calculated, as well as the contribution to perturbation theory.

It is difficult to show the behaviour of the multipole forces for a typical set of parameters since the observables of the ground states of spherical nuclei do provide enough information to give definite values to these parameters. Although calculations of excited states or deformed nuclei will be necessary to fit these parameters, there will be a contribution to spherical nuclei via the exchange term in the Hartree-Fock approximation and in perturbation theory, so these possible contributions are examined here.

The Λ-dependences of the higher multipole forces are controlled by parameters f_λ so it is not worthwhile to examine such dependence since it can be set freely. Instead, the results of varying the three strength parameters for the quadrupole force are examined in the $N = Z$ nucleus ^{40}Ca and the $N \neq Z$ nucleus ^{48}Ca which are close enough in mass that the uncertainty in the A-dependence is irrelevant. The function f_Q is chosen to be

$$f_Q = \frac{1}{A^{7/3}} \tag{5.4}$$

since this is the value used in Ref. [74]. This value is certainly not to be taken as fixed, but only as a choice made since some definiteness is necessary for this

study. The actual A-dependence of the force may need to be quite different since this density-dependent force used in the full space may be quite different from the traditional density-independent quadrupole forces used in a restricted space. Negative signs are chosen for the strengths since the quadrupole force is usually considered to be attractive. In the case of the spherical nuclei in which the largest contribution is from the HF exchange term, the effect is actually to lower the binding energy.

The results for the contribution to the HF exchange energy as a function of the strength parameters are shown in Table 5.7. In the case of ^{40}Ca the results for the pp and the nn force are almost the same, which is to be expected since their wavefunctions and relative single-particle spacing are almost identical. The HF energy contribution to the pn force is very close to that of the pp and nn forces, but the perturbation calculation is noticeably different. This is due to the fact that the proton and neutron states are shifted with respect to each other as a result of the Coulomb interaction so that the energy excitations from proton to neutron states and vice versa incur different energy denominators to those excitations which are between single particle states of the same isospin. In the case of ^{48}Ca the effect of the A-dependence is seen to reduce the strength of the pp interaction for a given W paramter. The addition of eight neutrons to the $f_{\frac{7}{2}}$ state results in quite a substantial increase in the contribution from the nn force, which shows that the quadrupole force has a large shell-dependence. Again, the pn force has a rather larger effect in perturbation theory than either the pp or nn forces.

The linear behaviour of the HF exchange energy is evident. This exact linearity is as a result of the approximation used, which neglects the effect upon the mean field due to the multipole forces. The extra contribution to the second order correction is seen to be quadratic in the strength parameter. This is a natural result of perturbation theory which orders terms by the number of interactions taking place. In second order, there is a squared matrix element proportional to W_Q^2. The quadratic behaviour is not exact since the quadrupole term cancels and augments the monopole term (and the dipole term, when used) as shown in Appendix F.

^{40}Ca

$W_{Q,pp}$ [MeV]	0.0	-100	-500	-1000	-5000	-10000	-50000
$E^{(Q)}$ [MeV]	0.0	0.051	0.254	0.508	2.359	5.078	25.393
$E_{(2)}$ [MeV]	-1.268	-1.268	-1.268	-1.269	-1.288	-1.348	-3.261
$E_{(2)}^{(Q)} - E_{(2)}^{(0)}$ [MeV]	0.0	0.0	0.0	0.001	0.020	0.080	1.993

$W_{Q,nn}$[MeV]	0.0	-100	-500	-1000	-5000	-10000	-50000
$E^{(Q)}$ [MeV]	0.0	0.052	0.258	0.517	2.584	5.169	25.843
$E_{(2)}$ [MeV]	-1.268	-1.268	-1.268	-1.269	-1.287	-1.347	-3.237
$E_{(2)}^{(Q)} - E_{(2)}^{(0)}$ [MeV]	0.0	0.0	0.0	0.001	0.019	0.079	1.969

$W_{Q,pn}$ [MeV]	0.0	-100	-500	-1000	-5000	-10000	-50000
$E^{(Q)}$ [MeV]	0.0	0.052	0.257	0.515	2.573	5.147	25.733
$E_{(2)}$ [MeV]	-1.268	-1.268	-1.269	-1.271	-1.347	-1.584	9.132
$E_{(2)}^{(Q)} - E_{(2)}^{(0)}$ [MeV]	0.0	0.0	0.001	0.003	0.0079	0.0316	7.864

^{48}Ca

$W_{Q,pp}$ [MeV]	0.0	-100	-500	-1000	-5000	-10000	-50000
$E^{(Q)}$ [MeV]	0.0	0.047	0.238	0.476	2.380	4.759	23.795
$E_{(2)}$ [MeV]	-3.149	-3.149	-3.149	-3.149	-3.165	-3.214	-4.778
$E_{(2)}^{(Q)} - E_{(2)}^{(0)}$ [MeV]	0.0	0.0	0.0	0.0	0.016	0.065	1.629

$W_{Q,nn}$[MeV]	0.0	-100	-500	-1000	-5000	-10000	-50000
$E^{(Q)}$ [MeV]	0.0	0.083	0.415	0.830	4.149	8.297	41.485
$E_{(2)}$ [MeV]	-3.149	-3.149	-3.149	-3.150	-3.175	-3.254	-5.795
$E_{(2)}^{(Q)} - E_{(2)}^{(0)}$ [MeV]	0.0	0.0	0.0	0.001	0.026	0.106	2.646

$W_{Q,pn}$ [MeV]	0.0	-100	-500	-1000	-5000	-10000	-50000
$E^{(Q)}$ [MeV]	0.0	0.054	0.271	0.542	2.711	5.421	27.107
$E_{(2)}$ [MeV]	-3.149	-3.149	-3.151	-3.155	-3.251	-3.535	-12.346
$E_{(2)}^{(Q)} - E_{(2)}^{(0)}$ [MeV]	0.0	0.0	0.002	0.006	0.102	0.386	9.197

Table 5.7: *Contribution from the quadrupole force to the HF exchange energy ($E^{(Q)}$). $E_{(2)}$ is the total second order correction and $E_{(2)}^{(Q)} - E_{(2)}^{(0)}$ is the change in second order correction due to the quadrupole force.*

Chapter 6

Nuclear Matter and Neutron Star Calculations

The purpose of nuclear structure theory is to describe the properties of observed nuclei given some kind of nuclear interaction or potential as input. The difficulties of performing full calculations and the desire to examine the properties of many candidate interactions have led to *infinite nuclear matter* calculations becoming a standard technique in examining the properties of nuclear potentials.

In its simplest form, infinite nuclear matter consists of an equal (and infinite) number of protons and neutrons interacting via a nuclear potential but with the Coulomb interaction "switched off". One may then calculate its binding energy per nucleon as a function of the nuclear density. The minimum point of this curve gives the equilibrium density and energy. The existence of the minimum at the correct energy and density is a necessary result which is a reflection of the saturation of nuclear forces.

The observables in nuclear matter are identified in a number of ways. The density is inferred from the central densities of heavy nuclei and is reasonably certain since there is not much variation in this value between nuclei (saturation of the density). For energies one considers terms in the simple semi-empirical mass formula of Weizsäcker–Bethe [76] which have the correct A-dependence to be finite in nuclear matter, namely the volume and asymmetry terms. Other observables are considered below.

More detailed descriptions of nuclear matter are widely available in textbooks on nuclear physics and many-body physics (see e.g. [34, 36, 37]) and in review articles (see e.g. [75]).

6.1 Symmetric Nuclear Matter

6.1.1 Single particle wavefunctions

Since infinite nuclear matter is infinite and homogeneous, the single particle wave functions must be translationally invariant, hence they are plane waves states. Nuclei also have intrinsic spin and isospin so each single particle state also has a spinor and isospinor associated with it:

$$\phi_\lambda(r) = \frac{1}{\sqrt{V}} e^{i k_\lambda \cdot r} \chi_\sigma \xi_\tau \tag{6.1}$$

where χ_σ is a spinor and ξ_τ is an isospinor.

6.1.2 Density

In nuclear matter theory, the system is a Fermi liquid, consisting of independent particles occupying states up to the Fermi level. In this picture we may write the number of particles as

$$A = \sum_{k\sigma\tau} \theta(k_F - k) \tag{6.2}$$

where $\theta(x)$ is the step function:

$$\theta(x) = \begin{cases} 1 & x > 0 \\ 0 & x < 0 \end{cases} . \tag{6.3}$$

As the size of the system increases to infinity the sum over momentum states becomes an integral and the expression for the number of particles becomes

$$
\begin{aligned}
A &= \frac{V}{(2\pi)^3} \sum_{\sigma\tau} \int d^3k \, \theta(k_F - k) \\
&+ \frac{4V}{(2\pi)^3} 4\pi \int_0^{k_F} k^2 \int dk \\
&= \frac{2V}{3\pi^2} k_F^3.
\end{aligned}
\tag{6.4}
$$

Dividing by the volume, the density $\rho = A/V$ is

$$\rho = \frac{2k_F^3}{3\pi^2}. \tag{6.5}$$

6.1.3 Kinetic Energy

The kinetic energy of a many-particle system may be written as the sum of the single particle kinetic energies, $T = \sum_i \langle i | \hat{T} | i \rangle$ which, in the case of the single particle states defined in Equation (6.1), is:

$$T = \sum_{k\sigma\tau} \frac{1}{V} \int d^3r \, e^{-ik\cdot r} \chi_\sigma^\dagger \xi_\tau^\dagger \left(-\frac{\hbar\nabla^2}{2m} \right) e^{ik\cdot r} \chi_\sigma \xi_\tau, \tag{6.6}$$

where χ_σ is a spinor and ξ_τ is an isospinor. Since the kinetic energy operator does not act in the spin or isospin spaces, the products of the spinors and their hermitian conjugates is unity. The action of the Laplacian on the exponential is just $\nabla^2 e^{ik\cdot r} = -k^2 e^{ik\cdot r}$ so that

$$
\begin{aligned}
T &= \sum_{k\sigma\tau} \frac{\hbar^2}{2m} k^2 \\
&= 4 \frac{V}{(2\pi)^3} \frac{\hbar^2}{2m} 4\pi \int_0^{k_F} k^4 dk \\
&= \frac{V\hbar^2 k_F^5}{5\pi^2 m} \\
&= \left(\frac{2k_F^3}{3\pi^2} \right) V \frac{3\hbar^2 k_F^2}{5 \, 2m} \\
&= A \frac{3}{5} \frac{\hbar^2 k_F^2}{2m}.
\end{aligned}
\tag{6.7}
$$

Hence

$$\frac{T}{A} = \frac{3}{5} \frac{\hbar^2 k_F^2}{2m} \tag{6.8}$$

which is the kinetic energy per particle. Using the relation between k_F and ρ (6.5), the kinetic energy per particle may also be expressed as

$$\frac{T}{A} = \frac{3}{5} \frac{\hbar^2}{2m} \left(\frac{3\pi^2}{2} \right)^{\frac{2}{3}} \rho^{\frac{2}{3}}. \tag{6.9}$$

In nuclear units, and taking the mass to be the average of the neutron and proton masses, $m \approx 938.8$ MeV, the kinetic energy per particle is approximately

$$\frac{T}{A} = a_k \rho^{\frac{2}{3}} \approx 75.0 \rho^{\frac{2}{3}} \text{ MeV} \tag{6.10}$$

6.1.4 Potential Energy

The total potential energy due to a two-body interaction in a many body system may be expressed as

$$V = \frac{1}{2} \sum_{\lambda\mu} \left(\langle \lambda\mu | V(1,2) | \lambda\mu \rangle - \langle \lambda\mu | V(1,2) | \mu\lambda \rangle \right) = E_D - E_E \tag{6.11}$$

where λ and μ each represent all the quantum numbers of the individual particles and the sums run over all occupied states. E_D is called the direct term, and E_E the exchange term. Considering first the direct term, with the central part of the two-body interaction acting between the plane wave states, the energy is

$$
\begin{aligned}
E_D &= \sum_{\xi=a,r} \frac{1}{2} \sum_{k_\lambda \sigma_\lambda \tau_\lambda}^{k<k_F} \sum_{k_\mu \sigma_\mu \tau_\mu}^{k<k_F} \langle k_\lambda \sigma_\lambda \tau_\lambda k_\mu \sigma_\mu \tau_\mu | W_\xi f_{\alpha_\xi}(\rho) \rho^{\beta_\xi} \rho^{\beta_\xi} | k_\lambda \sigma_\lambda \tau_\lambda k_\mu \sigma_\mu \tau_\mu \rangle \\
&= \sum_\xi \frac{1}{2} \left(\sum_{k\sigma\tau} \langle k\sigma\tau|\rho^\beta|k\sigma\tau\rangle \right)^2 W_\xi f_{\alpha_\xi}(\rho) \\
&= \sum_{\xi=a,r} \frac{1}{2} W_\xi \frac{1}{\int \rho^{\alpha_\xi} d^3 r} \left(4 \sum_k \frac{1}{V} \int d^3 r\, e^{-ik\cdot r} \rho^{\beta_\xi} e^{ik\cdot r} \right)^2 \quad (6.12)
\end{aligned}
$$

Using the fact that in infinite nuclear matter, the density is a constant, the functions ρ, may be taken outside of the integrals:

$$
\begin{aligned}
E_D &= \sum_{\xi=a,r} \frac{1}{2} W_\xi \frac{16}{\rho^{\alpha_\xi} V} \rho^{2\beta_\xi} \left(\sum_k^{k_F} 1 \right)^2 \\
&= \sum_{\xi=a,r} 8 W_\xi \rho^{2\beta_\xi - \alpha_\xi} V^{-1} \left(\frac{V}{(2\pi)^3} \int_0^{k_F} 4\pi k^2\, dk \right)^2 \\
&= \sum_{\xi=a,r} 8 W_\xi \rho^{2\beta_\xi - \alpha_\xi} V^{-1} \left(\frac{1}{3} k_F^3 V \frac{1}{(2\pi)^3} \right)^2 \\
&= \sum_{\xi=a,r} \left(\frac{2k_F^3 V}{3\pi^2} \right) \left(\frac{2k_F^3}{3\pi^2} \right) \frac{1}{2} W_\xi \rho^{2\beta_\xi - \alpha_\xi} \\
&= \sum_{\xi=a,r} A \frac{1}{2} W_\xi \rho^{2\beta_a - \alpha_\xi + 1} \quad (6.13)
\end{aligned}
$$

so that the contribution to the energy, per nucleon, is

$$
\frac{E_D}{A} = \frac{1}{2} W_a \rho^{2\beta_a - \alpha_a + 1} + \frac{1}{2} W_r \rho^{2\beta_r - \alpha_r + 1}. \quad (6.14)
$$

The exchange term, E_ξ is

$$
\begin{aligned}
E_\xi &= \sum_{\xi=a,r} \frac{1}{2} \sum_{k_\lambda \sigma_\lambda \tau_\lambda}^{k<k_F} \sum_{k_\mu \sigma_\mu \tau_\mu}^{k<k_F} \langle k_\lambda \sigma_\lambda \tau_\lambda k_\mu \sigma_\mu \tau_\mu | W_\xi f_{\alpha_\xi}(\rho) \rho^{\beta_\xi}(\mathbf{r}_1) \rho^{\beta_\xi}(\mathbf{r}_2) | k_\mu \sigma_\mu \tau_\mu k_\lambda \sigma_\lambda \tau_\lambda \rangle \\
&= \sum_\xi \frac{1}{2} W_\xi f_{\alpha_\xi}(\rho) \sum_{k_\lambda \sigma_\lambda \tau_\lambda}^{k<k_F} \sum_{k_\mu \sigma_\mu \tau_\mu}^{k<k_F} |\langle k_\lambda \sigma_\lambda \tau_\lambda|\rho^\beta|k_\mu \sigma_\mu \tau_\mu\rangle|^2 \\
&= \sum_\xi \frac{1}{2} W_\xi \frac{1}{\int d^3 r\, \rho} \sum_{k_\lambda \sigma_\lambda \tau_\lambda}^{k<k_F} \sum_{k_\mu \sigma_\mu \tau_\mu}^{k<k_F} \left| \frac{1}{V} \int d^3 r\, e^{-ik_\lambda \cdot r} \rho^\beta e^{ik_\mu \cdot r} \delta_{\sigma_\mu \sigma_\lambda} \delta_{\tau_\mu \tau_\lambda} \right|^2 \quad (6.15)
\end{aligned}
$$

Again taking ρ to be constant, the integral just gives a delta function:

$$
\begin{aligned}
E_\xi &= \sum_{\xi=a,r} \frac{1}{2} W_\xi \frac{4}{\rho^{\alpha_\xi} V} \rho^{2\beta_\xi} \sum_{k_\lambda}^{k_F} \sum_{k_\mu}^{k_F} \delta_{k_\lambda k_\mu} \\
&= \sum_{\xi=a,r} \frac{1}{2} W_\xi \frac{4}{\rho^{\alpha_\xi} V} \sum_k^{k_F} 1 \\
&= \sum_{\xi=a,r} 2 W_\xi \rho^{2\beta_\xi - \alpha_\xi} V^{-1} \left(\frac{V}{(2\pi)^3} \int_0^{k_F} 4\pi\, k^2\, dk \right) \\
&= \sum_{\xi=a,r} \frac{1}{2} W_\xi \rho^{2\beta_\xi - \alpha_\xi} \frac{2k_F^3}{3\pi^2} \\
&= \sum_{\xi=a,r} \frac{1}{2} \rho^{2\beta_\xi - \alpha_\xi + 1}
\end{aligned}
\tag{6.16}
$$

and the energy per nucleon, $E_\xi/A \to 0$ as $A \to \infty$. Note that this is in accord with the results presented in chapter 5 for the exchange contribution to the HF energy where the contributions are seen to become smaller as A is increased.

6.2   Asymmetric nuclear matter

In asymmetric nuclear matter the proton and neutron densities are not equal. The asymmetry is characterized by the quantity I, defined as

$$
I = \frac{N - Z}{A}
\tag{6.17}
$$

6.2.1   Density

The proton and neutron densities are defined in terms of the I parameter as

$$
\rho_p = -\frac{1}{2}(I - 1)\rho = \frac{1}{2}(1 - I)\rho
\tag{6.18}
$$

$$
\rho_n = \frac{1}{2}(1 + I)\rho.
\tag{6.19}
$$

In addition, the relation (6.5) between density and Fermi momentum may be derived for the case of a proton and a neutron Fermi momentum:

$$
\rho_n = \frac{k_{F(n)}^3}{3\pi^2}
\tag{6.20}
$$

$$
\rho_n = \frac{k_{F(p)}^3}{3\pi^2}.
\tag{6.21}
$$

Note that these expressions differ from Equation (6.5) each by a factor of two since there is not a sum over the isospin.

6.2.2   Kinetic Energy

Now the kinetic energy is the sum of proton and neutron kinetic energies:

$$
\begin{aligned}
T &= \sum_{k\sigma}^{k_{F(p)}} \frac{1}{V} \int d^3r\, e^{ik\cdot r} \chi_\sigma^\dagger \left(-\frac{\hbar^2 \nabla^2}{2m_p}\right) e^{ik\cdot r} \chi_\sigma + \sum_{k\sigma}^{k_{F(n)}} \frac{1}{V} \int d^3r\, e^{ik\cdot r} \chi_\sigma^\dagger \left(-\frac{\hbar^2 \nabla^2}{2m_n}\right) e^{ik\cdot r} \chi_\sigma \\
&= \sum_{k\sigma}^{k_{F(p)}} \frac{\hbar^2 k^2}{2m_p} + \sum_{k\sigma}^{k_{F(n)}} \frac{\hbar^2 k^2}{2m_n} \\
&= 2\frac{V}{(2\pi)^3}\frac{\hbar^2}{2m_p}\int_0^{k_{F(p)}} k^4\, dk\, 4\pi + 2\frac{V}{(2\pi)^3}\frac{\hbar^2}{2m_n}\int_0^{k_{F(n)}} k^4\, dk\, 4\pi \\
&= \frac{2}{5}\frac{V}{(2\pi)^3}4\pi\frac{\hbar^2 k_{F(p)}^5}{2m_p} + \frac{2}{5}\frac{V}{(2\pi)^3}4\pi\frac{\hbar^2 k_{F(n)}^5}{2m_n} \\
&= V\frac{\hbar^2}{2m_p}\frac{3}{5}(3\pi)^{2/3}\rho_p^{\frac{5}{3}} + V\frac{\hbar^2}{2m_n}\frac{3}{5}(3\pi)^{2/3}\rho_n^{\frac{5}{3}}
\end{aligned} \tag{6.22}
$$

and the kinetic energy per particle is

$$
\begin{aligned}
\frac{T}{A} &= \frac{\hbar^2}{2m_p}\frac{3}{5}(3\pi^2)^{2/3}\rho_p^{\frac{5}{3}}\frac{V}{A} + \frac{\hbar^2}{2m_n}\frac{3}{5}(3\pi^2)^{2/3}\rho_n^{\frac{5}{3}}\frac{V}{A} \\
&= \frac{\hbar^2}{2m_p}\frac{3}{5}(3\pi^2)^{2/3}\frac{\rho_p^{\frac{5}{3}}}{\rho} + \frac{\hbar^2}{2m_n}\frac{3}{5}(3\pi^2)^{2/3}\frac{\rho_n^{\frac{5}{3}}}{\rho}
\end{aligned} \tag{6.23}
$$

which is expressed in terms of the I parameter as

$$
\begin{aligned}
\frac{T}{A} &= \frac{\hbar^2}{2m_p}\frac{3}{5}(3\pi^2)^{2/3}\frac{1}{2^{5/3}}(1-I)^{5/3}\rho^{2/3} + \frac{\hbar^2}{2m_n}\frac{3}{5}(3\pi^2)^{2/3}\frac{1}{2^{5/3}}(1+I)^{5/3}\rho^{2/3} \\
&= c_p\frac{1}{2^{5/3}}(1-I)^{5/3}\rho^{2/3} + c_n\frac{1}{2^{5/3}}(1+I)^{5/3}\rho^{2/3}
\end{aligned} \tag{6.24}
$$

6.2.3   Potential Energy

The zero result for the exchange term in the case of symmetric nuclear matter was due to the exchange of the space coordinates. The character of the space part in the isospin-dependent term is exactly the same and the result is similarly zero. In addition, then, to the isospin-independent parts of the monopole interaction, there is an additional direct contribution from the "b"-terms of the isospin-dependent part of the force. The energy due to this term is

$$
E_D = \sum_{\xi=a,r} \frac{1}{2}W_\xi b_\xi f_{\alpha_\xi} \sum_{k_\lambda \sigma_\lambda \tau_\lambda} \sum_{k_\mu \sigma_\mu \tau_\mu} \langle \lambda\mu | \rho^{\beta_\xi} \rho^{\beta_\xi} \tau_{1z}\tau_{2z} | \lambda\mu \rangle \tag{6.25}
$$

In the case where $\tau_\lambda = \tau_\mu = q$ the energy is

$$
\begin{aligned}
E_{qq} &= \sum_{\xi=a,r} \frac{1}{2} W_\xi b_\xi f_{\alpha_\xi} \left(\sum_{k\sigma}^{k<k_{F(q)}} \int e^{-ik\cdot r} \rho^{\beta_\xi} e^{ik\cdot r} \, d^3r \right)^2 \\
&= \sum_{\xi=a,r} 2W_\xi b_\xi V^{-1} \rho^{2\beta_\xi - \alpha_\xi} \left(\sum_k^{k_{F(q)}} 1 \right)^2 \\
&= \sum_{\xi=a,r} 2W_\xi b_\xi V^{-1} \rho^{2\beta_\xi - \alpha_\xi} \left(\frac{V}{(2\pi)^3} 4\pi \int_0^{k_{F(q)}} k^2 \, dk \right)^2 \\
&= \sum_{\xi=a,r} \frac{1}{18\pi^4} V W_\xi b_\xi \rho^{2\beta_\xi - \alpha_\xi} k_{F(q)}^6 \\
&= \sum_{\xi=a,r} \frac{1}{18\pi^4} V W_\xi b_\xi \rho^{2\beta_\xi - \alpha_\xi} (3\pi^2 \rho_q)^2 \\
&= \sum_{\xi=a,r} \frac{1}{2} V W_\xi b_\xi \rho^{2\beta_\xi - \alpha_\xi} (\rho_p^2 + \rho_n^2)
\end{aligned}
\tag{6.26}
$$

and in the case $\tau_\lambda \neq \tau_\mu$ the combined action of the isospin operators gives a negative sign:

$$
\begin{aligned}
E_{q\bar{q}} &= -\sum_{\xi=a,r} \frac{1}{2} W_\xi b_\xi f_{\alpha_\xi} \left(\sum_{k\sigma}^{k<k_q} \int e^{-k\cdot r} \rho^{\beta_\xi} e^{ik\cdot r} \, d^3r \right) \left(\sum_{k\sigma}^{k<k_{F(\bar{q})}} \int e^{-k\cdot r} \rho^{\beta_\xi} e^{ik\cdot r} \, d^3r \right) \\
&= -\sum_{\xi=a,r} 2W_\xi b_\xi V^{-1} \rho^{2\beta_\xi - \alpha_\xi} \left(\sum_k^{k_{F(q)}} 1 \right) \left(\sum_k^{k_{F(\bar{q})}} 1 \right) \\
&= -\sum_{\xi=a,r} W_\xi b_\xi V^{-1} \rho^{2\beta_\xi - \alpha_\xi} \left(\frac{V}{(2\pi)^3} 4\pi \int_0^{k_{F(q)}} k^2 \, dk \right) \left(\frac{V}{(2\pi)^3} 4\pi \int_0^{k_{F(\bar{q})}} k^2 \, dk \right) \\
&= -\sum_{\xi=a,r} V W_\xi b_\xi \rho^{2\beta_\xi - \alpha_\xi} \rho_p \rho_n
\end{aligned}
\tag{6.27}
$$

Then the total energy due to the isospin-dependent term is

$$
E_D = \sum_{\xi=a,r} \frac{1}{2} W_\xi b_\xi \rho^{2\beta_\xi - \alpha_\xi} V (\rho_p - \rho_n)^2
\tag{6.28}
$$

and the energy per particle is

$$
E_D/A = \sum_{\xi=a,r} \frac{1}{2} W_\xi b_\xi \rho^{2\beta_\xi - \alpha_\xi - 1} (\rho_p - \rho_n)^2 .
\tag{6.29}
$$

The energy per particle of asymmetric nuclear matter, in terms of the total density and the asymmetry parameter I is:

$$
\begin{aligned}
\eta(\rho, I) \quad = \quad & c_p \frac{1}{2^{5/3}} (1 - I)^{5/3} \rho^{2/3} + c_n \frac{1}{2^{5/3}} (1 + I)^{5/3} \rho^{2/3} \\
+ \quad & \frac{1}{2} W_a \rho^{2\beta_a - \alpha_a + 1} + \frac{1}{2} W_r \rho^{2\beta_r - \alpha_r + 1} \\
+ \quad & \frac{1}{2} W_a b_a \rho^{2\beta_a - \alpha_a + 1} I^2 + \frac{1}{2} W_r b_r \rho^{2\beta_r - \alpha_r + 1} I^2
\end{aligned}
\tag{6.30}
$$

6.3 Observables

6.3.1 Symmetric nuclear matter

As a function of the density, the energy per particle in nuclear matter for a physical system has a minimum at the saturation density (ρ_0) with a value η_0. The observed value of $\eta = E/A$ at saturation density is determined from the liquid drop model to fits of a large number of finite nuclei and is taken to be[22]

$$
E_0 = -16.0 \pm 0.2 \ \text{MeV}.
\tag{6.31}
$$

One may expand the function $\eta = E/A$ about this minimum point:

$$
\eta(\rho) = \eta|_{\rho_0} + (\rho - \rho_0) \left. \frac{\partial \eta}{\partial \rho} \right|_{\rho_0} + \frac{(\rho - \rho_0)^2}{2} \left. \frac{\partial^2 \eta}{\partial \rho^2} \right|_{\rho_0} + \cdots
\tag{6.32}
$$

For the state of density ρ to be a minimum the first derivative must be zero. The physical parameter proportional to the first derivative is the pressure

$$
P = -\frac{\partial \eta}{\partial v} = \rho^2 \frac{\partial \eta}{\partial \rho}
\tag{6.33}
$$

where $v = 1/\rho$ is the volume per particle. The expression for the pressure in symmetric nuclei is

$$
P = \frac{2}{3} a_k \rho^{5/3} + \frac{1}{2} W_a (2\beta_a - \alpha_a + 1) \rho^{2\beta_a - \alpha_a + 2} + \frac{1}{2} W_r (2\beta_r - \alpha_r + 1) \rho^{2\beta_r - \alpha_r + 2}.
\tag{6.34}
$$

The quadratic term in the Taylor expansion is identified as the incompressibility, K,

$$
K = 9\rho^2 \left. \frac{\partial^2 \eta}{\partial \rho^2} \right|_{\rho_0}.
\tag{6.35}
$$

K is a measure of the energy needed to produce a density change in the nuclear matter. Its value is not well known, but is inferred from those excitation in finite

nuclei which correspond to density fluctuations (the *breathing mode*) to be 210 ± 20 MeV[85]. A generalized $K(\rho)$ may be defined for non-equilibrium densities [22]:

$$K = 9\rho^2 \frac{\partial^2 \eta}{\partial \rho^2} + 18\frac{P}{\rho} \tag{6.36}$$

where P is the pressure as defined above. Evaluated for the force in this thesis, the generalised incompressibility is

$$\begin{aligned} K &=& -2a_k\rho^{2/3} + \frac{9}{2}W_a(2\beta_a - \alpha_a + 1)(2\beta_a - \alpha_a)\rho^{2\beta_a - \alpha_a + 1} \\ &+& \frac{9}{2}W_r(2\beta_r - \alpha_r + 1)(2\beta_r - \alpha_r)\rho^{2\beta_r - \alpha_r + 1} + 18\frac{P}{\rho}. \end{aligned} \tag{6.37}$$

6.3.2 Asymmetric nuclear matter

Aside from the leading term in the Bethe-Weizsäcker mass formula, the asymmetry term also has an A-dependence such that it should be finite in asymmetric nuclear matter. Its form is

$$\eta|_{asym} = a_s \frac{(N-Z)^2}{A^2} \tag{6.38}$$

and the parameter a_s, like the leading term E_0 above is fitted to a large number of observed binding energies. This coefficient is identified in the expression (6.30) as

$$a_s = \frac{1}{2}\frac{\partial^2 \eta}{\partial I^2}. \tag{6.39}$$

Typical values for this parameter range from 18.6 Mev [77], to 23.7 MeV [78], to 33 MeV [79], the last value being the most recent. For the present case, the separable interaction gives for a_s:

$$a_s = \frac{5}{36}c_p\frac{\rho^{2/3}}{(1-I)^{1/3}} + \frac{5}{36}c_n\frac{\rho^{2/3}}{(1+I)^{1/3}} + \frac{1}{2}W_ab_a\rho^{2\beta_a - \alpha_a + 1} + \frac{1}{2}W_rb_r\rho^{2\beta_r - \alpha_r + 1}. \tag{6.40}$$

At $I = 0$ this expression becomes

$$a_s = \frac{5}{36}c_p\rho^{2/3} + \frac{5}{36}c_n\rho^{2/3} + \frac{1}{2}W_ab_a\rho^{2\beta_a - \alpha_a + 1} + \frac{1}{2}W_rb_r\rho^{2\beta_r - \alpha_r + 1}. \tag{6.41}$$

In addition one may consider the equation of state for pure neutron matter ($I = 1$). Although no observables as such are known, due to the fact that neutron matter is not bound by nuclear forces, this very fact may be used as a condition, i.e. neutron matter should not be predicted to be bound by the model. The binding energy of neutron matter is given from Equation 6.30 with $I = 1$ and $\rho = \rho_n$:

$$\eta = c_n 2^{2/3}\rho_n^{2/3} + \frac{1}{2}(1+b_a)W_a\rho_n^{2\beta_a - \alpha_a + 1} + \frac{1}{2}(1+b_r)W_r\rho_n^{2\beta_r - \alpha_r + 1} \tag{6.42}$$

6.4   Results

Results are presented for the parameter set used to fit finite nuclei. This values of the parameters are given at the beginning of the next chapter.

The curves of energy per particle in symmetric nuclear matter (SNM) and Pure Neutron Matter (PNM) are shown in Figure 6.1. The equilibrium point for symmetric nuclear matter occurs at $\rho_0 = 0.155$ fm^{-3} with an energy per nucleon of -15.56 MeV. This compares favourably with the inferred experimental[22] values of -16.0 ± 0.2 MeV at a saturation density of $\rho_0 = 0.16 \pm 0.005$ fm^{-3}, especially when one considers that the force parameters used were fitted to finite nuclei. In addition, different mass formula fits to the data give slightly different "experimental" results for nuclear matter properties, so, for instance, a recent paper of Heiselberg[86] gives $\eta_0 = -15.6 \pm 0.2$ MeV and they consider the value of the saturation to be more uncertain, at $\rho_0 = 0.16 \pm 0.02$ fm^{-3}. The curve for PNM shows the result that neutron matter is unbound at any density and everywhere less stable than symmetric matter, as it should be. This is in contrast to most Skyrme interactions fitted to finite nuclei which have PNM more stable than SNM above a threshold density which may be quite low (~ 0.4 fm^{-3} in the case of the force parameterisation SIII[22]).
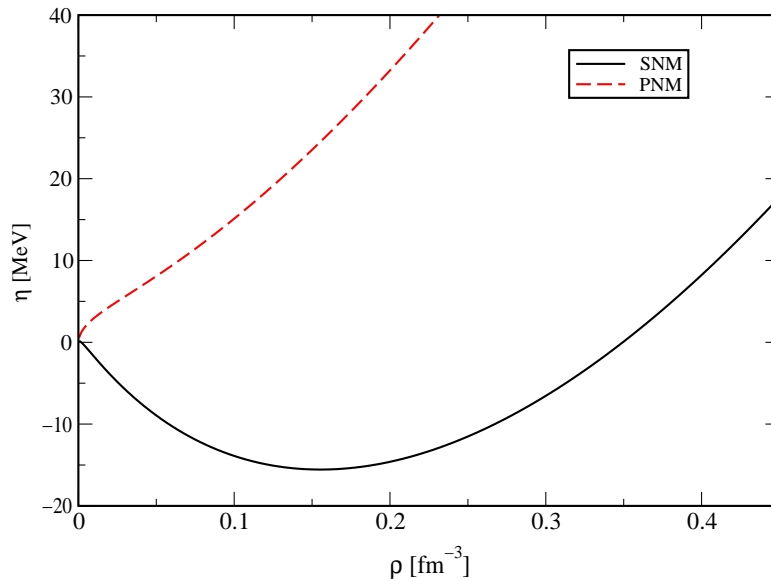

Figure 6.1: *Energy per particle in Symmetric Nuclear Matter (SNM) and Pure Neutron Matter (PNM). The saturation density is $\rho_0 = 0.155$ fm^{-3} and the energy per nucleon at saturation is -15.56 MeV.*

Force	Separable	SIII[80]	SGII[81]	SkM*[82]	SkP[83]	T6[84]	SLy230a[22]
ρ_0	0.155	0.145	0.158	0.160	0.162	0.161	0.160
k_F	1.319	1.291	1.328	1.333	1.340	1.355	1.133
r_0	1.155	1.180	1.147	1.143	1.137	1.141	1.143
η_0	-15.56	-15.85	-15.59	-15.77	-15.95	-15.96	-15.97
K_∞	218.2	355.4	214.6	216.6	201.0	135.9	229.9
m_∞^*/m	1.0	0.76	0.79	0.79	1.0	1.0	0.695
a_s	36.90	28.16	26.83	30.03	30.00	29.97	32.01

Table 6.1: *Properties of infinite nuclear matter at equilibrium for the separable interaction used in this thesis as well as some typical Skyrme interactions. The observables are the equilibrium density, ρ_0 [fm^{-3}], the Fermi momentum, k_F [fm^{-1}], $r_0 = (9\pi)^{1/3}/2k_f$ [fm] is the mean distance between two nucleons in the fluid, η_0 [MeV] is the energy at saturation density, K_∞ [MeV] is the incompressibility, m^*/m is the effective mass and a_s [MeV] is the asymmetry energy.*

A comparison of various observables between the selection of Skyrme forces used in the paper of Chabanat et. al.[22] and the separable force of this thesis is presented in Table 6.1. The first five Skyrme parameterisations listed were chosen to be a representative sample and the final one, SLy230a was the result of fitting to neutron-rich neutron matter and neutron star properties. Most of the observables compare favourably with those of the best Skyrme parameterization listed, SLy230a. The asymmetry parameter is perhaps too high, but it is closer to the value of that for SLy230a than the other listed parameterisations.

6.5   Neutron Star

One possible result of the collapse of a normal star at the end of its life is the formation of neutron star. Radio pulsars such as the object in the remnant of the Crab supernova are believed to be such stars which begin their life rotating rapidly but slow down rather quickly due to their high magnetic fields. The supposed structure of a neutron star is shown schematically in Figure 6.2. It is from the equations of state (EoS) of the *realistic* interactions that this picture is inferred and although the detailed results differ as one considers different models and interactions, the general features are the same. At the surface the density is only on the order of ~ 10 g cm^{-3}, which is about the same as 'normal' matter. The density rises rapidly through two layers of crust to $\sim 2 \times 10^{14}$ g cm^{-3}. The outer layer of crust consists of a gas of nuclei and electrons. Above the neutron drip density $\sim 4 \times 10^{11}$ g cm^{-3} the gas is supplemented by neutrons to form the inner crust. At
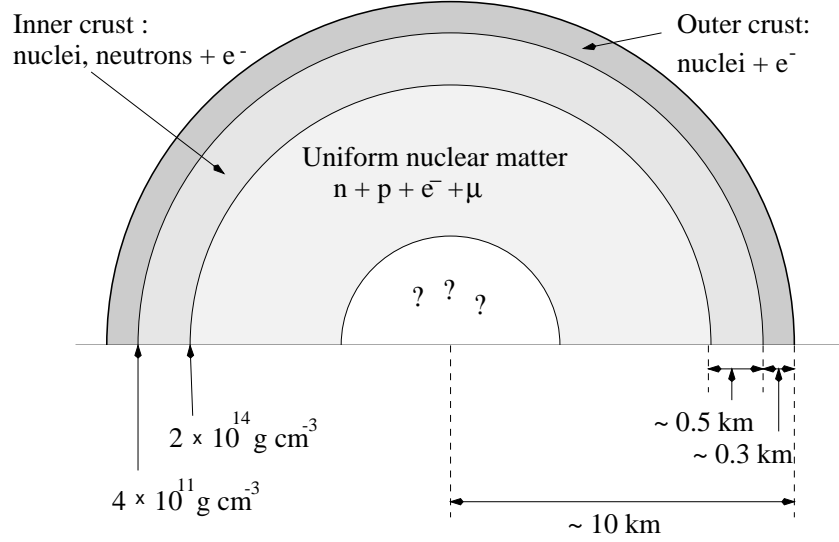
Figure 6.2: *Schematic view of the possible structure of a neutron star showing regions where nuclei and nuclear matter dominate. The central region may be quark matter. Figure is take from Ref.[86]*

greater densities, from about $\sim 4 \times 10^{11}$ g cm $^{-3}$ to $\sim 10^{15}$ g cm^{-3} the star consists of homogeneous nuclear matter with electrons and, above the threshold density for their creation, muons. At higher densities, in the core, hyperons may appear, or even quark matter. Since the interaction under study is between nucleons only, the $npe\mu$ region is extrapolated to the core. This is the technique adopted by Chabanat *et. al.*[22] and Wiringa *et. al.*[87].

In this section, the usual notation for describing neutron stars is used, which is somewhat contrary to the usual nuclear physicist's notation for nuclear matter. The number densities are written as n_b, n_p and n_n for baryons, protons and neutrons respectively. The symbol ρ is used as the mass density.

To describe a neutron star's properties an equation of state is derived which is the pressure as a function of the density

$$P(n_b) = n_b^2 \frac{d(e/n_b)}{dn_b} \tag{6.43}$$

where e is the energy density, and is related to the mass density $\rho(n_b) = e(n_b)/c^2$. The equation of state is derived in Appendix G.

EOS configuration	Separable M_{max}	SLy230a M_{max}	SLy230b M_{max}	Separable $1.4 M_\odot$	SLy230a $1.4 M_\odot$	SLy230b $1.4 M_\odot$
n_c (fm^{-3})	1.14	1.15	1.21	0.459	0.508	0.538
ρ_c (10^{14} g cm^{-3})	26.6	26.9	28.5	8.43	9.25	9.85
R (km)	10.3	10.25	9.99	12.1	11.8	11.7
M ($M_\odot$)	2.02	2.10	2.05	1.40	1.40	1.40
A (10^{57})	2.80	2.99	2.91	1.84	1.85	1.85
E_{bind} (10^{53} erg)	5.69	7.07	6.79	2.34	2.60	2.61
z_{surf}	0.539	0.591	0.593	0.233	0.240	0.244

Table 6.2: *Parameters of the neutron star models.* n_c *is the central number density and is the independent variable in the equation of state.* ρ_c *is the central mass density.* R *is the radius of the star,* M *is the mass in units of the solar mass.* A *is the number of baryons.* E_{bind} *is the binding energy of the star and* z_{surf} *is the gravitational red-shift (see ref [22])*

The calculation of a neutron star in this work is valid for non-rotating neutron stars. This is necessary for a simple calculation to be possible, and thanks to the Hubble telescope a non-rotating, non-accreting neutron star has actually now been observed due to its thermal emission alone[88]. For such a non-rotating star, Tolman, Oppenheimer and Volkoff (TOV) derived an equation of hydrostatic equilibrium[89, 90]:

$$\frac{dP}{dr} = -\frac{Gm\rho}{r^2} \frac{\left(1 + \frac{P}{\rho c^2}\right)\left(1 + \frac{4\pi r^3 P}{mc^2}\right)}{1 - \frac{2Gm}{rc^2}} \qquad (6.44)$$

with

$$m(r) = \int_0^r 4\pi r'^2 \rho(r')\, dr'. \qquad (6.45)$$

To solve these equations the following procedure is used:

- A central density, ρ_c is chosen. This gives from the EoS the central pressure, P_c. The boundary condition $m(r = 0) = 0$ is chosen.

- The TOV equation, (6.44), and the mass relation (6.45) are integrated numerically out from $r = 0$. This yields at each step a pressure, $P(r)$, given by the EoS.

- The condition $P = 0$ defines the surface of the star, at which $r = R$ is the radius and $m(R)$ is the mass.

With this prescription the TOV equation is solved for a number of central densities. A consequence of general relativity is that a maximum mass exists for the star. Results for some observables are shown in Table 6.2 for the maximum mass
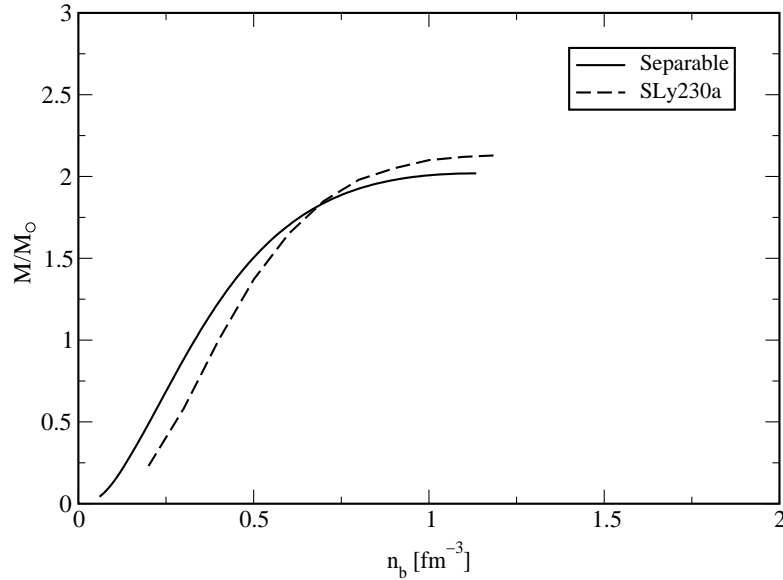
Figure 6.3: *Gravitational mass in units of solar mass of neutron star as a function of the central baryon density. Solid line is for the separable interaction in this thesis and the dashed line is for the Skyrme parameterisation SLy230a[22].*

star and for a star of mass $1.4M_{\odot}$ which is a commonly chosen benchmark in the literature. The results for the separable force are compared with results from Chabanat et. al. [22] which are for Skyrme force parameterisations fitted to nuclei at the extremes of density and isospin asymmetry.

Figure 6.3 shows the mass of the neutron star as a function of the central baryon density. The conclusion from these results is that the separable interaction gives rather similar results to the best Skyrme interactions used for neutron star calculations. The Skyrme forces to which the separable interaction is compared were themselves compared[22] to the "realistic" calculations of Wiringa et. al.[87] and found to be very similar. The separable force, then, predicts similar neutron star properties to other contemporary models, using both realistic and effective interactions.

Figure 6.4 shows neutron star binding energy as a function of mass. The box indicates the measured mass and binding energy, based on observed energy release, of the neutron star which presumably was created in the supernova 1987A[91]. The separable force calculations are consistent with this observation since part of the curve lies within the box.
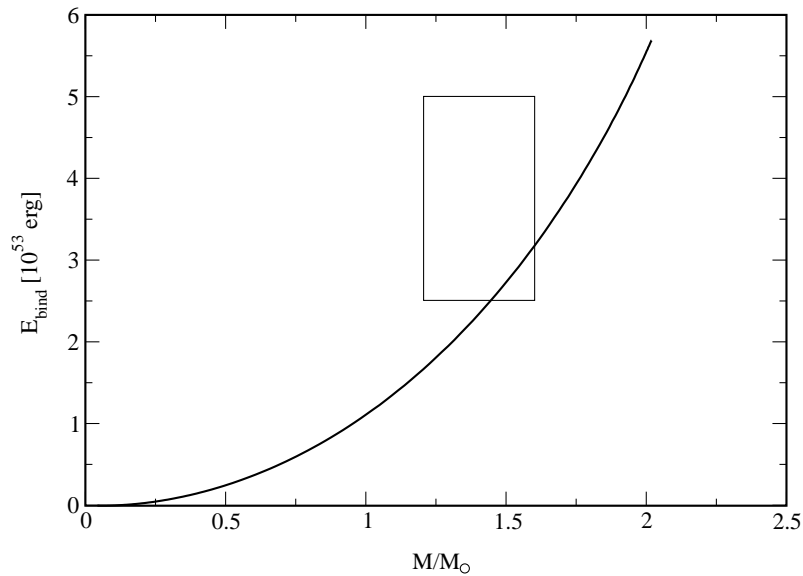
Figure 6.4: *Binding energy of a neutron star as a function of its mass. The box represents the possible values for the neutron star created in Supernova 1987A.*

6.6 Perturbation Calculations

So far the treatment of nuclear matter has been at the mean-field level with the single-particle states being plane waves. One would also like to calculate the corrections to this approximation since they could be quite large, particularly in the case of hard-core potentials. The usual approach taken in these cases is to include all the ladder diagrams which is facilitated by solving the Bethe-Goldstone equation[92, 36]. In the case of the separable interaction, the following remarkable property holds: In infinite nuclear matter the solution of the HF equations represents the exact ground state. To see this, one notes that the correlations to
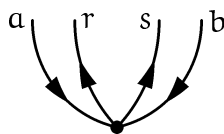

Figure 6.5: *Insertion appearing at the bottom of every Hugenholz diagram for the vacuum amplitude.*

the ground state energy can be described in terms of Hugenholz diagrams (See Appendix D). Following the rules given in the Appendix, one finds that all diagrams must include the insertion shown in Figure 6.5. This follows from the fact that a diagram must have a lowest dot, in the sense of being at the bottom of the diagram (i.e. earliest in time-ordering). Since four lines must leave this dot and they must connect to others, each of the lines must move upwards. Furthermore, by the rules of labelling lines, two of them must enter the dot and two must leave, so two are hole lines and two are particle lines. The matrix element associated with this dot is then

$$\langle ab|\tilde{V}|rs\rangle \qquad (6.46)$$

with a and b representing hole states and r and s representing particle states. Due to the nature of the separable interaction, the matrix element becomes

$$\langle ab|\tilde{V}|rs\rangle \propto \left(\langle a|\rho^\beta|r\rangle\langle b|\rho^\beta|s\rangle - \langle a|\rho^\beta|s\rangle\langle b|\rho^\beta|r\rangle\right) \qquad (6.47)$$

which is zero since the density is just a constant in infinite nuclear matter and each hole state is orthogonal to each particle state.

Chapter 7

Ground–State Properties of Nuclei

This chapter presents results for a set of parameters fitted according to the pre-scription of Chapter 3. All Hartree-Fock calculations are performed in a basis with 12 radial states per angular momentum state and iteration continues until the HF energy has converged to 10keV. The resulting set of basis states then forms the reference state used in the perturbation calculation. Since ample experimental data exist for finite nuclei, unlike infinite nuclear matter, the emphasis is on comparison to experimental data rather than to other interactions.

7.1 Force Parameters

The parameters for the monopole force are presented in Table 7.1. The higher multipole parameters are not included in this fit since their main contribution is to excited states and to deformations and fixing the parameters to a fit to ground–state properties of spherical nuclei is not appropriate. Some discussion of their possible role in the region of this fit is given.

W_a	α_a	β_a	a_a	b_a
-1543.8 MeV fm^3	2.0	1.0	-0.4295	-0.419825

W_r	α_r	β_r	a_r	b_r
1778.0 MeV fm$^{3.8265}$	2.2165	1.246	-1.4788	-0.314625

c			k	
160.0 Mev fm^5			16.0 Mev fm^{10}	

Table 7.1: *Monopole force parameters*

7.2   Nuclear Energies

The nuclear energies per particle of the nuclei in the fit are plotted in Figure 7.1 in the HF approximation and compared to the experimental results. Most of the experimental data are taken from Ref. [93] and have an experimental error of 300 keV or less, which makes the error bar smaller than the symbol on the plot in all cases. The value for ^{100}Sn was recently measured at 825.8(9) Mev[94]. The data for ^{48}Ni is extrapolated from a systematic study and is assumed to have an error of only about 200 keV [97]. The value for ^{78}Ni is also an extrapolated value. The contributions due to the perturbation theory are not shown in the figure since they are rather small and would not be readily distinguishable from the points for the Hartree-Fock energies for most of the nuclei. They are presented in Table 7.2 along with the experimental values.

The calculated energies are seen to follow the same trends as the theoretical curve, although there are some notable exceptions. ^{16}O is clearly very under-bound. Owing to the fact that the centre-of-mass correction is not treated, one
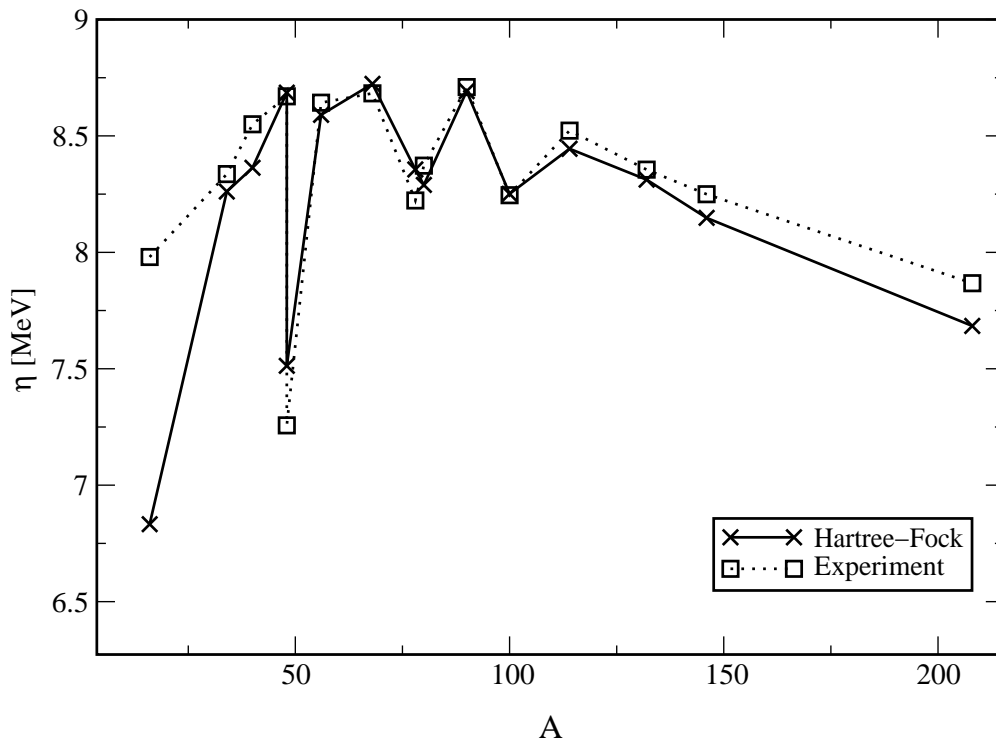

Figure 7.1: *Binding energy per nucleon in HF approximation*

Nucleus	E_{HF}	$E^{(2)}$	$E_{hh}^{(3)}$	$E_{pp}^{(3)}$	$E_{ph}^{(3)}$	E_{HF+2+3}	κ	Expt.
^{16}O	-109.32	-3.31	-0.1365	-0.3624	+0.921	-112.21	0.063	-127.68
^{34}Si	-280.88	-7.37	-0.0384	-0.4830	+1.223	-287.55	0.232	-283.43
^{40}Ca	-334.53	-2.51	-0.0323	-0.1114	+0.233	-336.95	0.052	-342.00
^{48}Ca	-417.01	-5.97	-0.0189	-0.2725	+0.273	-422.70	0.202	-416.16
^{48}Ni	-360.69	-6.57	-0.0130	-0.2058	+0.427	-367.05	0.234	-348.33
^{56}Ni	-481.25	-2.31	-0.0210	-0.0643	+0.123	-483.52	0.046	-483.99
^{68}Ni	-593.33	-6.00	-0.0109	-0.2091	+0.484	-598.85	0.221	-590.43
^{78}Ni	-651.90	-8.34	-0.0053	-0.1458	+0.477	-659.92	0.342	-641.38
^{80}Zr	-663.41	-1.87	-0.0087	-0.0411	+0.107	-665.22	0.044	-669.79
^{90}Zr	-782.70	-3.91	-0.0070	-0.1257	+0.103	-786.51	0.149	-783.89
^{100}Sn	-825.65	-1.71	-0.0060	-0.0220	+0.048	-827.35	0.039	-825.80
^{114}Sn	-963.20	-4.04	-0.0046	-0.1093	+0.226	-967.12	0.162	-971.57
^{132}Sn	-1097.65	-6.17	-0.0023	-0.0864	+0.209	-1103.70	0.287	-1102.92
^{146}Gd	-1190.32	-3.42	-0.0026	-0.0699	+0.142	-1193.66	0.146	-1204.44
^{208}Pb	-1599.04	-4.51	-0.0013	-0.0664	+0.108	-1603.51	0.233	-1636.45

Table 7.2: *Monopole Hartree-Fock energy and corrections from perturbation theory compared with experimental value. All energies are in MeV*

might expect to do quite badly in the lightest nuclei. On the other hand, typical values for the centre-of-mass correction in ^{16}O are about ten MeV[95] which is about half the difference between the experimental and calculated value presented here. Of course, one would need to re-fit the parameters in any case if the center-of-mass correction were included. An alternative possibility is that the value of the α-parameters are too large. From Fig. 5.3 it is seen that the contribution to the HF energy from the exchange term proportional to the α parameters is particularly large and positive for ^{16}O. Its value is selected to improve the overall fit, but it does so at the expense of the fit to ^{16}O. A possible solution lies in the multipole forces which for spherical nuclei act only in the exchange term which, like the monopole terms, presumably is strongest in the lightest nuclei, the choice of the A-dependent f_D and f_Q parameters notwithstanding.

The quality of the fit elsewhere is much better, with the next worst case after oxygen being ^{40}Ca, whose Hartree–Fock binding energy is about five percent off the experimental value. At the other end of the chart, ^{208}Pb is under-bound by quite a large amount in terms of total binding, but is not as serious a discrepancy in terms of energy per particle as in the lightest nuclei.

7.2.1   Perturbation Corrections

The smallness of the perturbation corrections in all the nuclei is notable. This work was predicated on the premise that it would be possible to find an effective

interaction which, when used in perturbation theory, would converge quickly with small corrections on top of the mean-field, and this is certainly a character of the chosen interaction. It is difficult to say how large the correlations ought to be since, as was pointed out in Chapter 2, the size of the correlations depend upon the efficacy of the single particle Hamiltonian. As a matter of comparison, correlation effects in Skyrme interactions have been estimated to be order of about ten MeV[96] for the total binding energy.

The A-dependence of the second order correction seems to be that the total correction to the HF energy remains of about the same order for nuclei across the periodic table. It has already been shown that the correction per nucleon in infinite nuclear matter is zero so the corrections for any diagram in finite nuclei must have an A-dependence weaker than $\propto A$. The reason for the lack in increase in binding energy correction in heavier nuclei may be explained in a similar way to the zero nuclear matter corrections. In that case it was the constant density which produced zero matrix elements. In the case of a heavy nucleus, the density is quite constant over the interior and only changes at surface, which may be of about the same width as in a light nucleus. In this way, the correlations may be seen as predominantly a surface effect, even though the force acts equally strongly over all ranges in the nucleus.

In addition, the corrections from perturbation theory are seen to be greater in $N{\neq}Z$ nuclei. From the discussion of the isospin-dependent term in Chapter 5, the reason for this is known to be that in $N{\neq}Z$ nuclei the isospin "flipping" operator, $\tau_1^+\tau_2^- + \tau_1^-\tau_2^+$, allows excitations in the same major shell to occur which give a large contribution. It is presumably not the case that N=Z nuclei in fact have less correlation energy than $N{\neq}Z$ nuclei so it may be necessary to consider reducing the strength of the isospin-dependent terms, although this would reduce the overall quality of the fit. On the other hand the inclusion of multipole forces which allow for a much broader range of excitations than the monopole force alone should smooth out these differences and increase the magnitude of the correlations.

In addition to the size of the correlations, the sign is also interesting. The second order correction is always negative definite but higher order corrections may be of any sign. In the third order the largest, by far, diagram – the particle-hole diagram – is always seen to be positive. This is in accord with studies of correlations with other forces [54, 96]. That it is the largest contribution suggests that long-range correlations are the most important effect arising from the monopole interaction.

7.3 Charge Radii and Densities

The root mean-square charge radii for the nuclei in the fit are given in Table 7.3 along with experimental data for those nuclei where it exists. The agreement with experiment is seen to be very good, with the main exception being ^{16}O, in which

Nucleus	r_{ch} HF (fm)	r_{ch} exp (fm)
^{16}O	2.85	2.69
^{34}Si	3.19	
^{40}Ca	3.54	3.48
^{48}Ca	3.47	3.48
^{48}Ni	3.88	
^{56}Ni	3.84	3.78
^{68}Ni	3.89	
^{78}Ni	3.87	
^{80}Zr	4.33	
^{90}Zr	4.29	4.27
^{100}Sn	4.60	
^{114}Sn	4.65	4.60
^{132}Sn	4.66	
^{146}Gd	5.02	4.96
^{208}Pb	5.50	5.50

Table 7.3: *Root mean-squared charge radii in HF approximation and experimentally. Experimental data is from [99]*

the error is about 5%, which is rather less than the error in the binding energy. The results are also displayed graphically in Fig. 7.2. The radii seem, in general, to be better reproduced than the binding energies, although data is not available for some of the more weakly bound nuclei presented. The radii for the under-bound light nuclei are somewhat too large, which is what one should reasonably expect to accompany under-binding. The relative good quality of the charge radii over the binding energy suggests that the single particle properties are comparatively better reproduced than many-body properties in the HF approximation.

Figures 7.3-7.17 show the point neutron, proton, charge and total densities for all the nuclei under consideration. In all plots, the total point density is the same on both sides of the y-axis. The left-hand side also gives the neutron point density and the right-hand side shows the proton point density as well as the charge density and, in cases where data is available, the experimental data.

The experimental data for the charge density is from the Fourier-Bessel decomposition in table IX of Ref. [99]. Even for those nuclei for which no data is available, the densities are plotted since they have a direct physical interpretation and they play an important role in the present interaction.

As shown by the moderate error in the charge radii, there is a visible discrepancy in the charge densities of ^{16}O and ^{40}Ca, particularly in the central region, though the error in the Fourier-transformed experimental data is the greatest in this region. This error should probably not be taken too seriously since no centre-of-mass correction is taken into account. The scale on all the plots is the same
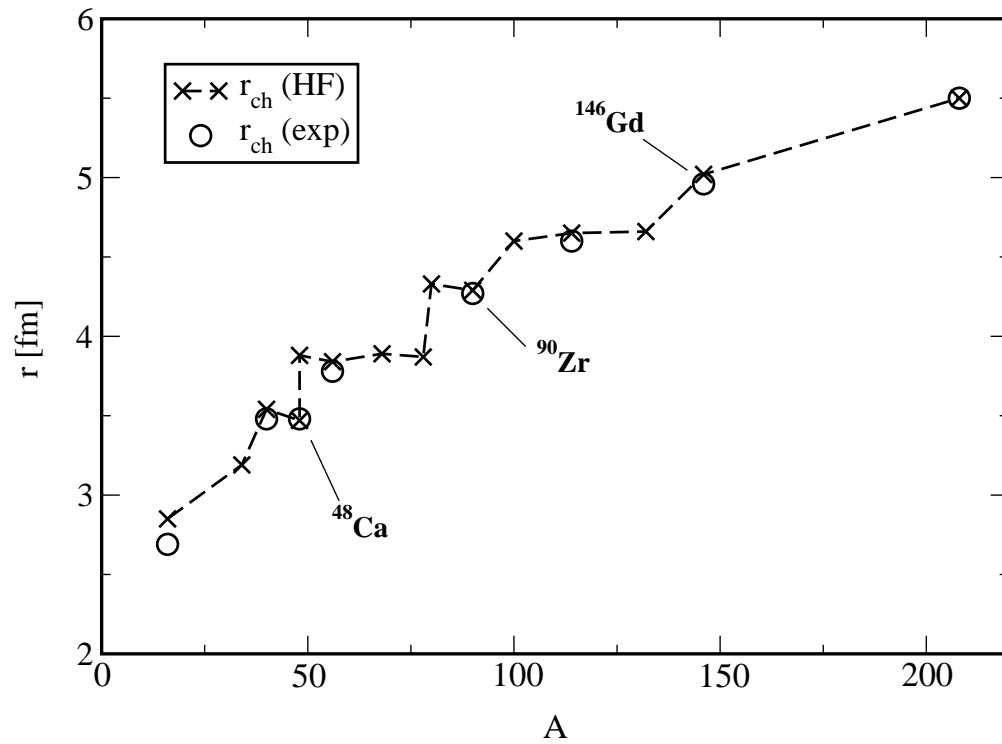
Figure 7.2: *Mean squared charge radii in HF approximation and experimentally. Experimental data is from the same reference as Table 7.3*

and it is easily seen that the central total densities for all the nuclei lie around the expected region of ~ 0.16 fm^{-3}.
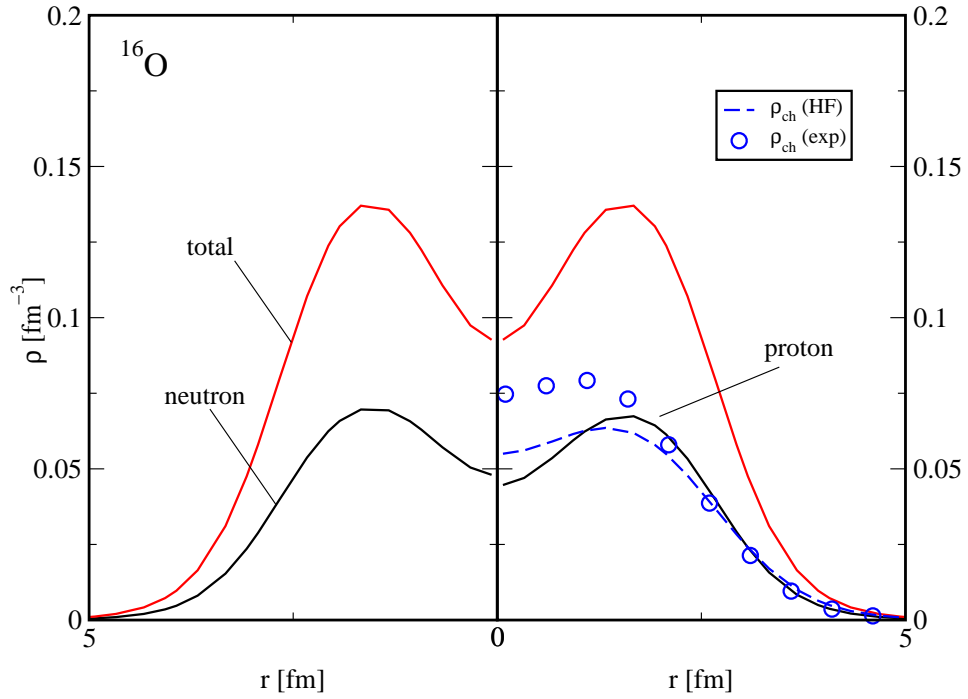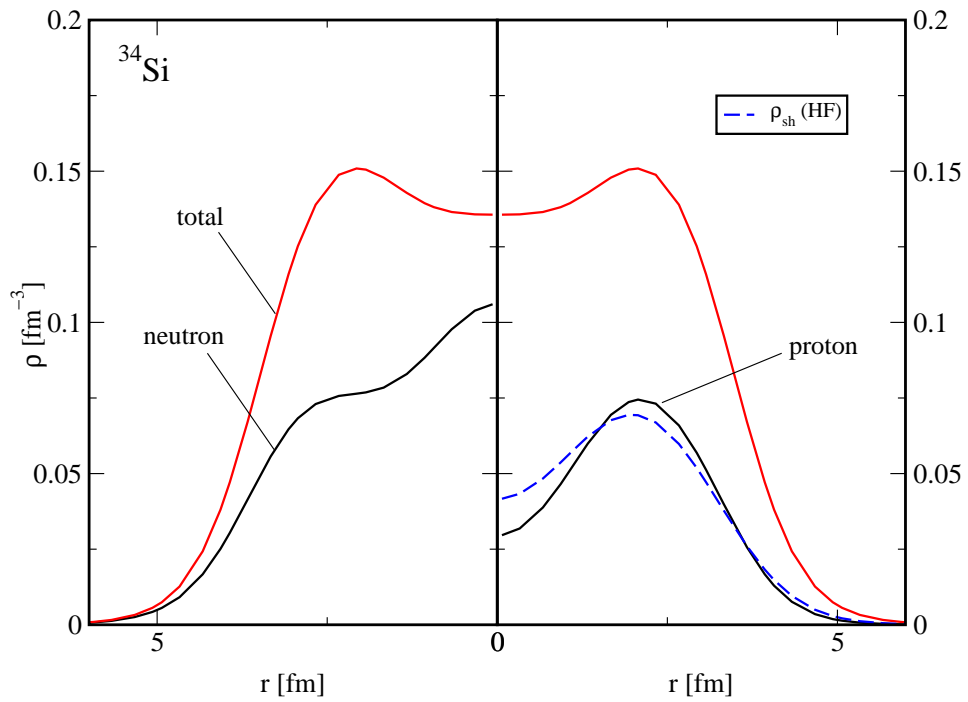
Figure 7.3: *Densities in ^{16}O*
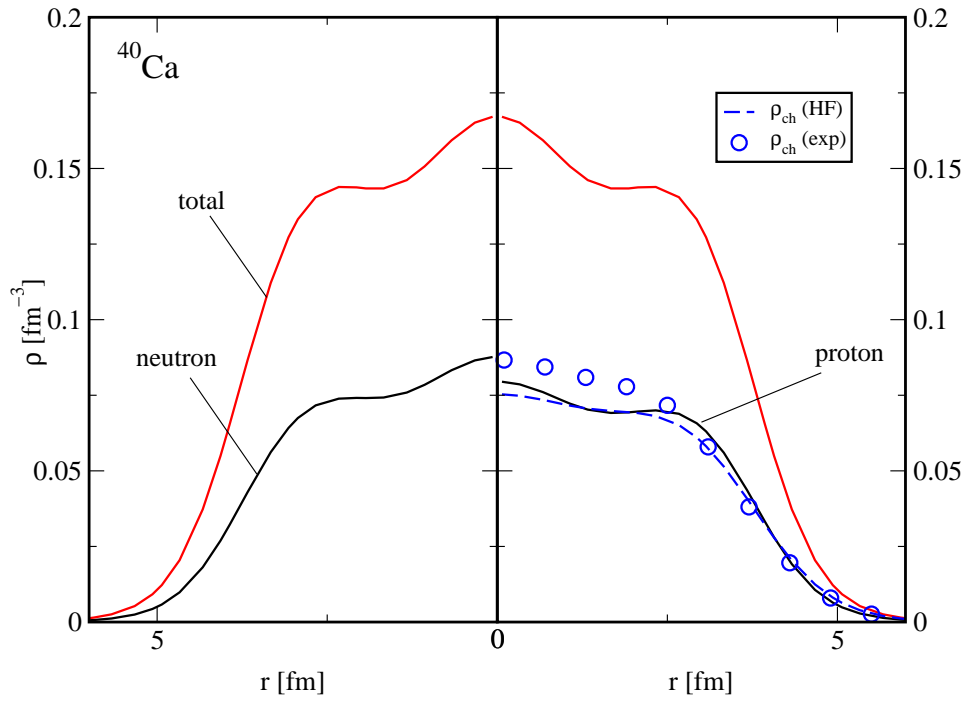

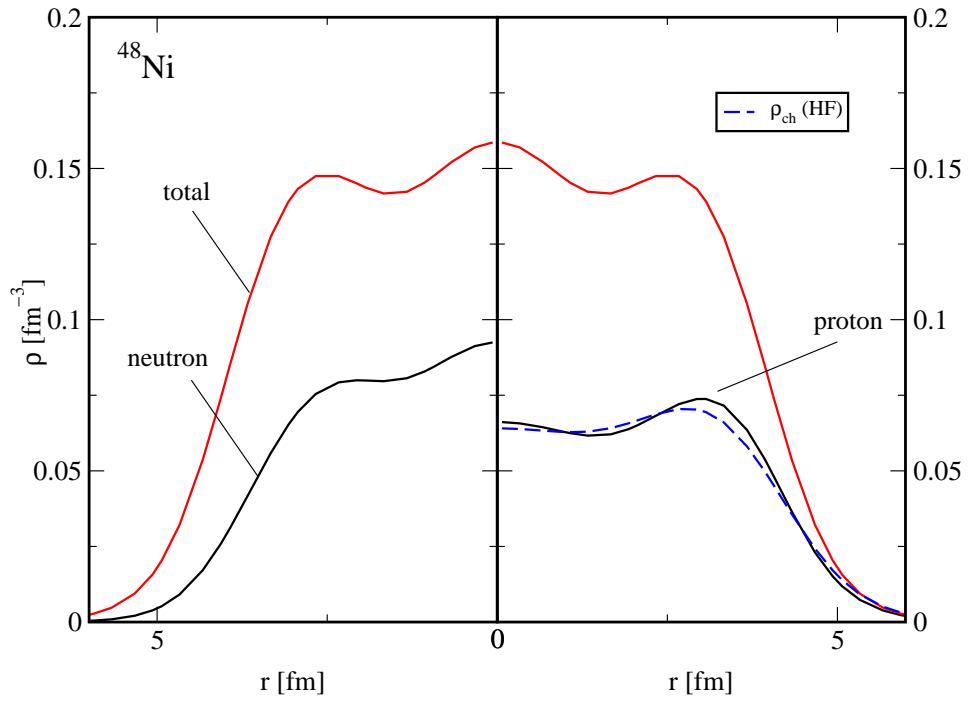Figure 7.4: *Densities in ^{34}Si*
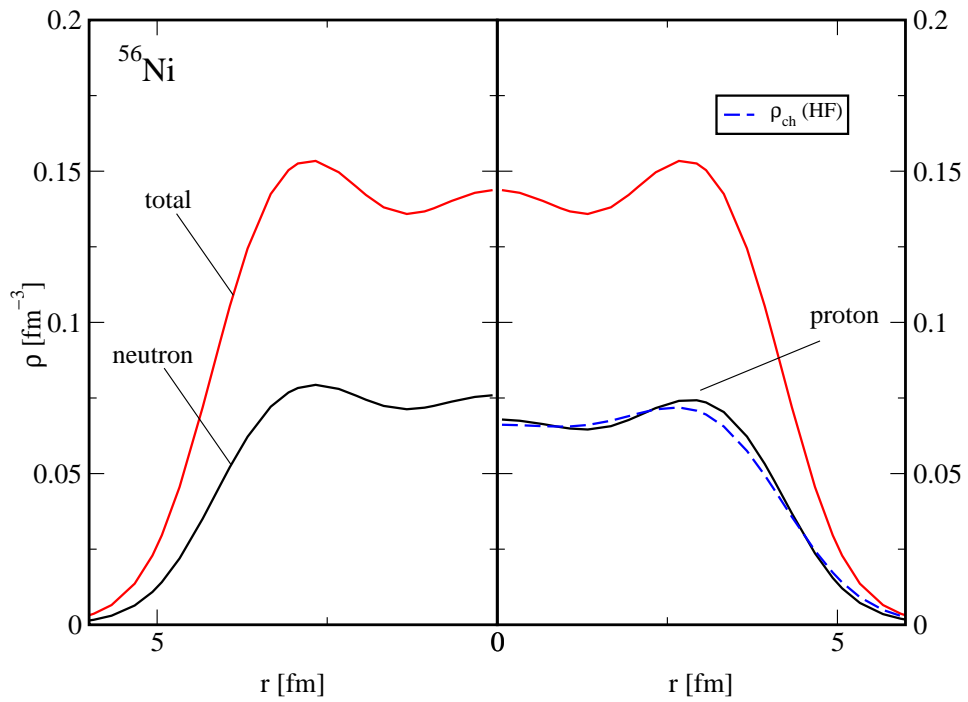
Figure 7.5: *Densities in* ^{40}Ca
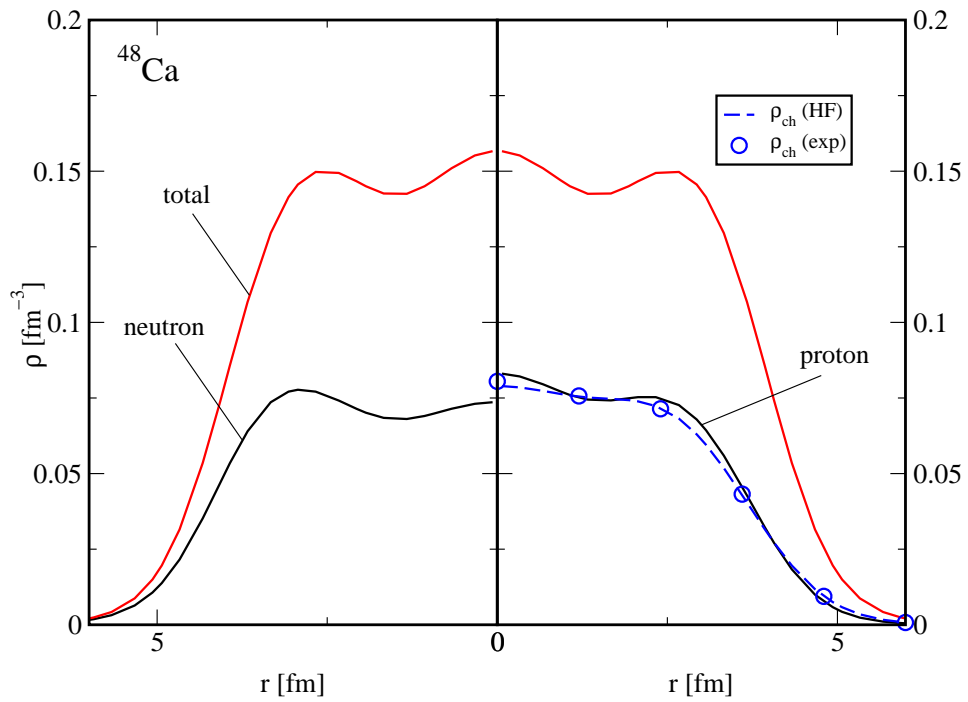
Figure 7.6: *Densities in* ^{48}Ca

Figure 7.7: *Densities in* ^{48}Ni

Figure 7.8: *Densities in* ^{56}Ni
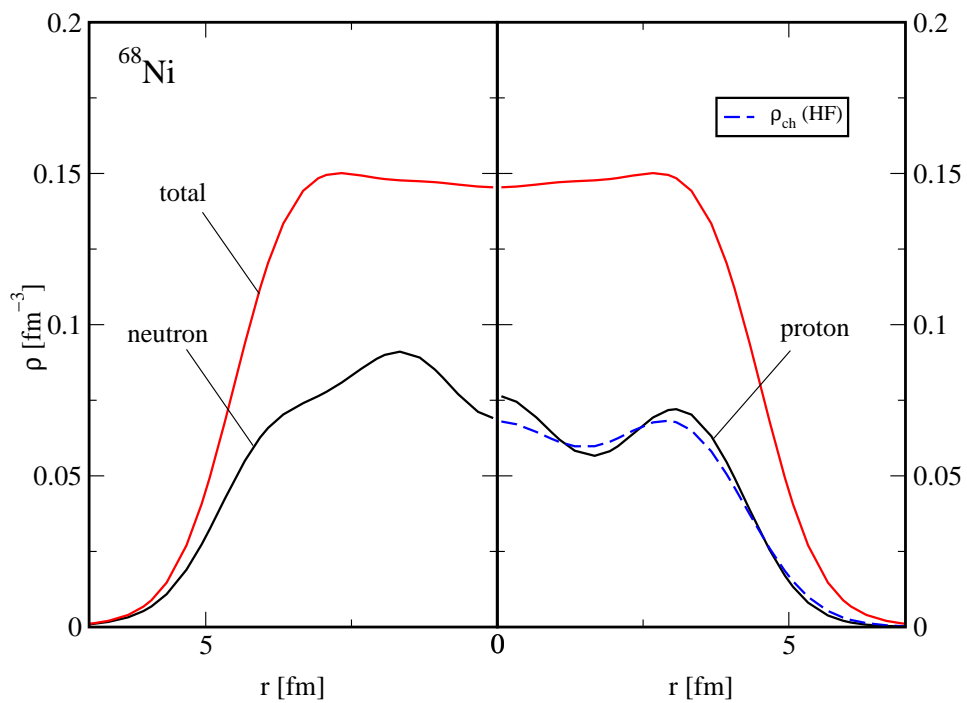
Figure 7.9: *Densities in ^{68}Ni*
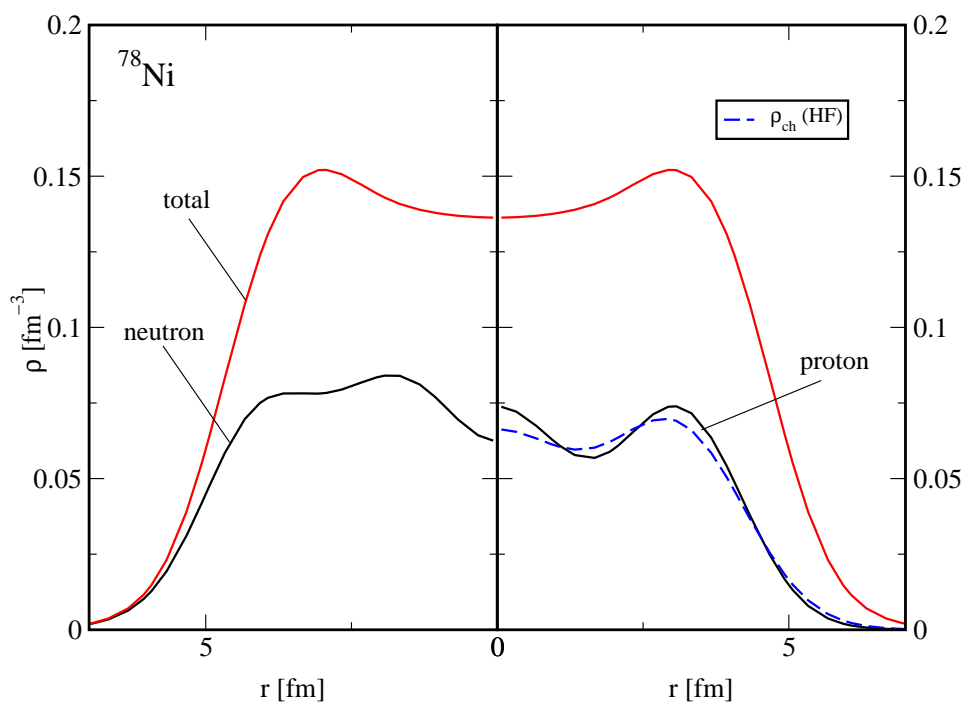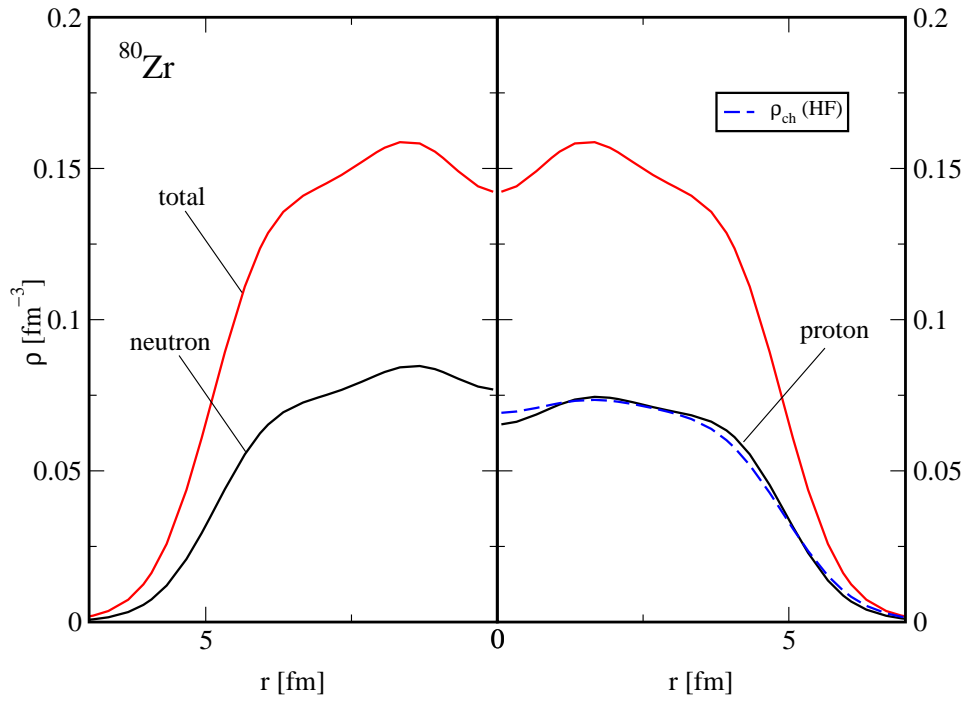

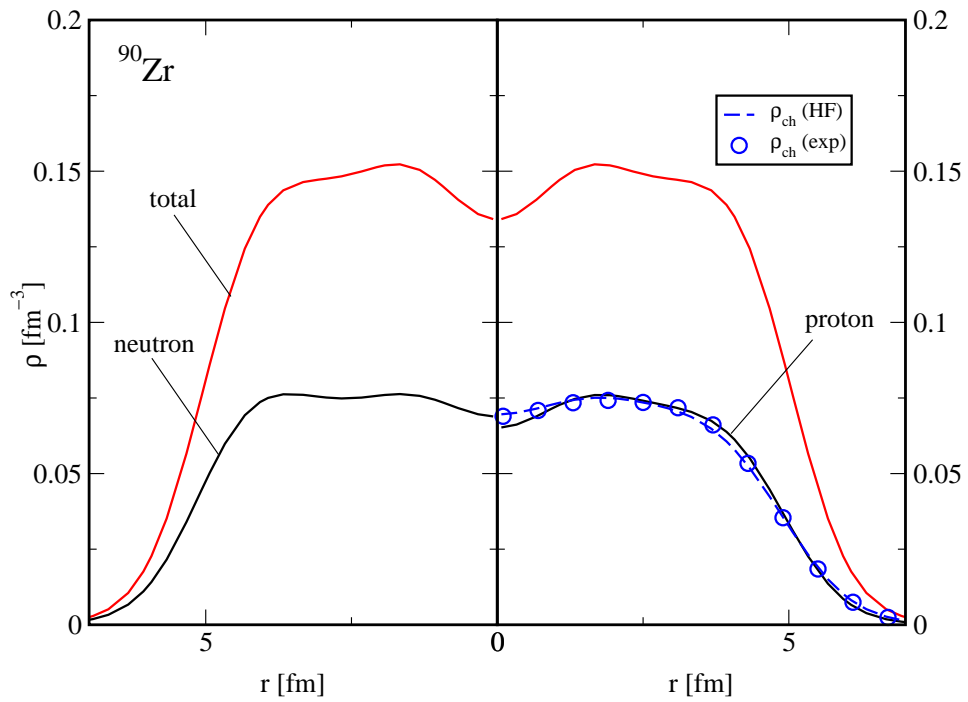Figure 7.10: *Densities in ^{78}Ni*
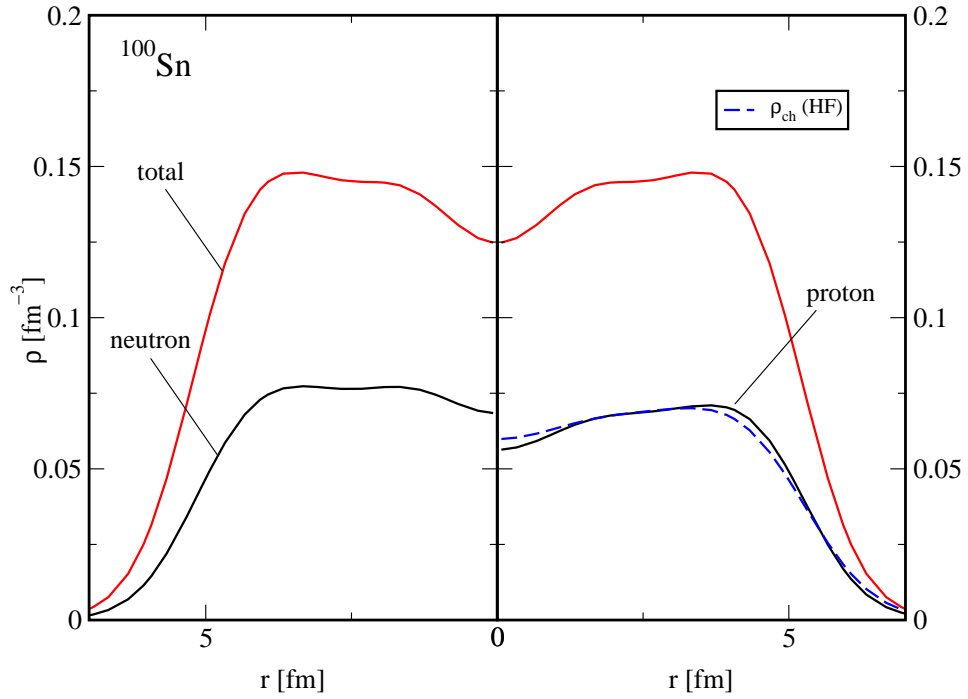
Figure 7.11: *Densities in ^{80}Zr*

Figure 7.12: *Densities in ^{90}Zr*

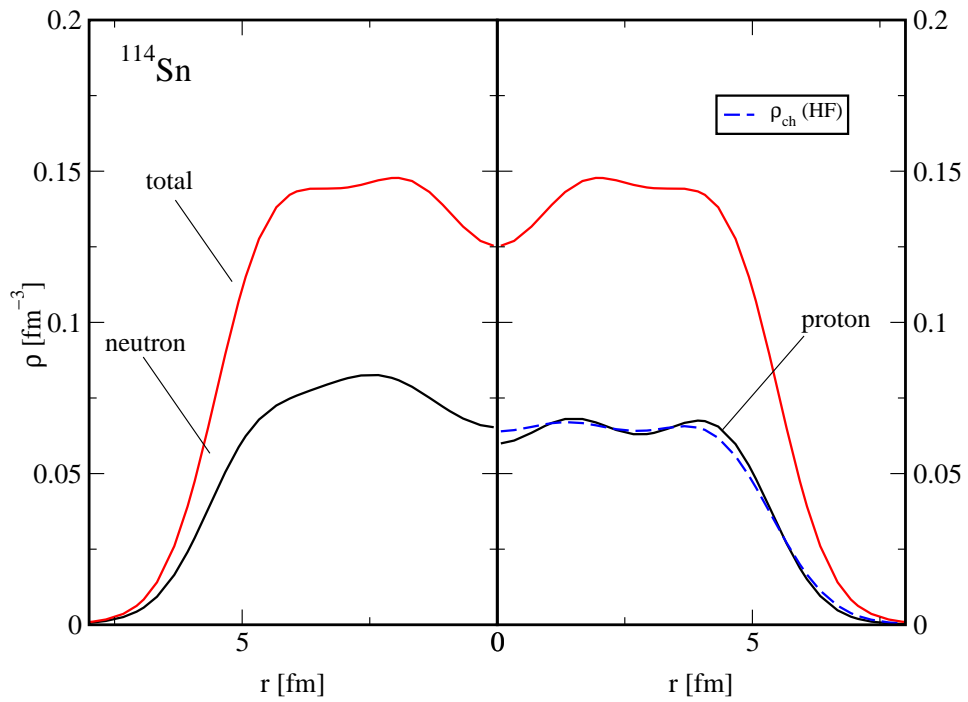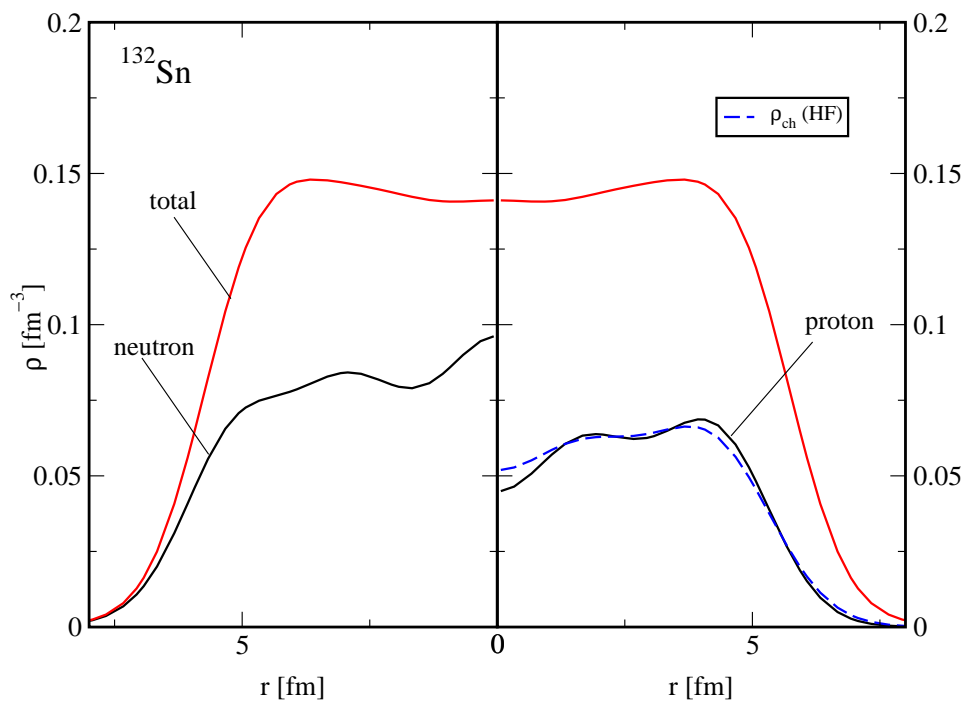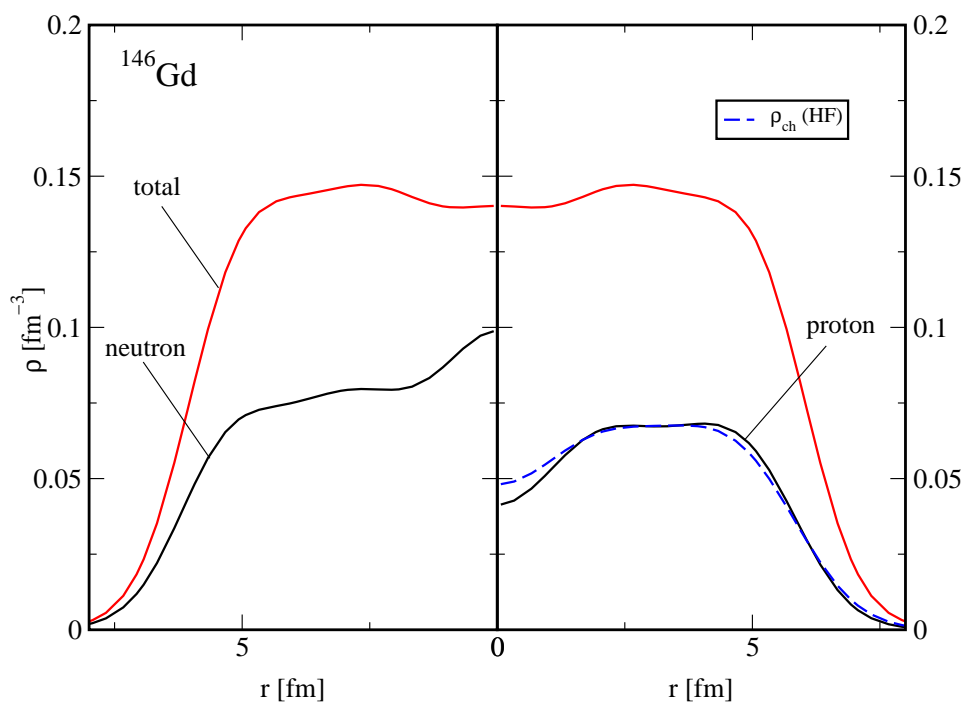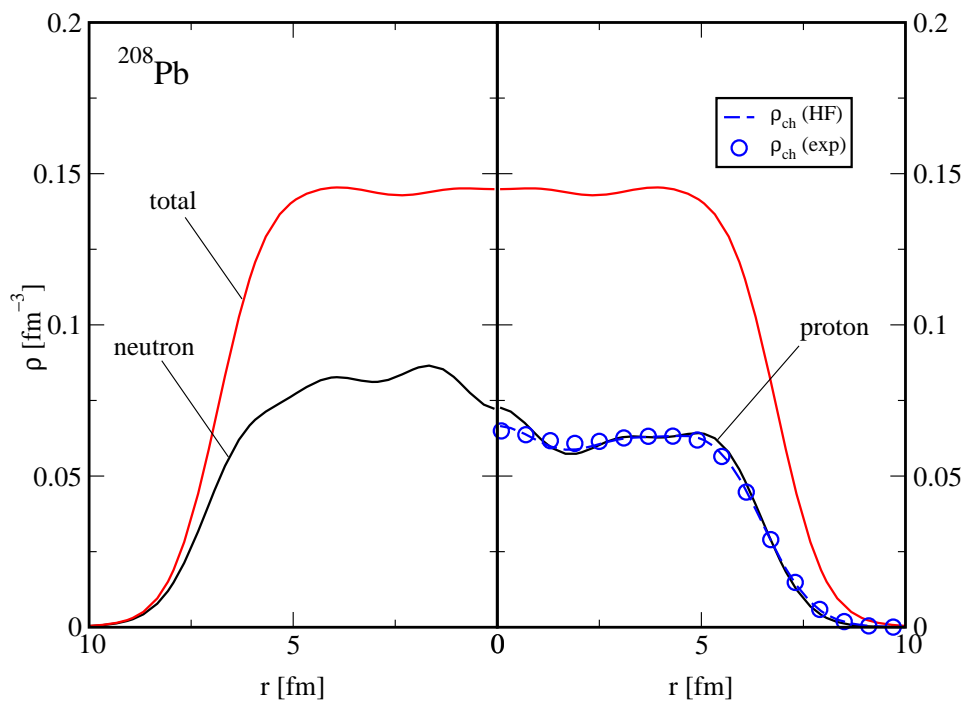Figure 7.13: *Densities in ^{100}Sn*

Figure 7.14: *Densities in ^{114}Sn*

Figure 7.15: *Densities in ^{132}Sn*

Figure 7.16: *Densities in ^{146}Gd*

Figure 7.17: *Densities in ^{208}Pb*

7.4   Form factors

The charge form factors are shown for those nuclei where experimental data is available, namely ^{16}O, ^{40}Ca, ^{48}Ca, ^{90}Zr and ^{208}Pb. The position of the first zero is clearly moves lower in momentum as Z increases, showing the increase in radius. As one would expect having already seen the fits to the densities, the quality of each fit to the Fourier transforms of the density are roughly equal in quality to the fits to the density. They are presented along with the densities since they are directly related to the experimental observables, as mentioned in Chapter 5.
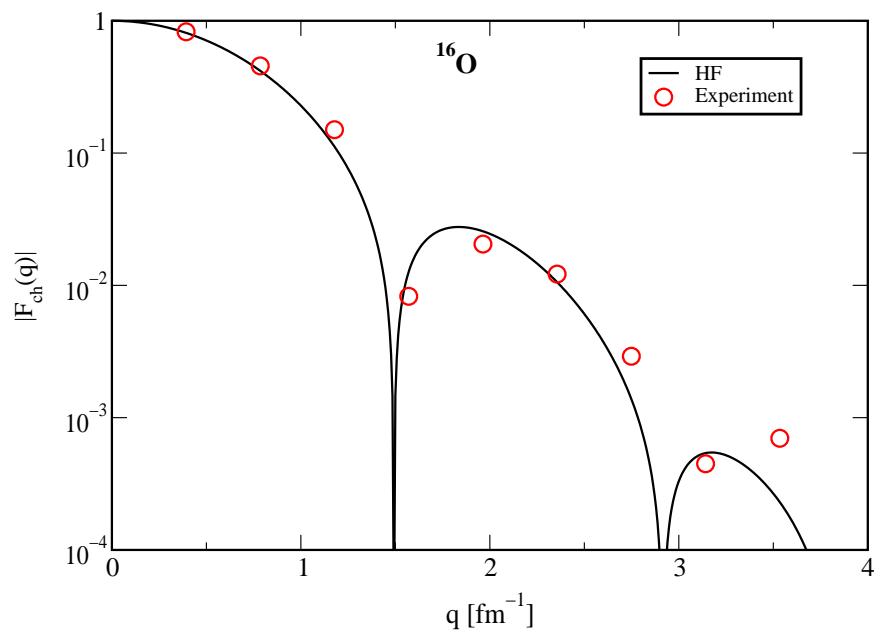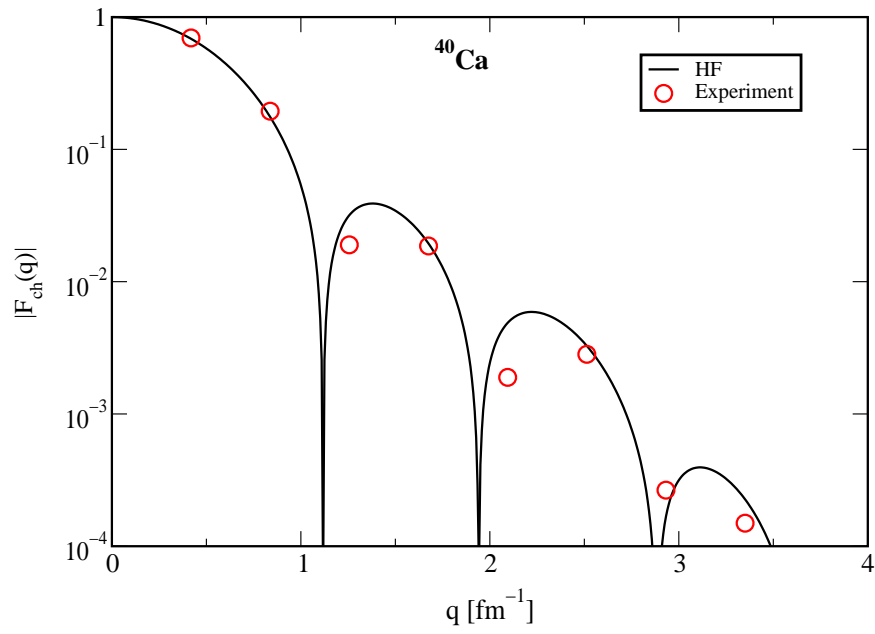

Figure 7.18: *Charge Form factor in* ^{16}O
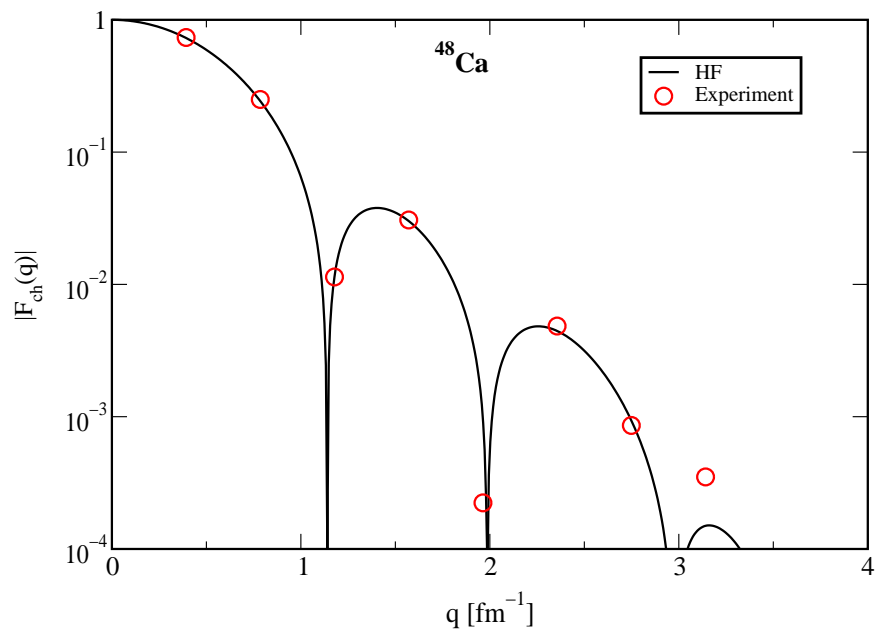
Figure 7.19: *Charge Form factor in ^{40}Ca*

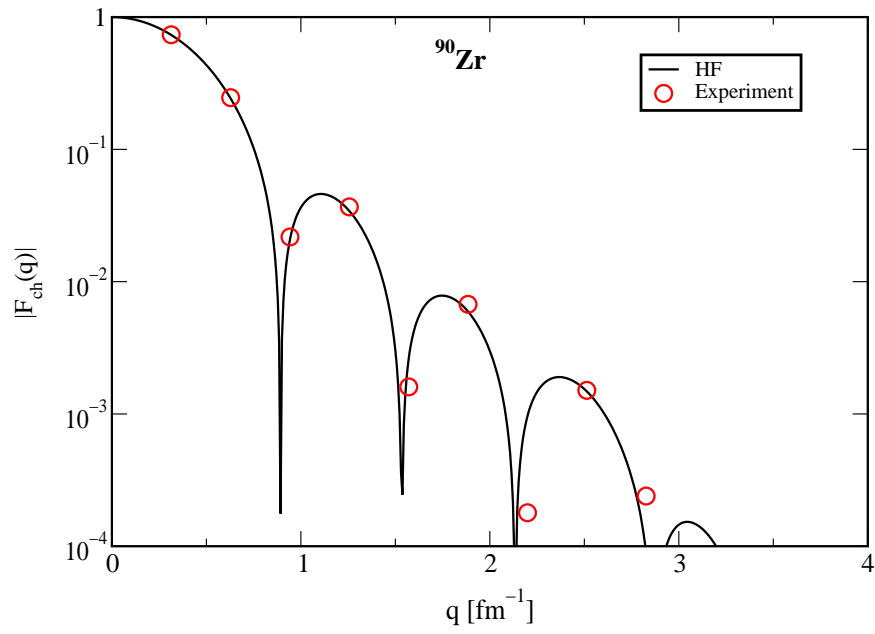Figure 7.20: *Charge Form factor in ^{48}Ca*

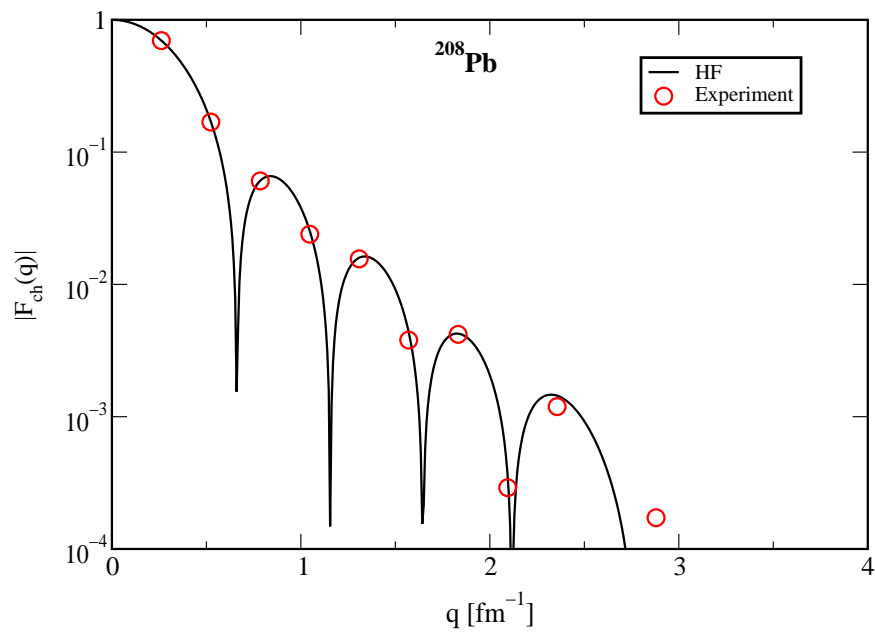Figure 7.21: *Charge Form factor in* ^{90}Zr

Figure 7.22: *Charge Form factor in* ^{208}Pb

7.5   Single-Particle energies

Calculated single particle energies are shown in Figures 7.23-7.28 compared to experimental data, taken from Refs.[21] and [97]. Only the nuclei for which experimental data were available are plotted, except ^{90}Zr for which neutron data are available. The position of the fermi level is indicated by the encircled number, which itself shows how many particles occupy the levels up to that point.

Firstly, one notes that the $N, Z = 8$ shell closures in ^{16}O are somewhat poor, as is the 20 particle shell closure in ^{40}Ca. This appears to be due in part to the overly-deep binding of the $d_{5/2}$ state above the $N, Z = 8$ shell and the $f_{7/2}$ state above the $N, Z = 20$ shell. The occupied states nearest the fermi level appear also to be pushed up, but given the underbinding in these light nuclei, the excessive depth of the unoccupied levels seems more remarkable. The effect does not take place for the $N, Z = 12$ or $N, Z = 28$ gaps. The fact that the pushed-down states are the lowest states of their given angular momentum may be of some significance. Since the monopole force only involves interactions between single-particles and other single-particles with exactly the same angular quantum numbers, the set of states of a given angular momentum for which not even the lowest N-state is unoccupied feel the exchange interaction differently to those states in which at least one state sharing angular quantum numbers is occupied. This effect was noticed earlier in Fig. 5.15 where it was seen that $0f_{7/2}$ and $0f_{5/2}$ states in ^{48}Ca had different single-particle energies in the absence of the spin-orbit force. Alternatively, since the smallness of the $Z = 20$ gap in ^{48}Ca is not so extreme, and the $N = 20$ gap in ^{34}Si is quite satisfactory, it could be that the problem is something to do with the properties of $N = Z$ nuclei.

In the heavier nuclei (^{132}Sn and ^{208}Pb) the level densities and shell gaps correspond much more closely to experiment than in the lighter nuclei. A possible factor here, as elsewhere, is the omission of the centre-of-mass correction is negligible in the heavy nuclei but not so in the lighter. Some of the details of the level ordering for neutron states in ^{132}Sn is seen to be at odds with experiment. It is noted that this is a common feature of Skyrme mean-field calculations[97].

The results in the light nuclei are similar to those in a recent work by Brown[97] in which a Skyrme paramaterisation was fitted to, amongst other things, the single particle spectra of light nuclei. He attributed the too-small gap in ^{16}O and ^{40}Ca as being due to not considering correlation effects in which single particles are excited across the gap. A calculation with just the monopole force alone would not account for the lowest energy excitations, but the quadrupole force might improve matters if its contribution to the mean-field is calculated, or it is used to evaluate corrections to the single-particle energies in perturbation theory.

Figure 7.23: *Single particle energies in ^{16}O compared to experiment*

Figure 7.24: *Single particle energies in ^{34}Si compared to experiment*

Figure 7.25: *Single particle energies in ^{40}Ca compared to experiment*

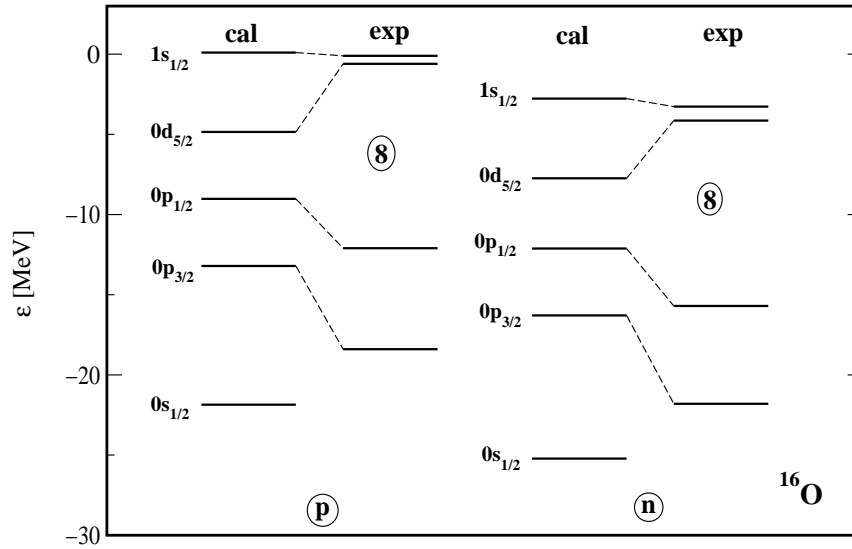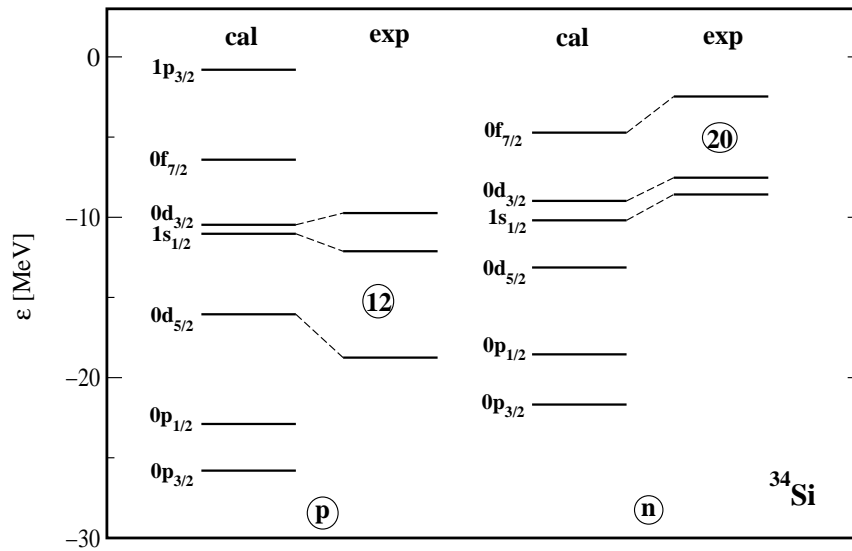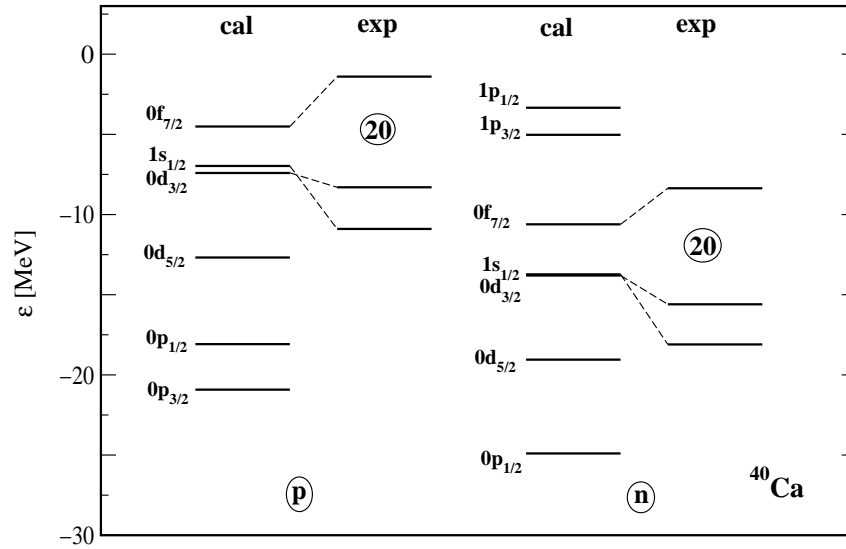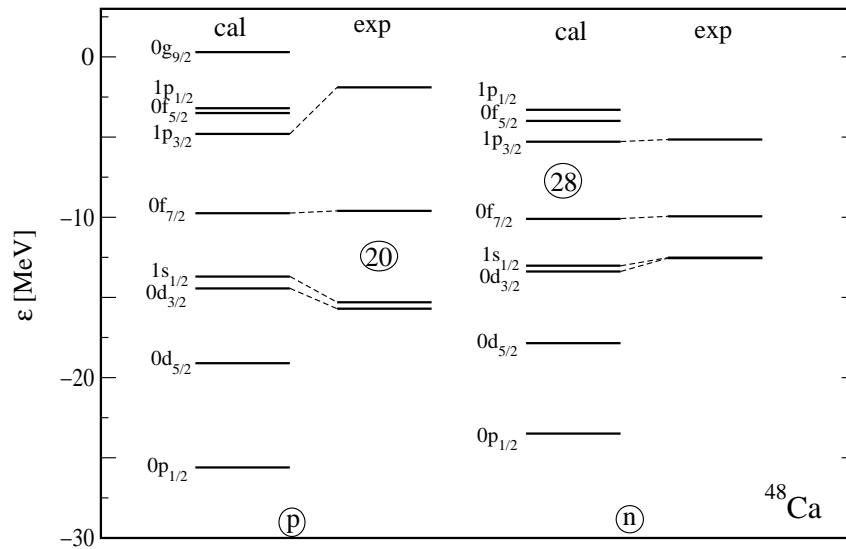Figure 7.26: *Single particle energies in ^{48}Ca compared to experiment*
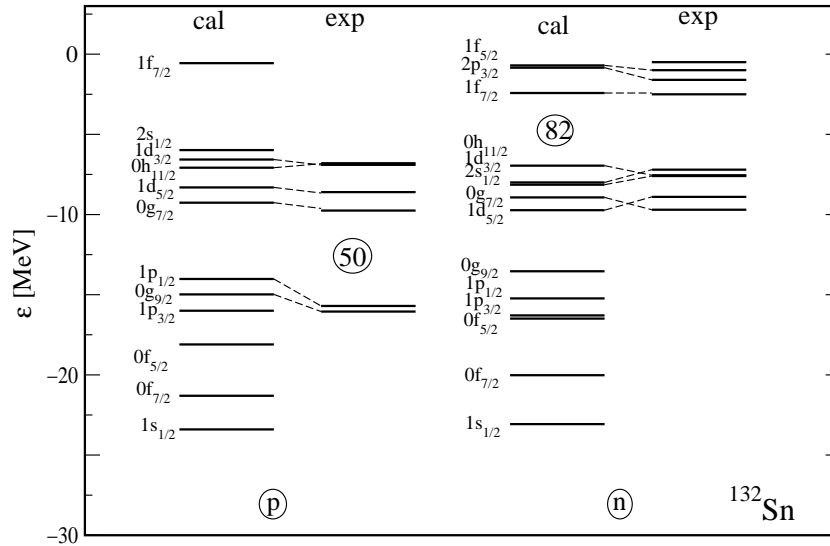
Figure 7.27: *Single particle energies in ^{132}Sn compared to experiment*
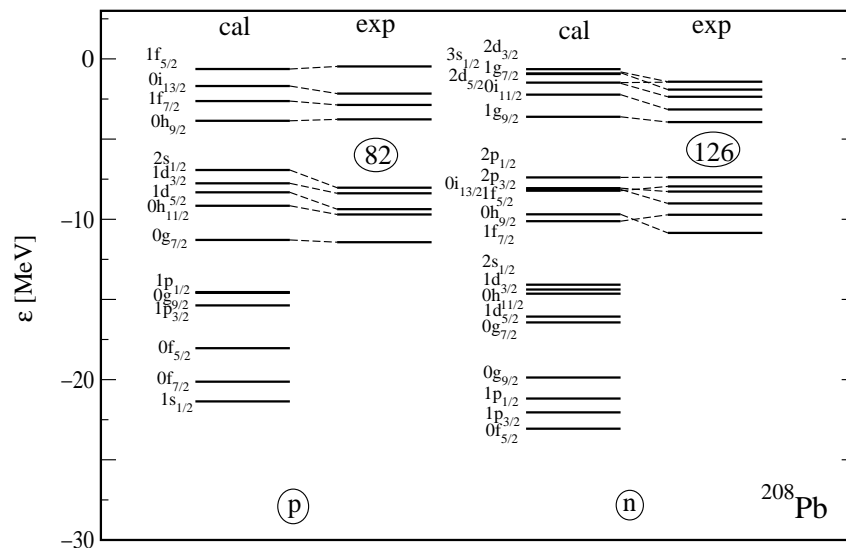
Figure 7.28: *Single particle energies in ^{208}Pb compared to experiment*

Chapter 8

Summary and Conclusions

A density-dependent separable multipole interaction has been presented and used in calculations of even-even spherical nuclei in the Hartree-Fock approximation on top of which corrections to third order in the energy have been calculated. In addition, the properties of symmetric and asymmetric nuclear matter have been studied as well as those of a neutron star.

From calculations of the perturbation series, it is found that the interaction is weak and the first terms in the perturbation series are small and appear to converge quite rapidly.

An approximate fit of the force parameters has been made to the ground-state properties of finite nuclei and the single-particle observables (single-particle energies and one-body densities) agree well with experiment. The agreement of the HF energy is quite reasonable, but not of the same quality as contemporary effective interactions used in HF models. However, this work represents the most successful application of the standard perturbation theory calculation in nuclei, improving quite significantly on the quality of the results compared to previous calculations, which were discussed in Chapter 3.

A deficiency of the present calculation is the uncertainty over the multipole parameters. Since the multipole effects manifest themselves in such ways as deformations and excited state spectra, it is not possible to determine their strengths with the calculation of the ground states of spherical nuclei. The next step therefore is to perform calculations of deformed nuclei to fit the multipole parameters and to develop techniques to calculate excited state properties using perturbation theory.

Appendix A

Hartree–Fock Equations

The Hartree-Fock (HF) approximation is based on the idea that a system of inter-acting fermions may be described as a system of fermions moving independently in a one-body potential. This "mean field" is supposed to describe the average of the interactions of a given particle with all the others.

This mean field is represented by a one-body Hamiltonian, the HF Hamilto-nian, the solution the one-dimensional Schrödinger equation with this Hamilto-nian gives the single particle states which the fermions occupy:

$$\hat{h}_{HF}(x)\varphi_b(x) = \epsilon_i\varphi_i(x). \tag{A.1}$$

To determine the HF potential one makes the *ansatz* of a Slater determinant of the single particle wavefunctions for the many-body wavefunction:

$$\Phi(r_1\cdots r_N) = \begin{vmatrix} \varphi_1(r_1) & \varphi_1(r_2) & \cdots & \varphi_1(r_N) \\ \varphi_2(r_1) & \varphi_2(r_2) & \cdots & \varphi_2(r_N) \\ \vdots & \vdots & \ddots & \vdots \\ \varphi_N(r_1) & \varphi_N(r_2) & \cdots & \varphi_N(r_N) \end{vmatrix} \tag{A.2}$$

and requires that the expectation value of the full Hamiltonian in this state be an extremum. One thus varies this expectation value with respect to the set of single particle wavefunctions and sets it to zero:

$$\frac{\delta}{\delta\varphi_i^*(x)}\left[\langle\Phi|\hat{H}|\Phi\rangle - \sum_{i=1}^N \epsilon_i \int dy\,\varphi^*(y)\varphi(y)\right] = 0 \tag{A.3}$$

where the N Lagrange multipliers serve to ensure the normalization of the single particle wave-functions. Note that the prescription for finding the HF Hamilto-nian depends on the single particle wavefunctions which are its solution, so there is a self-consistency condition which is usually dealt with by solving the HF equa-tions iteratively. These HF equations are derived from the variational equation

91

(A.3) by expressing the expectation value of the Hamiltonian in a Slater determinant in second quantization notation:

$$\langle \Phi | \hat{H} | \Phi \rangle = \sum_{i=1}^{N} \langle i | u | i \rangle + \frac{1}{2} \sum_{i,j=1}^{N} \langle ij | v \left[| ij \rangle - | ji \rangle \right],$$

(A.4)

where u is the one-body part of the interaction, including kinetic energy term, and v is the two-body part. Using the result from functional calculus

$$\int dy \sum_{i} \frac{\delta \varphi_i^*(y)}{\delta \varphi_b^*(x)} = \delta_{ib} \delta(x - y)$$

(A.5)

the variational equation becomes

$$
\begin{aligned}
0 \;=\; & \frac{\delta}{\delta \varphi_b^*(x)} \bigg\{ \sum_{i=1}^{N} \int dy \, \varphi_i(y) \left[u(y) \right] \varphi_i(y) \\
& + \frac{1}{2} \sum_{i,j=1}^{N} \iint dy \, dy' \varphi_i^*(y) \varphi_j^*(y') v(y, y') \varphi_i(y) \varphi_j(y') \\
& + \frac{1}{2} \sum_{i,j=1}^{N} \iint dy \, dy' \varphi_i^*(y) \varphi_j^*(y') v(y, y') \varphi_j(y) \varphi_i(y') \\
& - \sum_{i=1}^{N} \epsilon_i \int dy \, \varphi_i^*(y) \varphi_i(y) \bigg\} \\
=\; & \left[u(x) \right] \varphi_i(x) + \sum_{i=1}^{N} \int dy \, \varphi_i^*(y) \frac{\delta u(y)}{\delta \varphi_i^*(x)} \varphi_i(x) \\
& + \frac{1}{2} \sum_{j=1}^{N} \int dy' \varphi_j^*(y') v(x, y') \varphi_b(x) \varphi_j(y') \\
& + \frac{1}{2} \sum_{i=1}^{N} \int dy \, \varphi_i(y) v(y, x) \varphi_i(y) \varphi_b(x) \\
& + \frac{1}{2} \sum_{i,j=1}^{N} \iint dy \, dy' \varphi_i^*(y) \varphi_j^*(y') \frac{\delta v(y, y')}{\delta \varphi_b^*(x)} \varphi_i(y) \varphi_j(y') \\
& - \frac{1}{2} \sum_{j=1}^{N} \int dy' \varphi_j^*(y') v(x, y') \varphi_j(x) \varphi_b(y') \\
& - \frac{1}{2} \sum_{i=1}^{N} \int dy \, \varphi_i(y) v(y, x) \varphi_b(y) \varphi_i(x) \\
& - \frac{1}{2} \sum_{i,j=1}^{N} \iint dy \, dy' \varphi_i^*(y) \varphi_j^*(y') \frac{\delta v(y, y')}{\delta \varphi_b^*(x)} \varphi_j(y) \varphi_i(y') - \epsilon_b \varphi_b(x)
\end{aligned}
$$

by relabelling dummy indices and coordinate labels, the second and third and the fifth and sixth terms are seen to be equal. Furthermore, expressing the one-particle density and two-particle density matrix of a Slater determinant as

$$\rho(y) \;=\; \sum_{i=1}^{N} \varphi_i^*(y)\varphi_i(y)$$

$$\rho(y,y') \;=\; \sum_{i=1}^{N} \varphi_i^*(y')\varphi_i(y)$$

the equation (A.6) becomes

$$
\begin{aligned}
\epsilon_i\varphi_i(x) \;=\;& \left[u(x) + \int dy\,\rho(y)v(x,y)\right]\varphi_i(x) - \int dy\,\rho(x,y)v(x,y)\varphi_i(y) \\
&+ \int dy\,\rho(y)\frac{\delta u(y)}{\delta\varphi_i^*(x)} + \frac{1}{2}\int\int dy\,dy'\rho(y)\rho(y)\frac{\delta v(y,y')}{\delta\varphi_b^*(x)} \\
&- \frac{1}{2}\int\int dy\,dy'\rho(y,y')\rho(y',y)\frac{\delta v(y,y')}{\delta\varphi_b^*(x)}.
\end{aligned}
\tag{A.6}
$$

The first line of this equation is in the form of an eigenvalue problem and is the standard Hartree-Fock equation. From it, a one-body potential may be defined:

$$U_{HF}(x)\varphi_i(x) = \left[u(x) + \int dy\,\rho(y)v(x,y)\right]\varphi_i(x) - \int dy\,\rho(x,y)v(x,y)\varphi_i(y) \tag{A.7}$$

which is the Hartree-Fock potential. Note that it is inherently non-local in nature thanks to the exchange term. In addition, if the potentials $u(y)$ or $v(x,y)$ depend on the wavefunction - in practice this means dependent on the densities - then the second and third lines of (A.6) are non-zero and there is a further contribution to the Hartree-Fock potential, known as the *rearrangement* potential.

Appendix B

Many-Body Perturbation Theory

B.1 Hartree-Fock and Perturbation Theory

The Hamiltonian for a system of fermions interacting via one and two body interactions is written, in the language of second-quantization,

$$H = \sum_{ac} \langle a|u|c \rangle a_a^\dagger a_c + \frac{1}{4} \sum_{abcd} \langle ab|\tilde{v}|cd \rangle a_a^\dagger a_b^\dagger a_d a_c . \tag{B.1}$$

Here the one-body part of the Hamiltonian is labelled u. The two-body part is v and $a^\dagger$ and a are fermion creation and annihilation operators respectively. If one applies Wick's theorem[100], which states that a product of operators may be written as the sum of all contracted normal-ordered products, the Hamiltonian becomes

$$H = \sum_{ac} \langle a|u|c \rangle \left\{ : a_a^\dagger a_c : + \overparen{a_a^\dagger a_c} \right\} + \frac{1}{4} \sum_{abcd} \langle ab|\tilde{v}|cd \rangle \left\{ : a_a^\dagger a_b^\dagger a_d a_c : - \overparen{a_a^\dagger a_d} : a_b^\dagger a_c : \right.$$

$$\left. + \overparen{a_a^\dagger a_c} : a_b^\dagger a_d : - \overparen{a_b^\dagger a_d} : a_a^\dagger a_c : + \overparen{a_b^\dagger a_c} : a_a^\dagger a_d : - \overparen{a_a^\dagger a_d}\,\overparen{a_b^\dagger a_c} + \overparen{a_a^\dagger a_c}\,\overparen{a_b^\dagger a_d} \right\} \tag{B.2}$$

where the colons (:) denote normal-ordering of the operators within them and the braces denote contractions. Only contractions between a creation and annihilation operator have been retained since all other contractions are zero in the case of a sharp fermi surface, which is always true in the representation under consideration in this work.

The contractions $\overparen{a_a^\dagger a_c}$ are zero if either states a or c are unoccupied and δ_{ac} otherwise so the Hamiltonian reduces to

$$H = \sum_{h<\epsilon_F} \langle h|u|h \rangle + \sum_{ac} \langle a|u|c \rangle : a_a^\dagger a_c : + \frac{1}{4} \sum_{abcd} \langle ab|\tilde{V}|cd \rangle : a_a^\dagger a_b^\dagger a_d a_c :$$

$$- \frac{1}{4} \sum_{bc} \sum_{h<\epsilon_F} \langle hb|\tilde{v}|ch \rangle : a_b^\dagger a_c : + \frac{1}{4} \sum_{ac} \sum_{h<\epsilon_F} \langle ah|\tilde{v}|ch \rangle : a_a^\dagger a_c :$$

$$+ \ \frac{1}{4} \sum_{bd} \sum_{h<\epsilon_F} \langle hb|\tilde{v}|hd \rangle : a_b^\dagger a_d : -\frac{1}{4} \sum_{ad} \sum_{h<\epsilon_F} \langle ah|\tilde{v}|hd \rangle : a_a^\dagger a_d :$$

$$- \ \frac{1}{4} \sum_{hh'<\epsilon_F} \langle hh'|\tilde{v}|h'h \rangle + \frac{1}{4} \sum_{hh'<\epsilon_F} \langle hh'|\tilde{v}|hh' \rangle, \tag{B.3}$$

where h represent hole states, i.e., states which are occupied in the representation used. Since the matrix elements are anti-symmetrized and, using the symmetry $\langle ab|\tilde{v}|cd \rangle = \langle ba|\tilde{v}|dc \rangle$, the Hamiltonian reduces to

$$
\begin{aligned}
H \ = \ & \sum_{h<\epsilon_F} \langle h|u|h \rangle + \frac{1}{2} \sum_{hh'<\epsilon_F} \langle hh'|\tilde{v}|hh' \rangle \\
& + \ \sum_{ac} \{ \langle a|u|c \rangle + \langle ah|\tilde{v}|ch \rangle \} : a_a^\dagger a_c : \\
& + \ \frac{1}{4} \sum_{abcd} \langle ab|\tilde{v}|cd \rangle : a_a^\dagger a_b^\dagger a_d a_c :
\end{aligned} \tag{B.4}
$$

Taking the expectation value of the Hamiltonian in the reference state $|0\rangle$ of occupied orbitals below the Fermi surface, only the terms without normal-ordered products survive:

$$E_0 \equiv \langle 0|H|0 \rangle = \sum_{h<\epsilon_F} \langle h|u|h \rangle + \frac{1}{2} \sum_{hh'} \langle hh'|\tilde{v}|hh' \rangle. \tag{B.5}$$

The second line of Equation (B.4) describes a one-body field. It is written for in an arbitrary Hilbert space representation and one is free to choose a particular basis. A convenient choice is that which diagonalizes this single-particle Hamiltonian, i.e.

$$\langle a|u|c \rangle + \sum_{h<\epsilon_F} \langle ah|\tilde{v}|ch \rangle = \epsilon_a \delta_{ac} \tag{B.6}$$

which can be written as

$$\langle a|u + w|c \rangle = \epsilon_a \delta_{ac} \tag{B.7}$$

with the one-body field w defined as

$$\langle a|w|c \rangle \equiv \sum_{h<\epsilon_F} \langle ah|\tilde{v}|ch \rangle. \tag{B.8}$$

Equation (B.6) is just the Hartree-Fock equation in second quantized notation. This can be seen by taking equation (A.6) and acting left with $\int dx \varphi_a^*(x)$:

$$
\begin{aligned}
\epsilon_i \delta_{ia} \ = \ & \int dx \varphi_a^*(x) u(x) \varphi_i(x) + \int dx \int dy \sum_{h<\epsilon_F} \varphi_a^*(x) \varphi_h^*(y) v(x,y) \varphi_i(x) \varphi_h(y) \\
& - \ \int dx \int dy \sum_{h<\epsilon_F} \varphi_a^*(x) \varphi_h^*(y) v(x,y) \varphi_h(x) \varphi_i(y)
\end{aligned} \tag{B.9}
$$

which is just (B.6) in coordinate space, so that the Hamiltonian reduces to the form

$$H = E_0 + \underbrace{\sum_{a<\epsilon_F} \epsilon_a : a_a^\dagger a_a :}_{H_0} + \underbrace{\frac{1}{4} \sum_{abcd} \langle ab|\tilde{v}|cd\rangle : a_a^\dagger a_b^\dagger a_d a_c :}_{H_1} \qquad (B.10)$$

where a division of the Hamiltonian into parts labelled H_0 and H_1 is given for the purposes of performing perturbation theory.

B.2 Many-Body Perturbation Theory

Having partitioned the Hamiltonian into two parts, $H = H_0 + H_1$ it is assumed that the eigenvalue problem associated with H_0 has been solved:

$$H_0|\Phi_n\rangle = W_n|\Phi_n\rangle. \qquad (B.11)$$

A parameter is separated out of the perturbing term: $H_1 = \lambda \bar{H}_1$ so that it can be used to keep track of the order of perturbation theory. In the end it can be set to unity.

The full Schrödinger equation which needs to be solved is

$$H|\Psi_0\rangle = E_0|\Psi_0\rangle, \qquad (B.12)$$

for the ground state of the system. One has

$$\begin{aligned} H_1|\Psi_0\rangle &= (H - H_0)|\Psi_0\rangle = (E_0 - H_0)|\Psi_0\rangle \\ \text{then} \qquad \langle\Phi_0|H_1|\Psi_0\rangle &= \langle\Phi_0|E_0 - H_0|\Psi_0\rangle = (E_0 - W_0)\langle\Phi_0|\Psi_0\rangle. \end{aligned}$$

The *energy shift*, the difference between the exact and unperturbed energies is thus

$$\Delta E \equiv E_0 - W_0 = \frac{\langle\Phi_0|H_1|\Psi_0\rangle}{\langle\Phi_0|\Psi_0\rangle}. \qquad (B.13)$$

The operator which projects onto the ground state of the unperturbed problem is defined as

$$P \equiv |\Phi_0\rangle\langle\Phi_0|, \qquad (B.14)$$

and its complement is

$$Q \equiv 1 - P = \sum_{n=1}^{\infty} |\Phi_n\rangle\langle\Phi_n|. \qquad (B.15)$$

This operator, Q commutes with H_0 so

$$(E - H_0)Q|\Psi_0\rangle = Q(E - H_0)|\Psi_0\rangle = Q(E - E_0 + H_1)|\Psi_0\rangle, \qquad (B.16)$$

for an arbitrary number, E. Therefore

$$Q|\Psi_0\rangle = \frac{1}{E - H_0} Q(E - E_0 + H_1)|\Psi_0\rangle = |\Psi_0\rangle - |\Psi_0\rangle\langle\Phi_0|\Phi_0\rangle, \tag{B.17}$$

then by defining

$$|\xi\rangle = \frac{|\Psi_0\rangle}{\langle\Phi_0|\Psi_0\rangle}$$

equation (B.17) becomes

$$|\xi\rangle = |\Phi_0\rangle + \frac{1}{E_0 - H_0} Q(E - E_0 + H_1)|\xi\rangle \tag{B.18}$$

which can be iterated to give

$$
\begin{aligned}
|\xi\rangle &= |\Phi_0\rangle + \frac{1}{E_0 - H_0} Q(E - E_0 + H_1)\left\{|\Phi_0\rangle + \frac{1}{E_0 - H_0} Q(E - E_0 + H_1)\{\cdots\}\right\} \\
&= \sum_{n=0}^{\infty}\left[\frac{1}{E - H_0} Q(E - E_0 + H_1)\right]^n |\Phi_0\rangle \tag{B.19}
\end{aligned}
$$

Using this in the expression (B.13) for the energy shift, one obtains

$$\Delta E = \langle\Phi_0|\xi\rangle = \sum_{n=0}^{\infty}\langle\Phi_0|H_1\left[\frac{1}{E - H_0} Q(E - E_0 + H_1)\right]^n |\Phi_0\rangle. \tag{B.20}$$

This expression is true for any value of the number E. Setting $E = W_0$, the ground state eigenvalue of the unperturbed problem, the resulting expressions give the *Rayleigh-Schrödinger* perturbation theory:

$$|\xi\rangle = \sum_{n=0}^{\infty}\left[\frac{1}{W_0 - H_0} Q(W_0 - E_0 + H_1)\right]^n |\Phi_0\rangle \tag{B.21}$$

$$\Delta E = \sum_{n=0}^{\infty}\langle\Phi_0|H_1\left[\frac{1}{W_0 - H_0} Q(H_1 - \Delta E)\right]^n |\Phi_0\rangle. \tag{B.22}$$

Note that by setting $E = E_0$ one obtains the Brillouin-Wigner perturbation series.

To obtain the perturbation series order by order, terms in (B.21) and (B.22) are grouped according to the order of the coupling constant λ. For the energy:

$$n = 0: \qquad \langle\Phi_0|H_1|\Phi_0\rangle \sim \lambda \tag{B.23}$$

$$n = 1: \qquad \langle\Phi_0|H_1\frac{1}{W_0 - H_0} Q(H_1 - \Delta E)|\Phi_0\rangle$$

$$= \langle\Phi_0|H_1\frac{1}{W_0 - H_0} QH_1|\Phi_0\rangle - \langle\Phi_0|H_1\frac{1}{W_0 - H_0} Q\Delta E|\Phi_0\rangle$$

$$= \langle \Phi_0 | H_1 \frac{1}{W_0 - H_0} \sum_{n=1}^{\infty} |\Phi_n\rangle\langle\Phi_n|H_1|\Phi_0\rangle$$

$$= \sum_{n=1}^{\infty} \frac{\langle\Phi_0|H_1|\Phi_n\rangle}{W_0 - W_n}\langle\Phi_n|H_1|\Phi_0\rangle \sim \lambda^2$$

$$n = 2: \quad \langle\Phi_0|H_1 \left[\frac{1}{W_0 - H_0}Q(H_1 - \Delta E)\right]^2 |\Phi_0\rangle$$

$$= \langle\Phi_0|H_1 \frac{1}{W_0 - H_0}Q(H_1 - \Delta E)\frac{1}{W_0 - H_0}Q(H_1 - \Delta E)|\Phi_0\rangle$$

$$= \langle\Phi_0|H_1 \frac{1}{W_0 - H_0}Q(H_1 - \Delta E)\frac{1}{W_0 - H_0}QH_1|\Phi_0\rangle$$

$$\quad -\langle\Phi_0|H_1 \frac{1}{W_0 - H_0}Q(H_1 - \Delta E)\frac{1}{W_0 - H_0}Q\Delta E|\Phi_0\rangle$$

$$= \langle\Phi_0|H_1 \frac{1}{W_0 - H_0}Q(H_1 - \Delta E)\frac{1}{W_0 - E_0}\sum_{n=1}^{\infty}|\Phi_n\rangle\langle\Phi_n|H_1|\Phi_0\rangle$$

$$= \sum_{n=1}^{\infty}\langle\Phi_0|H_1 \frac{1}{W_0 - H_0}Q(H_1 - \Delta E)\frac{1}{W_0 - W_n}|\Phi_n\rangle\langle\Phi_n|H_1|\Phi_n\rangle$$

$$= \sum_{n=1}^{\infty}\frac{1}{W_0 - W_n}\langle\Phi_0|H_1 \frac{1}{W_0 - H_0}QH_1|\Phi_n\rangle\langle\Phi_n|H_1|\Phi_0\rangle$$

$$\quad -\Delta E \sum_{n=1}^{\infty}\langle\Phi_0|H_1 \frac{1}{(W_0 - W_n)^2}|\Phi_n\rangle\langle\Phi_n|H_1|\Phi_0\rangle$$

$$= \sum_{n=1}^{\infty}\frac{1}{W_0 - W_n}\langle\Phi_0|H_1 \frac{1}{W_0 - H_0}\sum_{m=1}^{\infty}|\Phi_m\rangle\langle\Phi_m|H_1|\Phi_n\rangle\langle\Phi_n|H_1|\Phi_0\rangle$$

$$\quad -\Delta E \sum_{n=1}^{\infty}\langle\Phi_0|H_1 \frac{1}{(W_0 - W_n)^2}|\Phi_n\rangle\langle\Phi_n|H_1|\Phi_0\rangle$$

$$= \sum_{n=1}^{\infty}\sum_{m=1}^{\infty}\frac{\langle\Phi_0|H_1|\Phi_m\rangle\langle\Phi_m|H_1|\Phi_n\rangle\langle\Phi_n|H_1|\Phi_0\rangle}{(W_0 - W_n)(W_0 - W_m)}$$

$$\quad -\Delta E \sum_{n=1}^{\infty}\frac{\langle\Phi_0|H_1|\Phi_n\rangle\langle\Phi_n|H_1|\Phi_n\rangle}{(W_0 - W_n)^2} \tag{B.24}$$

which consists of a term of order $\sim \lambda^3$ and a term which contains all orders of $\sim \lambda^3$ or greater. Taking the terms by order in λ the perturbation series for the energy is

$$\Delta E^{(1)} = \langle\Phi_0|H_1|\Phi_0\rangle$$

$$\Delta E^{(2)} = \sum_{n=1}^{\infty}\frac{\langle\Phi_0|H_1|\Phi_n\rangle\langle\Phi_n|H_1|\Phi_0\rangle}{W_0 - W_n}$$

$$\Delta E^{(3)} = \sum_{n=1}^{\infty} \sum_{m=1}^{\infty} \frac{\langle \Phi_0|H_1|\Phi_m\rangle\langle\Phi_m|H_1|\Phi_n\rangle\langle\Phi_n|H_1|\Phi_0\rangle}{(W_0 - W_n)(W_0 - W_m)}$$

$$-\langle\Phi_0|H_1|\Phi_0\rangle \sum_{n=1}^{\infty} \frac{\langle\Phi_0|H_1|\Phi_n\rangle\langle\Phi_n|H_1|\Phi_0\rangle}{(W_0 - W_n)^2}. \tag{B.25}$$

The first order energy correction is zero for the present case, since the perturbation is a normal-ordered product of operators which define the ground state in which their expectation value is being taken.

The second order correction to the energy is commonly obtained by creating a fictitious time-dependent problem in which the interaction H_1 is turned on adiabatically so that the full solution is obtained at $t = 0$. This approach is detailed in the textbooks[35, 39]. An alternative approach is to make use of the algebra of second quantization. The second order energy is

$$\Delta E^{(2)} = \sum_{n=1}^{\infty} \frac{\langle\Phi_0|H_1|\Phi_0\rangle\langle\Phi_n|H_1|\Phi_n\rangle}{W_0 - W_n}$$

$$= \sum_{n=1}^{\infty} \frac{|\langle\Phi_0|H_1|\Phi_n\rangle|^2}{W_0 - W_n} \tag{B.26}$$

The state $|\Phi_n\rangle$ must be of the form $a_r^\dagger a_s^\dagger a_a a_b |\Phi_0\rangle$, i.e. a state with two particles excited from the HF ground state so that the matrix element $\langle\Phi_0|H_1|\Phi_n\rangle$ is non-zero, H_1 containing two a-creation and two a-annihilation operators. To avoid double counting, the condtitions

$$s > r > \epsilon_F$$
$$a < b \leq \epsilon_F$$

apply. The eigenvalue of the unperturbed Hamiltonian of the excited state $|\Phi_n\rangle$ which appears in the denominator as W_n is

$$W_n = W_0 + \epsilon_r + \epsilon_s - \epsilon_a - \epsilon_b, \tag{B.27}$$

so that the second order energy correction is

$$\Delta E^{(2)} = \sum_{a<b\leq\epsilon_F} \sum_{r>s>\epsilon_F} \frac{\left|\langle\Phi_0|H_1 a_r^\dagger a_s^\dagger a_a a_b|\Phi_0\rangle\right|^2}{\epsilon_a + \epsilon_b - \epsilon_r - \epsilon_s}. \tag{B.28}$$

To evaluate the matrix elements a new set of creation and annihilation operators is defined whose action on the true vacuum $|\tilde{0}\rangle$ is the same as the of the a operators on the Hartree-Fock ground state $|\Phi_0\rangle$:

$$a_a^\dagger|\Phi_0\rangle = \begin{cases} c_a^\dagger|\tilde{0}\rangle, & a > \epsilon_F \\ c_a|\tilde{0}\rangle, & a < \epsilon_F \end{cases}$$

$$a_a|\Phi_0\rangle = \begin{cases} c_a|\tilde{0}\rangle, & a > \epsilon_F \\ c_a^\dagger|\tilde{0}\rangle, & a < \epsilon_F \end{cases}$$

so that the matrix element, with the normal-ordered product of operators is (see (B.10))

$$\frac{1}{4} \sum_{\alpha\beta\gamma\delta} \langle \alpha\beta|\tilde{v}|\gamma\delta\rangle \langle \Phi_0| : a_\alpha^\dagger a_\beta^\dagger a_\delta a_\gamma : c_r^\dagger c_s^\dagger c_a^\dagger c_b^\dagger |\tilde{0}\rangle \tag{B.29}$$

The matrix element will be non-zero if when translating the bra side to the c representation, four c-annihilation operators are produced. This means that α and β must be hole states in the HF representation and γ and δ must be particle states:

$$\frac{1}{4} \sum_{\alpha\beta\le\epsilon_F} \sum_{\gamma\delta>\epsilon_F} \langle \alpha\beta|\tilde{v}|\gamma\delta\rangle \langle \tilde{0}|c_\alpha c_\beta c_\delta c_\gamma c_r^\dagger c_s^\dagger c_a^\dagger c_b^\dagger |\tilde{0}\rangle \tag{B.30}$$

Since α and β are hole states and a and b are hole states, and the other operators pertain to particle states, the matrix element of the c-operators can be separated as

$$\langle \tilde{0}|c_\alpha c_\beta c_a^\dagger c_b^\dagger |\tilde{0}\rangle \langle \tilde{0}|c_\delta c_\gamma c_r^\dagger c_s^\dagger |\tilde{0}\rangle \tag{B.31}$$

The fist matrix element here will be unity if $b = \alpha$ and $a = \beta$ or -1 if $a = \alpha$ and $b = \beta$. This can be written as a generalized antisymmetric delta function:

$$\langle \tilde{0}|c_\alpha c_\beta c_a^\dagger c_b^\dagger |\tilde{0}\rangle = \delta_{\beta\alpha}^{ab} \equiv \begin{vmatrix} \delta_{\beta a} & \delta_{\beta b} \\ \delta_{\alpha a} & \delta_{\alpha b} \end{vmatrix} = \delta_{\beta a}\delta_{\alpha b} - \delta_{\beta b}\delta_{\alpha a} \tag{B.32}$$

so that the matrix element (B.30) becomes

$$\langle \Phi_0|H_1 a_r^\dagger a_s^\dagger a_a a_b|\Phi_0\rangle = \frac{1}{4} \sum_{\alpha\beta\gamma\delta} \langle \alpha\beta|\tilde{v}|\gamma\delta\rangle \delta_{\beta\alpha}^{ab}\delta_{\gamma\delta}^{rs} = -\langle ab|\tilde{v}|rs\rangle. \tag{B.33}$$

Hence the second order energy correction is

$$\Delta E^{(2)} = \sum_{a<b\le\epsilon_F} \sum_{r>s>\epsilon_F} \frac{|\langle ab|\tilde{v}|rs\rangle|^2}{\epsilon_a + \epsilon_b - \epsilon_r - \epsilon_s}. \tag{B.34}$$

Note that the numerator is always positive definite and the denominator is negative, so the second order energy correction always lowers the total energy from that of the Hartree-Fock result. It is often convenient to remove the restrictions $a < b$ and $r > s$. For each removal one doubles the set of states being summed over, so an extra factor of 1/2 is needed. The extra restrictions $a \ne b$ and $r \ne s$ are taken care of since the pairs of labels appear together in a bra or a ket and also in the energy denominator, although this is only true for second and third order diagrams. The second order energy then may be written

$$\Delta E^{(2)} = \frac{1}{4} \sum_{ab\le\epsilon_F} \sum_{rs>\epsilon_F} \frac{|\langle ab|\tilde{v}|rs\rangle|^2}{\epsilon_a + \epsilon_b - \epsilon_r - \epsilon_s}. \tag{B.35}$$

A dimensionless quantity related to the second order energy correction is the so-called "wound integral", κ[101], defined by

$$\kappa = \frac{1}{4} \sum_{ab \leq \epsilon_F} \sum_{rs > \epsilon_F} \frac{|\langle ab|\tilde{v}|rs\rangle|^2}{|\epsilon_a + \epsilon_b - \epsilon_r - \epsilon_s|^2}. \tag{B.36}$$

It is always positive and represents the number of particles in the wavefunction which are not in the ground-state Slater determinant.

This same procedure can be used for evaluation of higher order energy corrections and wavefunction corrections[54]. A more convenient method has been developed for the purposes of writing down the expressions for perturbation theory which is dealt with in the next Appendix.

Appendix C

Hugenholz Diagrams

C.1   Introduction

In 1949 Feynman found that perturbation series encountered in field theory could conveniently be represented diagramatically[102]. Following this lead, Goldstone[103] and Hugenholz[61] both used similar diagrammatic techniques in the treatment of many-fermion perturbation theory. Either set of diagrams may be used to calculate observables, but in this work the Hugenholz diagrams are used since for a given order of perturbation theory there are fewer diagrams to write down. The diagrammatic series for the ground state energy calculation is presented here.

C.2   Unlabelled Diagrams

For a given order, N, of perturbation theory, one draws N vertically ordered dots and then connects them up with lines in all possible ways subject to the following conditions:

- Each dot has four lines emanating from it

- Each diagram is topologically distinct

- Each diagram is linked

- No line connects a dot with itself

The first requirement is a consequence of the perturbation term consisting of a two-body interaction. The second conditions ensures that diagrams are counted only once. The third is a consequence of the *linked-cluster theorem* which shows that if a diagram consists of disconnected parts then each part will already have been included in lower order diagrams and should not be included again. The final

condition is a consequence of Brillouin's theorem and results from using the HF basis as the reference state for perturbation theory.

Using these rules one can see that there is only one possible second-order diagram, shown in Fig C.1. There is also only one unlabelled third order diagram (Fig C.2) but there are 12 unlabelled fourth order diagram, shown in Figure C.3.
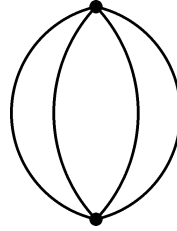
Figure C.1: **Unlabelled second-order Hugenholz diagram**
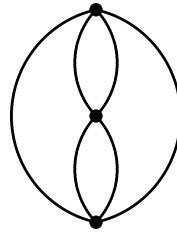
Figure C.2: **Unlabelled third-order Hugenholz diagram**

As one goes up in order of perturbation theory, the number of unlabelled Hugenholz diagrams to be calculated increases rather dramatically. Following the rules given in this section, one can develop an algorithm to count the number of diagrams in each order. This has been done by the author for unlabelled diagrams. Table C.1 shows these numbers. The large number of diagrams for higher orders suggests that explicit diagram-by-diagram evaluation of the perturbation theory will be impractical for systems in which the series has not sufficiently converged by the fourth, or perhaps fifth order.

Order	2	3	4	5	6	7
Unlabelled Diagrams	1	1	12	148	3150	90075

Table C.1: **Number of Hugenholz diagrams by order of perturbation theory**

C.3   Labelled diagrams

Once one has an unlabelled diagram, each of the lines needs to be labelled before it can be evaluated. Labelling consists of putting an arrow on each of the lines either pointing up or down subject to the following rules:
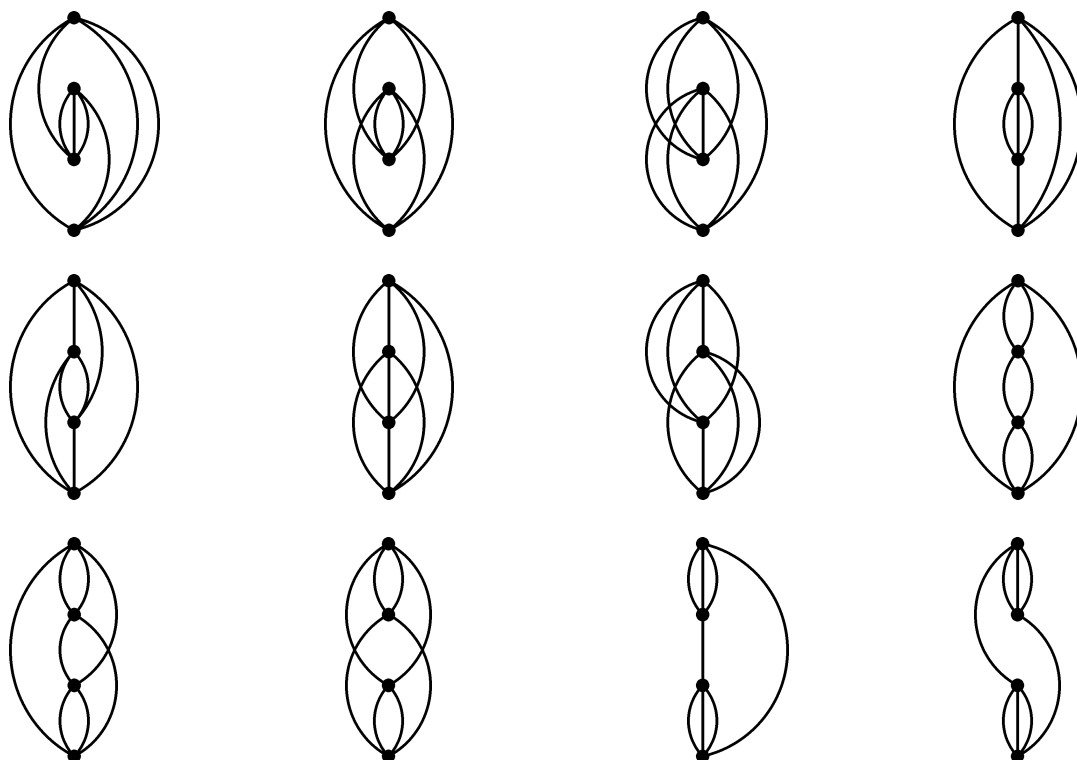
Figure C.3: **Unlabelled fourth-order Hugenholz diagrams**

- Each dot has two lines entering it and two leaving it.

- Each diagram is topologically unique.

An up-pointing arrow represents a particle state, which is to say a particle existing in an orbital unoccupied in the reference state. A down-pointing arrow represents a hole state, which is the absence of a particle in a state which is occupied in the reference state. Each unlabelled diagram may have more than one labelled representation. In the case of the second order there is only one, which is shown in Figure C.4.
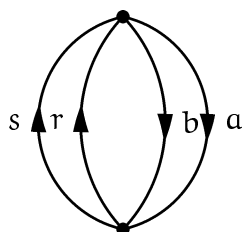
Figure C.4: **Labelled second-order Hugenholz diagram**

In third order, there are three distinct ways of labelling the unlabelled diagram, shown in Figure C.5
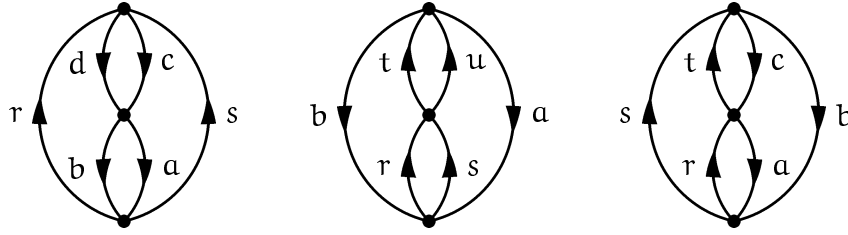
Figure C.5: **Labelled third-order Hugenholz diagrams**

The prescription for writing down the mathematical form of the energy contribution from each graph is as follows:

- For each dot, write down a factor of an *antisymmetric* matrix element of the interaction in the form $\langle$ label-in-1 label-in-2$|\tilde{V}|$ label-out-1 label-out-2$\rangle$. The ordering of the two "in" and "out" labels is not important here, although it will affect a phase later on.

  Between each successive pairs of dot, draw an imaginary horizontal line and for each such line contribute a factor in the denominator of $\left(\sum \epsilon_{\text{holes}} - \sum \epsilon_{\text{particles}}\right)$.

- Sum each hole label over all occupied HF states, and each particle label over unoccupied states.

- Multiply by a factor $1/2^k$ where k is the number of *equivalent pairs* of lines in the diagram. An equivalent pair is a pair of lines starting and ending at the same dot, and pointing in the same direction.

- Include a phase $(-1)^{h+l}$ where h is the number of hole lines and l is the number of closed loops. A prescription for calculating the number of closed loops appears below.

C.4   Second-order Energy Correction

Using the above rules, the expression for the second order ground state energy correction, given in expression (C.4), can be written down as

$$\Delta E^{(2)} = \frac{1}{2^2}(-1)^{2+l} \sum_{ab \leq \epsilon_F} \sum_{rs > \epsilon_F} \frac{\langle ab|\tilde{V}|rs\rangle\langle rs|\tilde{V}|ab\rangle}{\epsilon_a + \epsilon_b - \epsilon_r - \epsilon_s}. \tag{C.1}$$

To determine the number of closed loops, one writes down the series of matrix elements in this expression and starting with the first one follows through all the labels which appear in the same position on the other side of the matrix element until one arrives back at the starting label. If any labels are not included in the first

path, one starts on such a label and continues until all labels have been included. The number of separate paths is then the number of closed loops.

In the above case, the matrix elements are

$$\langle ab|\tilde{V}|rs\rangle\langle rs|\tilde{V}|ab\rangle,$$

so starting at a in the first matrix element, one proceeds:

$$\langle ab|\tilde{V}|rs\rangle\langle rs|\tilde{V}|ab\rangle, \tag{C.2}$$

which is one closed loop $a \to r \to a$. Starting from the first "unused" label, b, another loop exhausts the rest of the labels $b \to s \to b$:

$$\langle ab|\tilde{V}|rs\rangle\langle rs|\tilde{V}|ab\rangle, \tag{C.3}$$

so in this case $l = 2$ and the expression for the second order energy correction is

$$\Delta E^{(2)} = \frac{1}{4} \sum_{ab \leq \epsilon_F} \sum_{rs > \epsilon_F} \frac{\langle ab|\tilde{V}|rs\rangle\langle rs|\tilde{V}|ab\rangle}{\epsilon_a + \epsilon_b - \epsilon_r - \epsilon_s}. \tag{C.4}$$

This is exactly the same as the expression (B.35) derived in the previous Appendix.

C.5 Third-order Energy Correction

C.5.1 Hole-hole Scattering term

The first diagram in Fig (C.5) is called the *hole-hole scattering term* since the matrix element associated with the middle dot has a hole-hole state both as the initial and the final state. Following the rules to write down its expression gives

$$E_{hh}^{(3)} = \frac{1}{8} \sum_{a \neq b \leq \epsilon_F} \sum_{c \neq d \leq \epsilon_F} \sum_{r \neq s > \epsilon_F} (-1)^{4+l} \frac{\langle ab|\tilde{V}|rs\rangle\langle cd|\tilde{V}|ab\rangle\langle rs|\tilde{V}|cd\rangle}{(\epsilon_a + \epsilon_b - \epsilon_r - \epsilon_s)(\epsilon_c + \epsilon_d - \epsilon_r - \epsilon_s)} \tag{C.5}$$

The number of closed loops is evaluated as:

$$\langle ab|\tilde{V}|rs\rangle\langle cd|\tilde{V}|ab\rangle\langle rs|\tilde{V}|cd\rangle \tag{C.6}$$

where the numbers indicate the order in which the arrows operate to form the loop $a \to r \to c \to a$. A second loop exhausts the labels $b \to s \to d \to b$,

$$\langle ab|\tilde{V}|rs\rangle\langle cd|\tilde{V}|ab\rangle\langle rs|\tilde{V}|cd\rangle \tag{C.7}$$

so that $l = 2$ and the sign of the term is positive.

C.5.2 Particle-Particle Scattering term

Following the same procedure for writing down the expression and counting the number of closed loops, the second diagram in Figure C.5 is

$$
E_{pp}^{(3)} = \frac{1}{8} \sum_{a \neq b \leq \epsilon_F} \sum_{r \neq s > \epsilon_F} \sum_{t \neq u > \epsilon_F} \frac{\langle ab|\tilde{V}|rs\rangle \langle rs|\tilde{V}|tu\rangle \langle tu|\tilde{V}|ab\rangle}{(\epsilon_a + \epsilon_b - \epsilon_r - \epsilon_s)(\epsilon_a + \epsilon_b - \epsilon_t - \epsilon_u)} \tag{C.8}
$$

C.5.3 Particle-Hole Scattering term

The final diagram in Figure C.5 is

$$
E_{ph}^{(3)} = \sum_{a \neq b \neq c \leq \epsilon_F} \sum_{r \neq s \neq t > \epsilon_F} \frac{\langle ab|\tilde{V}|rs\rangle \langle cr|\tilde{V}|at\rangle \langle st|\tilde{V}|cb\rangle}{(\epsilon_a + \epsilon_b - \epsilon_r - \epsilon_s)(\epsilon_b + \epsilon_c - \epsilon_s - \epsilon_t)}. \tag{C.9}
$$

Note that there is no factor of 1/8 here since there are no "equivalent pairs".

Appendix D

Harmonic Oscillator Basis

D.1   Uncoupled representation

The HF wavefunctions are defined by their expansion coefficients in a spherical harmonic oscillator basis. The harmonic oscillator wavefunctions are separated into radial and angular parts:

$$\phi_{njl}(r) = R_{nl}(r)Y_{lm_l}(\theta, \phi), \tag{D.1}$$

and are the solution of the Schrödinger equation

$$-\frac{\hbar^2}{2m}\nabla^2\phi_a(r) - \frac{1}{2}m\omega^2r^2\phi_a(r) = e_{(nljm)_a}\phi_a(r). \tag{D.2}$$

With spherical symmetry assumed the angular parts of the wavefunction are sperical harmonics. The radial equation is analytically solvable to give

$$R_{nl}(r) = \sqrt{\frac{2^{l-n+1}(2n+2l+3)!!}{b^3\sqrt{\pi}\{(2l+1)!!\}^2}}r^l L_{n,l+1/2}(r^2/b^2)e^{-\frac{r^2}{2b^2}}, \tag{D.3}$$

where

$$b = \sqrt{\frac{\hbar}{m\omega}} \tag{D.4}$$

is the oscillator size parameter, and $L_{n,l+1/2}$ is an *associated Laguerre polynomial*. The ground state of the radial function is that which has $n = 0$. The full oscillator wavefunctions (D.1) are orthonormal and form a complete set. The orthogonality in the angular coordinates and quantum numbers comes from the spherical harmonics:

$$\int_0^\pi \sin\theta \, d\theta \int_0^{2\pi} d\phi \, Y^*_{lm_l}(\theta, \phi)Y_{l'm'}(\theta, \phi) = \delta_{ll'}\delta_{mm'} \tag{D.5}$$

and in the radial function

$$\int dr \, r^2 R_{nl}(r)R_{n'l}(r) = \delta_{nn'}. \tag{D.6}$$

D.2 Coupled representation

Since the eigenstates of the single particle Hamiltonian are eigenstates of the total angular momentum operator j^2 and not the orbital angular momentum operator l^2 it is useful to construct harmonic oscillator wavefunctions which share these symmetries. This is achieved by coupling the spherical harmonic to a spinor to give a spinor spherical harmonic:

$$\mathcal{Y}_{ljm}(\theta, \phi, \chi) = \left[Y_{lm_l}(\theta, \phi) \otimes \chi_{m_s}^{1/2} \right]_m^j, \tag{D.7}$$

where the m without a subscript is the magentic quantum number associated with the coupled angular momentum, and the symbol $\otimes$ represents a tensor coupling. Explicitly this may be written as

$$\mathcal{Y}_{ljm}(\theta, \phi, \chi) = \sum_{m_l m_s} \langle l m_l\, 1/2 m_s | jm \rangle Y_{lm_l}(\theta, \phi) \chi_{m_s}^{1/2} \tag{D.8}$$

where $\langle l m_l\, 1/2 m_s | jm \rangle$ is a Clebsch–Gordan coefficient.

The orthogonality relations are, in the coupled case, the same for the radial quantum number and, for the angular quantum numbers:

$$\int d\chi \int_0^\pi \sin\theta\; d\theta \int_0^{2\pi} d\phi\; \mathcal{Y}_{ljm}^*(\theta, \phi, \chi) \mathcal{Y}_{l'j'm'}(\theta, \phi, \chi) = \delta_{ll'}\delta_{jj'}\delta_{mm'} \tag{D.9}$$

D.3 Radial Derivatives

The radial derivative of a harmonic oscillator eigenfunction is quite simple since the derivatives of Laguerre polynomials are also Laguerre polynomials:

$$\frac{dL_{n,l+1/2}(r^2)}{dr} = L_{n-1,l+3/2}(r^2) \tag{D.10}$$

so that the derivative of the whole radial eigenfunction is

$$\begin{aligned}
\frac{d\mathcal{R}_{nl}(x)}{dx} = \; & \mathcal{N} \Bigg(l r^{l-1} L_{n,l+1/2}(r^2/b^2) e^{-\frac{r^2}{2b^2}} + r^l \left(\frac{2r}{b^2} \right) L_{n-1,l+3/2}(r^2/b^2) e^{-\frac{r^2}{2b^2}} \\
& - r^l L_{n,l+1/2}(r^2/b^2) \left(\frac{r}{b^2} \right) e^{-\frac{x^2}{2b^2}} \Bigg),
\end{aligned} \tag{D.11}$$

where N is the same normalization factor as in Equation (D.3). Thus any function of the density or its derivatives may be evaluated exactly in terms of the harmonic oscillator states.

Appendix E

Hartree–Fock Potential for the Separable Force.

This appendix contains derivations of the Hartree–Fock energy, potential and matrix elements for all the terms of the nuclear force used in the work.

The Hartree–Fock potential is obtained from a variation of the HF energy as detailed in Appendix A.

E.1   Variational principle

The normal functional variation is employed, viz.

$$\int dx \sum_a \frac{\delta \varphi_a^*(r)}{\delta \varphi_b^*(x)} = \int dx \sum_a \delta^3(r-x)\delta_{ab} \tag{E.1}$$

where a and b label all the good quantum numbers of a single particle state (N, l, j, m, τ) and x and r are the three-dimensional spatial coordinates plus spin and isospin coordinates. The wave functions, φ are the full single particle wave functions, including radial and angular parts, as well as a spinor and an isospinor The integral over x is really an integral over the continuous coordinates and a summation over the discrete ones and the Dirac delta includes a Kronecker delta for these coordinates. For most terms in the derivation which follows, this notation suffices and it is not necessary to break the wave functions φ up into their separate parts. However, for the terms which include spatial derivative operators, it is necessary to consider a variation acting only using the $\mathcal{R}$ part of the wave function. This is possible to do due to the assumed symmetries of the HF wave functions and the fact that only nuclei with completely full j-sub-shells are considered.

The appropriate variational principle is

$$\sum_a \int dx \frac{\delta \mathcal{R}_a^*(r)}{\delta \mathcal{R}_b(x)} = \sum_a \int dx \frac{1}{x^2}\delta(r-x)\frac{1}{2j_a+1}\delta_{ab}. \tag{E.2}$$

Here, the coordinates r and x are just the one-dimensional spatial coordinates. To show that this is true, one can consider a simple potential, which is just a constant, $V(r_1, r_2) = k$. Then the energy from this potential is

$$E = k \left(\int dr \rho(r) \right)^2 .$$

A single variation of which gives

$$\frac{\delta E}{\delta X} = k \int dr \rho(r) \cdot \int dr \frac{\delta \rho(r)}{\delta X} = kA \int dr \frac{\delta \rho(r)}{\delta X}.$$

Then choosing $X = \varphi_b^*(x)$:

$$
\begin{aligned}
\int d^3 r \frac{\delta \rho(r)}{\delta \varphi_b^*(x)} &= \int d^3 r \sum_{i < \epsilon_F} \frac{\varphi_i^*(r) \varphi_i(r)}{\delta \varphi_b^*(x)} \\
&= \int d^3 r \sum_{i < \epsilon_F} \varphi_i(r) \delta^3(r - x) \delta_{ib} = \varphi_b(x) \quad\quad (E.3)
\end{aligned}
$$

or $X = \mathcal{R}_b^*(x)$:

$$
\begin{aligned}
\int d^3 r \frac{\delta \rho(r)}{\delta \mathcal{R}_b^*(x)} &= \int d^3 r \sum_{i < \epsilon_F} \frac{\mathcal{R}(r)_i^* \mathcal{R}(r)_i \mathcal{Y}(\hat{r})_i^* \mathcal{Y}(\hat{r})_i \chi_i^* \chi_i}{\delta \mathcal{R}_b^*(x)} \\
&= \int r^2 d^1 r \sum_{N_i : i < \epsilon_F} (2j_i + 1) \delta_{ib} \delta^1(r - x) \mathcal{R}_i(x) \\
&= x^2 (2j_b + 1) \mathcal{R}_b(x) \quad\quad (E.4)
\end{aligned}
$$

where the dimensions of each spatial integration and delta function have been made explicit. The two methods of variation then result in the same one-dimensional HF potentials if the relation (E.2) is used. Of course, in the first case one has still to perform the angular and dimensional reduction, which accounts for these factors.

E.2 Hartree-Fock Energy

E.2.1 Monopole term

The monopole interaction is written in coordinate space as

$$
\begin{aligned}
V(r_1, r_2) &= W_a f_{\alpha_a} \rho^{\beta_a}(r_1) \rho^{\beta_a}(r_2) (1 + a_a(\tau_1^+ \tau_2^- + \tau_1^- \tau_2^+) + b_a(\tau_{1z} \tau_{2z})) \\
&+ W_r f_{\alpha_r} \rho^{\beta_r}(r_1) \rho^{\beta_r}(r_2) (1 + a_r(\tau_1^+ \tau_2^- + \tau_1^- \tau_2^+) + b_r(\tau_{1z} \tau_{2z})) \\
&+ k \nabla_1^2 \rho(r_1) \nabla_2^2 \rho(r_2) + \frac{c}{r} \frac{\partial \rho(r)}{\partial r} \mathbf{l} \cdot \mathbf{s}. \quad\quad (E.5)
\end{aligned}
$$

The physical interpretation of these terms is discussed in Chapter 3.

Since the first two terms of the force are functionally identical terms, it will suffice to go through the derivation for just one term. In what follows only the expressions for the attractive part of the potential, with subscript a, will be derived.

The energy contribution from this two-body force can be written

$$E = \frac{1}{2} \sum_{ij < \epsilon_f} \langle ij | V \left(|ij\rangle - |ji\rangle \right)$$ (E.6)

Central term

The energy contribution from the "central term", which is defined as that part of the attractive force with no isospin operator, is

$$\frac{1}{2} \sum_{ij < \epsilon_F} \langle ij | W_a f_{\alpha_a} \rho^{\beta_a}(r_1) \rho^{\beta_a}(r_2) | ij \rangle - \frac{1}{2} \sum_{ij < \epsilon_F} \langle ij | W_a f_{\alpha_a} \rho^{\beta_a}(r_1) \rho^{\beta_a}(r_2) | ji \rangle$$ (E.7)

The direct term in Equation (E.7) may be written

$$\frac{1}{2} W_a f_{\alpha_a} \sum_{ij < \epsilon_F} \int \int d^3 r_1 d^3 r_2 \, \varphi_i^*(r_1) \varphi_j^*(r_2) \rho^{\beta_a}(r_1) \rho^{\beta_a}(r_2) \varphi_i(r_1) \varphi_j(r_2)$$

$$= \frac{1}{2} W_a \left(\sum_{i < \epsilon_F} \int d^3 r_1 \, \varphi_i^*(r_1) \rho^{\beta_a}(r_1) \varphi_i(r_1) \right) \left(\sum_{j < \epsilon_F} \int d^3 r_2 \, \varphi_j^*(r_2) \rho^{\beta_a}(r_2) \varphi_j(r_2) \right)$$

$$= \frac{1}{2} W_a f_{\alpha_a} \left(\int d^3 r_1 \rho^{\beta_a+1}(r_1) \right) \left(\int d^3 r_2 \rho^{\beta_a+1}(r_2) \right)$$

$$= \frac{1}{2} W_a f_{\alpha_a} N_{\beta_a}^{\,2}$$ (E.8)

where the total density has been defined as the sum of the proton and neutron densities as

$$\rho(r) = \rho_p(r) + \rho_n(r) = \sum_{i \in p < \epsilon_F} \varphi_i^*(r) \varphi_i^*(r) + \sum_{i \in n < \epsilon_F} \varphi_i^*(r) \varphi_i(r)$$ (E.9)

and

$$N_{\beta_a} = \int d^3 r \rho^{\beta_a+1}(r).$$ (E.10)

We define N_{β_r} similarly for the repulsive term parameters. The exchange term cannot be simplified in terms of the one-body density. It may, however be expressed in terms of the nonlocal density, which for nucleon species q is

$$\rho_q(r_1, r_2) = \sum_{i \in q < \epsilon_F} \varphi_i^*(r_2) \varphi_i(r_1)$$ (E.11)

and a total nonlocal density $\rho(r_1, r_2)$ may be defined as $\rho(r_1, r_2) = \rho_p(r_1, r_2) + \rho_n(r_1, r_2)$. The exchange energy then can be written as

$$-\frac{1}{2} W_a f_{\alpha_a} \int \int d^3 r_1 d^3 r_2 \rho(r_1, r_2) \rho(r_2, r_1) \rho^{\beta_a}(r_1) \rho^{\beta_a}(r_2)$$

$$= -\frac{1}{2} W_a f_{\alpha_a} M_{\beta_a} \tag{E.12}$$

where the space part of the exchange integral has been defined as

$$M_{\beta_a} = \int \int d^3 r_1 d^3 r_2 \rho(r_1, r_2) \rho(r_2, r_1) \rho^{\beta_a}(r_1) \rho^{\beta_a}(r_2) \tag{E.13}$$

with a similar definition for M_{β_r}, with the parameter β_r.

Isospin-dependent term

To calculate the energy due to the isospin-dependent term of the monopole interaction, one needs to examine the properties of the isospin operators on the four possible combinations of uncoupled 2-body isospinors. We represent a proton state by the letter p and a neutron state by the letter n:

$$(a_a(\tau_1^+ \tau_2^- + \tau_1^- \tau_2^+) + b_a(\tau_{1z}\tau_{2z}))|pp\rangle = b_a|pp\rangle$$
$$(a_a(\tau_1^+ \tau_2^- + \tau_1^- \tau_2^+) + b_a(\tau_{1z}\tau_{2z}))|pn\rangle = a_a|np\rangle - b_a|pn\rangle$$
$$(a_a(\tau_1^+ \tau_2^- + \tau_1^- \tau_2^+) + b_a(\tau_{1z}\tau_{2z}))|np\rangle = a_a|pn\rangle - b_a|np\rangle$$
$$(a_a(\tau_1^+ \tau_2^- + \tau_1^- \tau_2^+) + b_a(\tau_{1z}\tau_{2z}))|nn\rangle = b_a|nn\rangle$$

so that the following isospin matrix elements are the only ones which are non-zero:

$$\langle \tau\tau|(a_a(\tau_1^+ \tau_2^- + \tau_1^- \tau_2^+) + b_a(\tau_{1z}\tau_{2z}))|\tau\tau\rangle = b_a$$
$$\langle \tau\bar{\tau}|(a_a(\tau_1^+ \tau_2^- + \tau_1^- \tau_2^+) + b_a(\tau_{1z}\tau_{2z}))|\tau\bar{\tau}\rangle = -b_a$$
$$\langle \tau\bar{\tau}|(a_a(\tau_1^+ \tau_2^- + \tau_1^- \tau_2^+) + b_a(\tau_{1z}\tau_{2z}))|\bar{\tau}\tau\rangle = a \tag{E.14}$$

where τ may represent either a neutron or a proton, and $\bar{\tau}$ represents the other nucleon species. To arrive at an expression for the contribution to the energy from this term, the sum is split into terms with $\tau_i = \tau_j$ and $\tau_i \neq \tau_j$. Firstly the direct term:

$$\frac{1}{2} \sum_{\substack{i,j < \epsilon_f \\ \tau_i = \tau_j}} \langle ij|W_a f_{\alpha_a} \rho^{\beta_a}(r_1) \rho^{\beta_a}(r_2)(a_a(\tau_1^+ \tau_2^- + \tau_1^- \tau_2^+) + b_a(\tau_{1z}\tau_{2z}))|ij\rangle$$

$$= \frac{1}{2} W_a b_a f_{\alpha_a} \sum_{\substack{i,j < \epsilon_F \\ \tau_i = \tau_j}} \int d^3 r_1 \varphi_i^*(r_1) \rho^{\beta_a}(r_1) \varphi_i(r_1) \int d^3 r_2 \varphi_j^*(r_2) \rho^{\beta_a}(r_2) \varphi_j(r_2)$$

$$= \frac{1}{2} W_a b_a f_{\alpha_a} \left(\left[\int d^3 r \rho^{\beta_a}(r) \rho_p(r) \right]^2 + \left[\int d^3 r \rho^{\beta_a}(r) \rho_n(r) \right]^2 \right)$$

$$= \frac{1}{2} W_a b_a f_{\alpha_a} \left(N_{\beta_a}^{(p)2} + N_{\beta_a}^{(n)2} \right), \tag{E.15}$$

where the function, $N_{\beta_a}^{(\tau)}$ is defined as

$$N_{\beta_a}^{(\tau)} = \int d^3 r \rho^{\beta_a}(r) \rho_\tau(r),$$

(E.16)

and $\rho_\tau(r)$ is the nuclear density for a particular species of nucleon. There is also a contribution from the terms with $\tau_i \neq \tau_j$:

$$\frac{1}{2} \sum_{\substack{i,j < \epsilon_f \\ \tau_i \neq \tau_j}} \langle ij | W_a f_{\alpha_a} \rho^{\beta_a}(r_1) \rho^{\beta_a}(r_2)(a_a(\tau_1^+ \tau_2^- + \tau_1^- \tau_2^+) + b_a(\tau_{1z}\tau_{2z})) | ij \rangle$$

$$= -\frac{1}{2} W_a b_a f_{\alpha_a} \sum_{\substack{i,j < \epsilon_F \\ \tau_i \neq \tau_j}} \int d^3 r_1 \varphi_i^*(r_1) \rho^{\beta_a}(r_1) \varphi_i(r_1) \int d^3 r_2 \varphi_j^*(r_2) \rho^{\beta_a}(r_2) \varphi_j(r_2)$$

$$= -W_a b_a f_{\alpha_a} \left(\int d^3 r \rho^{\beta_a}(r) \rho_p(r) \int d^3 r \rho^{\beta_a}(r) \rho_n(r) \right)$$

$$= -W_a b_a f_{\alpha_a} \left(N_{\beta_a}^{(p)} N_{\beta_a}^{(n)} \right).$$

(E.17)

so that the total energy contribution from these terms is

$$E_{\tau,\text{direct}} = \frac{1}{2} W_a b_a f_{\alpha_a} \left(N_{\beta_a}^{(p)} - N_{\beta_a}^{(n)} \right)^2$$

$$= \frac{1}{2} W_a b_a f_{\alpha_a} \left(\Delta N_{\beta_a} \right)^2,$$

(E.18)

in which the function

$$\Delta N_{\beta_a} = \left(N_{\beta_a}^{(p)} - N_{\beta_a}^{(n)} \right) = \int d^3 r \rho^{\beta_a}(r) \left(\rho_p(r) - \rho_n(r) \right)$$

(E.19)

is defined. The exchange term is also calculated by splitting it into two sums. For $\tau_i = \tau_j$, the contribution to the exchange energy is

$$= -(1/2) W_a f_{\alpha_a} \sum_{\substack{ij < \epsilon_f \\ \tau_i = \tau_j}} \langle ij | \rho^{\beta_a}(r_1) \rho^{\beta_a}(r_2)(a_a(\tau_1^+ \tau_2^- + \tau_1^- \tau_2^+) + b_a(\tau_{1z}\tau_{2z})) | ji \rangle$$

$$= -(1/2) W_a f_{\alpha_a} b_a \int \int d^3 r_1 d^3 r_2 \rho^{\beta_a}(r_1) \rho^{\beta_a}(r_2)(\rho_p(r_1, r_2)\rho_p(r_2, r_1)$$

$$+ \rho_n(r_1, r_2)\rho_n(r_2, r_1))$$

$$= -(1/2) W_a f_{\alpha_a} b_a M_{\beta_a}^{(\tau\tau)}$$

(E.20)

and for $\tau_i \neq \tau_j$:

$$= -(1/2) W_a f_{\alpha_a} \sum_{\substack{ij < \epsilon_f \\ \tau_i \neq \tau_j}} \langle ij | \rho^{\beta_a}(r_1) \rho^{\beta_a}(r_2)(a_a(\tau_1^+ \tau_2^- + \tau_1^- \tau_2^+) + b_a(\tau_{1z}\tau_{2z})) | ji \rangle$$

$$= -(1/2) W_a f_{\alpha_a} a_a \int \int d^3 r_1 d^3 r_2 \rho^{\beta_a}(r_1) \rho^{\beta_a}(r_2)(\rho_p(r_1, r_2)\rho_n(r_2, r_1)$$

$$+ \rho_n(r_1, r_2)\rho_p(r_2, r_1))$$

$$= -(1/2) W_a f_{\alpha_a} a_a M_{\beta_a}^{(\tau\bar\tau)}$$

(E.21)

so that the total energy contribution due to the exchange term of the isospin-dependent part of the force is

$$E_{\tau,\text{exch}} = -\frac{1}{2}W_a b_a f_{\alpha_a} M^{(\tau\tau)}_{\beta_a} - \frac{1}{2}W_a a_a f_{\alpha_a} M^{(\tau\bar{\tau})}_{\beta_a} \qquad (E.22)$$

Derivative term

The energy due to the direct part of this term is

$$E_{d,\text{dir}} = (k/2)\int d^3 r_1 \rho(r_1)\nabla^2\rho(r_1)\int d^3 r_2 \rho(r_2)\nabla^2\rho(r_2) = (k/2)\left[\int d^3 r \rho(r)\nabla^2\rho(r)\right]^2 = \frac{1}{2}kN^2_d, \qquad (E.23)$$

where N_d is

$$N_d = \int d^3 r \rho(r)\nabla^2\rho(r). \qquad (E.24)$$

The exchange term can be written

$$E_{d,\text{exch}} = (k/2)\int\int d^3 r_1 d^3 r_2 \rho(r_1, r_2)\rho(r_2, r_1)\nabla^2_1\rho(r_1)\nabla^2_2\rho(r_2). \qquad (E.25)$$

We may define the 6-dimension integral to be M_d in analogy with the other exchange integrals.

Spin-orbit term

To evaluate the energy contribution from the spin-orbit term, it is noted that

$$\hat{j}^2 = (\hat{l} + \hat{s})^2 = \hat{l}^2 + \hat{s}^2 + 2\hat{l}\cdot\hat{s} \qquad (E.26)$$

so that

$$\hat{l}\cdot\hat{s} = \frac{1}{2}\left(\hat{j}^2 - \hat{l}^2 - \hat{s}^2\right) \qquad (E.27)$$

and the act of this operator on a single particle state is

$$\hat{l}\cdot\hat{s}|i\rangle = \frac{1}{2}\left(j_i(j_i + 1) - l_i(l_i + 1) - \frac{3}{4}\right)|i\rangle \qquad (E.28)$$

This eigenvalue, w_i, is abbreviated for brevity as,

$$w_i = \frac{1}{2}\left(j_i(j_i + 1) - l_i(l_i + 1) - 3/4\right). \qquad (E.29)$$

The spin-orbit energy, then, can be written:

$$\begin{aligned}
E_{so} &= c\sum_{i<\epsilon_F}\langle i|\frac{1}{r}\frac{\partial\rho(r)}{\partial r}w_i|i\rangle \\
&= c\int d^3 r\frac{1}{r}\frac{\partial\rho(r)}{\partial r}\rho_w(r) \\
&= cN_w \qquad (E.30)
\end{aligned}$$

where the "weighted density" is defined as

$$\rho_w(r) = \sum_{i < \epsilon_F} w_i \varphi_i^*(r) \varphi_i(r). \tag{E.31}$$

and N_w to be the integral in the above expression. In summary, the complete expression of the energy due to the monopole and spin-orbit terms may be written as

$$
\begin{aligned}
E_{HF} &= \sum_{\xi=a,r} \left\{ \frac{1}{2} W_\xi f_{\alpha_\xi} N_{\beta_\xi}^2 - \frac{1}{2} W_\xi f_{\alpha_\xi} M_{\beta_\xi} \right. \\
&+ \left. \frac{1}{2} W_\xi b_\xi f_{\alpha_\xi} (\Delta N_{\beta_\xi})^2 - \frac{1}{2} W_\xi f_{\alpha_\xi} \left[b_\xi M_{\beta_\xi}^{(\tau\tau)} + a_\xi M_{\beta_\xi}^{(\tau\bar{\tau})} \right] \right\} \\
&+ \frac{1}{2} k N_d^2 - \frac{1}{2} k M_d + c N_w
\end{aligned}
\tag{E.32}
$$

Higher Multipole terms

The energy due to the dipole or quadrupole interactions may be written

$$E_{\Lambda,q_1,q_2} = \frac{f_\Lambda W_{\lambda,q_1,q_2}}{2} \sum_{i,j < \epsilon_F} \sum_{M=-\Lambda}^{\Lambda} (-1)^M \langle ij | (r_1^\Lambda \rho(r_1) Y_{\Lambda M}(\hat{r}_1))(r_2^\Lambda \rho(r_2) Y_{\Lambda-M}(\hat{r}_2)) \{ |ij\rangle - |ji\rangle \} \tag{E.33}$$

The direct contribution to the HF energy for a spherical nucleus in which each shell is filled is zero. To show this one notes that the force is separable so that the sums over i and j can be considered separately. Looking just at the angular part of the sum over i (which subscript can be dropped without confusion), one has

$$
\begin{aligned}
\sum_m \langle (l1/2)jm | Y_{\Lambda M} | (l1/2)jm \rangle &= \sum_m \sum_{m_l m_l'} \sum_{m_s m_s'} \langle l m_l 1/2 m_s | jm \rangle \langle l m_l' 1/2 m_s' | jm \rangle \\
&\quad \cdot \langle 1/2 m_s | 1/2 m_s' \rangle \langle l m_l | Y_{\Lambda M} | l m_l' \rangle \\
&= \sum_{m m_l m_s} |\langle l m_l 1/2 m_s | jm \rangle|^2 \langle l m_l | Y_{\Lambda M} | l m_l \rangle \\
&= \sum_{m m_l m_s} \frac{2j+1}{2l+1} |\langle 1/2 - m_s jm | l m_l \rangle|^2 \langle l m_l | Y_{\Lambda M} | l m_l \rangle \\
&= \sum_{m_l} \frac{2j+1}{2l+1} \langle l m_l | Y_{\Lambda M} | l m_l \rangle \\
&= \frac{2j+1}{4\pi} \int d^2\hat{r} Y_{\Lambda M}(\hat{r}) \\
&= \frac{2j+1}{\sqrt{4\pi}} \delta_{\Lambda 0} \tag{E.34}
\end{aligned}
$$

so for the values of Λ of interest, i.e. 1 and 2, there is no direct contribution to the Hartree-Fock energy. The exchange term is just evaluated directly from expression (E.33).

E.2.2   Hartree–Fock Potential

To determine the one-body Hartree–Fock potential, the variational principle is used, as described at the beginning of this Appendix, to minimize the energy. The contributions from the various terms in the energy are as follows:

Central Term

The variation of the direct part gives us

$$\frac{\delta}{\delta \varphi_b^*(x)} \left(\frac{1}{2} W_a f_{\alpha_a} N_{\beta_a}{}^2 \right) = \frac{1}{2} W_a \frac{\delta f_{\alpha_a}}{\delta \varphi_b^*(x)} N_{\beta_a}{}^2 + W_a f_{\alpha_a} N_{\beta_a} \frac{\delta N_{\beta_a}}{\delta \varphi_b^*(x)} \qquad (E.35)$$

The variation of f_{α_a} is

$$
\begin{aligned}
\frac{\delta f_{\alpha_a}}{\delta \varphi_b^*(x)} &= \frac{\delta}{\delta \varphi_b^*(x)} \left[\int \rho_a^\alpha(r) d^3 r \right]^{-1} \\
&= -\left[\int \rho_a^\alpha(r) d^3 r \right]^{-2} \int d^3 r \frac{\delta \rho_a^\alpha(r)}{\delta \varphi_b^*(x)} \\
&= -[f_{\alpha_a}]^2 \alpha_a \int d^3 r \rho^{\alpha_a - 1}(r) \frac{\delta \rho(r)}{\varphi_b^*(x)} \\
&= -[f_{\alpha_a}]^2 \alpha_a \int d^3 r \rho^{\alpha_a - 1}(r) \sum_k \varphi_k(r) \delta(x - r) \delta_{kb} \\
&= -[f_{\alpha_a}]^2 \alpha_a \rho^{\alpha_a - 1}(x) \varphi_b(x) \qquad (E.36)
\end{aligned}
$$

so that the first term in (E.35) is

$$-W_a(\alpha_a/2) \left(f_{\alpha_a} N_{\beta_a} \right)^2 \rho^{\alpha_a - 1}(x) \varphi_b(x) \qquad (E.37)$$

giving a contribution to the HF mean–field of

$$U(x) = -W_a(\alpha_a/2) \left(f_{\alpha_a} N_{\beta_a} \right)^2 \rho^{\alpha_a - 1}(x). \qquad (E.38)$$

Here $U(x)$ denotes the particular contribution to the HF potential, and the same function will be used throughout this derivation to denote other contributions. In the end $U(x)$ will be used to mean the sum of all the contributions together.
   The second term in (E.35) is

$$
\begin{aligned}
&W_a f_{\alpha_a} N_{\beta_a} \frac{\delta}{\delta \varphi_b^*(x)} \int d^3 r \rho^{\beta_a + 1}(r) \\
&= W_a f_{\alpha_a} N_{\beta_a} (\beta_a + 1) \int d^3 r \rho^{\beta_a}(r) \frac{\delta \rho(r)}{\delta \varphi_b^*(x)} \\
&= W_a f_{\alpha_a} N_{\beta_a} (\beta_a + 1) \rho^{\beta_a}(x) \varphi_b^*(x) \qquad (E.39)
\end{aligned}
$$

which gives a contribution to the Hartree–Fock potential of

$$U(x) = W_a f_{\alpha_a} N_{\beta_a} (\beta_a + 1) \rho^{\beta_a}(x) \tag{E.40}$$

Now is performed the variation of the exchange energy:

$$-\frac{\delta}{\delta\varphi_b^*(x)} \left(\frac{1}{2} W_a f_{\alpha_a} M_{\beta_a} \right)$$

$$= -\frac{1}{2} W_a \frac{\delta f_{\alpha_a}}{\delta\varphi_b^*(x)} M_{\beta_a} - \frac{1}{2} W_a f_{\alpha_a} \frac{\delta M_{\beta_a}}{\delta\varphi_b^*(x)} \tag{E.41}$$

The first term involves the variation of f_{α_a} as with the direct part, and the contribution to the (local) Hartree–Fock potential can be written down as

$$U(x) = +\frac{1}{2} W_a (f_{\alpha_a})^2 M_{\beta_a} \rho^{\alpha_a - 1}(x) \tag{E.42}$$

Variation of the function M_{β_a} is as follows:

$$\frac{\delta M_{\beta_a}}{\delta\varphi_b^*(x)} = \frac{\delta}{\delta\varphi_b^*(x)} \left(\sum_{ij<\epsilon_F} \int\int d^3r_1 d^3r_2 \varphi_i^*(r_1)\varphi_j(r_2)\rho^{\beta_a}(r_1)\rho^{\beta_a}(r_2)\varphi_j(r_1)\varphi_i(r_2) \right)$$

$$= \sum_{ij<\epsilon_F} \int\int d^3r_1 d^3r_2 \frac{\delta\varphi_i^*}{\delta\varphi_b^*(x)}\varphi_j(r_2)\rho^{\beta_a}(r_1)\rho^{\beta_a}(r_2)\varphi_j(r_1)\varphi_i(r_2)$$

$$+ \sum_{ij<\epsilon_F} \int\int d^3r_1 d^3r_2 \varphi_i^*(r_1)\frac{\delta\varphi_j^*(r_2)}{\delta\varphi_b^*(x)}\rho^{\beta_a}(r_1)\rho^{\beta_a}(r_2)\varphi_j(r_1)\varphi_i(r_2)$$

$$+ \sum_{ij<\epsilon_F} \int\int d^3r_1 d^3r_2 \varphi_i^*(r_1)\varphi_j^*(r_2)\frac{\delta\rho^{\beta_a}(r_1)}{\delta\varphi_b^*(x)}\rho^{\beta_a}(r_2)\varphi_j(r_1)\varphi_i(r_2)$$

$$+ \sum_{ij<\epsilon_F} \int\int d^3r_1 d^3r_2 \varphi_i^*(r_1)\varphi_j^*(r_2)\rho^{\beta_a}(r_1)\frac{\delta\rho^{\beta_a}(r_2)}{\delta\varphi_b^*(x)}\varphi_j(r_1)\varphi_i(r_2)$$

$$= \sum_{j<\epsilon_F} \int d^3r_2 \varphi_j^*(r_2)\rho^{\beta_a}(x)\rho^{\beta_a}(r_2)\varphi_j(x)\varphi_b(r_2)$$

$$+ \sum_{i<\epsilon_F} \int d^3r_1 \varphi_i^*(r_1)\rho^{\beta_a}(r_1)\rho^{\beta_a}(x)\varphi_b^*(r_1)\varphi_j^*(x)$$

$$+ \sum_{ij<\epsilon_F} \int d^3r_2 \varphi_i^*(x)\varphi_j(r_2)\beta_a\rho^{\beta_a-1}(x)\varphi_b(x)\rho^{\beta_a}(r_2)\varphi_j(x)\varphi_i(r_2)$$

$$+ \sum_{ij<\epsilon_F} \int d^3r_1 \varphi_i^*(r_1)\varphi_j(x)\rho^{\beta_a}(r_1)\beta_a\rho^{\beta_a-1}(x)\varphi_b(x)\varphi_j(r_1)\varphi_i(x) \tag{E.43}$$

By relabelling of indices and coordinates, the first and second terms are seen to be equal, as are the third and fourth terms. This variation then becomes:

$$\frac{\delta M_{\beta_a}}{\delta\varphi_b^*(x)} = 2 \sum_{i<\epsilon_F} \rho^{\beta_a}(x)\varphi_i(x) \int d^3r \varphi_i^*(r)\rho^{\beta_a}(r)\varphi_b(r)$$

$$+ \; 2 \sum_{ij<\epsilon_F} \varphi_i(x)\rho^{\beta_a-1}(x)\varphi_b(x)\varphi_j(x) \int d^3r \varphi_j(r)\rho^{\beta_a}(r)\varphi_i(r) \qquad (E.44)$$

The first term contributes to a nonlocal Hartree–Fock potential:

$$\mathcal{U}(x,x')\varphi_b(x') = -W_a f_{\alpha_a} \sum_{i<\epsilon_F} \rho^{\beta_a}(x)\varphi_i(x) \left[\int d^3r \varphi_i^*(r)\rho^{\beta_a}(r)\varphi_b(r) \right] \qquad (E.45)$$

and the other term contributes to the local Hartree–Fock potential:

$$U(x) = W_a f_{\alpha_a}\beta_a G_{\beta_a}(x)\rho^{\beta_a-1}(x) \qquad (E.46)$$

where $G_{\beta_a}(x)$ is defined as

$$G_{\beta_a}(x) = \int d^3r \rho(r,x)\rho(x,r)\rho^{\beta_a}(r) \qquad (E.47)$$

Isospin-dependent term

The functional variation of the energy which comes from the direct part of the isospin-dependent term (E.18) is

$$
\begin{aligned}
\frac{\delta E_{\tau,\text{direct}}}{\delta \varphi_b^*(x)} \;=\;& \frac{1}{2}V b_a \frac{\delta f_{\alpha_a}}{\delta \varphi_b^*(x)}(\Delta N_{\beta_a})^2 + W_a b_a f_{\alpha_a}(\Delta N_{\beta_a})\frac{\delta(\Delta N_{\beta_a})}{\delta \varphi_b^*(x)} \\
=\;& -W_a\alpha_a b_a \left[f_{\alpha_a}\Delta N_{\beta_a} \right]^2 \rho^{\alpha_a-1}(x)\varphi_b(x) \\
+\;& W_a b_a f_{\alpha_a}(\Delta N_{\beta_a})\Big[\beta_a \rho^{\beta_a-1}(x)\,(\rho_p(x)-\rho_n(x))\,\varphi_b(x) \\
+\;& \rho^{\beta_a}(x)\left(\varphi_b^{(p)}(x) - \varphi_b^{(n)}(x)\right)\Big]
\end{aligned}
\qquad (E.48)
$$

The first term contributes the following to the Hartree–Fock potential:

$$U(x) = -W_a b_a \left[f_{\alpha_a}\Delta N_{\beta_a} \right]^2 \rho^{\alpha_a-1}(x) \qquad (E.49)$$

From the variation of ΔN_{β_a} there is a contribution which applies equally to the proton and neutron Hartree–Fock potential:

$$U(x) = W_a b_a f_{\alpha_a}(\Delta N_{\beta_a})\beta_a \rho^{\beta_a-1}(x)\delta\rho(x) \qquad (E.50)$$

where $\delta\rho(x) = \rho_p(x) - \rho_n(x)$. There is also a contribution which depends on the nucleon species. The contribution to the proton potential is

$$U_p(x) = W_a b_a f_{\alpha_a}(\Delta N_{\beta_a})\rho^{\beta_a}(x) \qquad (E.51)$$

and the contribution to the neutron potential is

$$U_n(x) = -W_a b_a f_{\alpha_a}(\Delta N_{\beta_a})\rho^{\beta_a}(x). \qquad (E.52)$$

Define a quantity $\Delta_\tau N_{\beta_a}$, which equals ΔN_{β_a} for $\tau = p$ and is $-\Delta N_{\beta_a}$ for $\tau = n$, one can write the contribution in a unified term;

$$U_\tau(x) = W_a b_a f_{\alpha_a} (\Delta_\tau N_{\beta_a}) \beta_a \rho^{\beta_a}(x) \tag{E.53}$$

The variation of the exchange term is

$$
\begin{aligned}
\frac{\delta E_{\tau,\text{exch}}}{\delta \varphi_b^*(x)} &= W_a \frac{\delta f_{\alpha_a}}{\delta \varphi_b^*(x)} \left(\frac{1}{4} b_a M_{\beta_a}^{(\tau\tau)} + a_a M_{\beta_a}^{(\tau\bar\tau)} \right) \\
&+ \frac{1}{4} W_a b_a f_{\alpha_a} \frac{\delta M_{\beta_a}^{(\tau\tau)}}{\delta \varphi_b^*(x)} + W_a a_a f_{\alpha_a} \frac{\delta M_{\beta_a}^{(\tau\bar\tau)}}{\delta \varphi_b^*(x)}.
\end{aligned} \tag{E.54}
$$

The variation of f_{α_a} proceeds as before, giving rise to a contribution to the local Hartree–Fock potential of

$$U(x) = -\frac{1}{4} \alpha_a W_a b_a \, [f_{\alpha_a}]^2 \left(M_{\beta_a}^{(\tau\tau)} + M_{\beta_a}^{(\tau\bar\tau)} \right) \tag{E.55}$$

The varation of the exchange integrals, $M_{\beta_a}^{(\tau\tau)}$ and $M_{\beta_a}^{(\tau\bar\tau)}$, is rather complicated. Firstly, let's look at $M_{\beta_a}^{(\tau\tau)}$. It consists of a sum of two terms which differ only by the isospin index. Let us then consider the case where the index labels proton states. The result for the neutron states will be identical in form.

$$
\begin{aligned}
\frac{\delta M_{\beta_a}^{(pp)}}{\delta \varphi_b^*(x)} &= \sum_{ij<\epsilon_F \in p} \iint d^3 r_1 d^3 r_2 \frac{\delta \varphi_{i\in p}^*(r_1)}{\delta \varphi_b^*(x)} \varphi_{j\in p}^*(r_2) \rho^{\beta_a}(r_1) \rho^{\beta_a}(r_2) \varphi_{j\in p}(r_1) \varphi_{i\in p}(r_2) \\
&+ \sum_{ij<\epsilon_F \in p} \iint d^3 r_1 d^3 r_2 \varphi_{i\in p}^*(r_1) \frac{\delta \varphi_{j\in p}^*(r_2)}{\delta \varphi_b^*(x)} \rho^{\beta_a}(r_1) \rho^{\beta_a}(r_2) \varphi_{j\in p}(r_1) \varphi_{i\in p}(r_2) \\
&+ \sum_{ij<\epsilon_F \in p} \iint d^3 r_1 d^3 r_2 \varphi_{i\in p}^*(r_1) \varphi_{j\in p}^*(r_2) \frac{\delta \rho^{\beta_a}(r_1)}{\delta \varphi_b^*(x)} \rho^{\beta_a}(r_2) \varphi_{j\in p}(r_1) \varphi_{i\in p}(r_2) \\
&+ \sum_{ij<\epsilon_F \in p} \iint d^3 r_1 d^3 r_2 \varphi_{i\in p}^*(r_1) \varphi_{j\in p}^*(r_2) \rho^{\beta_a}(r_1) \frac{\delta \rho^{\beta_a}(r_2)}{\delta \varphi_b^*(x)} \varphi_{j\in p}(r_1) \varphi_{i\in p}(r_2) \\
&= \sum_{j<\epsilon_F \in p} \int d^3 r_2 \varphi_{j\in p}^*(r_2) \rho^{\beta_a}(x) \rho^{\beta_a}(r_2) \varphi_j(x) \varphi_{b\in p}(r_2) \\
&+ \sum_{i<\epsilon_F \in p} \int d^3 r_1 \varphi_{i\in p}^*(r_1) \rho^{\beta_a}(r_1) \rho^{\beta_a}(x) \varphi_{b\in p}(r_1) \varphi_{i\in p}(x) \\
&+ \sum_{ij<\epsilon_F \in p} \int d^3 r_2 \varphi_{i\in p}^*(x) \varphi_{j\in p}^*(r_2) \beta_a \rho^{\beta_a-1}(x) \varphi_{b\in p}(x) \rho^{\beta_a}(r_2) \varphi_{j\in p}(x) \varphi_{i\in p}(r_2) \\
&+ \sum_{ij<\epsilon_F \in p} \int d^3 r_i \varphi_{i\in p}^*(r_1) \varphi_{j\in p}^*(x) \rho^{\beta_a}(r_1) \beta_a \rho^{\beta_a-1}(x) \varphi_{b\in p}(x) \varphi_{j\in p}(r_1) \varphi_{i\in p}(x).
\end{aligned} \tag{E.56}
$$

Here, the first two terms are equal (with suitable relabelling of indices), as are the third and fourth terms. The expression simplifies to:

$$
\frac{\delta M^{(pp)}_{\beta_a}}{\delta \varphi^*_b(x)} = 2 \sum_{i < \epsilon_F \in p} \left\{ \int d^3r\, \varphi^*_{i \in p}(r) \rho^{\beta_a}(r) \varphi_{b \in p}(r) \right\} \rho^{\beta_a}(x) \varphi_{i \in p}(x)
$$

$$
+ 2 \sum_{ij < \epsilon_F \in p} \left\{ \int d^3r \varphi^*_{j \in p}(r) \rho^{\beta_a}(r) \varphi_{i \in p}(r) \right\} \beta_a \rho^{\beta_a - 1}(x) \varphi_{j \in p}(x) \varphi_b(x)
$$

Note that in the second term, the index b includes both proton and neutron states. The first term gives rise to a non-local potential which acts on protons only:

$$
\mathcal{U}_p(\mathbf{x}, \mathbf{x}') = \frac{1}{2} W_a b_a f_{\alpha_a} \rho_p(x', x) \rho^{\beta_a}(x') \rho^{\beta_a}(x) \tag{E.57}
$$

and the second term gives a contribution to the local Hartree–Fock potential, of both protons and neutrons, of

$$
U(x) = W_a (b_a) f_{\alpha_a} \rho^{\beta_a - 1}(x) G^{pp}_{\beta_a}(x), \tag{E.58}
$$

where

$$
G^{pp}_{\beta_a}(x) = \sum_{ij < \epsilon_F \in p} \left(\int d^3r \varphi^*_{j \in p}(r) \rho^{\beta_a}(r) \varphi_{i \in p}(r) \right) \varphi^*_{i \in p}(x) \varphi_{j \in p}(x). \tag{E.59}
$$

Replacing the proton label everywhere by a neutron label gives a non-local neutron potential

$$
\mathcal{U}_n(x, x') = \frac{1}{2} W_a b_a f_{\alpha_a} \rho_n(x', x) \rho^{\beta_a}(x') \rho^{\beta_a}(x) \tag{E.60}
$$

and a contribution to the one-body potential which applies to both nucleon species of

$$
U(x) = W_a (b_a) f_{\alpha_a} \rho^{\beta_a - 1}(x) G^{nn}_{\beta_a}(x) \tag{E.61}
$$

This leaves just the exchange terms where the isospins of states i and j differ:

$$
\frac{\delta M^{(pn)}_{\beta_a}}{\delta \varphi^*_b(x)} = \sum_{i \in p < \epsilon_F} \sum_{j \in n < \epsilon_F} \int d^3r_1 \int d^3r_2 \frac{\delta \varphi^*_i(r_1)}{\delta \varphi^*_b(x)} \varphi^*_j(r_2) \rho^{\beta_a}(r_2) \rho^{\beta_a}(r_1) \varphi_j(r_1) \varphi_i(r_2)
$$

$$
+ \sum_{i \in p < \epsilon_F} \sum_{j \in n < \epsilon_F} \int d^3r_1 \int d^3r_2 \varphi^*_i(r_1) \frac{\delta \varphi^*_j(r_2)}{\delta \varphi^*_b(x)} \rho^{\beta_a}(r_2) \rho^{\beta_a}(r_1) \varphi_j(r_1) \varphi_i(r_2)
$$

$$
+ \sum_{i \in p < \epsilon_F} \sum_{j \in n < \epsilon_F} \int d^3r_1 \int d^3r_2 \varphi^*_i(r_1) \varphi^*_j(r_2) \frac{\delta \rho^{\beta_a}(r_1)}{\delta \varphi^*_b(x)} \rho^{\beta_a}(r_1) \varphi_j(r_1) \varphi_i(r_2)
$$

$$
+ \sum_{i \in p < \epsilon_F} \sum_{j \in n < \epsilon_F} \int d^3r_1 \int d^3r_2 \varphi^*_i(r_1) \varphi^*_j(r_2) \rho^{\beta_a}(r_1) \frac{\delta \rho^{\beta_a}(r_2)}{\delta \varphi^*_b(x)} \varphi_j(r_1) \varphi_i(r_2)
$$

$$
= \sum_{j \in n < \epsilon_F} \int d^3r_2 \varphi^*_j(r_2) \rho^{\beta_a}(x) \rho^{\beta_a}(r_2) \varphi_j(x) \varphi_{b \in p}(r_2)
$$

$$+ \sum_{i \in p < \epsilon_F} \int d^3 r_1 \varphi_i^*(r_1) \rho^{\beta_a}(r_1) \rho^{\beta_a}(r_2) \varphi_b(r_1) \varphi_i(x)$$

$$+ \sum_{i \in p < \epsilon_F} \sum_{j \in n < \epsilon_F} \int d^3 r_2 \varphi_i^*(x) \varphi_j^*(r_2) \beta_a \rho^{\beta_a - 1}(x) \varphi_b(x) \rho^{\beta_a}(r_2) \varphi_j(x) \varphi_i(r_2)$$

$$+ \sum_{i \in p < \epsilon_F} \sum_{j \in n < \epsilon_F} \int d^3 r_1 \varphi_i^*(r_1) \varphi_j^*(x) \rho^{\beta_a}(r_1) \beta_a \rho^{\beta_a - 1}(x) \varphi_b(x) \varphi_j(r_1) \varphi_i(x) \tag{E.62}$$

The first term gives rise to a nonlocal potential, acting only on proton states:

$$\mathcal{U}_p(x, x') = \frac{1}{2} W_a a_a f_{\alpha_a} \rho_n(x, x') \rho^{\beta_a}(x) \rho^{\beta_a}(x') \varphi_b(x') \tag{E.63}$$

The next term produces a nonlocal neutron potential:

$$\mathcal{U}_n(x, x') = \frac{1}{2} W_a a_a f_{\alpha_a} \rho_p(x, x') \rho^{\beta_a}(x) \rho^{\beta_a}(x') \varphi_b(x') \tag{E.64}$$

The terms arising from the variation of the density apply both to neutron and proton states. The third term gives a local HF potential of

$$U(x) = \frac{1}{2} W_a a_a f_{\alpha_a} \beta_a \rho^{\beta_a - 1}(x) G_{pn}(x) \tag{E.65}$$

where $G_{\beta_a}^{(pn)}(x)$ is defined as

$$G_{\beta_a}^{(pn)}(x) = \int d^3 r \rho_p(r, x) \rho_n(x, r) \rho^{\beta_a}(r) \tag{E.66}$$

The fourth term differs from the third only by the exchanging of labels $p \leftrightarrow n$.

Derivative Term

The variation of the direct energy of the derivative term gives

$$\frac{\delta}{\delta \varphi_b^*(x)} E_{d,\text{dir}} = k N_d \frac{\delta N_d}{\delta \varphi_b^*(x)} = k N_D \frac{\delta}{\delta \varphi_b^*(x)} \int d^3 r \rho(r) \nabla^2 \rho(r).$$

$$= k N_d \int d^3 r \left\{ \frac{\delta \rho(r)}{\delta \varphi_b^*(x)} \right\} \nabla^2 \rho(r) + k N_d \int d^3 r \rho(r) \frac{\delta}{\delta \varphi_b^*(x)} \nabla^2 \rho(r) \tag{E.67}$$

The first terms is simply evaluated as

$$= k N_d \nabla^2 \rho(r) \cdot \varphi_b(x) \tag{E.68}$$

so that it gives a contribution to the HF potential of

$$U(x) = k N_d \nabla^2 \rho(x) \tag{E.69}$$

Since the density depends only on the radial coordinate, the operation of the laplacian on the density is

$$\nabla^2 \rho(r) = \frac{1}{r^2} \left(\frac{\partial}{\partial r} r^2 \frac{\partial}{\partial r} \right) \rho(r). \tag{E.70}$$

Then the variation of the second term, with partial derivatives with respect to the coordinate r, is best carried out by explicitly varying just the radial function. The variation of this term is

$$4\pi k N_d \int dr \rho(r) \frac{\delta}{\delta \mathcal{R}_b^*(x)} \frac{\partial}{\partial r} \left(r^2 \frac{\partial}{\partial r} \sum_{(Nlj\tau)_i} \frac{(2j_i + 1)}{4\pi} \mathcal{R}_i^*(r)\mathcal{R}_i(r) \right). \tag{E.71}$$

Integrating once by parts gives

$$-k N_d \int dr r^2 \frac{\partial \rho(r)}{\partial r} \frac{\delta}{\delta \mathcal{R}_b^*(x)} \frac{\partial}{\partial r} \sum_{(Nlj\tau)_i} (2j_i + 1)\mathcal{R}_i^*(r)\mathcal{R}_i(r), \tag{E.72}$$

and once more –

$$+k N_d \frac{1}{x^2} \frac{\partial}{\partial x} \left(x^2 \frac{\partial \rho(x)}{\partial x} \right) \mathcal{R}_b(x), \tag{E.73}$$

so this also gives a contribution to the HF potential of

$$U(x) = k N_d \nabla^2 \rho(x). \tag{E.74}$$

The exchange potential in this case is rather complicated and consists of calculating the action of the Laplacian on the density matrices. A simple approximation which can be made is to replace the density matrices with the local one-body density:

$$\iint d^3 r_1 d^3 r_2 \rho(r_1, r_2)\rho(r_2, r_1)f(r_1, r_2) \rightarrow \iint d^3 r_1 d^3 r_2 \rho(r_1)\delta^3(r_1 - r_2)f(r_1, r_2). \tag{E.75}$$

In the case that $f(r_1, r_2) = 1$ the replacement is an identity. For simplicity consider that the densities are of a single nucleon species, q

$$\begin{aligned}
\iint d^3 r_1 d^3 r_2 \rho_q(r_1, r_2)\rho_q(r_2, r_1) &= \iint d^3 r_1 d^3 r_2 \sum_{i=1}^{N_q} \sum_{j=1}^{N_q} \varphi_i^*(r_2)\varphi_j^*(r_1)\varphi_i(r_1)\varphi_j(r_2) \\
&= \sum_{i=1}^{N_q} \sum_{j=1}^{N_q} \left(\int d^3 r_1 \varphi_j^*(r_1)\varphi_i(r_1) \right) \left(\int d^3 r_2 \varphi_i^*(r_2)\varphi_i(r_2) \right) \\
&= \sum_{i=1}^{N_q} \sum_{j=1}^{N_q} \delta_{ij}\delta_{ij} = \sum_{i=1}^{N_q} 1 = N_q
\end{aligned} \tag{E.76}$$

and

$$\iint d^3 r_1 d^3 r_2 \rho_q(r_1)\delta^3(r_1 - r_2) = \int d^3 r \rho_q(r) = N_q. \tag{E.77}$$

For other values of $f(r_1, r_2)$ the replacement is an approximation. However, in cases where the exchange terms are directly calculable it is shown to be a good one and its use here should be considered better than ignoring the term completely. The exchange energy, then, is

$$E_{d,exch} = -\frac{1}{2}kM_d \approx -\frac{1}{2}k\int d^3r\rho(r)\left(\nabla^2\rho(r)\right)^2.$$ (E.78)

The variation of the first ρ gives simply a direct contribution to the HF potential:

$$U(x) = -\frac{1}{2}k\left[\nabla^2\rho(x)\right]^2.$$ (E.79)

The variation of the potential (the *rearrangement term*) proceeds:

$$-\frac{1}{2}k\int d^3r\rho(r)\frac{\delta}{\delta\varphi_b^*(x)}\left[\nabla^2\rho(r)\right]^2 = -k\int d^3r\rho(r)\nabla^2\rho(r)\frac{\delta}{\delta\varphi_b^*(x)}\nabla^2\rho(r).$$ (E.80)

In calculating the direct term it was shown that the action of the variational operator on a Laplacian was to move the Laplacian to act on the parts of the integral not subject to the variation. This would lead to a term of the form

$$\sim \nabla^2(\rho(r)\nabla^2\rho(r))$$ (E.81)

which includes calculating fourth derivatives of the density, which is too cumbersome to be considered an worthwhile approximation. If one returns to the full expression for the exchange energy and varies the potential in the matrix element to look at the rearrangement term, one has

$$-k\int\int d^3r_1d^3r_2\rho(r_2, r_1)\rho(r_1, r_2)\left[\frac{\delta}{\delta\varphi_b^*(x)}\nabla_1^2\rho(r_1)\right]\nabla_2^2\rho(r_2).$$ (E.82)

Here the factor of 1/2 has been dropped since there is also an identical term with the variational operator acting on the term of the potential in r_2. Since the Laplacian being varied only operates on r_1, when it is taken to act on all the terms not being varied, it does not then act on $\nabla_2^2\rho(r_2)$, but only on those parts dependent on r_1 – the density matrixes. At this stage the approximation may be applied to give

$$-k\int\int d^3r_1d^3r_2\nabla_2^2\rho(r_2)\nabla_1^2[\rho(r_1, r_2)\rho(r_2, r_1)]\varphi_b(r_1)\delta(r_1 - x)$$

$$\approx -k\int\int d^3r_1d^3r_2\nabla_2^2\rho(r_2)\nabla_1^2(\rho(r_1)\delta(r_1 - r_2))\varphi_b(x)\delta(r_1 - x)$$

$$= -k[\nabla^2\rho(x)]^2\varphi_b(x)$$ (E.83)

where the approximation is taken with some caution since the functon $f(r_1, r_2)$ contains derivative operators and delta functions. In any case the result here is

the same magnitude as with the safer invocation of the approximation above. It's numerical value in actual calculations, like the exchange terms elsewhere, is rather smaller than the direct term. This being so, the term may be neglected. If it is not, the entire contribution from the exchange part of the derivative term to the HF potential is approximated as

$$U(x) = -\frac{3}{2}(\nabla^2\rho(x))^2 \tag{E.84}$$

Spin-Orbit Term

The spin-orbit energy is

$$
\begin{aligned}
E_{so} &= cN_w = c\int d^3r \frac{1}{r}\frac{\partial\rho(r)}{r}\rho_w(r) \\
&= c\int rdr4\pi\frac{\partial}{\partial r}\left[\sum_{(Nlj\tau)_i}\frac{2j_i+1}{4\pi}\mathcal{R}_i^*(r)\mathcal{R}_i(r)\right]\sum_{(Nlj\tau)_j}\frac{2j_j+1}{4\pi}w_j\mathcal{R}_j^*(r)\mathcal{R}_j(r) \tag{E.85}
\end{aligned}
$$

which may be varied with respect to the radial wavefunction as

$$
\begin{aligned}
\frac{\delta E_{so}}{\delta\mathcal{R}_b(x)} &= c\int rdr\rho_w(r)\frac{\delta}{\delta\mathcal{R}_b^*(x)}\left\{\frac{\partial}{\partial r}\left[\sum_{(Nlj\tau)_i}(2j_i+1)\mathcal{R}_i^*(r)\mathcal{R}_i(r)\right]\right\} \\
&+ c\int rdr\frac{\partial\rho(r)}{\partial r}\sum_{(Nlj\tau)_j}w_j(2j_j+1)\frac{\delta\mathcal{R}_j^*(r)}{\delta\mathcal{R}_b^*(x)}\mathcal{R}_j(r).
\end{aligned}
$$

Using the variational principle for the radial wavefunctions (E.2), the second term is just

$$c\frac{1}{x}\frac{\partial\rho(x)}{\partial x}w_b\mathcal{R}_b(x) \tag{E.86}$$

which gives rise to a state-dependent potential

$$U(x)\varphi_b(x) = c\frac{1}{x}\frac{\partial\rho(x)}{\partial x}w_b\varphi_b(x). \tag{E.87}$$

The first term requires an integration by parts:

$$
\begin{aligned}
&= -c\int dr\frac{\partial}{\partial r}[r\rho_w(r)]\sum_{(Nlj\tau)_i}(2j_1+1)\frac{\delta\mathcal{R}_i^*(r)}{\delta\mathcal{R}_b^*(x)}\mathcal{R}_i(r) \\
&= -c\frac{1}{x^2}\left(x\frac{\partial\rho_w(x)}{\partial x}+\rho_w(x)\right)\mathcal{R}_b(x) \tag{E.88}
\end{aligned}
$$

so that the total HF potential arising from the spin-orbit force is

$$U_{so}(x)\varphi_b(x) = c\left(\frac{1}{x}w_b\frac{\partial\rho(x)}{\partial x}-\frac{1}{x}\frac{\partial\rho_w(x)}{\partial x}-\frac{1}{x^2}\rho_w(x)\right)\varphi_b(x). \tag{E.89}$$

The potential is finite at the origin since $\rho_w(x)$ disappears at $x = 0$ due to the fact that the weight w is zero for s-states, and the derivatives of the densities disappear also at $x = 0$ since the densities must be flat at the origin to ensure that it varies smoothly.

Collected Terms

Bringing all the terms together, the Local Hartree-Fock Potential due to the monopole interaction is

$$
\begin{aligned}
U_\tau(x) \;=\; & \sum_{\xi=a,r} \left\{ W_\xi f_{\alpha_\xi} \left[N_{\beta_\xi}(\beta_\xi + 1) + b_\xi \Delta_\tau N_{\beta_\xi} \right] \rho^{\beta_\xi}(x) \right. \\
& -\; W_\xi(\alpha_\xi/2) \left[f_{\alpha_\xi} \right]^2 \left[N_{\beta_\xi}^2 + b_\xi (\Delta N_{\beta_\xi})^2 \right] \rho^{\alpha_\xi - 1}(x) \\
& -\; W_\xi f_{\alpha_\xi} \beta_\xi \left[G_{\beta_\xi}(x) + b_\xi G_{\beta_\xi}^{pp}(x) + b_\xi G_{\beta_\xi}^{nn}(x) \right] \rho^{\beta_\xi - 1}(x) \\
& +\; W_\xi(\alpha_\xi/2)[f_{\alpha_\xi}]^2 M_{\beta_\xi} \rho^{\alpha_\xi - 1}(x) \\
& -\; W_\xi b_\xi \beta_\xi f_{\alpha_\xi} \left[\Delta N_{\beta_\xi} \right] \rho^{\beta_\xi - 1}(x) \delta\rho(x) \\
& +\; W_\xi(\alpha_\xi/2) \left[f_{\alpha_\xi} \right]^2 \left(b_\xi \left[M_{\beta_\xi}^{pp} + M_{\beta_\xi}^{nn} \right] + a_\xi \left[M_{\beta_\xi}^{pn} + M_{\beta_\xi}^{np} \right] \right) \rho^{\alpha_\xi - 1}(x) \\
& \left. -\; W_\xi a_\xi f_{\alpha_\xi} \beta_\xi \left(G_{\beta_\xi}^{pn}(x) + G_{\beta_\xi}^{np}(x) \right) \rho^{\beta_\xi - 1}(x) \right\} \\
& +\; 2kN_d \nabla^2 \rho(x) - k\frac{3}{2}(\nabla^2 \rho(x))^2 \qquad\qquad \text{(E.90)}
\end{aligned}
$$

and the nonlocal Hartree–Fock potential is

$$
\begin{aligned}
\mathcal{U}_\tau(x, x') \;=\; & -\sum_{\xi=a,r} \left\{ W_\xi f_\alpha \rho(x, x') \rho^{\beta_a}(x) \rho^{\beta_a}(x') \right. \\
& +\; W_\xi b_\xi f_{\alpha_\xi} \rho_\tau(x, x') \rho^{\beta_\xi}(x) \rho^{\beta_\xi}(x') \\
& \left. +\; W_\xi a_\xi f_{\alpha_\xi} \rho_{\bar\tau}(x, x') \rho^{\beta_\xi}(x) \rho^{\beta_\xi}(x') \right\}. \qquad \text{(E.91)}
\end{aligned}
$$

In addition there is a contribution to the local HF potential which depends upon the state on which it is acting:

$$
U(x)\varphi_b(x) = c \left(\frac{1}{x} w_b \frac{\partial\rho(x)}{\partial x} - \frac{1}{x}\frac{\partial\rho_w(x)}{\partial x} - \frac{1}{x^2}\rho_w(x) \right) \varphi_b(x). \qquad \text{(E.92)}
$$

Appendix F

Perturbation Terms for Separable Force

F.1   Second Order Energy Correction

As shown in Appendix B the second order correction to the total energy is obtained by evaluating the following sum:

$$E^{(2)} = \frac{1}{4} \sum_{a \neq b \leq \epsilon_F} \sum_{r \neq s > \epsilon_F} \frac{|\langle ab|\tilde{v}|rs \rangle|^2}{\epsilon_a + \epsilon_b - \epsilon_r - \epsilon_s} \tag{F.1}$$

where the labels a, b, c and d denote all the quantum numbers labelling each state, viz. N, l, j, m and τ, and $\tilde{v}$ is the two-body interaction.

Since the single-particle energies ϵ are independent of the m quantum numbers, it is possible to sum the squared matrix elements over m to give a closed-form expression. To do this, the matrix element is expanded as a sum of contributions from each of the terms in the potential, then each of the resulting terms may have its m numbers summed over. Defining the greek letters α, β, ρ and σ to be the subset of quantum numbers $\alpha = \{N, l, j, \tau\}_a$, the sum (F.1) may be written

$$E^{(2)} = \frac{1}{4} \sum_{\alpha, \beta \leq \epsilon_F} \sum_{\rho, \sigma > \epsilon_F} \frac{1}{\epsilon_\alpha + \epsilon_\beta - \epsilon_\rho - \epsilon_\sigma} \sum_{m_a \cdots m_s}$$
$$\cdot \quad (1 - \delta_{\alpha\beta} \delta_{m_a m_b})(1 - \delta_{\sigma\rho} \delta_{m_s m_r}) |\langle ab|\tilde{v}|rs \rangle|^2 \tag{F.2}$$

where the Kronecker delta symbols serve to restrict $m_a \neq m_b$ when all the other quantum numbers of particle a are the same as those of particle b and likewise for particles r and s. In this way the summation over the quantum numbers may is unrestricted. Looking at the terms which do include these delta symbols, it is easy to show that they disappear. For instance, the term with $\delta_{\alpha\beta} \delta_{m_a m_b}$ may be simple summed over $b = \beta$, m_b to give

$$-\frac{1}{4} \sum_{\alpha \leq \epsilon_F} \sum_{\rho, \sigma > \epsilon_F} \frac{1}{2\epsilon_\alpha - \epsilon_\rho - \epsilon_\sigma} \sum_{m_a m_r m_s} |\langle aa|\tilde{v}|rs \rangle|^2$$

which is zero since the antisymmetrized matrix element vanished when the two states in the bra (or the ket) are the same.

For the present purposes the potential (3.1, 3.4, 3.5) may be expressed in a way which hides all the dependence on the quantum numbers N, l, j and τ and puts them in functions F_M, F_D and F_Q for the monopole, dipole and quadrupole interactions respectively:

$$
\begin{aligned}
V(r_1, r_2) &= V_M(r_1, r_2) + V_D(r_1, r_2) + V_Q(r_1, r_2) \\
&= F_M(r_1, r_2) + F_D(r_1, r_2) \sum_{M=-1}^{1} (-1)^M Y_{1M}(\hat{r}_1) Y_{1-M}(\hat{r}_2) \\
&\quad + F_Q(r_1, r_2) \sum_{M=-2}^{2} (-1)^M Y_{2M}(\hat{r}_1) Y_{2-M}(\hat{r}_2).
\end{aligned}
\tag{F.3}
$$

Non-antisymmetrized matrix elements of each of these terms are then

$$
\langle ab|V_M|rs \rangle = F_M^{\alpha\beta\rho\sigma} \delta_{l_a l_r} \delta_{j_a j_r} \delta_{m_a m_r} \delta_{l_b l_s} \delta_{j_b j_s} \delta_{m_b m_s}
\tag{F.4}
$$

$$
\langle ab|V_D|rs \rangle = F_D^{\alpha\beta\rho\sigma} \sum_{M=-1}^{1} (-1)^M \langle j_a m_a|Y_{1M}|j_r m_r \rangle \langle j_b m_b|Y_{1-M}|j_s m_s \rangle
\tag{F.5}
$$

$$
\langle ab|V_Q|rs \rangle = F_Q^{\alpha\beta\rho\sigma} \sum_{M=-2}^{2} (-1)^M \langle j_a m_a|Y_{2M}|j_r m_r \rangle \langle j_b m_b|Y_{2-M}|j_s m_s \rangle
\tag{F.6}
$$

The matrix element of a spherical harmonic between spinor spherical harmonic states, in the case of the coupling order $l + 1/2 = j$ which is used throught this work, is [24]

$$
\langle jm|Y_{LM}|j'm' \rangle = \langle j'm'LM|jm \rangle (-1)^L \sqrt{\frac{\hat{L}}{4\pi}} \langle j\tfrac{1}{2}L0|j'\tfrac{1}{2} \rangle \frac{1}{2} \left(1 + (-1)^{l+L+l'} \right)
\tag{F.7}
$$

where the shorthand notation $\hat{L} = 2L + 1$ has been used. Here, the parts independent of m (the *reduced matrix elements*) may be subsumed into functions Γ_Λ so that

$$
\langle ab|V_D|rs \rangle = F_D^{\alpha\beta\rho\sigma} \Gamma_D^{\alpha\beta\rho\sigma} \sum_{M=-1}^{1} (-1)^M \langle j_r m_r 1M|j_a m_a \rangle \langle j_s m_s 1 -M|j_b m_b \rangle
$$

$$
\langle ab|V_Q|rs \rangle = F_Q^{\alpha\beta\rho\sigma} \Gamma_Q^{\alpha\beta\rho\sigma} \sum_{M=-2}^{2} (-1)^M \langle j_r m_r 2M|j_a m_a \rangle \langle j_s m_s 2 -M|j_b m_b \rangle.
$$

Note also that the monopole force may be expressed in this form, too:

$$
\langle ab|V_M|rs \rangle = F_M^{\alpha\beta\rho\sigma} \Gamma_M^{\alpha\beta\rho\sigma} \sum_{M=0}^{0} (-1)^M \langle j_r m_r 0M|j_a m_a \rangle \langle j_s m_s 0 -M|j_b m_b \rangle
\tag{F.8}
$$

since the sum is just $\delta_{m_r m_a} \delta_{m_s m_b}$. This means the monopole Γ is defined as $\Gamma_M^{\alpha\beta\rho\sigma} = \delta_{l_a l_r} \delta_{j_a j_r} \delta_{l_b l_s} \delta_{j_b j_s}$. This being so, it is convenient to consider only a generalized multipole form which corresponds to the monopole, dipole and quadrupole terms upon suitable substitution for a parameter Λ (0,1 or 2 respectively):

$$V_\Lambda(r_1, r_2) = F_\Lambda(r_1, r_2) \sum_{M=-\Lambda}^{\Lambda} (-1)^M Y_{\Lambda M}(\hat{r}_1) Y_{\Lambda -M}(\hat{r}_2). \tag{F.9}$$

Furthermore since the F and Γ numbers always appear together with the same super- and subscripts they may, to reduce notational clutter, be redefined as one number:

$$\tilde{F}_\Lambda^{\alpha\beta\gamma\delta} = F_\Lambda^{\alpha\beta\gamma\delta} \Gamma_\Lambda^{\alpha\beta\gamma\delta} \tag{F.10}$$

The multipole operators are constructed so as to be scalar. To take advantage of this, and also to verify it, the matrix elements may be evaluated by coupling the two body states to good total angular momentum. An antisymmetrized matrix element of given mutipole may be written

$$
\begin{aligned}
\langle ab|\tilde{v}_\Lambda|rs\rangle &= \sum_{JMJ'M'} \langle j_a m_a j_b m_b|JM\rangle \langle j_r m_r j_s m_s|j'M'\rangle \\
&\quad \cdot \left[\langle(\alpha\beta)JM|V_\Lambda|(\rho\sigma)J'M'\rangle - (-1)^{j_r + j_s - J'} \langle(\alpha\beta)JM|V_\Lambda|(\sigma\rho)J'M'\rangle \right].
\end{aligned}
\tag{F.11}
$$

This coupling was done to make the dependence of the matrix element on the quantum numbers $m_a \cdots m_s$ as simple as possible so that they may be summed out later in the expression for the energy correction. It is possible at this stage to greatly simplify the angular dependence still in the coupled matrix elements. To begin, they are uncoupled again:

$$
\begin{aligned}
\langle(\alpha\beta)JM|V_\Lambda|(\rho\sigma)J'M'\rangle &= F_\Lambda^{\alpha\beta\rho\sigma} \sum_\mu \sum_{m m' m'' m'''} \langle JM|j_a m j_b m'\rangle \langle j_r m'' j_s m'''|J'M'\rangle \\
&\quad \cdot \langle j_a m j_b m'|(-1)^\mu Y_{\Lambda\mu} Y_{\Lambda-\mu}|j_r m'' j_s m'''\rangle \\
&= \tilde{F}_\Lambda^{\alpha\beta\rho\sigma} \sum_\mu (-1)^\mu \sum_{m m' m'' m'''} \langle JM|j_a m j_b m'\rangle \\
&\quad \cdot \langle j_r m'' j_s m'''|J'M'\rangle \langle j_r m'' \Lambda\mu|j_a m\rangle \langle j_s m''' \Lambda\mu|j_b m'\rangle.
\end{aligned}
$$

This sum of four Clebsch–Gordan coefficients over four magnetic quantum numbers can be reduced to a 9-j symbol and two Clebsch–Gordan coefficients summed over one angular momentum and its projection. This gives for the matrix element

$$
\begin{aligned}
\langle(\alpha\beta)JM|V_\Lambda|(\rho\sigma)J'M'\rangle &= \tilde{F}_\Lambda^{\alpha\beta\rho\sigma} \sum_\mu (-1)^\mu \sum_{k\kappa} \langle \Lambda\mu\Lambda -\mu|k\kappa\rangle \langle J'M'k\kappa|JM\rangle \\
&\quad \cdot \sqrt{\hat{j}_a \hat{j}_b \hat{J}'\hat{k}} \left\{ \begin{array}{ccc} J & j_a & j_b \\ J' & j_r & j_s \\ k & \Lambda & \Lambda \end{array} \right\}.
\end{aligned}
$$

From the first Clebsch–Gordan coefficient one immediately has the condition $\kappa = 0$ so that κ may be summed out. Then this Clebsch–Gordan coefficient may be summed over μ:

$$(-1)^\Lambda \sum_\mu (-1)^{\Lambda-\mu} \langle \Lambda\mu\Lambda-\mu|k0\rangle = (-1)^\Lambda \delta_{k0}\sqrt{\hat\Lambda}. \tag{F.12}$$

Inserting this in the above expression and summing over k the matrix element becomes

$$\langle(\alpha\beta)JM|V_\Lambda|(\rho\sigma)J'M'\rangle = \tilde{F}_\Lambda^{\alpha\beta\rho\sigma}(-1)^\Lambda\sqrt{\hat{j}_a\hat{j}_b\hat{J}'\hat{\Lambda}}$$
$$\cdot\ \langle J'M'00|JM\rangle \begin{Bmatrix} J & j_a & j_b \\ J' & j_r & j_s \\ 0 & \Lambda & \Lambda \end{Bmatrix}. \tag{F.13}$$

The remaining Clebsch–Gordan coefficient is $\delta_{JJ'}\delta_{MM'}$. This shows that the multipole operators are indeed scalars. The 9–j symbol with a zero reduces to a 6–j symbol:

$$\begin{Bmatrix} J & j_a & j_b \\ J & j_r & j_s \\ 0 & \Lambda & \Lambda \end{Bmatrix} = \frac{(-1)^{j_r+j_b+\Lambda+J}}{\sqrt{\hat{J}\hat{\Lambda}}} \begin{Bmatrix} j_s & j_r & J \\ j_a & j_b & \Lambda \end{Bmatrix}. \tag{F.14}$$

thus the matrix element reduces to

$$\langle(\alpha\beta)JM|V_\Lambda|(\rho\sigma)J'M'\rangle = \tilde{F}_\Lambda^{\alpha\beta\rho\sigma}(-1)^{J+j_r+j_b}\delta_{JJ'}\delta_{MM'}\sqrt{\hat{j}_a\hat{j}_b} \begin{Bmatrix} j_s & j_r & J \\ j_a & j_b & \Lambda \end{Bmatrix}. \tag{F.15}$$

The full antisymmetrized matrix element which appears in the sum for the energy correction is thus

$$\langle ab|\tilde{v}_\Lambda|rs\rangle = \sum_{JM}\langle j_am_aj_bm_b|JM\rangle\langle j_rm_rj_sm_s|JM\rangle\sqrt{\hat{j}_a\hat{j}_b}$$
$$\cdot\ \left[\tilde{F}_\Lambda^{\alpha\beta\rho\sigma}(-1)^{J+j_r+j_b} \begin{Bmatrix} j_s & j_r & J \\ j_a & j_b & \Lambda \end{Bmatrix} + \tilde{F}_\Lambda^{\alpha\beta\sigma\rho}(-1)^{j_b+j_s} \begin{Bmatrix} j_r & j_s & J \\ j_a & j_b & \Lambda \end{Bmatrix}\right]$$
$$\tag{F.16}$$

In the expression (F.1) the sum over $m_a\cdots m_s$ of the square of these matrix elements needs to be evaluated. All possible terms appearing here can be considered by looking at two terms; $\langle ab|V_\Lambda|rs\rangle\langle ab|V_{\Lambda'}|rs\rangle$ and $\langle ab|V_\Lambda|rs\rangle\langle ab|V_{\Lambda'}|sr\rangle$. The first case is

$$\sum_{m_a\cdots m_s}\langle ab|V_\Lambda|rs\rangle\langle ab|V_{\Lambda'}|rs\rangle = \sum_{m_a\cdots m_s}\sum_{JM}\sum_{J'M'}\langle j_am_aj_bm_b|JM\rangle\langle j_rm_rj_sm_s|JM\rangle$$
$$\cdot\ \langle j_am_aj_bm_b|J'M'\rangle\langle j_rm_rj_sm_s|J'M'\rangle\hat{j}_a\hat{j}_b$$
$$\cdot\ \tilde{F}_\Lambda^{\alpha\beta\rho\sigma}\tilde{F}_{\Lambda'}^{\alpha\beta\rho\sigma} \begin{Bmatrix} j_s & j_r & J \\ j_a & j_b & \Lambda \end{Bmatrix}\begin{Bmatrix} j_s & j_r & J' \\ j_a & j_b & \Lambda' \end{Bmatrix}.$$

The quantum numbers m_a and m_b may be summed over the two Clebsch–Gordan coefficients in which they appear to give $\delta_{JJ'}\delta_{MM'}$. Likewise m_r and m_s. Summing over both M and M' then gives a factor of $(2J + 1)$. J' may be trivially summed over thanks to the Kronecker delta. This leaves one sum:

$$\sum_{m_a\cdots m_s} \langle ab|V_\Lambda|rs\rangle\langle ab|V_\Lambda|rs\rangle = \hat{\jmath}_a\hat{\jmath}_b \tilde{F}_\Lambda^{\alpha\beta\rho\sigma}\tilde{F}_{\Lambda'}^{\alpha\beta\rho\sigma} \sum_J \hat{J} \left\{ \begin{array}{ccc} j_s & j_r & J \\ j_a & j_b & \Lambda \end{array} \right\} \left\{ \begin{array}{ccc} j_s & j_r & J \\ j_a & j_b & \Lambda' \end{array} \right\}.$$

Providing the triplets (j_a, j_r, Λ) and (j_b, j_s, Λ') satisfy the triangle relation, the sum over J reduces to $\delta_{\Lambda\Lambda'}\hat{\Lambda}^{-1}$ [104]. The condition of satisfying the triangle relations is seen to already be true due to the Γ functions. The final answer for this term is then

$$\sum_{m_a\cdots m_s} \langle ab|V_\Lambda|rs\rangle\langle ab|V_\Lambda|rs\rangle = \frac{\hat{\jmath}_a\hat{\jmath}_b}{\hat{\Lambda}} \tilde{F}_\Lambda^{\alpha\beta\rho\sigma}\tilde{F}_{\Lambda'}^{\alpha\beta\rho\sigma}\delta_{\Lambda\Lambda'}. \tag{F.17}$$

The Kronecker delta in Λ and Λ' shows that there are no cross terms between multipoles.

The other possible term is

$$\begin{aligned}
\sum_{m_a\cdots m_s} \langle ab|V_\Lambda|rs\rangle\langle ab|V_{\Lambda'}|sr\rangle &= \sum_{m_a\cdots m_b}\sum_{JM}\sum_{J'M'} (-1)^{J+j_r+j_s}\langle j_a m_a j_b m_b|JM\rangle\langle j_r m_r j_s m_s|JM\rangle \\
&\quad \cdot \langle j_a m_a j_b m_b|J'M'\rangle\langle j_r m_r j_s m_s|J'M'\rangle\hat{\jmath}_a\hat{\jmath}_b \\
&\quad \cdot \tilde{F}_\Lambda^{\alpha\beta\rho\sigma}\tilde{F}_{\Lambda'}^{\alpha\beta\sigma\rho} \left\{ \begin{array}{ccc} j_s & j_r & J \\ j_a & j_b & \Lambda \end{array} \right\} \left\{ \begin{array}{ccc} j_r & j_s & J' \\ j_a & j_b & \Lambda' \end{array} \right\}.
\end{aligned}$$

Again the four Clebsch–Gordan coefficients sum out and M, M' and J' may be summed over:

$$\begin{aligned}
\sum_{m_a\cdots m_s} \langle ab|V_\Lambda|rs\rangle\langle ab|V_\Lambda|sr\rangle &= (-1)^{j_r+j_s}\hat{\jmath}_a\hat{\jmath}_b\tilde{F}_\Lambda^{\alpha\beta\rho\sigma}\tilde{F}_{\Lambda'}^{\alpha\beta\sigma\rho} \\
&\quad \cdot \sum_J \hat{J}(-1)^J \left\{ \begin{array}{ccc} j_s & j_r & J \\ j_a & j_b & \Lambda \end{array} \right\} \left\{ \begin{array}{ccc} j_r & j_s & J \\ j_a & j_b & \Lambda' \end{array} \right\}.
\end{aligned}$$

This sum over two 6-j symbols can be reduced to a single 6-j symbol [104]:

$$\sum_J \hat{J}(-1)^J \left\{ \begin{array}{ccc} j_s & j_r & J \\ j_a & j_b & \Lambda \end{array} \right\} \left\{ \begin{array}{ccc} j_r & j_s & J \\ j_a & j_b & \Lambda' \end{array} \right\} = (-1)^{\Lambda+\Lambda'} \left\{ \begin{array}{ccc} j_r & j_b & \Lambda' \\ j_s & j_a & \Lambda \end{array} \right\} \tag{F.18}$$

so that the summed matrix elements are

$$\sum_{m_a\cdots m_s} \langle ab|V_\Lambda|rs\rangle\langle ab|V_\Lambda|sr\rangle = (-1)^{j_r+j_s+\Lambda+\Lambda'}\tilde{F}_\Lambda^{\alpha\beta\rho\sigma}\tilde{F}_{\Lambda'}^{\alpha\beta\sigma\rho}\hat{\jmath}_a\hat{\jmath}_b \left\{ \begin{array}{ccc} j_r & j_b & \Lambda' \\ j_s & j_a & \Lambda \end{array} \right\} \tag{F.19}$$

Now there is no Kronecker delta in Λ and Λ' so that there may appear cross terms of this form between multipoles.

When expanding the squared matrix element in (F.1) over the six terms of V (one direct and one exchange matrix element from each of the three multipoles) there are $7!/5!2! = 21$ terms. Many of these can be combined since the sum over r runs over exactly the same states as s so, for example, the summed direct $\times$ direct term for a given multipole is the same as the summed exchange $\times$ exchange. Furthermore it has been show that some terms are zero. In fact, of the 21 terms, just 9 remain. The final expression for the second order energy correction is obtained by inserting the appropriate combinations of Λ and Λ' in the above expression. After simplifying the cases in which one or more of Λ, Λ' and Λ'' equals zero, the result is:

$$
\begin{aligned}
E^{(2)} = {} & \frac{1}{2} \sum_{\alpha,\beta \leq \epsilon_F} \sum_{\rho,\sigma > \epsilon_F} \frac{1}{\epsilon_\alpha + \epsilon_\beta - \epsilon_\rho - \epsilon_\sigma} \Bigg[\left(\tilde{F}_M^{\alpha\beta\rho\sigma} \right)^2 \hat{\jmath}_a \hat{\jmath}_b - \tilde{F}_M^{\alpha\beta\rho\sigma} \tilde{F}_M^{\alpha\beta\sigma\rho} \hat{\jmath}_a \\
& - 2\tilde{F}_M^{\alpha\beta\rho\sigma} (-1)^{j_b - j_a} \sqrt{\hat{\jmath}_a \hat{\jmath}_b} \left(\tilde{F}_D^{\alpha\beta\sigma\rho} + \tilde{F}_Q^{\alpha\beta\sigma\rho} \right) + \frac{1}{3} \left(\tilde{F}_D^{\alpha\beta\rho\sigma} \right)^2 \hat{\jmath}_a \hat{\jmath}_b \\
& + (-1)^{j_r - j_s} \tilde{F}_D^{\alpha\beta\rho\sigma} \tilde{F}_D^{\alpha\beta\sigma\rho} \hat{\jmath}_a \hat{\jmath}_b \left\{ \begin{matrix} j_a & j_r & 1 \\ j_b & j_s & 1 \end{matrix} \right\} \\
& - (-1)^{j_r + j_s} \tilde{F}_D^{\alpha\beta\rho\sigma} \tilde{F}_Q^{\alpha\beta\sigma\rho} \hat{\jmath}_a \hat{\jmath}_b \left\{ \begin{matrix} j_a & j_r & 1 \\ j_b & j_s & 2 \end{matrix} \right\} \\
& + \frac{1}{5} \left(\tilde{F}_Q^{\alpha\beta\rho\sigma} \right)^2 \hat{\jmath}_a \hat{\jmath}_b + (-1)^{j_r - j_s} \tilde{F}_Q^{\alpha\beta\rho\sigma} \tilde{F}_Q^{\alpha\beta\sigma\rho} \hat{\jmath}_a \hat{\jmath}_b \left\{ \begin{matrix} j_a & j_r & 2 \\ j_b & j_s & 2 \end{matrix} \right\} \Bigg]
\end{aligned}
$$
(F.20)

F.2 Third Order Energy Correction

F.2.1 Hole-Hole Scattering term

The energy correction due to the hole–hole–scattering diagram is

$$
E_{hh}^{(3)} = \frac{1}{8} \sum_{a \neq b \leq \epsilon_F} \sum_{c \neq d \leq \epsilon_F} \sum_{r \neq s > \epsilon_F} \frac{\langle ab | \tilde{v} | rs \rangle \langle cd | \tilde{v} | ab \rangle \langle rs | \tilde{v} | cd \rangle}{(\epsilon_a + \epsilon_b - \epsilon_r - \epsilon_s)(\epsilon_c + \epsilon_d - \epsilon_r - \epsilon_s)}
$$
(F.21)

Again, since the single particle energies are independent of m, the m quantum numbers may be summed out of product of matrix elements. As in the second order term, one must be careful to exclude terms in which $b = a$ or $c = d$. It is seen, however, that these terms vanish so may be included in the sum without danger.

The product of three antisymmetrized matrix elements expands to a sum of 8 terms of products of three non-antisymmetrized matrix elements. Using the following facts,

$$
\begin{aligned}
\langle ab | V | rs \rangle &= \langle ba | V | sr \rangle \\
\langle ab | V | rs \rangle &= \langle rs | V | ab \rangle,
\end{aligned}
$$

one can show that these eight terms pair up into four terms. Furthermore, since these terms are summed over labels which run over the same states as other labels summed over, one may swap pairs of these labels without affecting the result. This operation enables one to identify the four terms as really being two independent terms. Going through this process, then, one can show that the above sum (F.21) can be written

$$
E_{hh}^{(3)} = \frac{1}{2} \sum_{\alpha,\beta \leq \epsilon_F} \sum_{\gamma,\delta \leq \epsilon_F} \sum_{\rho,\sigma > \epsilon_F} \frac{1}{(\epsilon_\alpha + \epsilon_\beta - \epsilon_\rho - \epsilon_\sigma)(\epsilon_\gamma + \epsilon_\beta - \epsilon_\rho - \epsilon_\sigma)}
$$
$$
\cdot \sum_{m_a \cdots m_s} \langle ab|V|rs\rangle \langle cd|V|ab\rangle \left(\langle rs|V|cd\rangle - \langle rs|V|dc\rangle\right). \tag{F.22}
$$

This involves two different terms, each of which needs to be evaluated. Looking at the first, with the possibility of a different multipolarity for each;

$$
\sum_{m_a \cdots m_s} \langle ab|V_\Lambda|rs\rangle \langle cd|V_{\Lambda'}|ab\rangle \langle rs|V_{\Lambda''}|cd\rangle = \sum_{m_a \cdots m_s} \tilde{F}_\Lambda^{\alpha\beta\rho\sigma} \tilde{F}_{\Lambda'}^{\gamma\delta\alpha\beta} \tilde{F}_{\Lambda''}^{\rho\sigma\gamma\delta}
$$
$$
\cdot \sum_{JM} \sum_{J'M'} \sum_{J''M''} \langle j_a m_a j_b m_b|JM\rangle \langle j_r m_r j_s m_s|JM\rangle \langle j_c m_c j_d m_d|J'M'\rangle
$$
$$
\cdot \langle j_a m_a j_b m_b|J'M'\rangle \langle j_r m_r j_s m_s|J''M''\rangle \langle j_c m_c j_d m_d|J''M''\rangle
$$
$$
\cdot \sqrt{\hat{j}_a \hat{j}_b \hat{j}_c \hat{j}_d \hat{j}_r \hat{j}_s}
$$
$$
\cdot (-1)^{J+J'+J''+j_a+j_b+j_c+j_d+j_r+j_s} \left\{ \begin{array}{ccc} j_s & j_r & J \\ j_a & j_b & \Lambda \end{array} \right\} \left\{ \begin{array}{ccc} j_b & j_a & J' \\ j_c & j_d & \Lambda' \end{array} \right\} \left\{ \begin{array}{ccc} j_d & j_c & J'' \\ j_r & j_s & \Lambda'' \end{array} \right\}.
$$

As in the case of the second order correction, the numbers $m_a \cdots m_s$ may be summed over giving delta functions in the J and M numbers, all of which but one J may be trivially summed, to give:

$$
\tilde{F}_\Lambda^{\alpha\beta\rho\sigma} \tilde{F}_{\Lambda'}^{\gamma\delta\alpha\beta} \tilde{F}_{\Lambda''}^{\rho\sigma\gamma\delta} \sqrt{\hat{j}_a \hat{j}_b \hat{j}_c \hat{j}_d \hat{j}_r \hat{j}_s} \sum_J \hat{J} (-1)^{3J+j_a+j_b+j_c+j_d+j_r+j_s}
$$
$$
\cdot \left\{ \begin{array}{ccc} j_s & j_r & J \\ j_a & j_b & \Lambda \end{array} \right\} \left\{ \begin{array}{ccc} j_b & j_a & J \\ j_c & j_d & \Lambda' \end{array} \right\} \left\{ \begin{array}{ccc} j_d & j_c & J \\ j_r & j_s & \Lambda'' \end{array} \right\}.
$$

This sum of three 6-j symbols is known[104] and gives for the sum of three matrix elements;

$$
\sum_{m_a \cdots m_s} \langle ab|V_\Lambda|rs\rangle \langle cd|V_{\Lambda'}|ab\rangle \langle rs|V_{\Lambda''}|cd\rangle = \tilde{F}_\Lambda^{\alpha\beta\rho\sigma} \tilde{F}_{\Lambda'}^{\gamma\delta\alpha\beta} \tilde{F}_{\Lambda''}^{\rho\sigma\gamma\delta}
$$
$$
\cdot \sqrt{\hat{j}_a \hat{j}_b \hat{j}_c \hat{j}_d \hat{j}_r \hat{j}_s} (-1)^{\Lambda+\Lambda'+\Lambda''} \left\{ \begin{array}{ccc} \Lambda & \Lambda' & \Lambda'' \\ j_a & j_c & j_r \end{array} \right\} \left\{ \begin{array}{ccc} \Lambda & \Lambda' & \Lambda'' \\ j_b & j_d & j_s \end{array} \right\}. \tag{F.23}
$$

The other term, after summing out the Clebsch–Gordan Coefficients, is

$$
-\sum_{m_a \cdots m_s} \langle ab|V|rs\rangle \langle cd|V|ab\rangle \langle rs|V|dc\rangle = \tilde{F}_\Lambda^{\rho\sigma\alpha\beta} \tilde{F}_{\Lambda'}^{\gamma\delta\alpha\beta} \tilde{F}_{\Lambda''}^{\rho\sigma\delta\gamma} \hat{j}_r \hat{j}_s \sqrt{\hat{j}_c \hat{j}_d}
$$

$$
\cdot \sum_J \hat{J}(-1)^{2J+2j_s+2j_a+2j_d}
\begin{Bmatrix} j_b & j_a & J \\ j_r & j_s & \Lambda \end{Bmatrix}
\begin{Bmatrix} j_b & j_a & J \\ j_c & j_d & \Lambda' \end{Bmatrix}
\begin{Bmatrix} j_c & j_d & J \\ j_r & j_s & \Lambda'' \end{Bmatrix}
$$

$$
= -\tilde{F}^{\rho\sigma\alpha\beta}_{\Lambda} \tilde{F}^{\gamma\delta\alpha\beta}_{\Lambda'} \tilde{F}^{\rho\sigma\delta\gamma}_{\Lambda''} \hat{j}_r \hat{j}_s \sqrt{\hat{j}_c \hat{j}_d}
\begin{Bmatrix} j_r & j_d & \Lambda'' \\ j_a & \Lambda' & j_c \\ \Lambda & j_b & j_s \end{Bmatrix}
\tag{F.24}
$$

Now all that remains is to evaluate these contributions for the possible values of Λ, Λ' and Λ'' which arise. Since each of these numbers can take on three different values there are $3^3 = 27$ different terms to evaluate. By observing that the labels a and b run over the same states and always appear together in the energy denominator, they may be interchanged without effect, likewise c and d, and r and s. Then, 9 of the 27 terms may be identified with another 9 to give 18 independent terms. Of these, 7 vanish for the 'direct' term (F.23), but all are finite in the exchange term (F.24). For those terms in which at least one of Λ, Λ' and Λ'' is zero, the 6- and 9-j symbols simplify. The full expression for the third order energy correction due the the h-h diagram is then

$$
E^{(3)}_{hh} = \frac{1}{2} \sum_{\alpha,\beta \le \epsilon_F} \sum_{\gamma,\delta \le \epsilon_F} \sum_{\rho,\sigma > \epsilon_F} \frac{1}{(\epsilon_\alpha + \epsilon_\beta - \epsilon_\rho - \epsilon_\sigma)(\epsilon_\gamma + \epsilon_\delta - \epsilon_\rho - \epsilon_\sigma)}
$$

$$
\cdot \left[\tilde{F}^{\alpha\beta\rho\sigma}_M \tilde{F}^{\gamma\delta\alpha\beta}_M \hat{j}_a \left(\tilde{F}^{\rho\sigma\gamma\delta}_M \hat{j}_d - \tilde{F}^{\rho\sigma\delta\gamma}_M \right) \right.
$$

$$
- 2\tilde{F}^{\alpha\beta\rho\sigma}_M \tilde{F}^{\gamma\delta\alpha\beta}_M \left(\tilde{F}^{\rho\sigma\delta\gamma}_D + \tilde{F}^{\rho\sigma\delta\gamma}_Q \right) \sqrt{\hat{j}_r \hat{j}_s}
$$

$$
- \tilde{F}^{\alpha\beta\rho\sigma}_M \left(\tilde{F}^{\gamma\delta\alpha\beta}_D + \tilde{F}^{\gamma\delta\alpha\beta}_Q \right) \tilde{F}^{\rho\sigma\delta\gamma}_M \sqrt{\hat{j}_r \hat{j}_s}
$$

$$
+ 2\tilde{F}^{\alpha\beta\rho\sigma}_M \tilde{F}^{\gamma\delta\alpha\beta}_D \left(\frac{1}{3} \tilde{F}^{\rho\sigma\gamma\delta}_D \hat{j}_a \hat{j}_b - (-1)^{j_a+j_b} \tilde{F}^{\rho\sigma\delta\gamma}_D \sqrt{\hat{j}_r \hat{j}_s \hat{j}_c \hat{j}_d} \begin{Bmatrix} j_c & j_a & 1 \\ j_d & j_s & 1 \end{Bmatrix} \right)
$$

$$
+ 2(-1)^{j_a+j_b} \tilde{F}^{\alpha\beta\rho\sigma}_M \tilde{F}^{\gamma\delta\alpha\beta}_D \tilde{F}^{\rho\sigma\delta\gamma}_Q \sqrt{\hat{j}_r \hat{j}_s \hat{j}_c \hat{j}_d} \begin{Bmatrix} j_c & j_a & 1 \\ j_d & j_s & 2 \end{Bmatrix}
$$

$$
+ 2(-1)^{j_a+j_b} \tilde{F}^{\alpha\beta\rho\sigma}_M \tilde{F}^{\gamma\delta\alpha\beta}_Q \tilde{F}^{\rho\sigma\delta\gamma}_D \sqrt{\hat{j}_r \hat{j}_s \hat{j}_c \hat{j}_d} \begin{Bmatrix} j_c & j_a & 2 \\ j_d & j_s & 1 \end{Bmatrix}
$$

$$
+ 2\tilde{F}^{\alpha\beta\rho\sigma}_M \tilde{F}^{\gamma\delta\alpha\beta}_Q \left(\frac{1}{5} \tilde{F}^{\rho\sigma\gamma\delta}_Q \hat{j}_a \hat{j}_b - (-1)^{j_a+j_b} \tilde{F}^{\rho\sigma\delta\gamma}_Q \sqrt{\hat{j}_r \hat{j}_s \hat{j}_c \hat{j}_d} \begin{Bmatrix} j_c & j_a & 2 \\ j_d & j_s & 2 \end{Bmatrix} \right)
$$

$$
+ \hat{j}_r \hat{j}_s \tilde{F}^{\alpha\beta\rho\sigma}_D \tilde{F}^{\gamma\delta\alpha\beta}_M \left(\frac{1}{3} \tilde{F}^{\rho\sigma\gamma\delta}_D \delta_{j_a j_r} \delta_{j_b j_s} - (-1)^{j_a+j_b} \tilde{F}^{\rho\sigma\delta\gamma}_D \begin{Bmatrix} j_r & j_a & 1 \\ j_s & j_b & 1 \end{Bmatrix} \right)
$$

$$
+ 2(-1)^{j_a+j_b} \tilde{F}^{\alpha\beta\rho\sigma}_D \tilde{F}^{\gamma\delta\alpha\beta}_M \tilde{F}^{\rho\sigma\delta\gamma}_Q \hat{j}_r \hat{j}_s \begin{Bmatrix} j_r & j_a & 1 \\ j_s & j_b & 2 \end{Bmatrix}
$$

$$
+ \hat{j}_r \hat{j}_s \tilde{F}^{\alpha\beta\rho\sigma}_Q \tilde{F}^{\gamma\delta\alpha\beta}_M \left(\frac{1}{5} \tilde{F}^{\rho\sigma\gamma\delta}_Q \delta_{j_a j_r} \delta_{j_b j_s} - (-1)^{j_a+j_b} \tilde{F}^{\rho\sigma\delta\gamma}_Q \begin{Bmatrix} j_r & j_a & 2 \\ j_s & j_b & 2 \end{Bmatrix} \right)
$$

$$
\left. + \cdots \right]
\tag{F.25}
$$

Λ	Λ'	Λ''	factor
1	1	1	1
1	1	2	2
1	2	1	1
1	2	2	2
2	1	2	1
2	2	2	1

Table F.1: Terms missing from expression (F.25) for the third order hole–hole energy correction

Here the ellipsis represents the terms which cannot be reduced, i.e. those for which none of Λ, Λ' or Λ'' are zero. These terms are shown in table F.1 and are just the expressions (F.23) and (F.24) with the appropriate values of Λ, Λ' and Λ'' and the factor as indicated in the table.

F.2.2 Particle-Particle Scattering term

The energy correction due to the particle–particle scattering diagram is

$$E_{pp}^{(3)} = \frac{1}{8} \sum_{a \neq b \leq \epsilon_F} \sum_{r \neq s > \epsilon_F} \sum_{t \neq u > \epsilon_F} \frac{\langle ab|\tilde{v}|rs\rangle\langle rs|\tilde{v}|tu\rangle\langle tu|\tilde{v}|ab\rangle}{(\epsilon_a + \epsilon_b - \epsilon_r - \epsilon_s)(\epsilon_a + \epsilon_b - \epsilon_t - \epsilon_u)} \qquad \text{(F.26)}$$

If one relabels this using $a \to r$, $b \to s$, $r \to a$, $s \to b$, $t \to c$, $u \to d$, then the matrix elements are exactly of the same form as the hole–hole expression, and the labels pair up with others running over the same states in the same way as in the hole–hole expression. The summation of the magnetic quantum numbers in the matrix elements may be carried out in exactly the same way. The expression for the energy correction is then

$$E_{pp}^{(3)} = \frac{1}{2} \sum_{\alpha,\beta \leq \epsilon_F} \sum_{\rho,\sigma > \epsilon_F} \sum_{\tau \upsilon > \epsilon_F} \frac{1}{(\epsilon_\alpha + \epsilon_\beta - \epsilon_\rho - \epsilon_\sigma)(\epsilon_\alpha + \epsilon_\beta - \epsilon_\tau - \epsilon_\upsilon)} \left[\cdots\right] \qquad \text{(F.27)}$$

where the expression elided in the square brackets is just that for the hole–hole case with the transformation of labels as above.

F.2.3 Particle-Hole Scattering term

In the previous terms the fact that each single particle state occurred always with the same partner in the two-particle state vector greatly simplified things. Specifically it enabled one to couple the two-body states to good J and then sum out

the Clebsch-Gordan coefficients which resulted in a trivial way. For the p-h term the situation is somewhat different. The energy correction is

$$E_{ph}^{(3)} = \sum_{a \neq b \neq c \leq \epsilon_F} \sum_{r \neq s \neq t > \epsilon_F} \frac{\langle ab|\tilde{v}|rs\rangle \langle cr|\tilde{v}|at\rangle \langle st|\tilde{v}|cb\rangle}{(\epsilon_a + \epsilon_b - \epsilon_r - \epsilon_s)(\epsilon_b + \epsilon_c - \epsilon_s - \epsilon_t)}. \tag{F.28}$$

Fortunately, the need to worry about the restriction on the sum is again obviated by the fact that the matrix elements are antisymmetric and that for each restriction both labels involved appear somewhere together in a bra or a ket and also together in the energy denominator. It is not until one attempts to calculate selected fourth order diagrams that this becomes a difficult issue.

Fewer reductions can be made in the expansion of the product of three antisymmetric matrix elements than in the previous cases. Only two pairs of the 8 may be identified to give for the energy correction:

$$
\begin{aligned}
E_{ph}^{(3)} &= \frac{1}{2} \sum_{\alpha, \beta, \gamma \leq \epsilon_F} \sum_{\rho\sigma\tau > \epsilon_F} \frac{1}{(\epsilon_\alpha + \epsilon_\beta - \epsilon_\rho - \epsilon_\sigma)(\epsilon_\beta + \epsilon_\gamma - \epsilon_\sigma - \epsilon_\tau)} \\
&\quad \cdot \sum_{m_a \cdots m_t} \big[2\langle ab|V|rs\rangle\langle st|V|cb\rangle\langle cr|V|at\rangle - 2\langle ab|V|rs\rangle\langle st|V|cb\rangle\langle cr|V|ta\rangle \\
&\quad \cdot -\langle ab|V|rs\rangle\langle st|V|bc\rangle\langle cr|V|at\rangle + \langle ab|V|rs\rangle\langle st|V|bc\rangle\langle cr|V|ta\rangle \\
&\quad \cdot -\langle ab|V|sr\rangle\langle st|V|cb\rangle\langle cr|V|at\rangle + \langle ab|V|sr\rangle\langle st|V|cb\rangle\langle cr|V|ta\rangle \big] \tag{F.29}
\end{aligned}
$$

To evaluate the sum over the 6 m quantum numbers it is still easier to couple the bras and kets to good J rather than to attempt to sum 6 dependent Clebsch-Gordan symbols. For the first two terms of (F.29), the coupling of the matrix elements gives:

$$
\begin{aligned}
\sum_{m_a \cdots m_t} &\langle ab|V_\Lambda|rs\rangle\langle st|V_{\Lambda'}|cb\rangle\langle cr|\tilde{v}_{\Lambda''}|at\rangle = \\
&\langle ab(JM)|V_\Lambda|rs(JM)\rangle\langle st(J'M')|V_{\Lambda'}|cb(J'M')\rangle\langle cr(J''M'')|\tilde{v}_{\Lambda''}|at(J''M'')\rangle \\
&\quad \cdot \sum_{m_a \cdots m_t} \sum_{JM} \sum_{J'M'} \sum_{J''M''} \langle j_a m_a j_b m_b|JM\rangle\langle j_r m_r j_s m_s|JM\rangle\langle j_s m_s j_t m_t|J'M'\rangle \\
&\quad \cdot \langle j_c m_c j_b m_b|J'M'\rangle\langle j_c m_c j_r m_r|J''M''\rangle\langle j_a m_a j_t m_t|J''M''\rangle \tag{F.30}
\end{aligned}
$$

To perform this sum, one takes the first four Clebsch-Gordan coefficients and sums them over the magnetic numbers which appear twice:

$$
\begin{aligned}
&= (-1)^{1+j_a+j_s+j+r+j_c-J'} \sum_{MM'm_b m_s} \langle j_b m_b j_a m_a|JM\rangle\langle j_s m_s j_r m_r|JM\rangle \\
&\quad \cdot \langle j_s m_s j_t m_t|J'M'\rangle\langle j_b m_b j_c m_c|J'M'\rangle \\
&= (-1)^{1+j_c-j_b-J'}\hat{J}\hat{J}' \sum_{k\kappa} \langle j_c m_c j_r m_r|k\kappa\rangle\langle j_t m_t j_a m_a|k\kappa\rangle
\begin{Bmatrix} J & j_b & j_a \\ j_s & J' & j_t \\ j_r & j_c & k \end{Bmatrix} .
\end{aligned}
$$

This result is then combined with the remaining two Clebsch–Gordan coefficients and sums over magnetic numbers

$$= (-1)^{1+j_c-j_b-J'}\hat{J}\hat{J}' \sum_k \left\{ \begin{array}{ccc} J & j_b & j_a \\ j_s & J' & j_t \\ j_r & j_c & k \end{array} \right\}$$

$$\cdot \sum_\kappa \sum_{M'} \sum_{m_a m_c} \sum_{m_t m_r} \langle j_c m_c j_r m_r | k\kappa \rangle \langle j_t m_t j_a m_a | k\kappa \rangle \langle j_c m_c j_r m_r | J''M'' \rangle \langle j_a m_a j_t m_t | J''M'' \rangle.$$

Now the sums over the remaining m states are carried out to give for the sum (F.30)

$$\sum_{m_a \cdots m_t} \langle ab | V_\Lambda | rs \rangle \langle st | V_{\Lambda'} | cb \rangle \langle cr | \tilde{v}_{\Lambda''} | at \rangle =$$

$$\langle ab(JM) | V_\Lambda | rs(JM) \rangle \langle st(J'M') | V_{\Lambda'} | cb(J'M') \rangle \langle cr(J''M'') | \tilde{v}_{\Lambda''} | at(J''M'') \rangle$$

$$\cdot \sum_{JJ'J''} (-1)^{1+j_a+j_t+j_c-j_b-J'-J''} \hat{J}\hat{J}'\hat{J}'' \left\{ \begin{array}{ccc} J & j_b & j_a \\ j_s & J' & j_t \\ j_r & j_c & J'' \end{array} \right\}. \qquad (F.31)$$

Now the representation of the reduced matrix elements in terms of the 6–j symbols (F.15) may be substituted. Looking first at the direct part of the one antisymmetric matrix element, one has:

$$\sum_{m_a \cdots m_t} \langle ab | V_\Lambda | rs \rangle \langle st | V_{\Lambda'} | cb \rangle \langle cr | V_{\Lambda''} | at \rangle =$$

$$\cdot \tilde{F}_\Lambda^{\alpha\beta\rho\sigma} \tilde{F}_\Lambda^{\sigma\tau\gamma\beta} \tilde{F}_\Lambda^{\gamma\rho\alpha\tau} \sum_{JJ'J''} \hat{J}\hat{J}'\hat{J}'' (-1)^{1+J} \left\{ \begin{array}{ccc} j_s & j_r & J \\ j_a & j_b & \Lambda \end{array} \right\} \left\{ \begin{array}{ccc} j_b & j_c & J' \\ j_s & j_t & \Lambda' \end{array} \right\}$$

$$\cdot \left\{ \begin{array}{ccc} j_t & j_a & J'' \\ j_c & j_r & \Lambda'' \end{array} \right\} \left\{ \begin{array}{ccc} J & j_b & j_a \\ j_s & J' & j_t \\ j_r & j_c & J'' \end{array} \right\} \qquad (F.32)$$

The sum of three 6–j symbols and one 9–j symbol in this case may be obtained in steps. The sum over J'' of a factor, and one 6–j and one 9–j may be performed to give two 6–j symbols. This leaves a sum over two indices of four 6–j symbols:

$$-\sum_{JJ'} (-1)^J \hat{J}\hat{J}' \left\{ \begin{array}{ccc} j_s & j_r & J \\ j_a & j_b & \Lambda \end{array} \right\} \left\{ \begin{array}{ccc} j_b & j_c & J' \\ j_s & j_t & \Lambda' \end{array} \right\} \left\{ \begin{array}{ccc} j_r & j_t & \Lambda'' \\ J' & J & j_s \end{array} \right\} \left\{ \begin{array}{ccc} J' & J & \Lambda'' \\ j_a & j_c & j_b \end{array} \right\}. \quad (F.33)$$

Now J', appearing in three of the 6–j symbols may be summed over to give a 9–j symbol, leaving

$$-\sum_J (-1)^J \hat{J} \left\{ \begin{array}{ccc} j_s & j_r & J \\ j_a & j_b & \Lambda \end{array} \right\} \left\{ \begin{array}{ccc} j_b & J & j_a \\ j_t & j_r & \Lambda'' \\ \Lambda' & j_s & j_c \end{array} \right\}. \qquad (F.34)$$

Finally the last sum, over J may be performed. The result is two 6-j symbols so that the sum over $m_a \cdots m_t$ of the non–antisymmetrized matrix elements is

$$\sum_{m_a \cdots m_t} \langle ab|V_\Lambda|rs\rangle\langle st|V'_\Lambda|cb\rangle\langle cr|V_{\Lambda''}|at\rangle = \sqrt{\hat{\jmath}_a\hat{\jmath}_b\hat{\jmath}_c\hat{\jmath}_r\hat{\jmath}_s\hat{\jmath}_t}\,\tilde{F}_\Lambda^{\alpha\beta\rho\sigma}\tilde{F}_\Lambda^{\sigma\tau\gamma\beta}\tilde{F}_\Lambda^{\gamma\rho\alpha\tau}$$

$$\cdot(-1)^{j_a+j_b+j_c+j_r+j_s+j_t+\Lambda'+\Lambda''}\left\{\begin{matrix} j_c & j_t & \Lambda \\ j_b & j_s & \Lambda' \end{matrix}\right\}\left\{\begin{matrix} j_c & j_t & \Lambda \\ j_r & j_a & \Lambda'' \end{matrix}\right\}. \tag{F.35}$$

The other 5 terms in (F.29) can be reduced in a similar manner. The results are:

$$\sum_{m_a \cdots m_t} \langle ab|V_\Lambda|rs\rangle\langle st|V_{\Lambda'}|cb\rangle\langle cr|V_{\Lambda''}|ta\rangle = \sqrt{\hat{\jmath}_a\hat{\jmath}_b\hat{\jmath}_c\hat{\jmath}_r\hat{\jmath}_s\hat{\jmath}_t}\,\tilde{F}_\Lambda^{\alpha\beta\rho\sigma}\tilde{F}_\Lambda^{\sigma\tau\gamma\beta}\tilde{F}_\Lambda^{\gamma\rho\tau\alpha}$$

$$\cdot(-1)^{j_c+j_b+j_r+j_s}\frac{\delta_{\Lambda\Lambda'}}{\hat{\Lambda}}\left\{\begin{matrix} j_s & j_b & \Lambda'' \\ j_t & j_c & \Lambda' \end{matrix}\right\} \tag{F.36}$$

$$\sum_{m_a \cdots m_t} \langle ab|V_\Lambda|rs\rangle\langle st|V_{\Lambda'}|bc\rangle\langle cr|V_{\Lambda''}|at\rangle = \sqrt{\hat{\jmath}_a\hat{\jmath}_b\hat{\jmath}_c\hat{\jmath}_r\hat{\jmath}_s\hat{\jmath}_t}\,\tilde{F}_\Lambda^{\alpha\beta\rho\sigma}\tilde{F}_\Lambda^{\sigma\tau\gamma\beta}\tilde{F}_\Lambda^{\gamma\rho\alpha\tau}$$

$$\cdot(-1)^{j_a+j_b+j_c+j_r+j_s+j_t+\Lambda'+\Lambda''}\frac{\delta_{\Lambda\Lambda'}}{\hat{\Lambda}}\left\{\begin{matrix} j_a & j_r & \Lambda' \\ j_t & j_c & \Lambda'' \end{matrix}\right\} \tag{F.37}$$

$$\sum_{m_a \cdots m_t} \langle ab|V_\Lambda|sr\rangle\langle st|V_{\Lambda'}|bc\rangle\langle cr|V_{\Lambda''}|ta\rangle = -\sqrt{\hat{\jmath}_a\hat{\jmath}_b\hat{\jmath}_c\hat{\jmath}_r\hat{\jmath}_s\hat{\jmath}_t}\,\tilde{F}_\Lambda^{\alpha\beta\rho\sigma}\tilde{F}_\Lambda^{\sigma\tau\beta\gamma}\tilde{F}_\Lambda^{\gamma\rho\tau\alpha}$$

$$\cdot(-1)^{j_a+j_b+j_c+j_r+j_s+j_t}\frac{\delta_{\Lambda\Lambda'}\delta_{\Lambda\Lambda''}}{\hat{\Lambda}} \tag{F.38}$$

$$\sum_{m_a \cdots m_t} \langle ab|V_\Lambda|rs\rangle\langle st|V_{\Lambda'}|cb\rangle\langle cr|V_{\Lambda''}|at\rangle = \sqrt{\hat{\jmath}_a\hat{\jmath}_b\hat{\jmath}_c\hat{\jmath}_r\hat{\jmath}_s\hat{\jmath}_t}\,\tilde{F}_\Lambda^{\alpha\beta\rho\sigma}\tilde{F}_\Lambda^{\sigma\tau\gamma\beta}\tilde{F}_\Lambda^{\gamma\rho\alpha\tau}$$

$$\cdot\left\{\begin{matrix} \Lambda & \Lambda' & \Lambda'' \\ j_t & j_r & j_b \end{matrix}\right\}\left\{\begin{matrix} \Lambda & \Lambda' & \Lambda'' \\ j_c & j_a & j_s \end{matrix}\right\} \tag{F.39}$$

$$\sum_{m_a \cdots m_t} \langle ab|V_\Lambda|sr\rangle\langle st|V_{\Lambda'}|cb\rangle\langle cr|V_{\Lambda''}|ta\rangle = \sqrt{\hat{\jmath}_a\hat{\jmath}_b\hat{\jmath}_c\hat{\jmath}_r\hat{\jmath}_s\hat{\jmath}_t}\,\tilde{F}_\Lambda^{\alpha\beta\sigma\rho}\tilde{F}_\Lambda^{\sigma\tau\gamma\beta}\tilde{F}_\Lambda^{\gamma\rho\tau\alpha}$$

$$\cdot(-1)^{j_b+j_c+j_r+j_s+\Lambda+\Lambda'}\left\{\begin{matrix} j_a & j_r & \Lambda' \\ j_b & j_s & \Lambda \end{matrix}\right\}\left\{\begin{matrix} j_s & j_b & \Lambda'' \\ j_t & j_c & \Lambda' \end{matrix}\right\}. \tag{F.40}$$

Now the expression (F.29) can be evaluated using the reduced sums over the m quantum numbers. For each of the six terms in (F.29) there are 27 ways of labelling Λ, Λ' and Λ''. This being the case, that there are $27 \times 6 = 162$ terms, they are not explicitly listed here. It is noted, however, that for any term in which at least one of Λ, Λ' and Λ'' is zero, the 6-j symbols will simplify, and the terms, although more numberous for the particle-hole correction, are individually no more complicated than for the particle-particle or hole-hole terms.

Appendix G

Neutron Star Equation of State

To obtain the equation of state for the nuclear matter region of a neutron star, the energy density of the neutron, proton, electron and muon ($npe\mu$) matter is written as a sum of nucleon and lepton contributions[22]:

$$
\begin{aligned}
e(n_p, n_n, n_e, n_\mu) &= e_N(n_p, n_n) + n_n m_n c^2 + n_p m_p c^2 + e_e(n_e) \\
&+ e_\mu(n_\mu) + n_e m_e c^2 + n_\mu m_\mu c^2 + e_\nu
\end{aligned}
\tag{G.1}
$$

The matter is considered to be in equilibrium with respect to weak interactions:

$$
n \leftrightarrow p + e^- \leftrightarrow p + \mu^-
$$

which implies the conditions on the chemical potentials:

$$
\mu_n = \mu_p + \mu_e, \qquad \mu_\mu = \mu_e
\tag{G.2}
$$

where the chemical potential is defined as

$$
\mu_j = \frac{\partial e}{\partial n_j}.
\tag{G.3}
$$

A second condition arises from the fact that the matter must be electrically neutral, which implies

$$
n_p = n_e + n_\mu.
\tag{G.4}
$$

For each baryon number density fractions are defined as

$$
Y_{n,p} = \frac{n_{n,p}}{n_b}
\tag{G.5}
$$

where $n_b = n_p + n_n$ is the number of baryons. Lepton fractions are constrained by the above conditions. Given these definitions and conditions, the EOS is given by two expressions: The mass density

$$
\rho(n_b) = \frac{e(n_b)}{c^2}
\tag{G.6}
$$

and the pressure

$$P(n_b) = n_b^2 \frac{d(e/n_b)}{dn_b}. \tag{G.7}$$

By eliminating n_b from these equations the EOS results giving pressure as a function of mass density of the matter.

From 6.30, the energy density of asymmetric matter can be rendered in the notation of neutron star theory as

$$
\begin{aligned}
e_N(n_b, n_p, n_n) &= c_p n_p^{5/3} + c_n n_n^{5/3} + \frac{1}{2} W_a n_b^{2\beta_a - \alpha_a + 2} + \frac{1}{2} W_r n_b^{2\beta_r - \alpha_r + 2} \\
&+ \frac{1}{2} W_a b_a n_b^{2\beta_a - \alpha_a}(n_n - n_p)^2 + \frac{1}{2} W_r b_r n_b^{2\beta_r - \alpha_r}(n_n - n_p)^2 \quad \text{(G.8)}
\end{aligned}
$$

or, as a function of n_b and the baryon fractions as

$$
\begin{aligned}
e_N(n_b, Y_p, Y_n) &= c_p n_b^{5/3} Y_p^{5/3} + c_n n_b^{5/3} Y_n^{5/3} + \frac{1}{2} W_a n_b^{2\beta_a - \alpha_a + 2} + \frac{1}{2} W_r n_b^{2\beta_r - \alpha_r + 2} \\
&+ \frac{1}{2} W_a b_a n_b^{2\beta_a - \alpha_a + 2}(Y_n - Y_p)^2 + \frac{1}{2} W_r b_r n_b^{2\beta_r - \alpha_r + 2}(Y_n - Y_p)^2 \quad \text{(G.9)}
\end{aligned}
$$

To simplify the calculation, the numbers c_p and c_n (which are defined in Chapter 6) are taken to be the same value, β, using an average nucleon mass $m_n = (1/2)(m_p + m_n)$. The first two terms thus become $\beta n_b^{5/3}(Y_n^{5/3} + Y_p^{5/3})$.

This expression is then used to work out the chemical potentials:

$$\mu_i = \frac{\partial e}{\partial n_i} = \frac{\partial(e/n_b)}{\partial(n_i/n_b)} = \frac{\partial \mathcal{E}}{\partial Y_i} \tag{G.10}$$

where $\mathcal{E} = \mathcal{E}_N + \mathcal{E}_e + \cdots = e/n_b$ is the energy density per particle. $\mathcal{E}_N$ is thus

$$
\begin{aligned}
\mathcal{E}_N(n_b, Y_p, Y_n) &= \beta n_b^{2/3} \left(Y_p^{5/3} + Y_n^{5/3}\right) + \frac{1}{2} W_a n_b^{2\beta_a - \alpha_a + 1} + \frac{1}{2} W_r n_b^{2\beta_r - \alpha_r + 1} \\
&+ \frac{1}{2} W_a b_a n_b^{2\beta_a - \alpha_a + 1}(Y_n - Y_p)^2 + \frac{1}{2} W_r b_r n_b^{2\beta_r - \alpha_r + 1}(Y_n - Y_p)^2 \quad \text{(G.11)}
\end{aligned}
$$

so the chemical potentials are

$$
\begin{aligned}
\mu_p &= \frac{\partial \mathcal{E}_N}{\partial Y_p} = \frac{5}{3} \beta n_b^{2/3} Y_p^{2/3} \\
&- W_a b_a n_b^{2\beta_a - \alpha_a + 1}(Y_p + Y_n)^{2\beta_a - \alpha_a}(Y_n - Y_p) \\
&- W_r b_r n_b^{2\beta_r - \alpha_r + 1}(Y_p + Y_n)^{2\beta_r - \alpha_r}(Y_n - Y_p)
\end{aligned}
\tag{G.12}
$$

and

$$
\begin{aligned}
\mu_n &= \frac{\partial \mathcal{E}_N}{\partial Y_p} = \frac{5}{3} \beta n_b^{2/3} Y_p^{2/3} \\
&+ W_a b_a n_b^{2\beta_a - \alpha_a + 1}(Y_p + Y_n)^{2\beta_a - \alpha_a}(Y_n - Y_p) \\
&+ W_r b_r n_b^{2\beta_r - \alpha_r + 1}(Y_p + Y_n)^{2\beta_r - \alpha_r}(Y_n - Y_p)
\end{aligned}
\tag{G.13}
$$

and their difference is

$$
\begin{aligned}
\mu_n - \mu_p \;=\;& \frac{5}{3}\beta n_b^{2/3}\left(Y_n^{2/3} - Y_p^{2/3}\right)\\
&+\; 2W_a b_a n_b^{2\beta_a-\alpha_a+1}Y_p\\
&+\; 2W_r b_r n_b^{2\beta_r-\alpha_r+1}Y_p.
\end{aligned}
\tag{G.14}
$$

From the equilibrium condition (G.2) one has

$$
\mu_n - \mu_p - \mu_e = 0
\tag{G.15}
$$

The electron chemical potential μ_e can be calculated as [106, 107]

$$
\mu_e = \hbar c \,(3\pi^2 Y_e n_b)^{1/3}.
\tag{G.16}
$$

The electron fraction, Y_e must be equal to the proton fraction to ensure charge neutrality, at least below muon threshold. Furthermore since Y_p and Y_n are related by the condition $Y_p + Y_n = 1$, the equation (G.15) can be used to combine (G.14) and (G.16) to give an expression which can be solved for the equilibrium proton fraction (and so the equilibrium neutron fraction) given just n_b

$$
\begin{aligned}
0 \;=\;& \frac{5}{3}\beta n_b^{2/3}\left((1-Y_p)^{2/3} - Y_p^{2/3}\right)\\
&+\; 2W_a b_a n_b^{2\beta_a-\alpha_a+1}Y_p\\
&+\; 2W_r b_r n_b^{2\beta_r-\alpha_r+1}Y_p\\
&-\; \hbar c\,(3\pi^2 Y_p n_b)^{1/3}
\end{aligned}
\tag{G.17}
$$

Above muon threshold, i.e. the difference between neutron and proton chemical potentials exceeds the rest mass of the muon, the following condition also holds

$$
\mu_n - \mu_p = \mu_\mu
\tag{G.18}
$$

where μ_μ is [106]

$$
\mu_\mu = \sqrt{(m_\mu c^2)^2 + \hbar^2 c^2 (3\pi^2 Y_\mu n_b)^{2/3}}
\tag{G.19}
$$

and it is known from (G.2) that $\mu_\mu = \mu_e$. Now the condition for charge neutrality gives

$$
Y_p = Y_e + Y_\mu.
\tag{G.20}
$$

From (G.16) and (G.19) and the condition $\mu_e = \mu_\mu$, the electron fraction and the muon fraction can be related as

$$
Y_e = \left[\left(\frac{m_\mu c^2}{\hbar c}\right)^2 \frac{1}{(3\pi^2 n_b)^{2/3}} + Y_\mu^{2/3}\right]^{3/2}
\tag{G.21}
$$

Now the expressions arising from the conditions

$$\mu_n - \mu_p - \mu_e = 0$$
$$\mu_n - \mu_p - \mu_\mu = 0$$

can be solved to give Y_p, Y_e and Y_μ as a function of the baryon density n_b.

Going back to (G.1) the energy densities for electrons, muons and neutrinos still need to be evaluated. They are [107, 105]:

$$e_e \approx \frac{1}{4\pi^2} \frac{\mu_e^4}{(\hbar c)^3} \tag{G.22}$$

$$e_\mu = \frac{1}{4\pi^2 (\hbar c)^3} \left[\mu_\mu k(\mu_\mu^2 - \frac{1}{2} m_\mu^2 c^4) - \frac{1}{2} m_\mu^4 c^8 \ln\left(\frac{\mu_\mu + k}{m_\mu c^2}\right) \right] \tag{G.23}$$

$$e_\nu = \frac{1}{8\pi^2} \frac{\mu_\nu^4}{(\hbar c)^3} \tag{G.24}$$

where $k = (3\pi^2 Y_\mu n_b)^{1/3} \hbar c$ and $\mu_\nu = \hbar c (6\pi^2 Y_\nu n_b)^{1/3}$. The electron energy is approximated to be ultrarelativistic. In addition there is a contribution from the Coulomb interaction. The direct term is zero due to the charge neutrality of the system, but the exchange term provides a small contribution:

$$e_{ce} = -\frac{3}{2} \left(\frac{3}{\pi}\right)^{1/3} e^2 (Y_e n_b)^{4/3} \tag{G.25}$$

Now that the entire expression for the energy density is known, the pressure may be evaluated. Since the protons and neutrons interact strongly their partial pressures cannot be defined. Instead, the nucleon pressure is calculated:

$$
\begin{aligned}
P_N &= n_b^2 \frac{\partial(e_N/n_b)}{\partial n_b} = n_b^2 \frac{\partial \mathcal{E}_N}{\partial n_b} \\
&= \frac{2}{3} \beta n_b^{5/3} \left(Y_n^{5/3} + Y_p^{5/3}\right) \\
&+ \frac{1}{2}(2\beta_a - \alpha_a + 1) W_a n_b^{2\beta_a - \alpha_a + 2} \\
&+ \frac{1}{2}(2\beta_r - \alpha_r + 1) W_r n_b^{2\beta_r - \alpha_r + 2} \\
&+ \frac{1}{2}(2\beta_a - \alpha_a) W_a b_a n_b^{2\beta_a - \alpha_a + 2} (Y_n - Y_p)^2 \\
&+ \frac{1}{2}(2\beta_r - \alpha_r) W_r b_r n_b^{2\beta_r - \alpha_r + 2} (Y_n - Y_p)^2
\end{aligned}
\tag{G.26}
$$

The electron, muon and neutrino pressures and the Coulomb exchange pressure are calculated in the same way to be

$$P_e = \frac{1}{12\pi^2} \frac{\mu_e^4}{(\hbar c)^3} \tag{G.27}$$

$$P_\mu = \frac{1}{12\pi^2}\left[\mu_\mu k(\mu_\mu^2 - \frac{5}{2}m_\mu^2 c^4) + \frac{3}{2}m_\mu^4 c^8 \ln\left(\frac{\mu_\mu + k}{m_\mu c^2}\right)\right] \tag{G.28}$$

$$P_\nu = \frac{1}{24\pi^2}\frac{\mu_\nu^4}{(\hbar c)^3} \tag{G.29}$$

$$P_{ce} = -\frac{1}{2}\left(\frac{3}{\pi}\right)^{1/3} e^2(Y_e n_b)^{4/3} \tag{G.30}$$

Now there is an expression for the pressure as a function of the species fractions and the baryon density. The fractions are themselves solvable given just the baryon density, so by solving the equations given, one can evaluate the pressure for a given density, which gives us then the equation of state.

To relate the number density to the mass density the following relation is used

$$c^2\rho(n_b) = e_N + n_b Y_p m_p + n_b Y_n m_n + n_b Y_e m_e + n_b Y_\mu m_\mu. \tag{G.31}$$

This gives ρ in nuclear units ($\mathrm{MeV\,fm^{-3}\,c^{-2}}$). To covert to astrophysical units, the following factor is necessary:

$$\frac{\mathrm{MeV}}{\mathrm{fm}^3}\frac{1}{c^2} \approx 1.782465 \times 10^{12}\frac{\mathrm{g}}{\mathrm{cm}^3} \tag{G.32}$$

Bibliography

[1] S. Hofmann *et al.*, *Z.Phys.* **A350**, 277 (1995).

[2] Yu. A. Lazarev, *Phys. Rev.* **C 54**, 620 (1996).

[3] S. Hofmann *et al.*, *Z.Phys* **A 354**, 229 (1996).

[4] H. A. Bethe, *Sci. Am.* **189**, No.3, 58 (1956).

[5] T. Barnes, N. Black, D. J. Dean, and E. S. Swanson *Phys. Rev.* **C** Accepted for publication (1999).

[6] R. B. Wiringa *et al.* *Phys. Rev.* **C 51**, 38 (1995).

[7] S. A. Coon, M. D. Scadron, P. C. McNamee, B. R. Barrett, D. W. E. Blatt, and B. H. J. McKellar, *Nucl. Phys.* **A317**, 242 (1979).

[8] J. Carlson, V. R. Pandharipande, and R. B. Wiringa, *Nucl. Phys.* **A401**, 59 (1983).

[9] R. Schiavilla, V. R. Pandharipande, and R. B. Wiringa, *Nucl. Phys.* **A449**, 219 (1986).

[10] K. A. Brueckner, C. A. Levinson and H. M. Mahmoud, *Phys. Rev.* **95**, 217 (1954).

[11] C. R. Chen, G. L. Payne, J. L. Friar and B. F. Gibson, *Phys. Rev.* **C 31**, 2266 (1985).

[12] R. B. Wiringa *et al.* *Phys. Rev.* **C 43**, 1585 (1991)

[13] B. S. Pudliner *et al.* *Phys. Rev.* **C 56**, 1720 (1997).

[14] A. Fabrocini, F. Arias de Saaverda, G. Co' and P. Fogarait, *Phys. Rev.* **C 57**, 1668 (1998).

[15] J. G. Zabolitsky, *Nucl. Phys.* **A226**, 285 (1974).

[16] B. Mihaila, *Ph.D. Thesis*, University of New Hampshire, (1998).

[17] B. D. Day, *Rev. Mod. Phys.* **50**, 495 (1978).

[18] W. C. Haxton and C.-L. Song *nucl-th/9906082* (1999).

[19] D. Hartree, *The Calculation of Atomic Structure*, Wiley, New York (1957)

[20] J. P. Svenne, *Adv. Nucl. Phys.* **11** 179 (1979)

[21] D. Vautherin and D. M. Brink, *Phys. Rev.* **C 5**, 626 (1972).

[22] E. Chabanat *et al.*, *Nucl. Phys* **A 627**, 710 (1997).

[23] J. W. Negele, *Phys. Rev.* **C 5**, 1472 (1972).

[24] K. L. G. Heyde, *The Nuclear Shell Model, Second Edition*, Springer Verlag, Berlin (1994).

[25] M. Waroquier, G. Wenes, K. Heyde, *Nucl. Phys.* **A 404**, 298 (1983)

[26] M. Leuschner, *et al.*, *Phys. Rev.* **C 49**, 855 (1994).

[27] A. deShalit and H. Feshbach, *Theoretical Nuclear Physics, Volume I.*, John Wiley and Sons, New York (1974).

[28] P. Ring and P. Schuck, *The nuclear Many-Body Problem*, Springer, New York (1980).

[29] M. G. Mayer and J. H. Jensen, *Elementary Theory of Nuclear Shell Structure*, John Wiley and Sons, New York (1955).

[30] S. G. Nilsson, *Mat. Fys. Medd. Dan. Vid. Selsk.* **29** No. 16. (1955).

[31] D. C. Zheng, B. R. Barrett, J. P. Vary, W. C. Haxton and C. L. Song, *Phys. Rev.* **C52**, 2488 (1995).

[32] B. A. Brown and B. H. Wildenthal, *Ann. Rev. Nucl. Part. Sci.* **38**, 29 (1988).

[33] M. Hjorth-Jensen, T. T. S. Kuo and E. Osnes, *Phys. Rep.* **261**, 125 (1995)

[34] N. H. March, W. H. Young and S. Sampanthar, *The Many-Body Problem in Quantum Mechanics*, Cambridge University Press, London (1967).

[35] E. K. U. Gross, E. Runge and O. Heinonen, *Many-Particle Theory*, Adam Hilger, Bristol (1991).

[36] A. L. Fetter and J. D. Walecka, Quantum theory of many particle systems, McGraw-Hill, New York (1971).

[37] R. D. Mattuck, A guide to Feynman diagrams in the many-body problem, McGraw-Hill, New York (1976).

[38] D. J. Thouless, *The Quantum Mechanics of Many-Body Systems*, Academic Press, New York (1961).

[39] J. M. Eisenberg and W. Greiner, Nuclear Theory, Volume 3, North-Holland, Amsterdam (1972).

[40] A. Szabo and N. S. Ostlund, *Modern Quantum Chemistry*, McGraw Hill, New York (1989).

[41] S. E. Koonin, *Ph.D. Thesis*, M.I.T. (1975).

[42] D. Bohm and D. Pines, *Phys. Rev.* **92**,609 (1953).

[43] R. J. Blin-Stoyle, *Phil. Mag.* **46**, 973 (1955).

[44] J. W. Ehlers and S. A. Moszkowski, *Phys.Rev.* **C 6**, 217 (1972).

[45] D. Vautherin and M. Veneroni, Phys. Letters **26 B**, 552 (1968).

[46] J. C. Slater, *Phys. Rev.* **81**, 385 (1951).

[47] D. R. Bès and Z. Szymanski, *Nucl. Phys.* **28**, 42 (1961).

[48] M. Baranger and K. Kumar, *Nucl. Phys.* **62**, 113 (1965).

[49] M. Baranger and K. Kumar, *Nucl. Phys.* **A 110**, 490 (1968).

[50] K. Kumar and M. Baranger, *Nucl. Phys.* **A 100**, 529 (1968).

[51] R. Devi and S. K. Khosa, *Phys. Rev.* **C 54**, 1661 (1996).

[52] M. Dufour and A. Zuker, *Phys. Rev.* **C54**, 1641 (1996).

[53] A. Kerman, *Cargèse Lectures in Physics* **3**, 396 (1969).

[54] M. R. Strayer, *Ph.D. thesis*, MIT (1971).

[55] C. N. Bressel, A. K. Kerman and B. Rouben, *Nucl. Phys.* **A 124**, 624 (1969).

[56] B. Rouben, *Ph.D. Thesis*, MIT (1969).

[57] J. Zipse, *Ph.D. Thesis*, MIT (1970).

[58] E. Riihimäki, *Ph.D. Thesis*, MIT (1970).

[59] F. Tabakin, *Phys. Rev.* **174**, 1208 (1968).

[60] A. Kerman and M. K. Pal, *Phys. Rev.* **162**, 970 (1967).

[61] N. M. Hugenholz, *Physica* **23**, 481 (1957).

[62] D. Gogny, *Proceedings of the International Conference on Nuclear Selfconsistent Fields*, Trieste, 1975. G. Ripka and M. Porneuf, Eds. North Holland, Amsterdam, (1975).

[63] R. Machleidt, *Phys. Lett.* **B459**, 1 (1999).

[64] V. G. J. Stokes, R. A. M. Klomp, M. C. M. Rentmeester and J. J. de Swart, *Phys. Rev.* **C 48**, 792 (1993).

[65] T. Koopmans, *Physica* **1**, 104 (1933).

[66] J. M. Eisenberg and W. Greiner, Nuclear Theory, Volume 2, North-Holland, Amsterdam (1976).

[67] J. W. Negele, *Phys. Rev.* **C 1**, 1260 (1970).

[68] K. A. Brueckner and D. T. Goldman, *Phys. Rev.* **117**, 207 (1960).

[69] H. S. Köhler, *Nucl. Phys.* **A 162**, 385 (1971).

[70] W. H. Press, S. A. Teukolsky and M. Metcalf, *Numerical Recipes in Fortan 90*, Cambridge University Press, Cambridge (1996).

[71] C. C. J. Roothan, *Rev. Mod. Phys.* **23**, 69 (1951).

[72] F. James, *CERN Program Library Long Writeup* **D506** Version 94.1 (1998)

[73] M. Bender, *Dissertation zur Erlangung des Doktorgrades der Naturwissenschaft*, Johann Wolfgang Goethe Universität (1997).

[74] D. R. Bes and R. A. Sorensen *Adv. Nucl. Phys.* **2** 129, (1969).

[75] H. Bethe, *Annu. Rev. Nucl. Part. Sci.* **21**, 93 (1971).

[76] C. F. Von Weizsäcker, *Z. Phys.* **96**, 431 (1935).

[77] W. D. Myers and W. J. Swiatecki, *Nucl. Phys.* **81**, 1 (1966).

[78] A. E. S. Green, *Phys. Rev.* **95**, 1006 (1964).

[79] W. J. Swiatecki, *Nucl. Phys,* **A 574**, 237C (1994).

[80] M. Beiner, H. Flocard, Nguyen Van Giai and P. Quentin, *Nucl. Phys.* **A 238** 29 (1975).

[81] Nguyen Van Giai and N. Sagawa, *Nucl. Phys.* **A 371** 1 (1981).

[82] J. Bartel, P. Quentin, M. Brack, C. Guet and H.-B. Håkansson, *Nucl. Phys.* **A 386**, 79 (1982).

[83] J. Dobaczewski, H. Flocard and J. Treiner, *Nucl. Phys.* **A 422**, 103 (1984).

[84] F. Tondeur, M. Brack, M. Farine and J. M. Pearson, *Nucl. Phys.* **A 420** 297 (1984).

[85] J. P. Blaizot, *Phys. Rep.* **64**, 171 (1980)

[86] H. Heiselberg and M. Hjorth-Jensen, *Phys. Rep.* To be published (1999).

[87] R. B. Wiringa, V. Fiks and A. Fabrocini, *Phys. Rev.* **C 38**, 1010 (1988).

[88] F. M. Walter and L. D. Metthews, *Nature* **389**, 358 (1997).

[89] J. R. Oppenheimer and G. M. Volkoff, *Phys. Rev.* **55**, 374 (1939).

[90] S. L. Shapiro and S. A. Teukolsky, *Black Holes, White Dwarves and Neutron Stars*, John Wiley and Sons, New York (1983).

[91] R. Schaeffer, Y. Declais and S. Jullian, *Nature* **300**, 434 (1987).

[92] H. A. Bethe and J. Goldstone, *Proc. Roy. Soc. (London)* **A238**, 551 (1957).

[93] G. Audi and A. H. Wapstra, *Nucl. Phys.* **A595**, 409 (1995).

[94] M. Chartier *et al.*, *Phys. Rev. Lett.* **77**, 2400 (1996).

[95] M. Bender, K. Rutz, P.-G. Reinhard and J. A. Maruhn, *nucl-th/9910025* Accepted by *Eur. Phys. J.* **A** (1999).

[96] P. G. Reinhard and J. Friedrich, *Z. Phys.* **A 321**, 619 (1985)

[97] B. A. Brown, *Phys. Rev.* **C 58**, 220 (1998).

[98] A. L. Goodman, *Adv. Nucl. Phys.* **11**, 263 (1979).

[99] G. Fricke *et al.*, *At. Data Nucl. Data Tables* **60**, 177 (1995).

[100] G. C. Wick, *Phys. Rev.* **80**, 268 (1950).

[101] B. H. Brandow, *Phys. Rev.* **152**, 863 (1966).

[102] R. P. Feynman, *Phys. Rev.* **76**, 769 (1949).

[103] J. Goldstone, *Proc. Roy. Soc.* **A239**, 267 (1957).

[104] D. A. Varshalovich, A. N. Moskalev and V. K. Khersonskii, *Quantum Theory of Angular Momentum*, World Scientific, Singapore (1988).

[105] N. K. Glendenning, *Compact Stars : Nuclear Physics, Particle Physics, and General Relativity*, Springer Verlag, Berlin (1996).

[106] M. Onsi, H. Przsiezniak and J. M. Pearson, *Phys. Rev.* **C 55**, 3139 (1997).

[107] Latimer *et al.*, *Phys. Rev.* **C 50**, 460 (1994).